THE REDOX CHEMISTRY OF METAL PHTHALOCYANINES AND RELATED COMPOUNDS

Roderick C.S. McQueen

Ph.D. Thesis
University of Edinburgh
1982

To the family

Acknowledgements

I am indebted to Dr. G.A. Heath for his constant inspiration and assistance throughout this work. I am grateful to my industrial supervisor Dr. J.D.R. Vass, and to the many other members of staff at I.C.I. Grangemouth, especially Dr. R.V.H. Jones, Mr. R. MacKay and Mr. C. Bennie, for aiding a novice in the synthesis of phthalocyanines. I wish to thank all those members of the academic and technical staff of Edinburgh University, Chemistry Department for their help and advice, especially Miss Annette Erskine for typing this thesis.

I am also grateful to the Science and Engineering Research Council and Imperial Chemical Industries P.L.C. for financial support under the C.A.S.E. scheme and to the University of Edinburgh for the use of their facilities.

For the gift of Bonellin I wish to thank Professor Pelter.

Finally, much of this work was greatly aided by the generous gift of porphyrins. For this I am deeply grateful to Professor Alan Johnson, who tragically died before this work was completed.

Abstract

Phthalocyanines and porphyrins are structurally related tetrapyrrolic macrocycles of considerable technical and biological significance respectively, and are equally of fundamental academic interest due to their remarkable electronic properties and stability. This thesis is concerned with the stepwise electron-transfers of these systems and their metallated derivatives, as revealed by intensive voltammetric studies in widely differing non-aqueous media.

Chapter 1 reviews some general aspects of porphyrin and phthalocyanine chemistry, including earlier studies of their oxidations and reductions, and particularly traces the emergence of electrochemical methods as a valuable adjunct or alternative to purely "wet chemical" investigations.

Chapter 2 recounts the development of techniques for routine a.c., d.c. and cyclic voltammetry in 1-methylnaphthalene (and other liquid naphthalenes) at 150°C. This medium was examined initially because of the extreme insolubility of common phthalocyanine pigments in conventional solvents however the new electrochemical medium is remarkable for its strictly non-polar, non-coordinating, aprotic (and completely anhydrous) qualities, as well as its solubilizing power and wide temperature range, and should have wider application.

Chapter 3 recounts the rigorous voltammetric examination of the first and second one-electron reductions of phthalocyanines and its metal complexes in true solution in

1-methylnaphthalene at 150°C. Subsequent studies of the more soluble tetra-t-butyl phthalocyanines in the same medium at 150°C, and in dichloromethane at 20°C, provide parallel results. The evident inconsistencies in previous attempts to provide an orderly set of reduction potentials for metallophthalocyanines are examined and resolved.

Chapter 4 describes the voltammetric characterisation of the stepwise reduction of octa-ethyl and tetra-phenyl porphyrins and their metal derivatives in metal derivatives in methyl naphthalene. This enables exact comparison of the reduction potentials of the phthalocyanines and porphyrins in the same medium. The origins of the intrinsic differences in electron affinities of the two systems are elucidated by study of zinc tetrabenzoporphin, a compound of intermediate structure. Further studies confirm that dichloromethane provides a convenient room-temperature non-coordinating medium and the influence on the electrode potentials of metallo-porphyrins and butyl phthalocyanines of added Lewis bases or coordinating solvents is examined.

The extensive and accurate compilation of reduction potentials for two series of metallo phthalocyanines and metallo porphyrins in this work makes possible a reassessment of the widely accepted correlation between electrode potentials and central ion electronegativity. It is concluded in Chapter 5 that such relationships are by no means as exact or soundly based as hitherto suggested.

In Chapter 6 the oxidative behaviour of phthalocyanines and porphyrins is discussed. Unlike porphyrins, phthalocyanines are generally found to have poorly defined or anomalous anodic voltammetric responses. Fortunately the zinc complexes of both phthalocyanine and tetra-t-butyl phthalocyanine give well defined oxidations in methyl naphthalene and 1,2-dichlorobenzene. The separation between first oxidation and first reduction does not match the energy (in eV) of the prominent visible absorption band and indicates that in contrast to the situation prevailing in porphyrins, the electrochemical and optical experiments are not mapping the same region of the molecular orbital diagram.

Bonellin is a physiologically active chlorin of unique structure. Voltammetric measurements on its dimethyl ester in methyl-naphthalene and acetonitrile reveal well-defined reversible electron-transfer steps reported in Chapter 7. The separation between first oxidation and first reduction (well-matched to the prominent π to π^* transition energy) is characteristically smaller than in porphyrins due to the relative ease of chlorin oxidation. The spectroscopic changes accompanying exhaustive one-electron reduction of Bonellin dimethyl ester establish the presence of an intermediate, possibly involving complexation of the neutral chlorin and its radical anion.

Chapter 8 details the synthetic and purification procedures for the macrocyclic compounds prepared in the course of this work. Particular emphasis is given to the route to t-butyl phthalic acid and its subsequent conversion to tetra-t-butyl phthalocyanine derivatives, and to the 'one-pot' synthesis of zinc tetrabenzoporphin. Detailed infra-red and optical spectral data are provided where otherwise unavailable.

Contents

Dedication		(i)
Declaration		(ii)
Acknowledgements		(iii)
Abstract		(iv)
Contents		(viii)
List of Figures		(xi)
List of Tables		(xv)
Chapter 1	Aspects of Phthalocyanine and Porphyrin Chemistry	1
1.1	Introduction	2
1.2	Porphyrin and Phthalocyanine Structures	4
1.3	Chemistry of Metalloporphyrins and Metallophthalocyanines	9
1.4	Redox Chemistry of Phthalocyanine and Porphyrin Complexes	14
Chapter 2	Voltammetric Methods for High Temperature Liquid Naphthalene Media	26
2.1	Introduction	27
2.2	Electrochemical Techniques	27
2.3	Electrochemistry in Non-Aqueous Solvents	31
2.4	The Use of Naphthalene Solvents in Voltammetric Studies	37
2.5	Determination of Solution Resistance	47
2.6	Experimental Methods	48

Chapter 3 Stepwise Reduction Potentials of Phthalocyanines in Strictly Non-Coordinating Media 53

3.1 Introduction 54

3.2 Results 58

3.3 Discussion 73

(i) Nomenclature 73

(ii) Assignment of Reduction Site 79

(iii) Comparison with Literature Data 83

3.4 Electrochemistry of Phthalocyanines at Ambient Temperature 91

3.5 Characterisation of Silver and Molybdenum Phthalocyanines 93

Chapter 4 Direct Comparison of Phthalocyanine and Porphyrin Cathodic Behaviour 99

4.1 Introduction 100

4.2 Results 100

4.3 Disucssion 108

4.4 Comparative Redox Behaviour of Phthalocyanines and Porphyrins 114

4.5 Solvent Coordination and its Effect on Redox Behaviour 122

4.6 The Relationship between Macrocycle Structure and Electron Affinity 132

Chapter 5 Reduction Potential/Electronegativity Correlations for Metallophthalocyanines and Metalloporphyrins 137

Chapter 6	The Anodic Behaviour of Porphyrins and Phthalocyanines	152
6.1	Introduction	153
6.2	Porphyrin Oxidations at Elevated Temperatures	154
6.3	Oxidations of Phthalocyanines	160
Chapter 7	Bonellin Dimethyl Ester	175
7.1	Introduction	176
7.2	Results	177
7.3	Experimental	184
Chapter 8	Synthetic Procedures	185
8.1	Introduction	186
8.2	Synthesis of Porphyrins	189
8.3	Synthesis of Phthalocyanines	189
8.4	Synthesis of Zinc Tetrabenzoporphin	207
8.5	Experimental Procedure	208
References		222

List of Figures

Chapter 1

1.1 Typical Porphyrin Structure 2

1.2 Phthalocyanine Structure 3

1.3 Porphin Ring 4

1.4 Protohaem 5

1.5 Porphin Delocalisation 6

1.6 Phthalocyanine Delocalisation 6

1.7 Chlorophyll a 11

1.8 Corrin Ring 12

1.9 Historical Survey 15

1.10 Zinc Tetrabenzoporphin 17

1.11 Magnesium Octaphenyl tetra-aza-porphin 17

1.12 Reduction of Porphins 18

1.13 Copper Tetrasulphonato phthalocyanine 22

Chapter 2

2.1 Voltammetric Wave-Forms 28

2.2 Voltammetry of Ferrocene in MeN 41

2.3 Ferrocene - A.C. Frequency Dependence 42

2.4 Cyclic Voltammogram of Ferrocene 43

2.5 Ferrocene - C.V. Scan Rate Dependence 44

2.6 Ferrocene - Reversibility Test 46

2.7 Variation of $E_{\frac{1}{2}}$ with i in uncompensated solution. $Fe(cp)_2/CH_2Cl_2$ 49

2.8 Variation of $E_{\frac{1}{2}}$ with i in uncompensated solution. $Fe(cp)_2$/MeN 50

Chapter 3

3.1	Trends in Phthalocyanine Reduction Potential	55
3.2	Copper Tetra(4-t-butyl)phthalocyanine	57
3.3	Voltammetry of [H_2Pc]	59
3.4	Voltammetry of [ZnPc]	60
3.5	Typical "mix" experiment	62
3.6	(a) Polarogram of [PtPc]	65
	(b) A.C. Frequency Dependence [PtPc]	66
3.7	(a) Cyclic Voltammogram of [V(O)Pc]	67
	(b) C.V. Scan Rate Dependence [V(O)Pc]	68
3.8	A.C. Polarogram of [Ag(H)Pc]	70
3.9	A.C. Frequency Dependence [Ag(H)Pc]	71
3.10	Voltammetry of [H_2Bu_4Pc]	74
3.11	Voltammetry of [$CuBu_4Pc$]	75
3.12	A.C. Frequency Dependence [$ZnBu_4Pc$]	76
3.13	Cyclic Voltammogram of [$Ti(O)Bu_4Pc$]	77
3.14	C.V. Scan Rate Dependence [$Ti(O)Bu_4Pc$]	78
3.15	Comparisons of Phthalocyanine Reduction Potential	85
3.16	Trends in Phthalocyanine 2nd Reduction Potential	86
3.17	Phthalocyanine Reduction Potentials	90
3.18	Phthalocyanine Visible Spectra	95
3.19	Infra-Red Spectra of Phthalocyanines	98

Chapter 4

4.1	A.C. Polarogram of [CuTPP]	101
4.2	Cyclic Voltammogram of [Fe(Cl)OEP]	106
4.3	Trends in Porphyrin Reduction Potential	109
4.4	[MTPP] Reduction Potentials	111
4.5	[MOEP] Reduction Potentials	113
4.6	Relative Trends in Reduction Potential	115
4.7	Trends in Reduction Potential	117
4.8	Trends in [MOEP] Reduction Potential	125
4.9	A.C. Polarogram	126
4.10	Variation of Reduction Potential with Solvent	130
4.11	Tetrabenzoporphyrin	132
4.12	Tetra-aza-porphyrin	132
4.13	Observed Reduction Potential	134
4.14	Calculated Differencies in LUMO Energy	135

Chapter 5

5.1	Variation of [MOEP] Reduction Potential with Allred-Rochow Electronegativity	142
5.2	Variation of [MOEP] Reduction Potential with Pauling Electronegativity	143
5.3	Variation of [MPc] Reduction Potential with Allred-Rochow Electronegativity	145
5.4	Variation of [MPc] Reduction Potential with Pauling Electronegativity	146
5.5	Variation of [MPc] Reduction Potential with Work Function	149

Chapter 6

6.1	Voltammetry of [ZnTPP]	156
6.2	A.C. Polarogram of [Mo(O)Pc]	161
6.3	A.C. Polarogram of [$ZnBu_4Pc$]	162
6.4	Voltammetry of [CoTPP]	166
6.5	Voltammetry of [$CuBu_4Pc$]	167
6.6	Cyclic Voltammogram of [H_2Bu_4Pc]	169
6.7	Cyclic Voltammogram of [$CuBu_4Pc$]	170
6.8	Cyclic Voltammogram of [$NiBu_4Pc$]	171
6.9	Voltammetry of [$Ti(O)Bu_4Pc$]	172

Chapter 7

7.1	Bonellin Structure	176
7.2	Cyclic Voltammogram of [H_2BDME]	178
7.3	A.C. Polarogram of [H_2BDME]	181

Chapter 8

8.1	Cyclisation of Phthalocyanine	188
8.2	Synthetic Routes to [MBu_4Pc]	191

List of Tables

Chapter 2

2.1	Reversibility Criteria	32
2.2	Dielectric Constants for Selected Solvents	35
2.3	Physical Properties of 1-methyl naphthalene and its Electrolyte Solution	40

Chapter 3

3.1	Reduction Potentials of Metallophthalocyanines	63
3.2	Electrochemical Reversibility Criteria at 150°C	64
3.3	Reduction Potentials of [MBu_4Pc]	72
3.4	Reduction Potentials of [MBu_4Pc] at 25°C	92

Chapter 4

4.1	Reduction Potentials of [MTPP]	102
4.2	Reduction Potentials of [MOEP]	104
4.3	Reduction Potentials of [MOEP] in Selected Solvents	124

Chapter 6

6.1	Redox Potentials of Porphyrins at Elevated Temperatures	157
6.2	[MOEP] Redox Potential Separations	157
6.3	Oxidation Potentials of Phthalocyanines	163

Chapter 7

7.1	Redox Potentials of [H_2BDME]	180

Chapter 8

8.1	Infra-Red Spectra of [MBu_4Pc]	203
8.2	Visible Spectra of [MBu_4Pc]	205

Infra-Red Spectra

A	1-t-butyl-3,4-dimethyl-benzene (neat liquid)	209
B	4-t-butyl phthalic anhydride (KBr Disc)	210
C	4-t-butyl phthalic acid (KBr Disc)	211
D	4-t-butyl phthalimide (KBr Disc)	212
E	4-t-butylphthalamide (KBr Disc)	213
F	4-t-butyl phthalonitrile (KBr Disc)	214
G	Copper Phthalocyanine [CuPc] (KBr Disc)	215
H	Phthalocyanine [H_2Pc] (KBr Disc)	216
J	Tetra(4-t-butyl)phthalocyanine [H_2Bu_4Pc] (KBr Disc)	217
K	Copper tetra(4-t-butyl)phthalocyanine [$CuBu_4Pc$] (KBr Disc)	218
L	Zinc tetra(4-t-butyl)phthalocyanine [$ZnBu_4Pc$] (KBr Disc)	219
M	Titanyl tetra(4-t-butyl)phthalocyanine [$Ti(O)Bu_4Pc$] (KBr Disc)	220
N	Zinc tetrabenzoporphin [ZnTBP] (KBr Disc)	221

CHAPTER 1

Aspects of Phthalocyanine and Porphyrin Chemistry

1.1 Introduction

The porphyrins (Figure 1) represent a class of fundamentally important biologically active compounds. They are widespread in nature, being found in both plant and animal kingdoms in species from the blue-green algae tc Man. They have a variety of biochemical roles, all of which appear to depend on their redox behaviour. A knowledge of the redox properties of these species is therefore of great importance in understanding their natural function.

Figure1.1 Typical Porphyrin Structure

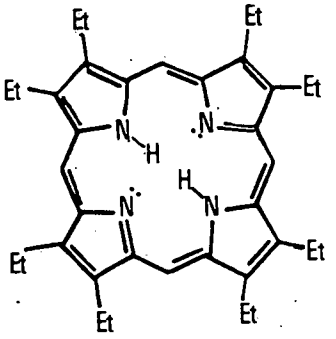

Octaethylporphyrin

[H_2OEP]

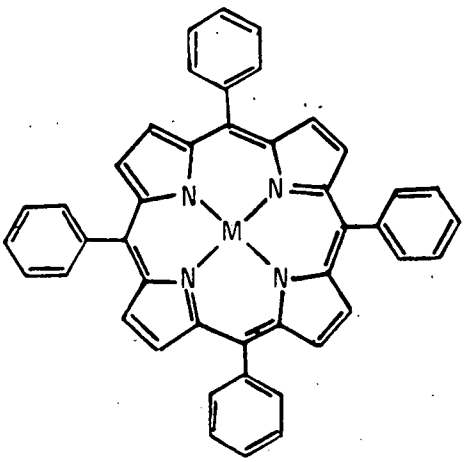

Metallo tetraphenylporphyrin

[M = Co, Ni, Cu, Zn]

In recent years extensive investigation of the redox chemistry of porphyrins has been carried out, particularly by the techniques of electrochemistry as will be outlined later.

Paralleling this work there have been a number of studies on porphyrin analogues. This interest is twofold; firstly such compounds may provide useful models of porphyrin activity and therefore aid in elucidating the mechanisms of biological processes. Secondly, the physical properties of such macrocycles mean that they could be of great practical value whereas the porphyrins are themselves generally unsuited to commercial processes, being uneconomic to prepare or isolate in quantity. Among such porphyrin analogues, the most intensely studied and most closely related structurally are the Phthalocyanines (Figure1.2), which are tetra-azaporphyrins. These synthetic macrocyclic compounds are used primarily as pigments. Industrial manufacture began in the 1930's and now stands at several thousands of tonnes per annum.

Figure1.2 Phthalocyanine Structure

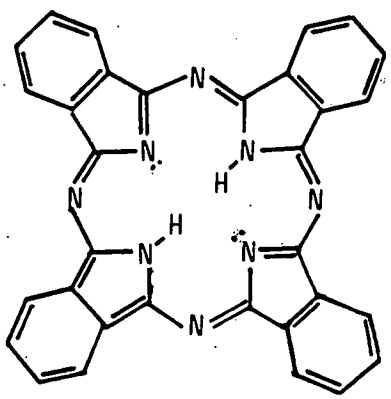

Phthalocyanine

[H_2Pc]

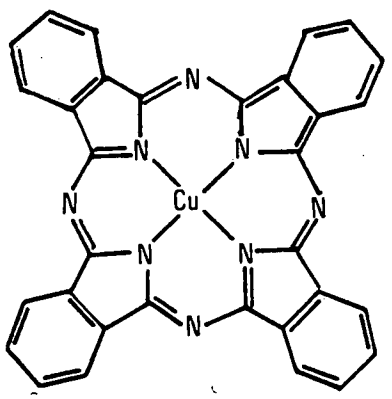

Copper Phthalocyanine

[CuPc]

The electrochemical behaviour of various metallo-phthalocyanines has been studied previously, but only to a limited extent and with conflicting results due mainly to the insolubility of these compounds, a factor which is intrinsic to their performance as colour-fast pigments. This Thesis reports the genuine redox chemistry of phthalocyanines in true solution using novel electrochemical methods, and discusses the relationships thus revealed between the redox characteristics of phthalocyanines and porphyrins.

1.2 Porphyrin and Phthalocyanine Structures

The central structural unit of the porphyrins is the porphin ring (Figure1.3) from which all porphyrins are formally derived by substitution of some or all the peripheral positions.

Figure1.3 Porphin Ring

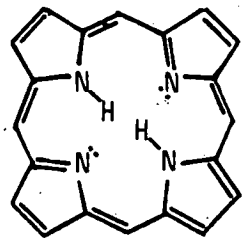

Although certain naturally occurring porphyrins had been discovered during the nineteenth century, it was not until 1912 that Kuster[1] suggested the compounds were tetrapyrroles linked by methine bridges. Final confirmation

of this proposal was provided by the total synthesis of Protohaem (Figure I.4) by Fischer[2] in 1929.

Figure I.4 Protohaem.

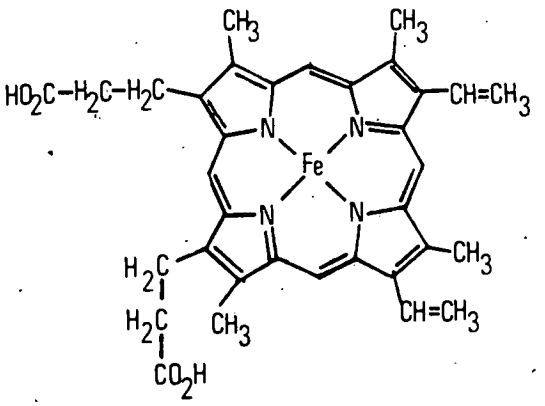

The Phthalocyanines are apparently wholly synthetic in origin. They were discovered by accident at the Grangemouth Works of Scottish Dyes Ltd. (now I.C.I. Organics Division) in 1928 when a dark blue insoluble material was observed during the production of phthalimide from phthalic anhydride and urea. The compound, later shown to be ferrous phthalocyanine, was formed as a result of a flaw in the glass lining of the reaction vessel which allowed the hot phthalimide to come into contact with the iron container.

It is likely that phthalocyanines had been observed but not identified previously by other workers. For example in 1927 de Diesbach and van der Weid[3] reported the formation of a highly insoluble blue product in the reaction of o-dibromobenzene, cuprous cyanide and pyridine. They assigned this to a phthalonitrile/pyridine complex of copper although it was almost certainly copper phthalocyanine.

The tetrapyrrolic macrocyclic structure of phthalocyanine was established by Linstead and co-workers in a series of classic studies[4-8] and is shown in Figure I.2.

Unlike porphin, the pyrrole rings of phthalocyanine are linked by nitrogen atoms (aza bridges), which are isoelectronic with the CH bridge. Additionally, phthalocyanine has a benzenoid ring fused to each pyrrole ring and therefore phthalocyanine might be given the alternative nomenclature of tetra-aza-tetrabenzoporphin.

Both macrocycles are highly conjugated and it is possible to devise a number of resonance forms for each. The conjugation system of the Porphin ring has 22 π-electrons but only 18 of these can be included in any delocalisation pathway (Figure I.5). Phthalocyanine possesses 38 π-electrons with a delocalisation train of 26 electrons being possible (Figure I.6).

Figure I.5 Porphin Delocalisation

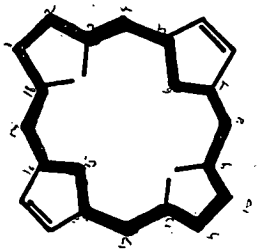

Figure I.6 Phthalocyanine Delocalisation

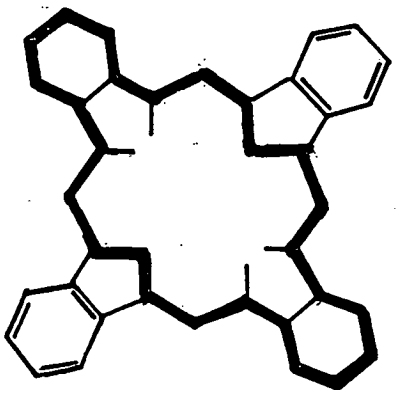

Each macrocycle therefore conforms to the Hückel $(4n + 2)\pi$-electron rule for aromaticity (n = 4 for Porphin, n = 6 for Phthalocyanine) and the compounds exhibit many of the features expected for extended aromatic systems. In particular they are highly coloured, with principal π-π^* absorption bands having very high extinction coefficients. Porphyrins are generally red with a highly characteristic absorption band known as the Soret band[9] at approximately 400 nm with typical molar extinction coefficients of 4×10^5, however the intensely green phthalocyanines (the blue colour is pigmentary in origin) have primary absorption in the visible region at approximately 660-700 nm with extinction coefficients of about 2×10^5.

Commercial exploitation is based on the high chemical stability of these compounds. The copper complex can be sublimed at atmospheric pressure at 580°C, and is stable under vacuum to 900°C [10]. Metallophthalocyanines are generally stable to light, resistant to attack by acid and base, and insoluble in the majority of common organic solvents. The best solvents are substituted benzenes and naphthalenes but, even here, maximum solubility is of the order of 10^{-6} Molar. However phthalocyanines dissolve freely in concentrated sulphuric acid where the blue colour is replaced by a straw-brown solution. This exceptional solubility is attributed to protonation of the aza bridges and provides a useful method for the purification of Phthalocyanines, which are easily regenerated on dilution.

Industrial production is primarily of the copper compound under the trade name Monastral Blue and of greener shades which are produced by peripheral chlorination of the fused benzene rings up to the exhaustively substituted 16-chloro derivative.

Both porphyrins and phthalocyanines having such highly conjugated aromatic systems might be expected to be strictly planar, as is largely confirmed by X-ray crystallography.

In a series of papers[11-14] Robertson showed that the phthalocyanine molecule was planar and, within the limits of the experiment, square. He also showed that in the nickel and copper compounds the metal was in a square planar environment. Longer range interactions were observed between molecules in the crystal structure with bridging nitrogens of neighbouring molecules positioned above and below each metal ion, requiring the molecules to adopt a staggered configuration with respect to each other.

A number of further X-ray studies have been carried out on porphyrins since the mid 1960's. Examination of porphin itself[15] shows the molecule to be planar to within ±0.02 Å while a study of metal free octaethylporphyrin[16] indicates a deviation from planarity of ±0.05 Å. The Porphyrin macrocycle seems more flexible than Phthalocyanine. For example, different crystalline forms of [NiOEP] can be obtained. In the tetragonal form[17] the nickel atom and coordinating nitrogens form a square plane and the pyrrole rings are inclined by 14° from this plane. This "ruffled"

form of the compound has S_4 symmetry, the angle between adjacent rings being 28°. In contrast in the triclinic form[18] the pyrrole ring deviate from true planarity by less than 2°.

It has been noted that metallo-porphyrins and metallo-phthalocyanines will accept axial ligands, even in cases where d-orbital ligand stabilisation effects are not operative, e.g. in a zinc porphyrin mono-pyridinate[19] the zinc adopts a square pyramidal environment, the fifth coordination site being occupied by pyridine.

1.3 Chemistry of Metalloporphyrins and Metallophthalocyanines

Many parallels exist in the chemistry of porphyrins and phthalocyanines and many of the biological functions of porphyrins can be mimicked by phthalocyanines.

All biologically-active porphyrins are metallated; a variety of metals are utilized, the most abundant being the iron porphyrins or haems. These are active in various processes, including the vital functions of direct electron-transfer and oxygen-transport.

In higher animals oxygen transport is carried out by two haem proteins; tetrameric haemoglobin, the oxygen carrier in blood, and myoglobin, responsible for oxygen transport and storage within muscle tissue[20]. Dioxygen binding occurs at the iron atom, the protein chain providing a controlled environment for the haem group[20]. If removed from the globin, the haem group loses its ability to bind dioxygen

reversibly and in an aqueous environment is irreversibly oxidised forming Fe(III) hydroxy species.

Similar activity is seen in phthalocyanine chemistry. Cobalt phthalocyanine will bind dioxygen at low temperature[32,33] although the complex may have the formulation $[(Co^{III}Pc)^{+}O_2^{-}]$. Remarkably, insertion of either iron- or cobalt-phthalocyanines into a globin is possible, producing a phthalocyanine-globin; which can bind dioxygen reversibly at ambient temperatures[34].

Manganese phthalocyanine offers one of the earliest examples of phthalocyanine-oxygen interaction. Reaction with dioxygen gave a μ-oxo bridged dimer, one of the predicted intermediates in this process being the adduct $MnPc(O_2)$[28]. This was later detected by Uchida[29] and fully characterised by Lever, Wilshire and Quan[30,31]. In dry solvents (particularly dimethyl acetamide) this adduct is the final product; it can be isolated and, like simple manganese porphyrins[26,27], the dioxygen binding is fully reversible. It is interesting to note that manganese phthalocyanine has a greater affinity for dioxygen than iron porphyrins[30,35].

In contrast to the oxygen carriers, other haems called oxygenases activate dioxygen towards chemical reaction. These enzymes can transfer either both oxygen atoms of coordinated O_2 to the substrate, as in the case of tryptophan oxygenase[21], or only one, as is found in the mono-oxygenases or hydroxylases[21,22].

The electroreduction of dioxygen to water mediated by cobalt phthalocyanine was first observed by Jasinski in 1964, and the cobalt, iron and manganese systems have been intensively investigated by a number of workers[37-42] with particular reference to applications in fuel cell technology.

The cleavage of dioxygen by manganese phthalocyanine is of interest in elucidating the mechanism of photosynthesis. The final stage of the biological process is the production of water from dioxygen and it is believed that this is achieved by an as yet unidentified manganese complex. Recently[23-25] it has been proposed a manganese porphyrin would be capable of performing this function, having both dioxygen-binding capability[26,27] and a series of available oxidation states for the storage of the four electrons necessary for the production of water from oxygen.

Photosynthesis is, in any event, ultimately dependent on the magnesium pigments known as Chlorophylls; the structure of a typical chlorophyll being shown in Figure 1.7.

Figure 1.7 Chlorophyll a

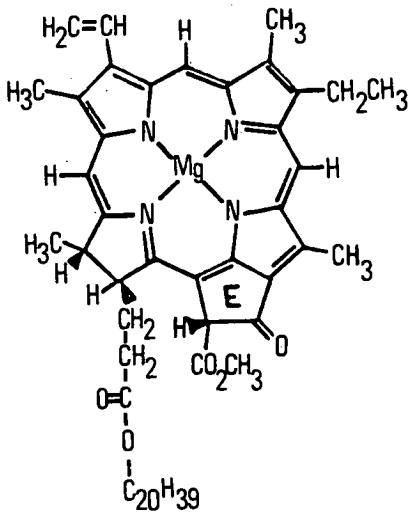

These complexes are examples of the chlorin ring system in which one double bond has been "saturated" as indicated in Figure 1.7 (c.f. Figure 1.1). As a class Chlorophylls also have a fifth ring, labelled E in Figure 1.7, fused to the macrocycle. The pigments in varying states of aggregation are responsible for the collection of light photons and for the relay and storage of this energy until conversion into useful chemical work. The intense optical absorption of phthalocyanines has already been noted. Their photoconductivity was first observed in 1948 by Putseiko[43] and they have been investigated extensively[44-48] both as models for understanding the photochemistry of Chlorophyll[45,49], and as useful solar energy converters in their own right[93,94,95].

The ubiquitous requirement for cobalt in living organisms is known. This essential element is primarily found in the corrin ring of vitamin B_{12} (Figure 1.8) and closely related molecules. The most important of the many roles of B_{12} is the transfer of hydride or C_1 groups, and rests fundamentally on Co(III)/Co(I) transformations.

Figure 1.8 The Corrin Ring

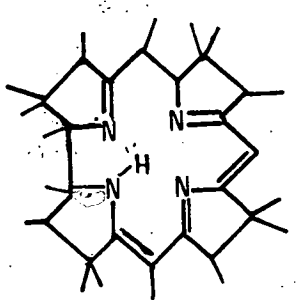

Similar tranformations are observed in cobalt phthalocyanine chemistry and the reaction of cobalt(I) phthalocyanine with alkyl halides has been used extensively by Ugi and co-workers[51-55] in the cleavage of protecting groups in peptide synthesis. As in B_{12} the chemistry is dependent upon the ability for linked valency/coordination-number changes. The excellent nucleophilic properties of such square planar cobalt complexes has led to their description as "supernucleophiles".

A further vital role of iron porphyrins not discussed above is the function of the cytochromes in the electron transport chain, for example in the final stages of the catabolism of carbohydrates to produce chemical energy. The members of the chain constitute a series of redox couples. Electrons (made available from previous stages of carbohydrate degradation) pass from one member to the next at ever-decreasing potential, and the free energy released is converted to useful chemical energy.

The catalytic properties of phthalocyanines have been under investigation ever since their discovery[56] and have been reviewed in depth[44,57]. They have been shown to catalyse hydrogen peroxide decomposition[56], the oxidation of various organic molecules such as phenol[58] and cumene[59], and many other processes.

Throughout this discussion both phthalocyanine and porphyrin complexes have been seen to function because of (or in some cases in spite of) their redox capability. Hence an understanding of the redox chemistry of these systems is vital in appreciating how they function, and the development of our existing knowledge of these complexes is reviewed below.

1.4 Redox Chemistry of Phthalocyanine and Porphyrin Complexes

In these systems, two distinct sites of redox activity are available. Oxidation or reduction at the metal centre may occur, as exemplified by the transition metals iron, cobalt or manganese. Alternatively, the macrocycle itself may undergo changes of oxidation state. The macrocycle π-system acts as a "reservoir" to which electrons can be added or removed. Naturally, in the free bases, only macrocycle-based electron-transfer can occur and the redox chemistry of these molecules provides a useful reference point from which metal complex behaviour can be assessed.

It is now appreciated that under favourable conditions tetrapyrrolic macrocycles, whether metallated or not, can undergo up to four one-electron reductions steps and two one-electron oxidations.

This represents the culmination of extensive and intensive study spanning the last forty years as outlined in Figure1.9.

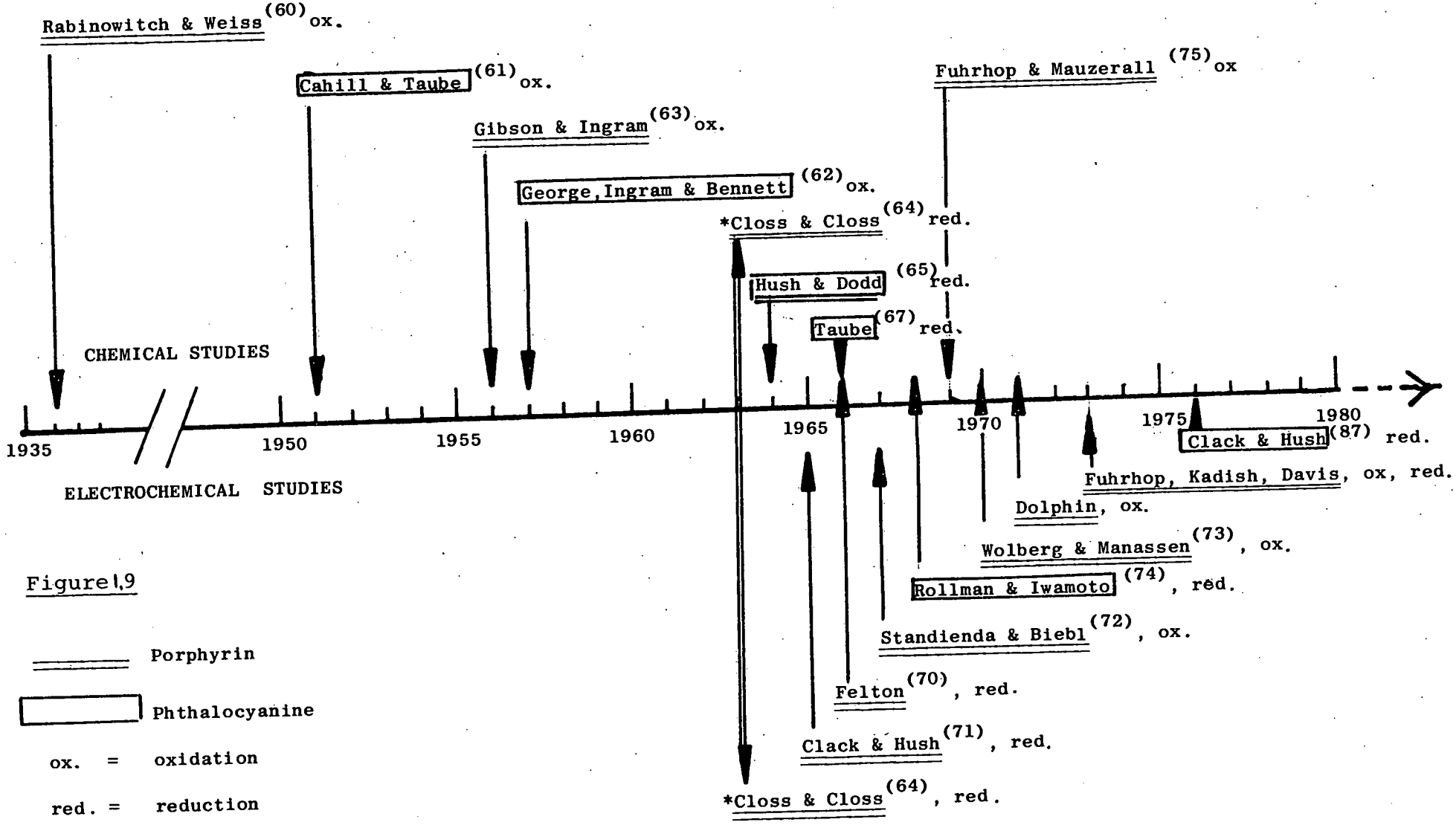

Figure 1.9

Porphyrin

Phthalocyanine

ox. = oxidation

red. = reduction

In 1937, the treatment of chlorophyll a with ferric chloride, by Rabinowitch and Weiss[60] produced a species which, although not fully characterised, was probably the π-cation radical of chlorophyll a. Considerably later cerium(IV) oxidations of Phthalocyanine[61,62] and Porphyrin derivatives were studied and the resulting species characterised in solution by e.s.r. spectroscopy.

In 1963 Closs and Closs[64] prepared the π-monoanion and π-dianion of zinc tetraphenylporphin. These species were isolated as salts and were the first fully characterised examples of porphyrin systems driven to unfamiliar oxidation states. Selective use of various reducing agents allowed approximate estimation of the reduction potentials necessary for the production of the reduced species, and Closs and Closs found these values were consistent with polarographic measurements which indicated successive one-electron reduction potentials of -1.30, -1.75 (and -2.43 V) vs S.C.E. This pioneering study is of considerable significance. It was the first demonstration of the reduction of these macrocycles to anionic rather than hydrogenated states. The successful use of polarography gave results directly corresponding to previous observations and therefore suggested a general means to evaluate the redox activity of these compounds precisely and conveniently without the need for bulk chemical methods. As will become clear later, the pattern of electrode potential values can itself yield information on the nature of the redox process.

Hush and coworkers soon demonstrated that the reduction phenomena observed by Closs and Closs were not unique to Zinc TPP by studying an assortment of macrocycles, initially by chemical and spectroscopic studies[65], and later by polarographic methods[66]. Free base porphin, tetrabenzoporphin (Figure 1.10) and octaphenyltetraazaporphin (Figure 1.11) or their metallated (Mg, Zn) complexes were examined in DMF solution. The low solubility of phthalocyanine compounds meant that electrochemical methods were <u>not</u> applied to them,[66] although anionic CuPc species had been obtained chemically and their absorption spectra presented[65].

Figure 1.10

Zinc Tetrabenzoporphin

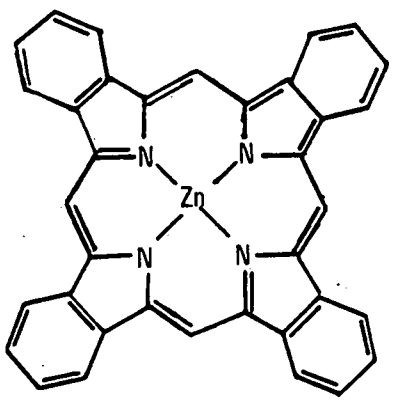

Figure 1.11

Magnesium octaphenyltetra-azaporphin

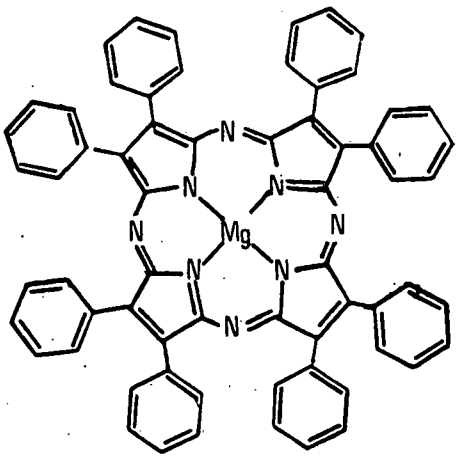

A consistent pattern emerged with each compound undergoing three or four one-electron reductions. While the absolute position of first reduction potential varied widely, the difference between first and second reductions was effectively constant at 0.42 V over all the compounds studied. Similarly characteristic E^{o} separations were seen between second and third (0.7V) and third and fourth (0.26V) steps. This reactivity pattern was recognised to be consistent with the stepwise filling of a degenerate e_g pair of lowest unoccupied macrocycle molecular orbitals (Figure 1.12), the separation between successive reduction potentials being a reflection of the electron repulsion and spin-exchange energies encountered on each reduction step.

Figure 1.12 Reduction of Porphins

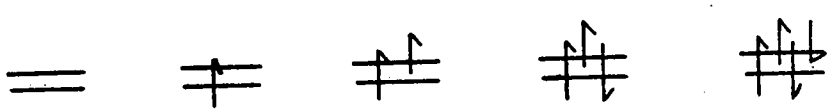

Later, theoretical work by Zerner and Gouterman[68] confirmed the assignment of the lowest vacant π^{*} orbital as an e_g pair.

Independently of Hush's work, R. Taube prepared and characterised reduced phthalocyanines species by the action of lithium in tetrahydrofuran solution. Successive species up to $[MPc]^{4-}$ ($[MPc]^{5-}$ for reducible metals) could be isolated as crystalline T.H.F.-solvated salts of formula $Li_n^{+}[MPc]^{n-}$,

stable in the absence of oxygen or moisture.

$$MPc \xrightarrow[THF]{Li} [MPc]^{-} \longrightarrow [MPc]^{2-} \longrightarrow [\ ]^{3-} \longrightarrow [\ ]^{4-} \longrightarrow ([MPc]^{5-})$$

The first systematic investigation of the effect of the coordinated metal on the reduction properties of porphyrins is due to Felton[76,71]. Polarography of metallotetraphenylporphins (MTPP, M = Co, Ni, Cu, Zn) in DMSO solution generally revealed two one-electron reductions. The electrogenerated monoanions were characterised by spectroscopic methods. While most compounds showed behaviour similar to that observed by Clack and Hush, indicating ligand-based reductions, the much larger gap of 1.05 V between the two reductions of CoTPP was seen to indicate a different process. It is now accepted that the first reduction involves the Co^{II}/Co^{I} couple.

Felton envisaged a correlation between reduction potential and metal electronegativity, the more electronegative the metal the less negative the ligand reduction potential[70], due to partial withdrawal of charge by the metal ion.

The tetraphenylporphins were also the subject of the first voltammetric study of the oxidative properties of porphyrins. Stanienda and Biebl[72] observed two oxidations of metallo-tetraphenylporphins, etioporphyrins and haematoporphyrins (M = H_2, Co, Ni, Cu, Zn) in butyronitrile solution. Correlations of oxidation potentials with metal ionisation energy, metal ion radius or absorption maxima in the visible region were all considered.

Characterisation of the oxidised [MTPP] species by e.s.r., magnetic susceptibility and visible spectroscopic methods was undertaken by Wolberg and Manassen[73].

The metallooctaethylporphyrins [MOEP] were first investigated by Fuhrhop and Mauzerall utilizing classical potentiometry. The one-electron oxidation products of the zinc, copper, nickel and palladium complexes were characterised by spectroscopic methods as ligand π-cation radicals. In contrast Dolphin and co-workers[76] found that stepwise oxidation in [CoOEP] gave $[Co(III)OEP^{+}]^{2+}$; metal oxidation intervening before macrocycle oxidation.

The most comprehensive study of octa-ethylporphyrins to date is that of Fuhrhop, Kadish and Davis[77]. Oxidation and reduction steps, in butyronitrile and D.M.S.O. solution respectively, were detected voltammetrically for a range of 25 metallo-octaethylporphyrins. In the case of redox-inert metal ions, where only ligand redox activity is seen, an almost constant separation between first oxidation and first reduction was observed. This was taken as a measure of the gap between highest occupied and lowest unoccupied molecular orbitals. The value of 2.25 ± 0.15 V is consistent with the separation previously estimated by Zerner and Gouterman[68] in their theoretical work on the electronic structure of porphins, and is a good match with the observed $\pi \rightarrow \pi^*$ optical transition energy of 16000 cm^{-1} (2.0 eV). Fuhrhop et al demonstrated the variation of ligand oxidation and reduction potential with metal electronegativity for a limited set of divalent metals for which suitable electro-negativity values could be found. The authors went on to

define a new "metal induction parameter", evaluated from E° data so that all compounds necessarily fell on a linear E°/induction parameter plot, and such correlations are now widely accepted in porphyrin and phthalocyanine chemistry. Departures from the 2.25 V gap between E_{ox} and E_{red} were used to identify intervening metal-based redox processes.

Investigations of the porphyrin complexes of the redox active metals have been numerous. Particular significance has been attached to the iron porphyrins. Davis and Orleron,[78,83] Lexa and co-workers[79a,b] and Kadish and co-workers[80a→e] have all observed the Fe(III)/(II) couple in various iron porphyrins, and detailed discussions of solvent, axial ligation and macrocyclic substitution effects on the metal redox activity have been presented. Similar effects have been discussed in relation to cobalt porphyrins[81,82] and manganese complexes[84,85]. These aspects along with investigations of the redox behaviour of natural porphyrin derivatives and the influence of protic "biologically relevant" solvents, has recently been reviewed in some detail[86]. The influence of solvent polarity and donor ability on metalloporphyrins and related complexes is explored in some depth in this thesis.

In contrast to the intensive and apparently comprehensive study of the redox chemistry of porphyrins, studies of the solution redox chemistry of phthalocyanines have been only rarely reported.

Insolubility of phthalocyanine had prevented polarographic study by Clack and Hush[66]; in 1968 Rollman and Iwamoto[74] reported circumvention of this by the use of the tetrasulphonato-phthalocyanines (Figure 1.13) which are more readily soluble in conventional media.

Figure 1.13 Copper tetrasulphonato-phthalocyanine tetra sodium salt

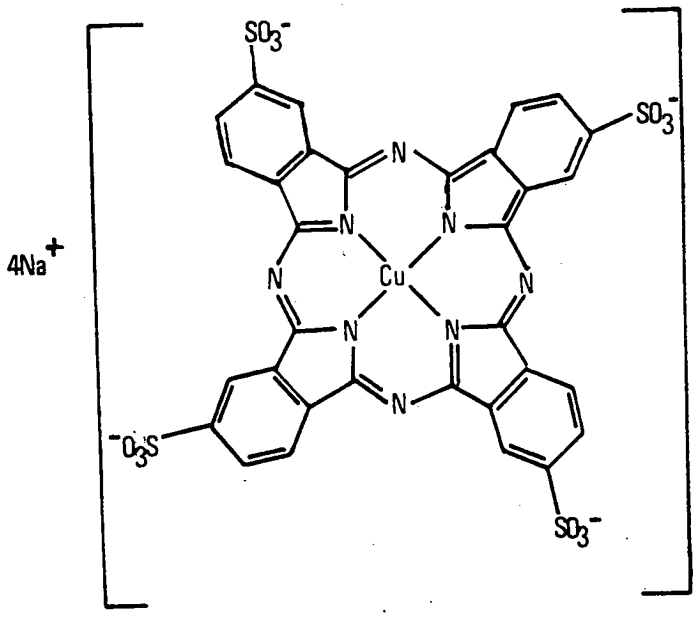

Two or three reductions were seen in DMSO solution for the cobalt, nickel, copper and free base (H_2) derivatives and esr and visible spectroscopic data for the mono- and di-anions were obtained.

After a gap of some years, Clack, Hush and Woolsey reported their polarographic investigation of the unsubstituted complexes in DMF solution. These were examined as the soluble $Li^+[MPc]^-$ salts (M = H_2, Mn, Fe, Co, Ni, Cu, Zn, Mg), obtained by generating the mono-anion by lithium reduction. Four waves were generally observed,

the first being associated with the oxidative generation of $[MPc]^{o}$ (which should be immaterial to the measurement of the reversible electrode potential for $[MPc]+e \rightleftharpoons [MPc]^{-}$ and the others represent the reduction of $[MPc]^{-}$ to $[MPc]^{4-}$. Thus the stepwise formal reduction potentials for a series of phthalocyamine complexes were presented. Disappointingly, however, these results did not parallel those obtained earlier by Rollman and Iwamoto[74]. The relative order of first reduction potentials obtained by Hush and Clack was different from that of Rollman and Iwamoto, as was the gap between first and second reductions, and furthermore no convincing correlation could be drawn between these latest results and the earlier electrochemical studies on porphyrin reductions by Hush himself and others.

The oxidative behaviour of phthalocyanines has been even less well documented. Rollman and Iwamoto[74] briefly reported degradation of the tetrasulphonato compounds on oxidation, and recently (while this work was in progress) studies in the Soviet Union on the oxidation of tetraalkyl-phthalocyanines[90,91] have indicated completely anomalous voltammetric responses for many of the compounds despite potentiometric evidence for discrete one-electron oxidation. The apparently well-ordered oxidative behaviour of phthalocyanines in chloronaphthalene at room temperature mentioned in passing by Wolberg and Manassen[73] is quite incapable of experimental verification for reasons which will become apparent later in this thesis.

Chemical oxidation of phthalocyanines with $SOBr_2$ and $SOCl_2$ [92] leads to oxidative addition, forming products such as $[BrMn^{III}Pc]$. The earlier work on the generation of $[MPc^+]$ cations[61,62] has not generally been pursued, and as has been mentioned results obtained in later voltammetric studies of soluble derivatives are not informative for reasons still to be explained.

Phthalocyanines are however sufficiently soluble for electrochemical measurementsin pyridine, and Lever and Wilshire[88,89] have demonstrated the strong influence of the coordinating medium on both the anodic and cathodic behaviour of [MPc](M = Mn, Fe, Co). The differing central ion coordination number and spin states exhibited by the various metal ionsin this medium preclude systematic comparisons with other data (or even within the pyridine study).

The aim of this work therefore has been to study the electrochemistry of metal phthalocyanines in true solution in non-coordinating media. This has meant the development of novel high-temperature electrochemical methods using low dielectric constant solvents such as 1-methylnaphthalene (this will be outlined in Chapter 2).

The redox characteristics of a series of unsubstituted metallophthalocyanines dissolved in hot (150°C) liquid naphthalenes are presented and, in order that absolute comparisons can be made, a series of porphyrin derivatives has been studied under identical conditions. The synthesis of

alkylated phthalocyanine derivatives soluble in more conventional media has been undertaken, and the consistency of the electrochemical behaviour at high and ambient temperature is established.

In order that the nature of the differences between phthalocyanines and porphyrins might be further elucidated, compounds of intermediate structure, tetrabenzoporphin and tetraazaporphins, have been prepared and studied, and the fundamental structural influence on the electron affinity of such macrocycles is discussed.

CHAPTER 2

Voltammetric Methods for High Temperature Liquid Naphthalene Media

2.1 Introduction

In this chapter a brief account of electrochemical methodology is presented. This is followed by a discussion on the use of non-aqueous solvents with particular reference to relevant physical properties of such solvents, and from this foundation, the principles underlying the novel experimental techniques evolved in this work are outlined.

2.2 Electrochemical Techniques

Modern electrochemical practices have as their origin the classical works of Heyrovsky performed in the nineteen-twenties. He developed the technique of direct current (d.c.) polarography whose central feature is the Dropping Mercury Electrode (d.m.e.)[98,99]. This electrode consists of a fine capillary through which mercury slowly issues dropwise into the test solution. The potential between this "working" electrode and a standard reference electrode is externally controlled and the resulting cell current response measured. Many other voltammetric techniques have evolved subsequently, including the use of stationary solid working electrodes (strictly polarography applies only to systems using the d.m.e.) and these have been extensively documented[99,100,101]. Of considerable importance amongst these techniques are the methods of cyclic voltammetry (c.v.) and alternating current (a.c.) voltammetry or polarography[100,102]. These methods, in conjunction with d.c. polarography, have been used throughout this work and are briefly described below.

Typical d.c. and a.c. polarograms and the cyclic voltammogram for a reversible one-electron process are shown in Figure 2.1.

Figure 2.1 * Voltammetric Wave-forms for one-Electron Transfer.

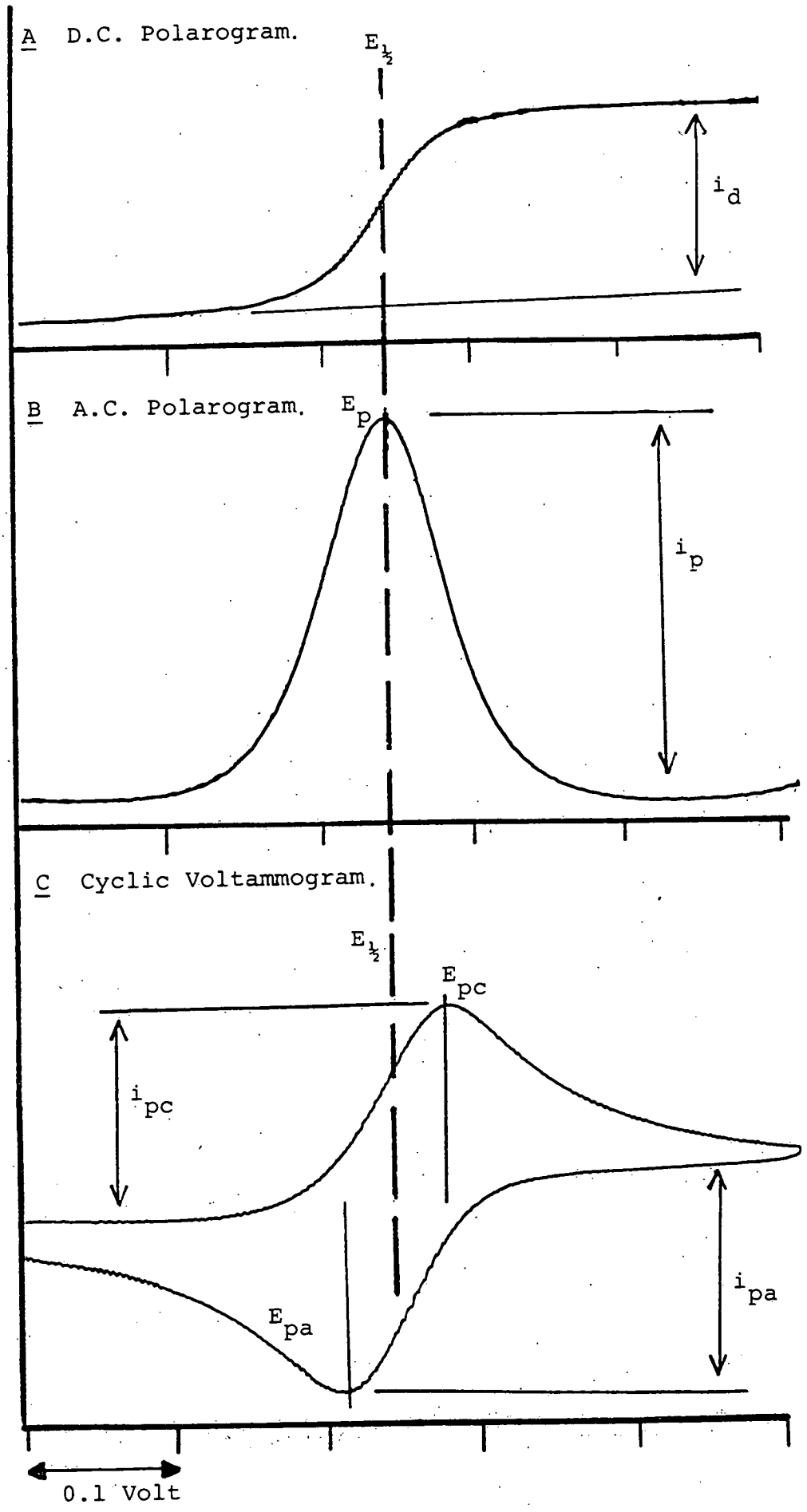

*Reproduced from actual recordings [H_2Bu_4Pc]

(i) d.c. polarogram

For the case of an ideally behaved one-electron process, Fig. 2.1(a) shows the classical Nernstian wave reflecting the direct-current response upon application of a linearly increasing potential. As the species under investigation undergoes electron-transfer, the current reaches a maximum plateau value, the diffusion current (i_d), determined by the rate of diffusion of substrate to the electrode surface and, given that rate of diffusion is a function of concentration, then i_d is ultimately dependent on concentration. For an ideal, reversible system, the midpoint potential of the wave (where $i=\frac{1}{2}\ i_d$), termed $E_{\frac{1}{2}}$, can be shown to equal the standard electrode potential E^o, as defined by the Nernst equation. The observed $E_{\frac{1}{2}}$-value is of course characteristic of each particular species. Hence both qualitative and quantitative measurements can be made using this technique. In the course of an experiment only minute quantities of substrate are electrolysed, the bulk being unreacted. This contrasts markedly with classical potentiometry where establishment of comparable concentrations of both members of the redox couple in homogeneous solution is necessary for determination of E^o.

(ii) a.c. polarography

Fig. 2.1(b) shows the a.c. polarogram corresponding to the d.c. polarogram of 2.1(a). In this technique, first developed in 1947,[103] a small sinusoidal alternating potential (typically 10 mV, 200 Hz) is superimposed on the d.c. potential. The alternating component of current is then monitored selectively as a function of the "d.c." linearly increasing potential, resulting in a symmetric peak form

superimposed on the d.c. wave. In the case of reversible electron transfer the potential E_p corresponding to maximum current coincides with $E_{\frac{1}{2}}$. This particular technique offers a number of advantages over conventional d.c. polarography. For example, the method provides phase-sensitive discrimination against the background charging current, arising from the non-informative capacitative element of the cell. Hence greater sensitivity is achieved (sample concentrations of 10^{-6} M can be used compared with 10^{-4} M for d.c. polarography). The method is very sensitive to deviations from full reversibility. (Reversibility may be assessed by certain critical features of the wave and these are discussed in full later in this section).

(iii) cyclic voltammetry[100,102]

As the name implies, the technique involves the application of a triangular potential ramp to the cell, that is the potential is scanned in a cyclic manner between initial and "switching" potentials spanning the region of interest and care is taken not to disturb the electrode/solution interface during this cycle. Stationary electrodes (platinum, gold, carbon or a static mercury drop) are used in quiescent solution and fast potential scanning rates are necessary to minimise the effects of diffusion and convection (typically 100 mV s^{-1} compared with 10 mV s^{-1} polarography). This results in a situation where the electrolysis proceeding at the electrode is reflected by depletion of substrate and generation of product in the immediately adjacent solution. Fig. 2.1(c) shows the typical cyclic voltammogram for a fully reversible one electron transfer. The potential midway

between the cathodic and anodic peak potentials (E_{pc} and E_{pa} respectively) is equal to $E_{\frac{1}{2}}$ as determined by d.c. polarography. The technique is particularly attractive since deviations from reversibility graphically alter the current response in a readily interpretable manner.

Reversibility Criteria

In the preceding discussion it has been assumed that the electrode reaction under investigation is reversible i.e. that electron transfer is rapid in either direction, and the species produced by electron transfer is stable so that no further chemical reaction occurs on the experimental time scale. If these conditions are not satisfied then the current responses will vary from those shown in Figure 1, and consideration of the voltammetric behaviour provides a means by which reversibility can be determined and departures from reversibility analysed. For a diffusion-controlled, fully reversible electron-transfer these various well-established criteria hold, as set out in Table 1.

It should be noted that the numerical values of some of these criteria are temperature-dependent and at temperatures well removed from ambient, as found in this work, different values are appropriate. Those modified values will be detailed later.

2.3 Electrochemistry in Non-Aqueous Solvents

While polarography was originally devoted to aqueous solvent systems, extension of these techniques to non-aqueous solvents is clearly desirable, particularly for investigation of organic and organometallic compounds, thus necessitating refinement of electrochemical technology.

Table 2.1 Reversibility Criteria

n = no. of electrons transferred. Other symbols defined in Fig. 1 and text.

d.c. Polarography

$E_{\frac{1}{2}}$ independent of concentration and t_d (drop time)

Plot of E vs. $\log[(i_d-i)/i]$ is linear with slope = (59/n) mV at 25°C.

a.c. Polarography

$E_p = E_{\frac{1}{2}}$ independent of concentration, t_d, ω (a.c. frequency)

Wave symmetric, width at half height = (90/n) mV at 25°C.

Plot of I_p vs. $\omega^{\frac{1}{2}}$ linear through the origin.

Cyclic Voltammetry

$E_{\frac{1}{2}} = \frac{1}{2}[E_{pc}+E_{pa}]$ independent of concentration and scan rate ν

$I_{pa} = I_{pc}$

$\Delta E_p = (59/n)$ mV

Plot of I_p vs. $\nu^{\frac{1}{2}}$ linear through the origin.

It is crucial that any electrochemical cell system has only modest internal resistance (R). As a current (i) flows in a cell then a dissipation of applied potential difference equal to iR, the so-called "ohmic loss" or "iR drop",[104-106] is encountered, and the effective potential (V_{eff}) between working electrode and solution is less than the applied potential (V_{appl}), i.e. $V_{eff} = V_{appl} - iR$. If a large resistance is present then a considerable attenuation of the voltammetric wave is seen and serious errors in measurement of electrode potential can occur; in the limit the wave becomes uncharacterisable or even undetectable.

Cell resistance is, of course, a function of both solution composition and electrode configuration. While only two electrodes, "reference" and "working", are essential in a primitive cell to provide a circuit through which a current can flow, most conventional reference electrodes are high-resistance components and not designed for the passage of current. Therefore it is now usual to employ an "auxiliary" or "counter" electrode and sophisticated circuitry such that current flows through working and counter electrodes only, and reference electrode polarisation is avoided. This three-electrode configuration and electronic potentiostat control system is well known[107-109] and is routinely used in modern electrochemistry.

Suitable electrochemical solvents must fulfil a number of constraints. Apart from dissolving the substrate and the carrier electrolyte (added to facilitate current transfer across the cell), and having a suitably wide potential "window" where it is redox-inactive, the solvent must support ion formation and conduct ionic currents. Both

these requirements can best be assessed by consideration of the appropriate dielectric constant (ε); and Table 2.2 lists ε values[110,111] for a range of selected solvents. The dielectric constant of a medium is a measure of its insulating properties and hence of its ability to promote dissociation into ions of electrolytes, the larger the value of ε, the larger the ionising effect. Accordingly, useful electrochemical solvents such as water and aqueous media have the largest dielectric constants while organic solvents commonly used in electrochemistry have ε greater than 30.

Solvents with dielectric constants less than 30 are rather non-polar and, particularly in solvents of ε less than 15, substantial ion-association must occur[111]. For most purposes therefore solvents of ε=10 or less are considered as being at the limits of usefulness in electrochemistry.

Cell resistances in these latter solvents can be significant; for example, a dichloromethane-containing cell with a typical tip-to-tip working electrode to reference electrode resistance (R_u) of 1000 Ω (see below) will produce a voltage drop of 0.2 V when a 200 μA current flows; this represents a gross error since potentials are normally measured correct to 10-20 mV over a span of $\pm$2 volts.

Although its many advantages include overcoming the high internal resistance of the reference electrode, the 3-electrode potentiostat is not immune to the ohmic loss in solution represented by iR_u. Solution resistance phenomena in non-aqueous media can be at least partially

Table 2.2 Dielectric Constants[110,111] for Selected Solvents*

Solvent	ε
Water	78.54
Dimethylsulphoxide	46.7
Acetonitrile	37.5
Dimethylformamide	36.7
Nitromethane	35.74
Acetone	20.7
1,2-Dichloroethane	10.65
1,2-Dichlorobenzene	9.93
Dichloromethane	9.08
1-Chloronaphthalene	3.67[111]
1-Methylnaphthalene	2.71[111]

* By definition these are derived by comparison with a vacuum where ε = 1.00.

corrected however by the use of positive feedback compensation[106,107,112,116]. This circuitry, incorporated into most modern electrochemical apparatus, samples the current flowing in the cell and boosts the potential at the working electrode to nullify the voltage drop appropriate to the predetermined cell resistance.

The resistance R_u can be calculated if the specific resistance of the solution (ρ ohm cm) and the cell geometry are known, according to equation (2.1)[117].

$$R_u = \frac{\rho}{2\pi}\left[\frac{1}{r_1} - \frac{1}{r_2}\right] \qquad \text{(Eqn. 2.1)}$$

where r_1 = radius of Hg drop at d.m.e.

r_2 = distance from centre of Hg drop to reference electrode tip.

More commonly, the cell resistance is compensated empirically[101,118], as follows. In a potential region where only double-layer charging current is found (i.e. no Faradic current), the extent of positive-feedback is increased gradually until the onset of instability, signalled by current oscillation which indicates over-compensation, and then slightly reduced. This method has been used through the present work.

Thus with care regarding experimental design and cell geometry, and employment of a three-electrode potentiostat incorporating positive feedback compensation, undistorted voltammograms are readily obtained in polar organic solvents such as dimethylsulphoxide, acetonitrile, acetone or even dichloromethane.

2.4 The Use of Naphthalene Solvents in Voltammetric Studies

As has been outlined previously optimum solubility of phthalocyanines is attained in substituted benzenes and naphthalenes. However, the dielectric constants of these liquids, as shown in Table 2 are evidently very low, particularly when we consider that $\varepsilon=1$ for a vacuum. Equally their ability to dissolve possible supporting electrolytes is limited and the likelihood of strong ion-pairing of such solutes is very high. The specific resistance of such solutions is therefore expected to be very high, and quite beyond the scope of potentiostat and resistance compensation technology. As a consequence such a solvent would ordinarily be regarded as impractical for electrochemical studies.

However, in view of their exceptional ability to dissolve phthalocyanine pigments, research was initiated in this laboratory to determine the feasibility of using the low-polarity solvents 1-chloronaphthalene and 1-methyl-naphthalene in a.c. and d.c. polarography and cyclic voltammetry, using tetra-alkylammonium salt electrolytes at elevated temperature on a routine basis. This innovation was predicted to produce a number of advantages. Solubility of the electrolyte was found to increase greatly and moreover as hoped the increased thermal energy of the solution tended to disrupt ion-pairs, dramatically increasing conductivity. These advantages, combined with the increase of ion-mobility resulting from the decrease in solvent viscosity, were discovered to enable full ohmic compensation for fast-scan voltammetry and for the more sensitive and demanding technique of a.c. polarography.

Concomitant with this, elevated temperatures naturally promised increased phthalocyanine solubility.

Full compensation for d.c. voltammetric work is achieved at 60°C while 125°C represents the threshold temperature for full compensation in the a.c. polarographic mode using commercially available cells and instrumentation (the P.A.R. 170 system). Our routine practice is to work at 150°C using nominally 2 M tetrabutylammonium perchlorate (TBAP) or tetrabutylammonium fluoroborate ($TBABF_4$). (Either salt can be used although the latter is preferred for reasons of safety). These conditions are well below the boiling points of the liquid naphthalene solvents and provide a margin in compensation for ohmic loss while solvent evaporation and thermal decomposition of solvent and electrolyte are kept to a minimum.

The coordinating ability of solvents is also of significance in studies of metallated species. As will be discussed later, solvation of a coordinatively unsaturated metal ion may materially effect its redox potentials and even its electronic configuration. One aspect of this present work therefore has been to examine the redox activity of the phthalocyanines in the absence of such axial ligation effects, in strictly non-polar media. Conventional organic solvents such as D.M.S.O. or D.M.F. are invariably coordinating media to some degree, having high donor numbers on the Gutmann-scale[119]. Naphthalene or its simple derivatives however have no appreciable σ-donor character and thus provide a medium free from metal complexation effects. Thus the naphthalenes represent a range of non-polar, non-protic, non-coordinating

high-boiling solvents, in which the redox activity of phthalocyanines can be investigated in a remarkable temperature domain.

While 1-methylnaphthalene, 1-chloronaphthalene and even naphthalene itself have been used under these conditions, the former solvent has been used throughout the present work because of its larger potential range, approximately 3.2 V compared with 2.5 V for 1-chloronaphthalene. Table 2.3 lists the relevant physical properties of this solvent/electrolyte system[126].

Preliminary investigations* to characterise cell response under these unusual conditions in the new electrochemical medium were carried out by studying the well-defined reversible ferrocene-ferrocenium redox couple[126]. Figure 2.2 shows the a.c. polarogram and cyclic voltammogram of ferrocene in 1-methylnaphthalene at 150°C.

The electron transfer was confirmed to be reversible by a.c. polarography over the a.c. frequency range 20.5 Hz - 1005 Hz. (Figure 2.3 shows the linear dependence of I_p with $\omega^{\frac{1}{2}}$). Similarly, the cyclic voltammetric behaviour (Figure 2.4) indicates full reversibility for scan rates in the range 20 mV s^{-1} - 20 V s^{-1}. Figure 2.5 shows the linear I_p vs. $\nu^{\frac{1}{2}}$ dependence.

A particularly sensitive test of electrode reversibility and of uncompensated resistance is the a.c.

*Note Initial investigations were carried out at Stirling University using TBAP/MeN and ClN mixtures and have been confirmed and extended in this thesis using $TBABF_4$ which proves equally effective.

Table 2.3 Selected Physical Properties of 1-methylnaphthalene, and its Electrolyte Solution*, at 150°C.[a]

		Ref.
Melting Point/°C	-30.5	127,128
Boiling Point/°C	244.7	127,128
Vapour Pressure/mmHg	60	127
Density/g cm^{-3}	0.933[b]	111,128,129
Density*/g cm^{-3}	0.957	126
Viscosity/cp	0.56	126
Viscosity*/cp	1.93	126
Surface Tension/dyne cm^{-1}	26.3[b]	129
Dielectric Constant	2.71(20°C)	111,130
Dipole Moment D	0.4	111,131
Conductivity Ω^{-1} cm^{-1}	1.2×10^{-9}	126
Conductivity* Ω^{-1} cm^{-1}	5.5×10^{-3}	126
Potential Range (Hg)*[c] V	+0.4 to -2.8	126
Potential Range (Pt)*[c] V	+0.5 to -2.7	126

(a) All values (except M.Pt. and B.Pt.) at 150°C and 1 atmosphere unless otherwise stated.

(b) Extrapolation from results at lower temperatures.

(c) Potentials vs. Ferrocene/Ferrocenium couple

* Indicates 1 M Bu_4NClO_4 Solution.

Figure 2.2 Voltammetry of Ferrocene in Methylnaphthalene

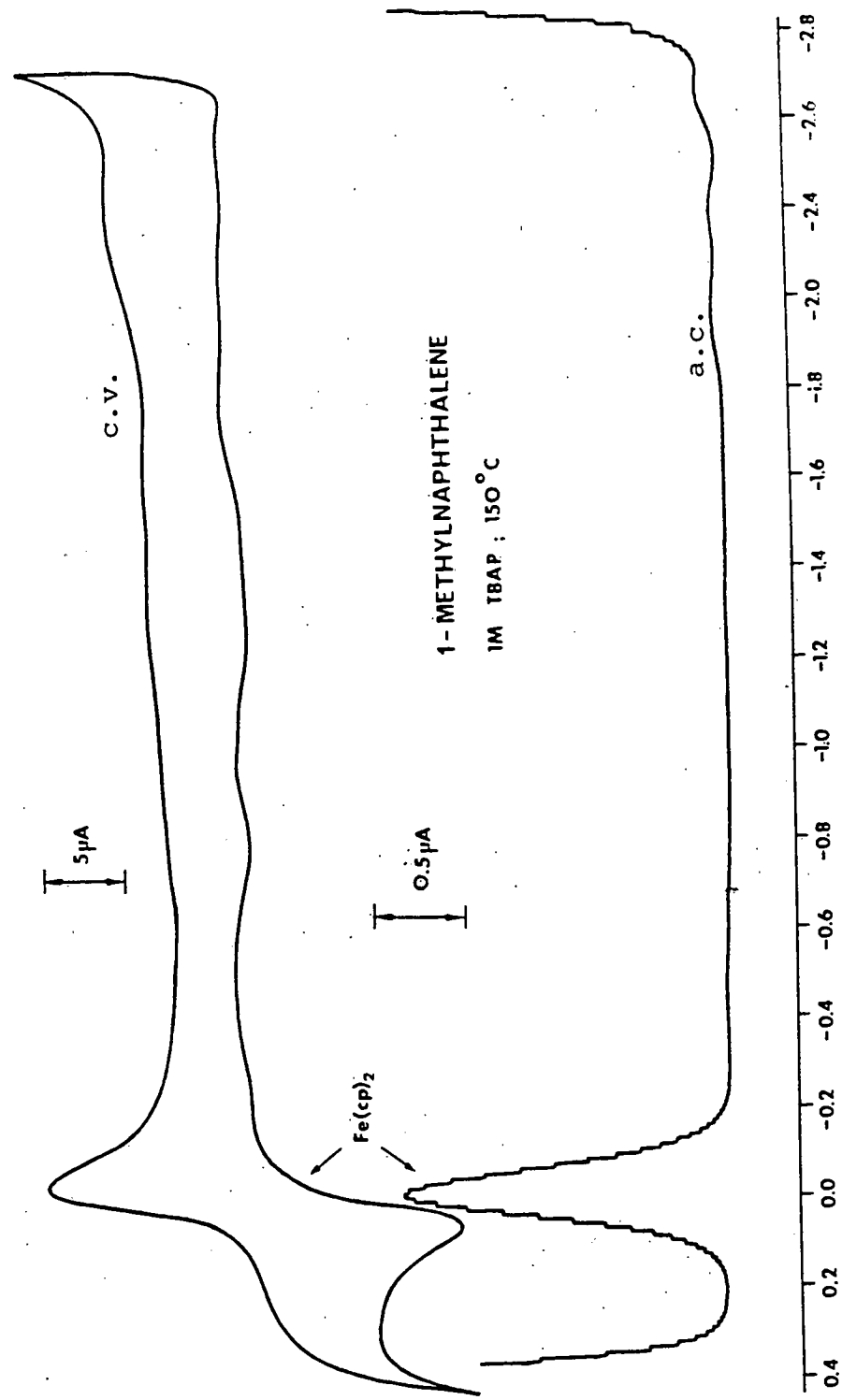

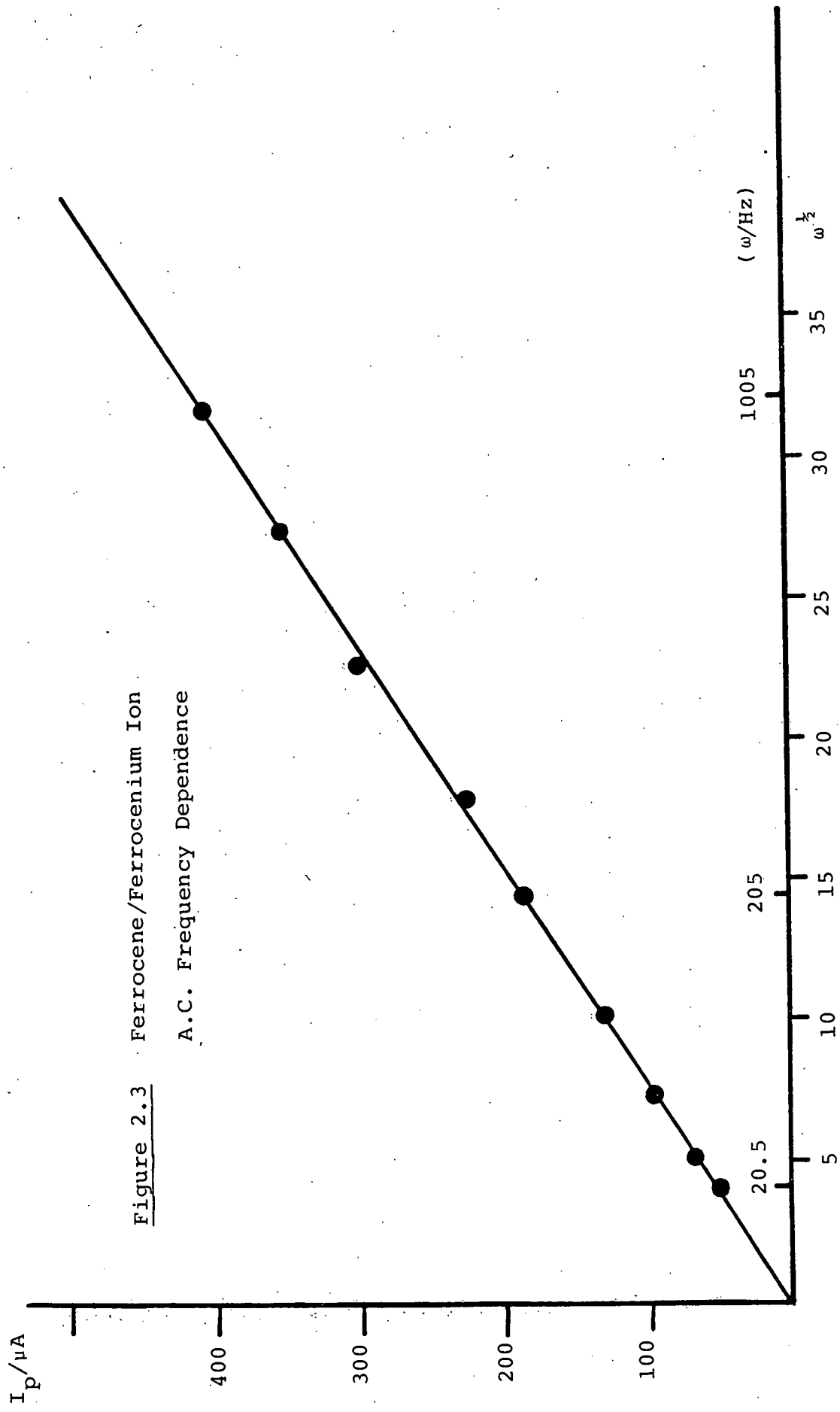

Figure 2.3 Ferrocene/Ferrocenium Ion

A.C. Frequency Dependence

Figure 2.4 Ferrocene/Ferrocenium Ion Couple
Cyclic Voltammogram, 50-500 mVs^{-1}

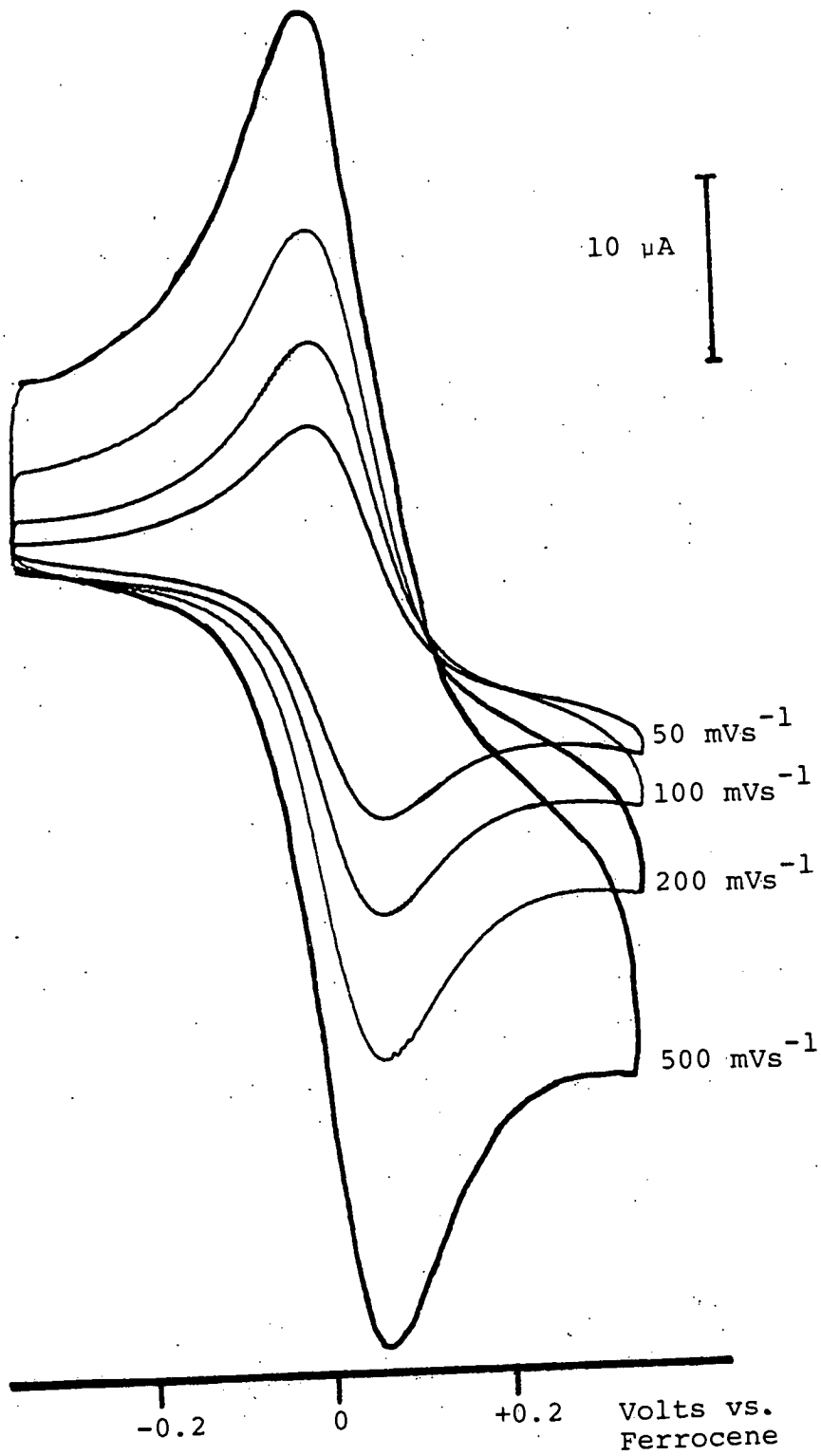

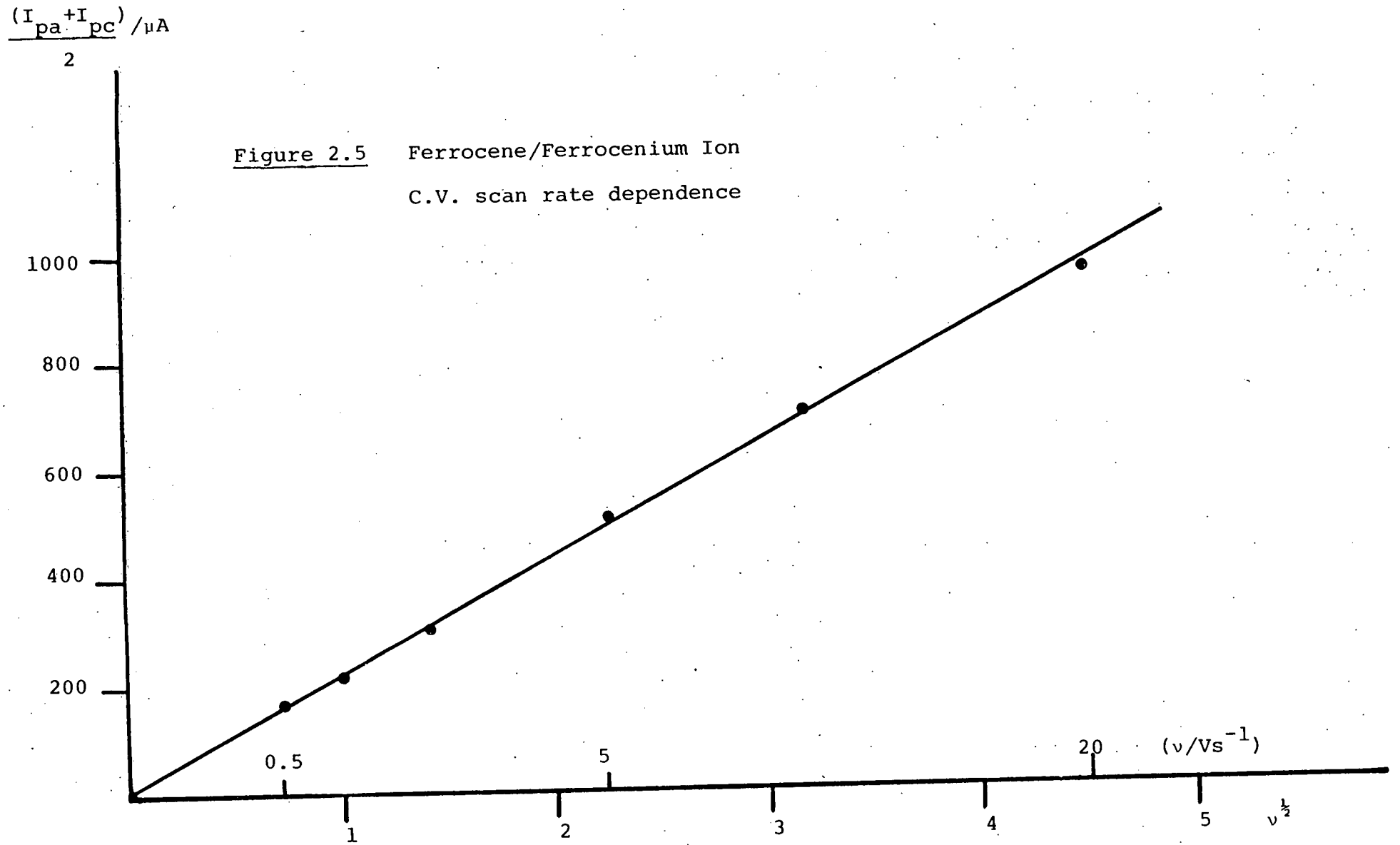

Figure 2.5 Ferrocene/Ferrocenium Ion
C.V. scan rate dependence

waveform. The shape of a reversible diffusion-controlled a.c. wave can be shown[120,121] to be represented by the equation:

$$I/I_p = 4e^j/1+e^j \quad \text{where} \quad j = (E-Ep)nF/RT$$

$$= f(E-E_p) \qquad \text{(Eqn. 2.2)}$$

Fig. 2.6 shows the plot of I/I_p vs. $E-E_p$ for ferrocene in MeN and almost perfect agreement between experiment and calculation is obtained, indicating the full reversibility of the ferrocene system and complete compensation for solution resistances.

The provision of a reference electrode for use in high temperature solvents presents a technical challenge; conventional aqueous reference electrodes clearly cannot be immersed in the cell operating near or above 100°C. In the initial stages of this work therefore a platinum wire was used as a quasi-reference electrode[101]. The potential of this electrode is sufficiently stable for immediate purposes but accurate determination of potentials was achieved by introducing ferrocene into the cell at a convenient stage and employing the $E_{\frac{1}{2}}$(ferrocene/ ferrocenium) as the internal reference point. Electrode potentials of all couples were determined directly in terms of their separation from $E_{\frac{1}{2}}(Fe(cp)_2/Fe(cp)_2^+)$, with ferrocene and the test compound co-existing in the cell. More recently, in the course of this work, an Ag/Ag^+ molten-salt reference electrode[101] has been introduced but nonetheless all potentials are quoted with respect to the ferrocene/ ferrocenium ion couple set at 0.00 V throughout this thesis, unless otherwise stated.

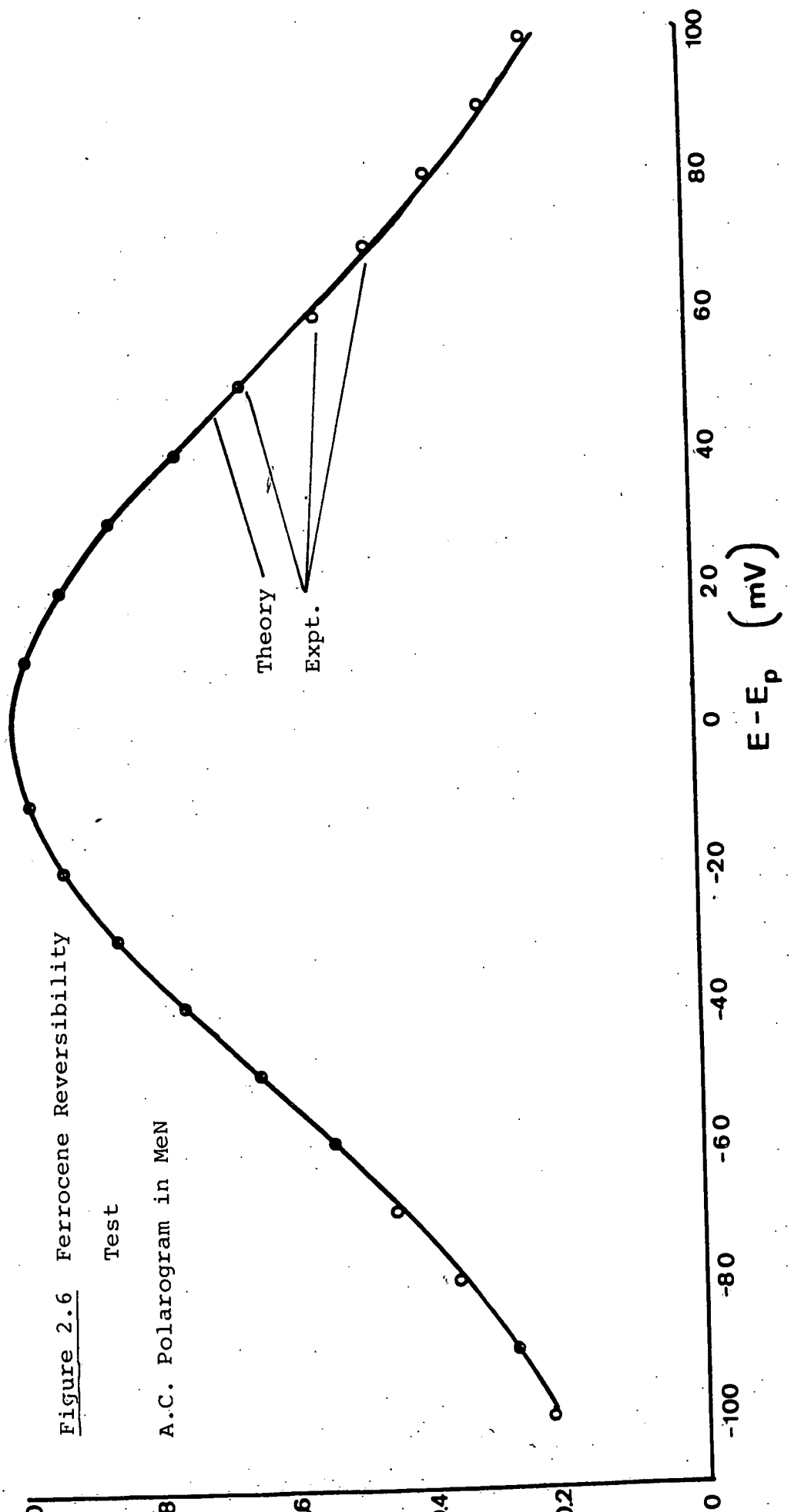

Figure 2.6 Ferrocene Reversibility Test

A.C. Polarogram in MeN

2.5 Determination of Solution Resistance

We tend to refer to the 1-methylnaphthalene electrolyte system as a relatively "high resistance" electrochemical medium, even at 150°C, and it was felt necessary to quantify this. Hence measurements were undertaken to determine the cell resistance under typical operating conditions.

Many methods of evaluating cell resistance are available. If cell geometry and the specific resistance of the solutions are known then equation 2.1[117] can be used. Alternatively d.c.[122] or preferably a.c. conductance[123-125] measurement can be utilised. However a simpler empirical method was employed in this work.

As explained previously, as a current i flows across a cell with resistance R_u (between working and reference electrodes) then a potential drop $V = iR_u$ is encountered. The effective potential between working electrode and solution is decreased and hence the apparent $E_{\frac{1}{2}}$ for electron transfer shifts. The greater the concentration of electroactive species, the greater the current and hence the greater the shift of $E_{\frac{1}{2}}$. Thus in the absence of any resistance compensation, a plot of $E_{\frac{1}{2}}$ vs. $\frac{1}{2}i_d$ for a series of differing concentration of substrate should be linear with slope equal to R_u. This must, of course, be derived from a range of substrate concentrations where the couple is known to be behaving ideally so that E^o is independent of substrate concentration.

This practice was tested initially for a more conventional fairly high resistance medium, dichloromethane,

at room temperature. The ferrocene oxidation was again convenient to study and the variation of $E_{\frac{1}{2}}$ with $\frac{1}{2}i_d$ vs. a Ag/AgCl reference electrode in 0.2 M $TBABF_4$ solution in CH_2Cl_2 is shown in Figure 2.7. A value of cell resistance (R_u) of 950 ohms is obtained and is in agreement with resistance values obtained independently for the same cell electrode configuration by a.c. conductance measurements.

Figure 2.8 shows the $E_{\frac{1}{2}}/i$ variation for the ferrocene oxidation in 1-methylnaphthalene at 150°C using a Ag/Ag^+ reference electrode. The variation of measured $E_{\frac{1}{2}}$ with cell current ($\frac{1}{2}i_d$) and hence with concentration is again satisfyingly linear and a working electrode/reference electrode cell resistance of 420 ohms is calculated.

These measurements refer to a typical commercial cell (Metrohm EA875-5) with tip-to-tip separation of 5 mm and electrode areas of 3.14 mm^2 (working electrode) and 7 mm^2 (reference electrode). In our experience placement of electrodes is not critical to successful positive feedback compensation in such cells.

Thus at elevated temperatures these apparently unpromising naphthalene solvents provide excellent voltammetric media with electrical resistances comparable with conventional electrochemical solvent systems.

2.6 Experimental Methods

All electrochemical experiments were carried out using a Princeton Applied Research (P.A.R.) Model 170 electrochemical system with P.A.R. 172 d.m.e. and drop timer. Platinum wire and double wire electrodes (Metrohm EA235 and EA285) were used as counter and reference electrodes and as working electrodes for cyclic voltammetry.

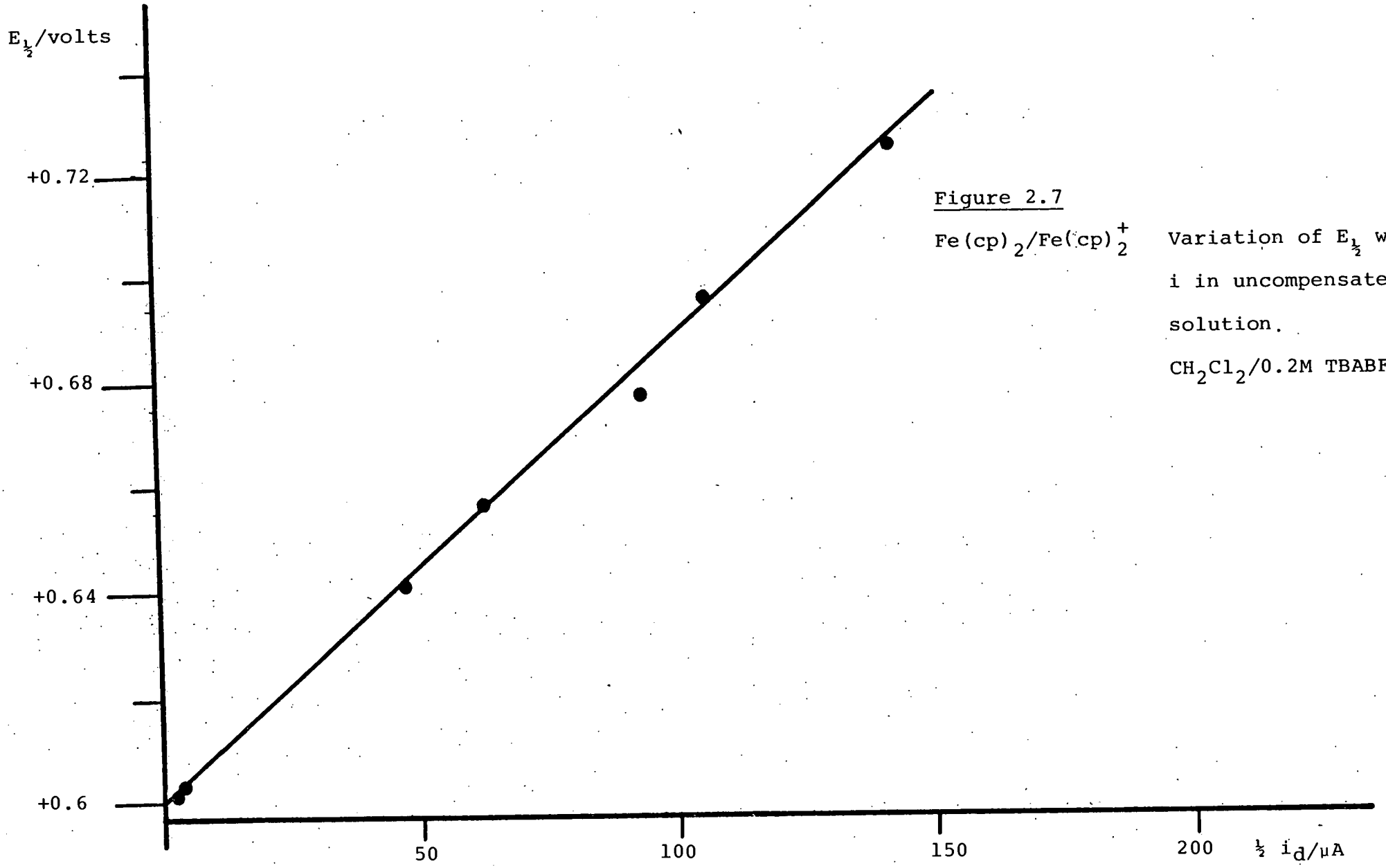

Figure 2.7

$Fe(cp)_2/Fe(cp)_2^+$ Variation of $E_{\frac{1}{2}}$ with i in uncompensated solution.

CH_2Cl_2/0.2M $TBABF_2$/25°C

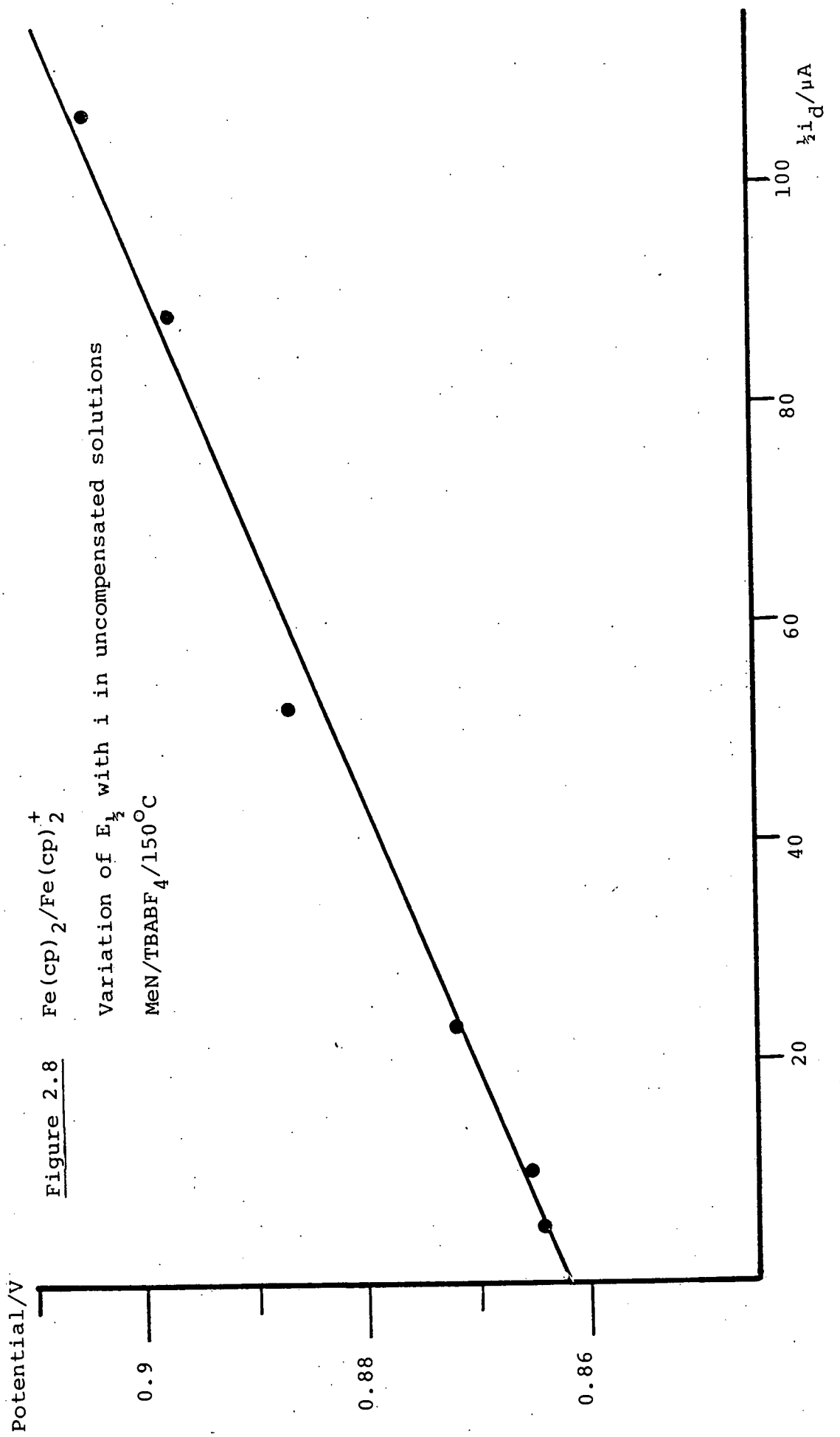

Figure 2.8 $Fe(cp)_2/Fe(cp)_2^+$

Variation of $E_{\frac{1}{2}}$ with i in uncompensated solutions

MeN/$TBABF_4$/150°C

A Metrohm 5 ml jacketed cell linked to a digitally controlled Haake F3S circulator/heating bath was used with silicone oil (Dow Corning GC 200) as circulating fluid. Cell temperature was maintained at 150 $\pm$ 0.5^{o}C throughout experimental work.

In a typical experiment the cell was heated to 100^{o}C, 1-methylnaphthalene (5 ml) was added and heating continued to 150^{o}C where tetrabutylammonium fluoroborate ($TBABF_4$) (3.2 g) was added. Solutions were then degassed with argon for 10 mins and kept under argon throughout the experiment. Temperatures were independently monitored using a Comark Digital Thermometer and thermocouple probe.

Experiments in dichloromethane, butyronitrile or dimethyl sulphoxide were carried out at room temperature using 0.2 M $TBABF_4$ as supporting electrolyte with an Ag/AgCl reference electrode (Metrohm EA441/5) containing 0.02 M TBACl and 0.18 M $TBABF_4$ as electrolyte.

Solvents

1-methylnaphthalene (Aldrich reagent grade) was purified by chromotography on neutral Alumina (Fisons "Camag" 100-250 mesh) and stored at 0^{o}C in the absence of light until required.

Dichloromethane was stored over potassium hydroxide for 48 hours and distilled from phosphorus pentoxide before use. Dimethyl sulphoxide and butyronitrile (B.D.H. reagent grade) were used without further purification.

Electrolytes

(i) Tetrabutylammonium Fluoroborate ($TBABF_4$)

Tetrabutylammonium hydroxide 160 ml (B.D.H. 40% solution, 160 ml) was neutralised with fluoroboric acid (B.D.H. technical grade, 40% solution, 40 ml) and the resulting precipitate filtered, washed liberally with cold water and dried. Recrystallisation from methanol/water yielded tetrabutylammonium fluoroborate which was dried under vacuum (0.1 torr, 80°C) for 24 hours.

Yield 53.8 g (69%) white needles

Analysis Calc. 58.39% C; 10.95% H; 4.26% N

Obs. 58.30% C; 10.69% H; 4.09% N.

A similar method was used for the preparation of tetrabutylammonium perchlorate,[126] which was scrupulously washed and recrystallised to avoid explosive hazards arising from trace impurity.

(ii) Tetrabutylammonium Hexafluorophosphate ($TBAPF_6$)

Ammonium hexafluorophosphate (4.89 g) was dissolved in 30 ml of water and added dropwise to tetrabutylammonium hydroxide solution (18.5 ml) in water (50 ml). The white precipitate formed was washed with water until washings were neutral. The solid was then recrystallised from methanol and dried under vacuum.

Yield = 10.6 g (91%)

Analysis Calc. 49.61% C; 9.30% H; 3.62% N

Obs. 49.88% C; 9.29% H; 3.58% N.

CHAPTER 3

Stepwise Reduction Potentials of Phthalocyanines in Strictly Non-Coordinating Media

3.1 Introduction

It has been established in porphyrin chemistry that, irrespective of the nature of the peripheral substituents, a systematic dependence of reduction potentials on the identity of the central metal ion is observed. One might expect a parallel dependence to exist in phthalocyanine chemistry. However, as outlined in Chapter 1, previous investigations by Rollman and Iwamoto[74] on tetrasulphonato-phthalocyanines [$M(SO_3)_4Pc$] and by Clack and Hush[87] on unsubstituted phthalocyanines [MPc] have proved inconsistent and disappointing in this respect.

Examination of the cobalt, nickel, copper and free-base compounds was common to both studies. Rollman and Iwamoto found the numerical order of first reduction potentials, from easiest to hardest (most negative) was

$$H_2 < Co < Ni < Cu$$

while Clack and Hush observed

$$Co << H_2 < Cu < Ni$$

This disparity is shown very clearly in Figure 3.1* where first and second reduction potentials of the relevant compounds are plotted as a function of central ion. First reduction potentials for the two series disagree substantially, both in absolute values and in relative order although it should be noted that, when presented in this manner, parallels do emerge in second reduction potentials.

---

* Note .

In this and subsequent figures arbitrary relative displacements enable better visual comparison of systems which are chemical distinct or related to differing solvents or reference electrodes The numerical displacements are indicated on each figure.

Figure 3.1 Trends in Phthalocyanine Reduction Potential

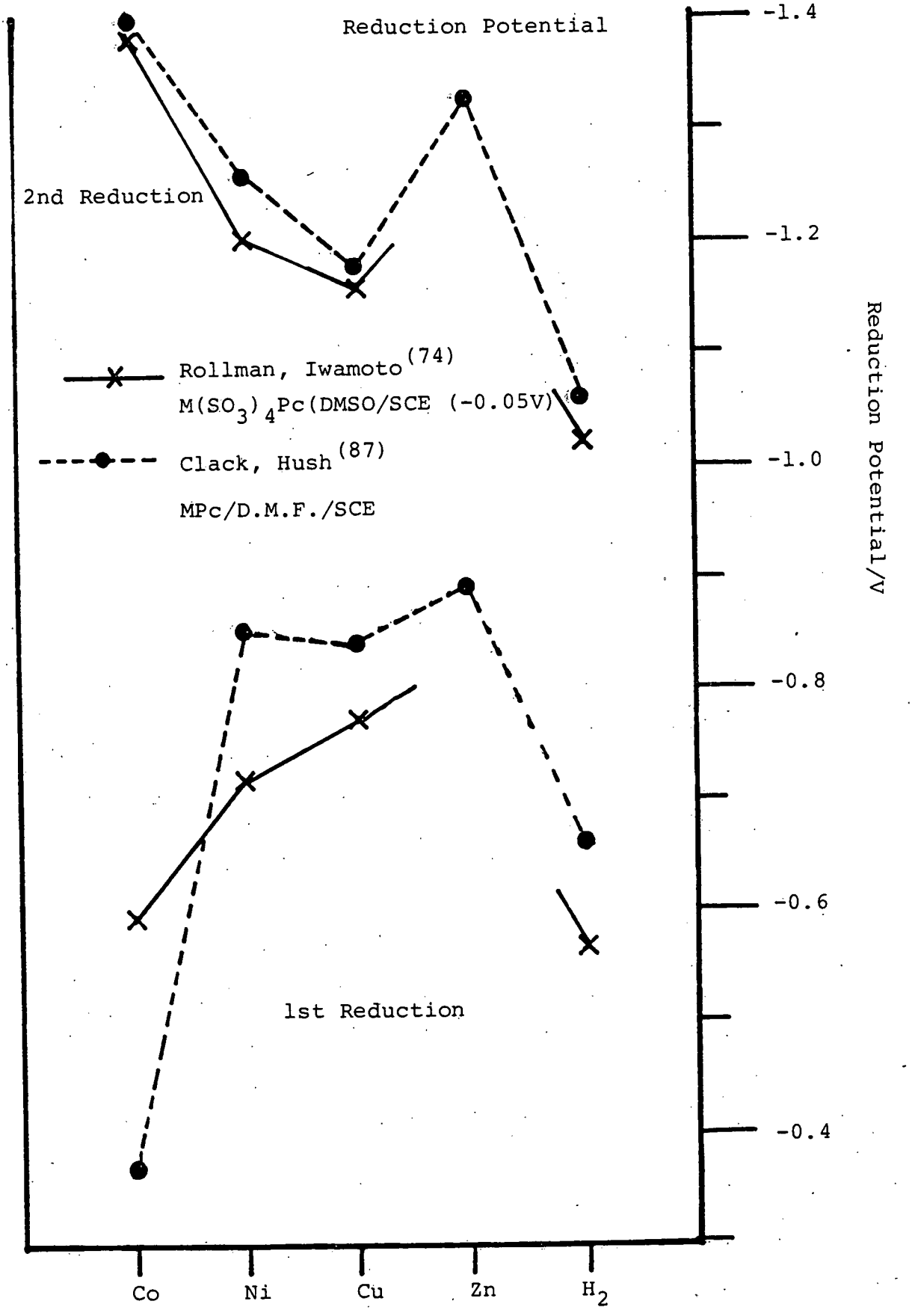

It was against this background that studies of the redox chemistry of phthalocyanines in our novel high-temperature medium were initiated. These studies have succeeded in resolving the contradictions existing in the literature with respect to the phthalocyanines themselves and, further, in determining absolutely the characteristic differences in electron affinity between the porphyrin and phthalocyanine macrocycles.

The very low solubility of phthalocyanines arises from the strong intermolecular forces within the close-packed crystal structure. More soluble derivatives have been sought but these have largely been confined to the water soluble tetra-sulphonato derivatives. Simple alkyl-substituted derivatives which are relatively soluble in common organic solvents have received surprisingly little attention in the literature. Therefore in order to consolidate our conclusions derived from the pigments themselves, and in conjunction with Imperial Chemical Industries, P.L.C., the synthesis of a series of tetra(tertiarybutyl)phthalocyanines [$M^{t}Bu_4Pc$] (figure 3.2) was undertaken. (The detailed synthetic methods used will be discussed in Chapter 8).

Figure 3.2 Copper Tetra(^{t}butyl)phthalocyanine

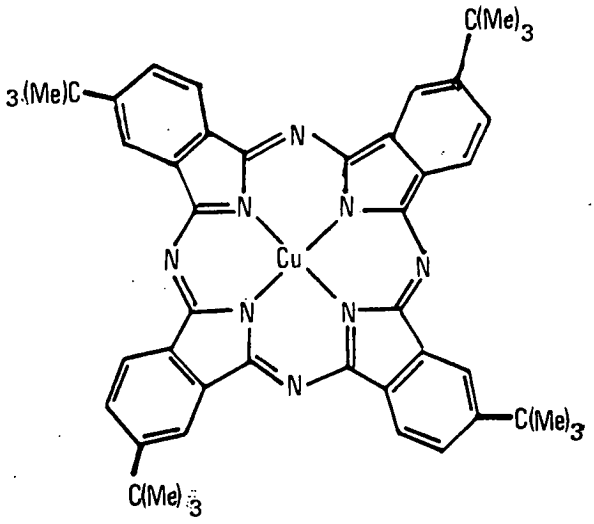

The choice of ^{t}butyl group as substituent was made primarily on grounds of its bulk. Its size should prevent close crystal packing and hence lower intermolecular forces thus enhancing solubility. While this work was in progress, the synthesis of octa-methyl and octa-n-butyl phthalocyanines was reported by Cueller and Marks[144]. These were soluble only in aromatic solvents (toluene, tri-chlorobenzene). In contrast we have found the tetra-tertiary butyl derivatives although having fewer "solubilizing" groups to be soluble even in simple aliphatic hydrocarbons (heptane, hexane). This arises not simply from the bulk of the ^{t}butyl group but is also related to the symmetry of the resulting phthalocyanine.

The asymmetry of the alkylated precursors means that MBu_4Pc exist as a mixture of isomers. The four possible isomers have been identified in an apparently statistical distribution by n.m.r. spectroscopy. This structural isomerism apparently exerts no observable effect on the redox behaviour of the macrocycles.

The preparation of alkylated phthalocyanines offers a number of advantages. Increased solubility should, of course, result in more normal current responses in polarographic and voltammetric work. The effect of t-butyl substitution on reduction potentials should be small yet well-defined. The group has an essentially electron-donating effect, and the increased electron density should result in macrocycle reduction potentials being shifted to slightly more negative values. It was hoped that these soluble derivatives would reinforce the conclusions obtained for the unsubstituted compounds in our high-temperature medium. Furthermore electrochemical investigations of [MBu_4Pc] in more familiar organic solvents might be possible, allowing comparison of high- and low-temperature behaviour, and exploration of any axial solvent interactions.

3.2 Results

The cathodic behaviour of a series of phthalocyanine compounds has been studied in 1-methylnaphthalene solution at 150°C using the methods outlined in Chapter 2. In general the compounds are seen to undergo two well-defined reduction steps in the available range, as exemplified by [H_2Pc] and [ZnPc], in Figures 3.3 and 3.4 respectively.

The first-reduction potentials, E_{red} (1), were all found to lie in a relatively narrow band of approximately 200 mV. Given our interest in determining accurately the relative reduction potential values of the various derivatives,

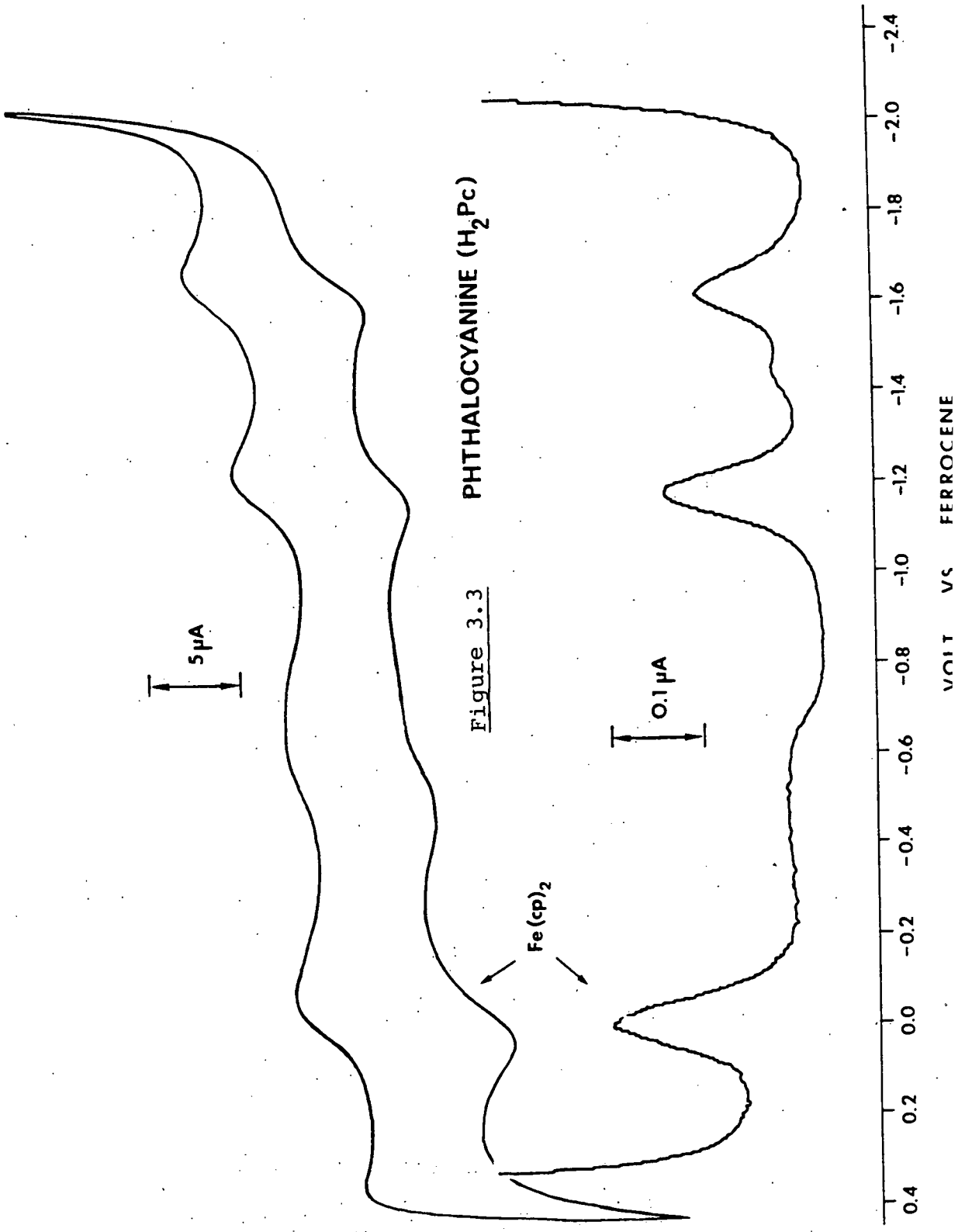
PHTHALOCYANINE (H_2Pc)
5 μA
0.1 μA
$Fe(cp)_2$
0.4
0.2
0.0
-0.2
-0.4
-0.6
-0.8
-1.0
-1.2
-1.4
-1.6
-1.8
-2.0
-2.4
VOLT VS FERROCENE

Figure 3.3

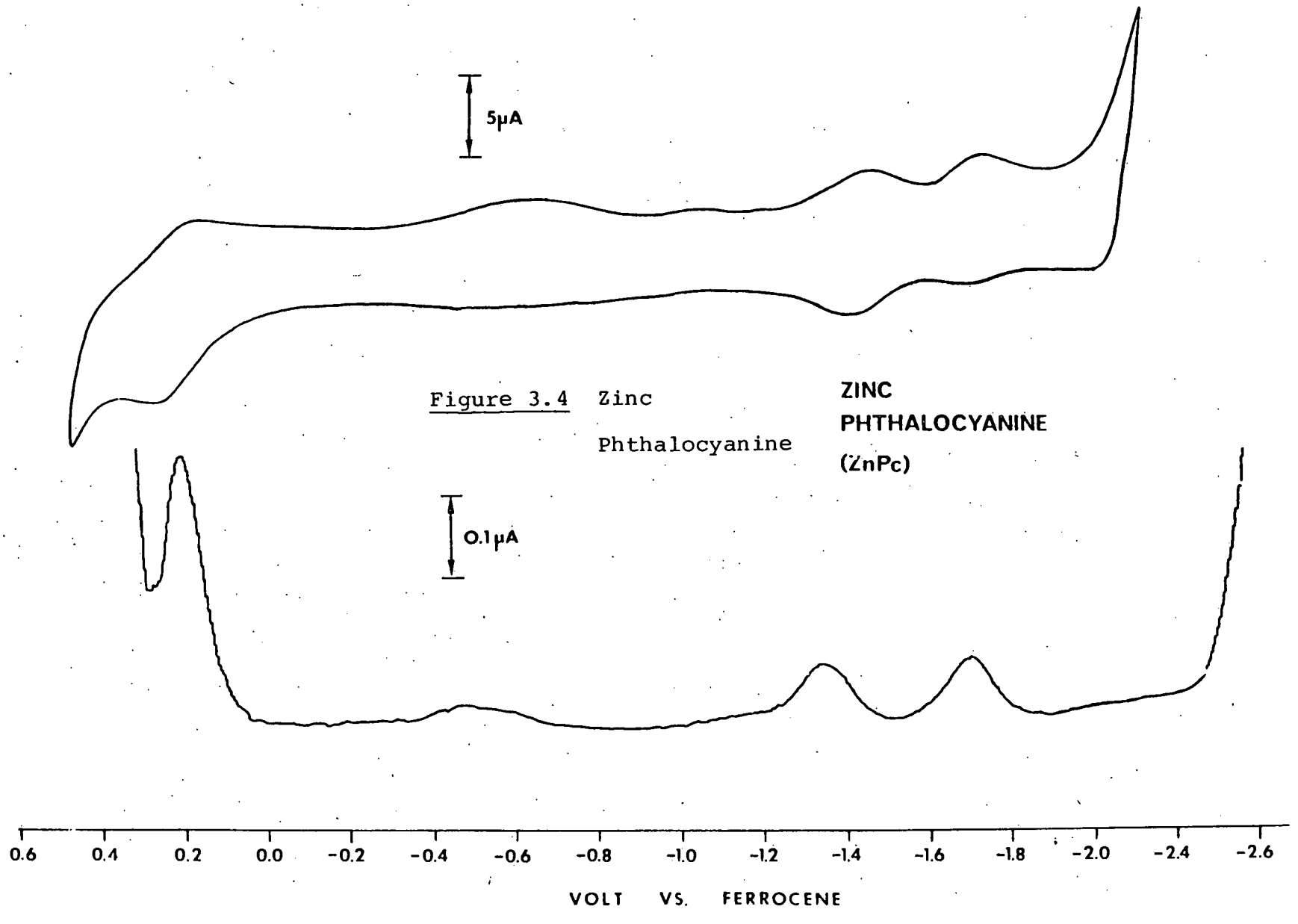

Figure 3.4 Zinc Phthalocyanine

conventional measurements on the individual compounds in isolation was felt to be inadequate. A rigorous scheme of cross-referenced experiments were devised, where in each case two or more compounds were studied simultaneously in the same solution as in Figure 3.5.

From a series of such experiments, accurate differences in reduction potential between various compounds were established unequivocally in a self-consistent network, and absolute values were assigned with reference to a suitable standard. These refined values are listed in Table 3.1.

These reduction steps are all shown to be diffusion-controlled reversible one-electron transfers, by analysis of the a.c. polarographic and cyclic voltammetric behaviour. High-temperature operation leads to considerable numerical change in the reversibility criteria previously outlined and Table 3.2 compares the modified values appropriate to 150°C with room temperature norms. For example Figure 3.6(a) shows the a.c. polarogram of platinum phthalocyanine [PtPc] over the applied a.c. frequency range 205-1005 Hz, while Figure 3.6(b) shows the wide domain of linear variation of I_p with $\sqrt{w}$. Figure 3.7(a) shows the cyclic voltammogram of vanadyl phthalocyanine [V(O)Pc] over the range of scan rates 100-500 mVs^{-1} while Figure 3.7(b) shows the linear dependence of peak current on $(\text{scan rate})^{\frac{1}{2}}$.

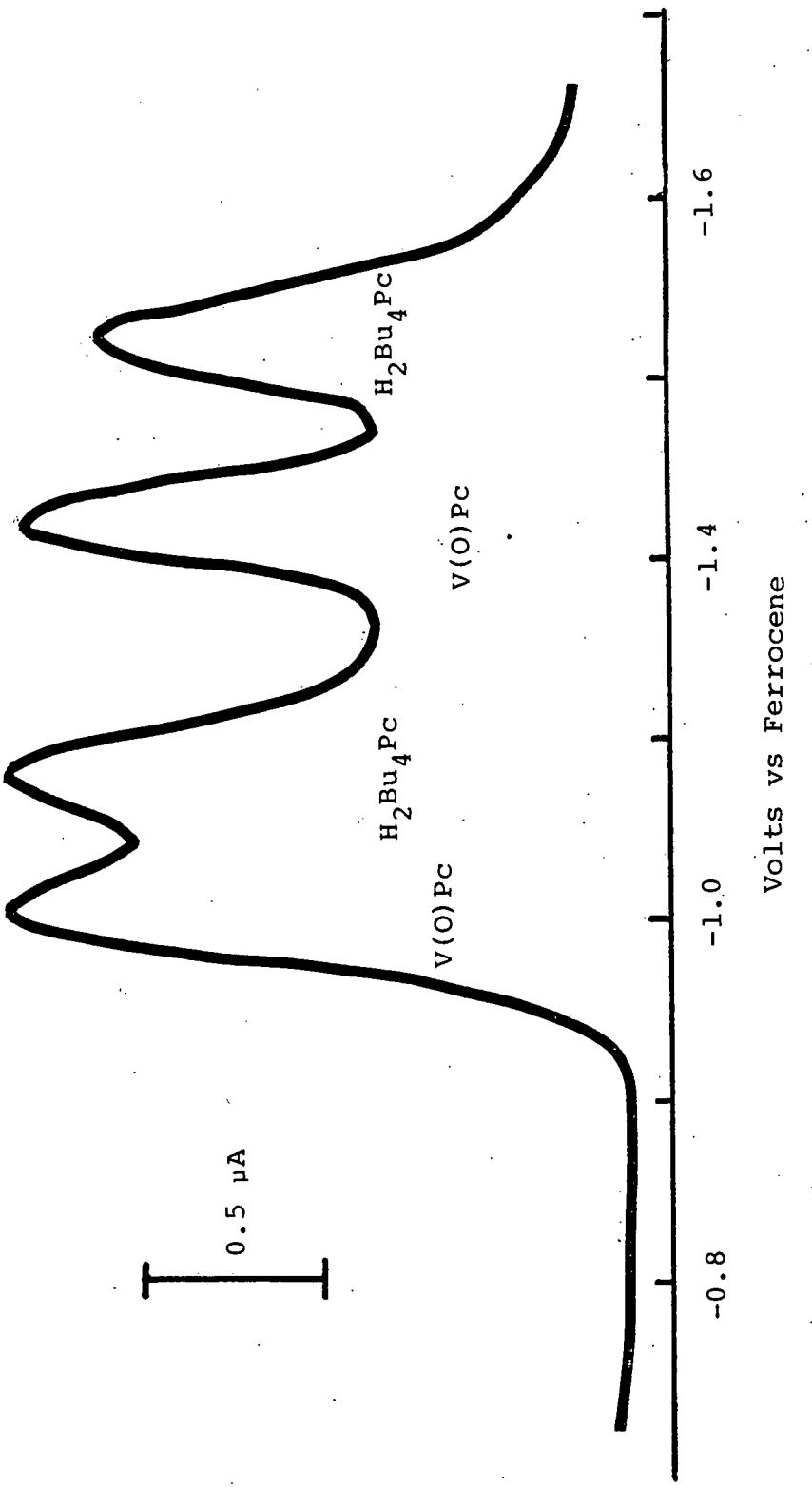

Figure 3.5 A.C. Polarogram of typical "mix" experiment

V(O)Pc + H_2Bu_4Pc/MeN/150°C

Table 3.1 Reduction Potentials of Metallophthalocyanines[b]

MPc M=	$E_{\frac{1}{2}}(1)$[a]	$E_{\frac{1}{2}}(2)$[a]	ΔE[c]
H_2	-1.16	-1.60	0.44
Fe	-1.29	-1.69	0.40
Co	-1.20	-1.90	0.70
Ni	-1.28	-1.76	0.48
Cu	-1.26	-1.70	0.44
Zn	-1.34	-1.70	0.36
Mg	-1.53	$\sim$-2.0	$\sim$0.47
Pb	-1.26	-1.57	0.31
Pt	-1.23	-1.61	0.38
$V^{IV}(O)$	-1.02	-1.45	0.43
$Mo^{IV}(O)$[d]	-0.92	-1.34	0.42
AgH[d]	-1.13	-1.58	0.45

(a) all potentials quoted vs $Fe(cp)_2$ = 0.00 V

(b) MeN solution, $TBABF_4$ as supporting electrolyte at 150°C

(c) $\Delta E = E_{\frac{1}{2}}(2) - E_{\frac{1}{2}}(1)$

(d) characterisation of these compounds see later

Table 3.2 Electrochemical Reversibility Criteria at 150°C

d.c. polarography

Plot of E vs $\log[(i_d-i)/i]$ linear with slope of 85 mV (59 mV)*

a.c. polarography

Width at half height = 120 mV (90 mV)*

cyclic voltammetry

$\Delta E_p = E_{pc} - E_{pa} = 85$ mV (59 mV)*

* values in brackets indicate 25°C norms

Figure 3.6(a) A.C. Polarogram of PtPc/MeN/150°C
Variation of Current with ω

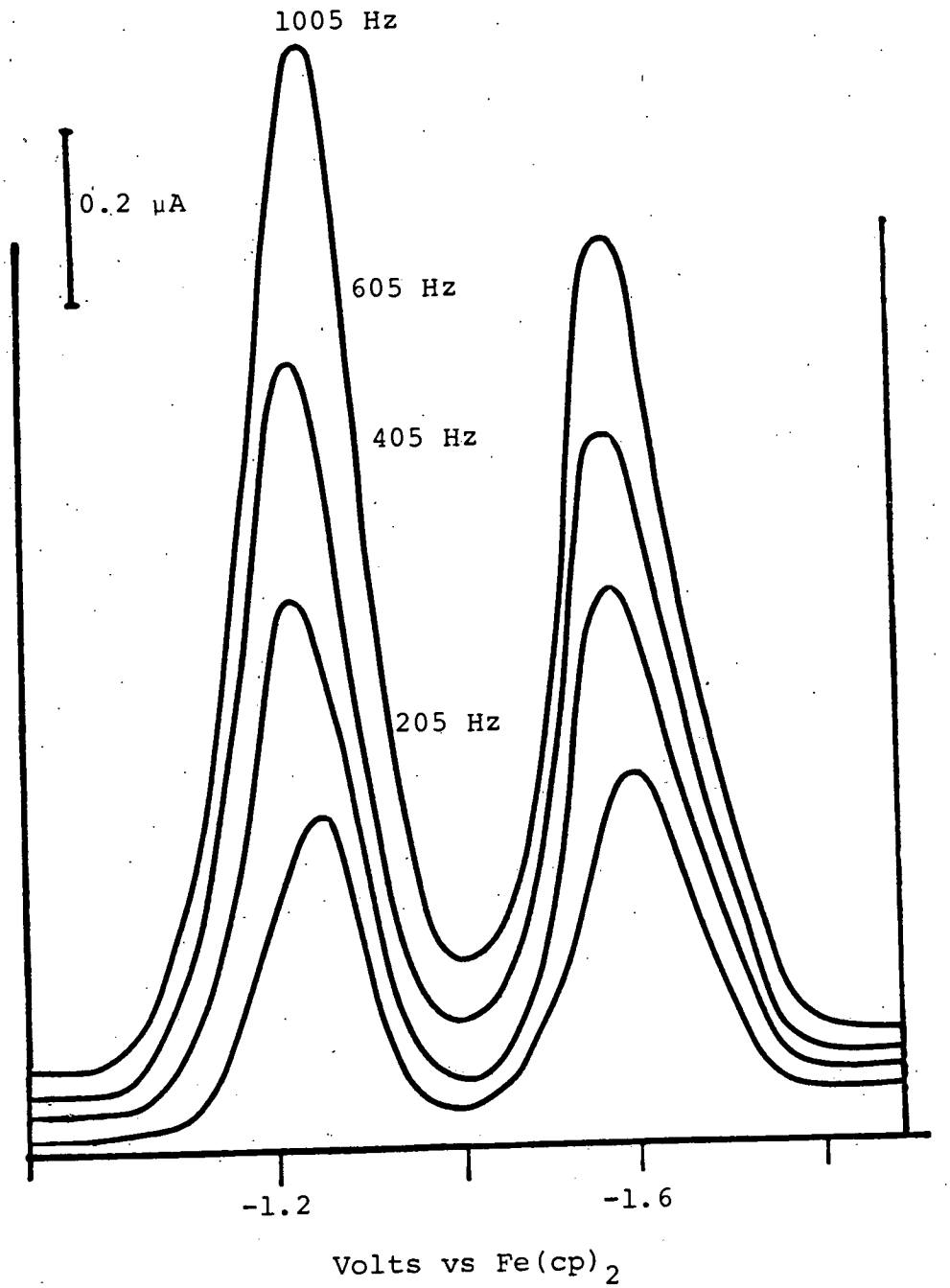

Figure 3.6(b) A.C. frequency dep[illegible]

PtPc/MeN/150°C

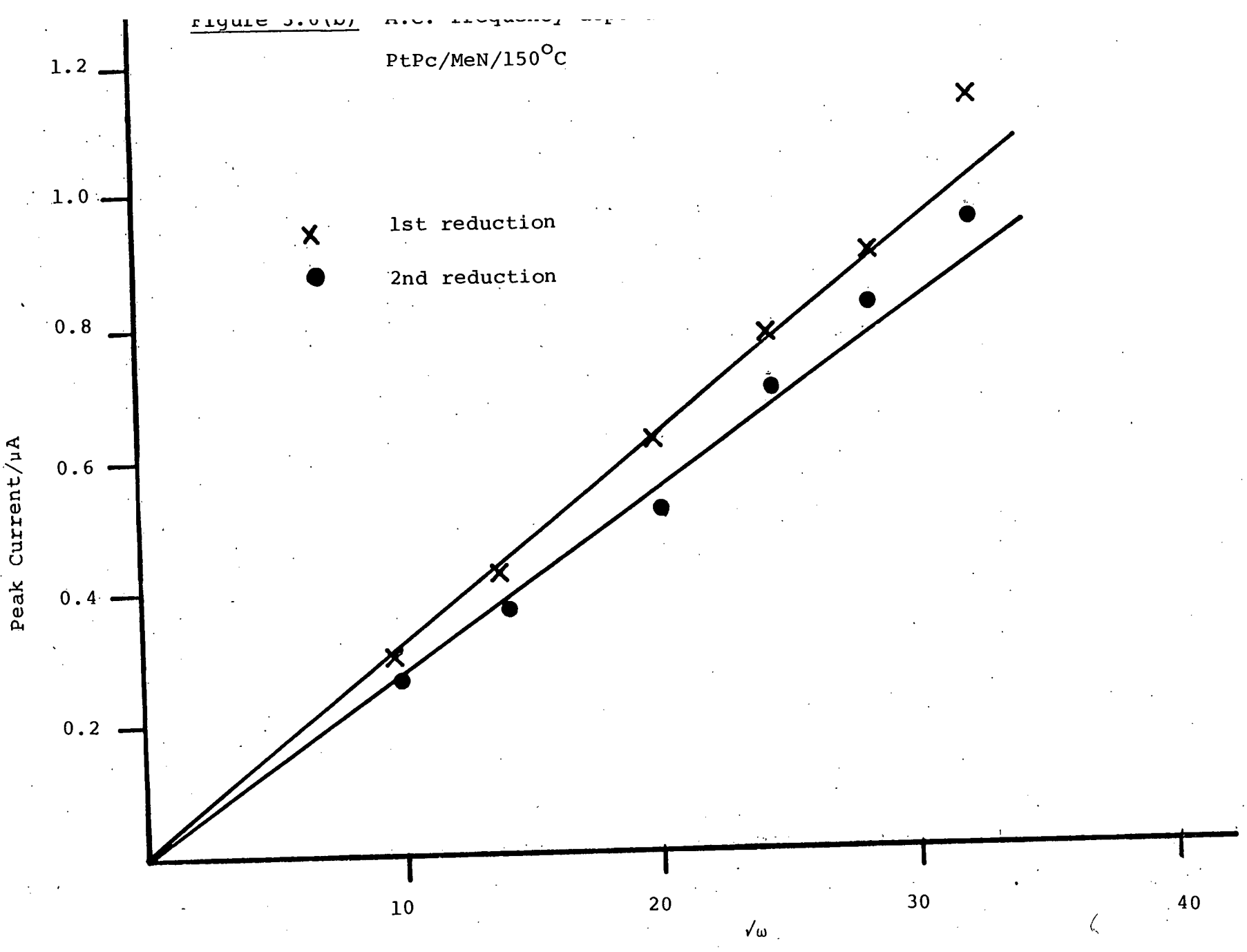

Figure 3.7(a) Cyclic Voltammogram of V(O)Pc

Variation with scan rate

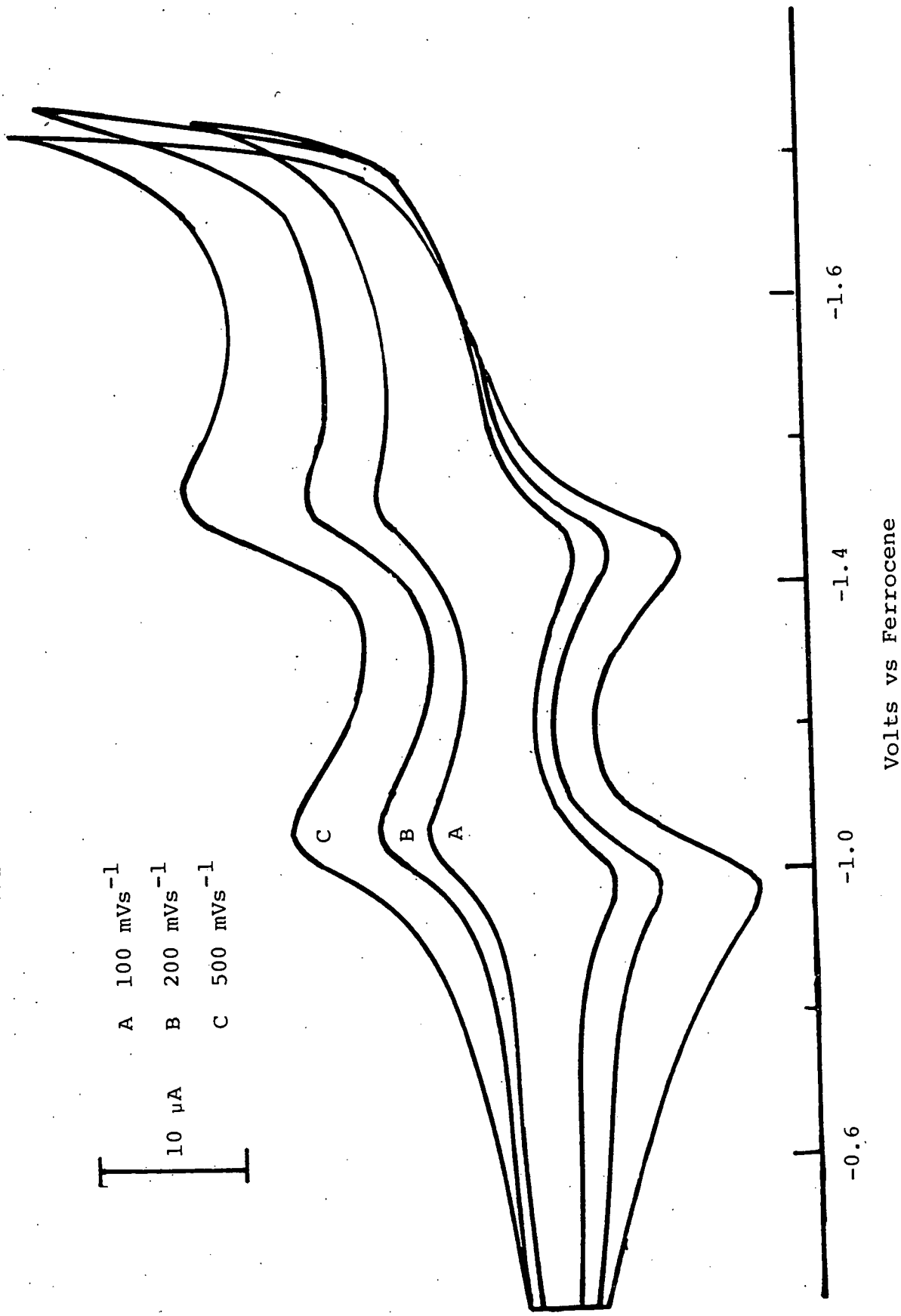

Figure 3.7(b) C.V. Scan rate dependence

V(O)Pc/McN/150°C

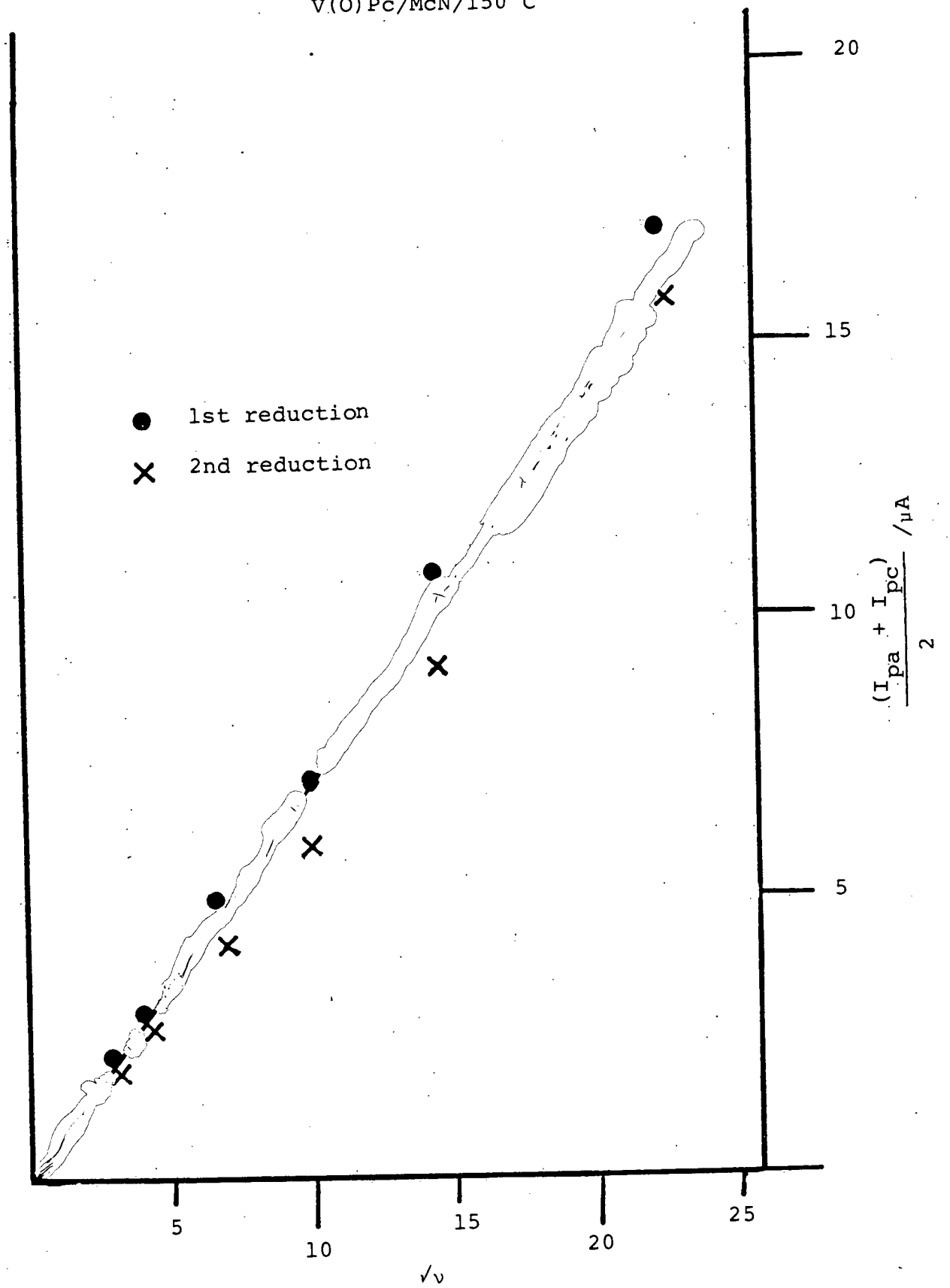

While a.c. peak currents for first and second one-electron reductions were expected to be equal, it was observed that in several compounds the peak current for the first step was substantially enhanced with respect to that of the second. For example, Figure 3.8 shows the a.c. polarographic response of silver phthalocyanine [Ag(H)Pc] at the d.m.e. The enhancement of first reduction increases excessively at higher applied a.c. frequency and is thus manifested by deviation from linearity in the a.c. frequence dependence, as shown in Figure 3.9. This effect, which is at its most extreme in the case of highly insoluble compounds such as [H_2Pc] or [CoPc], is attributed to adsorption of the neutral compounds at the electrode surface, a phenomenon well known to give enhanced a.c. signals.

Of the compounds studied here, only [MgPc], with the most negative E_{red} (1), fails to show two well-defined reductions within the available solvent range. The second [MgPc] reduction can actually be discovered at ca. -2.0 V *vs.* $Fe(cp)_2$ although its proximity to the solvent limit precludes detailed analysis.

The reduction potentials of the series of metallo-tetra-tertiary-butyl-phthalocyanines [MBu_4Pc] in 1-methylnaphthalene (MeN) at 150°C are presented in Table 3.3.

Figure 3.8 Silver Phthalocyanine

MeN/150°C

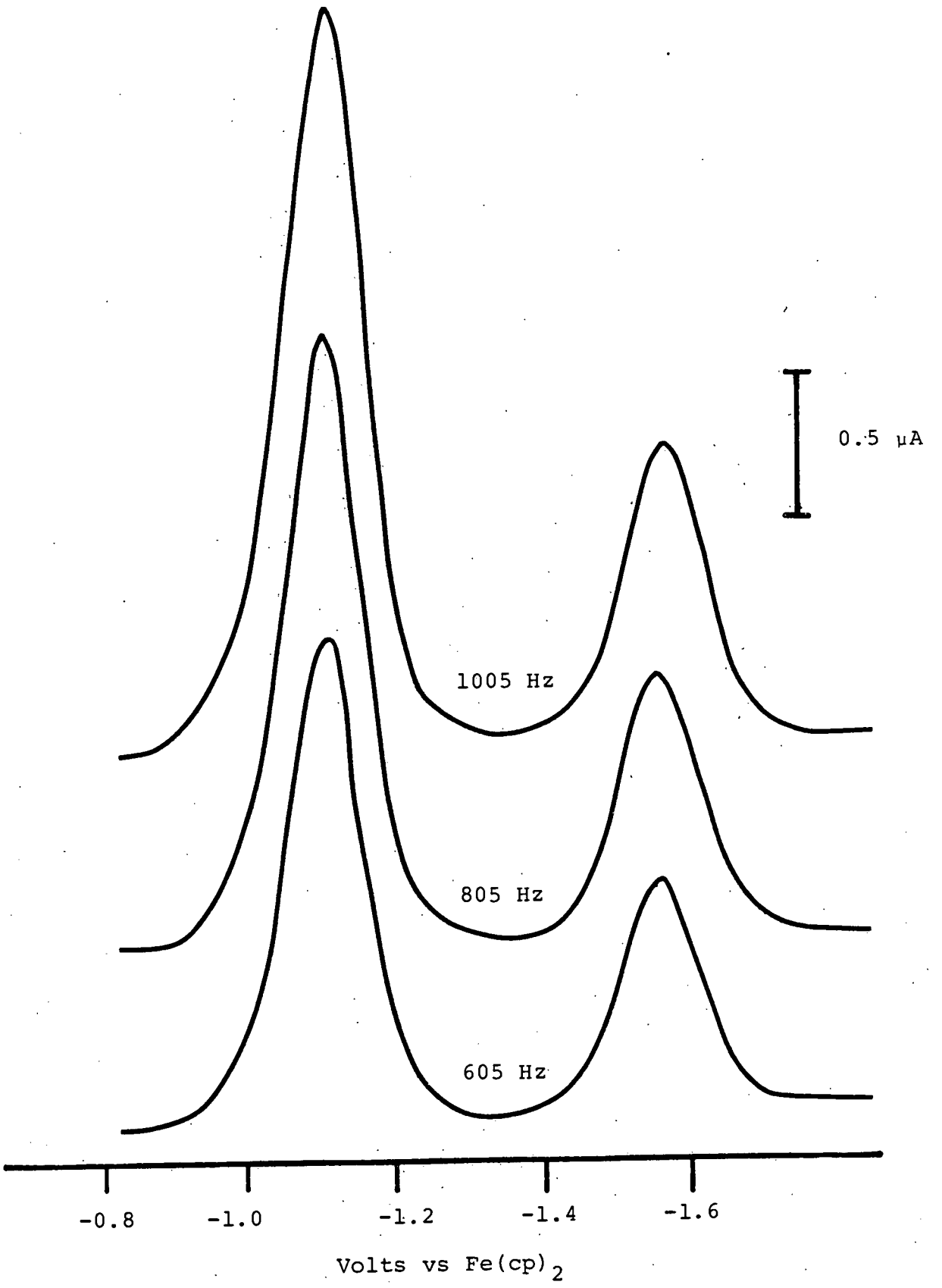

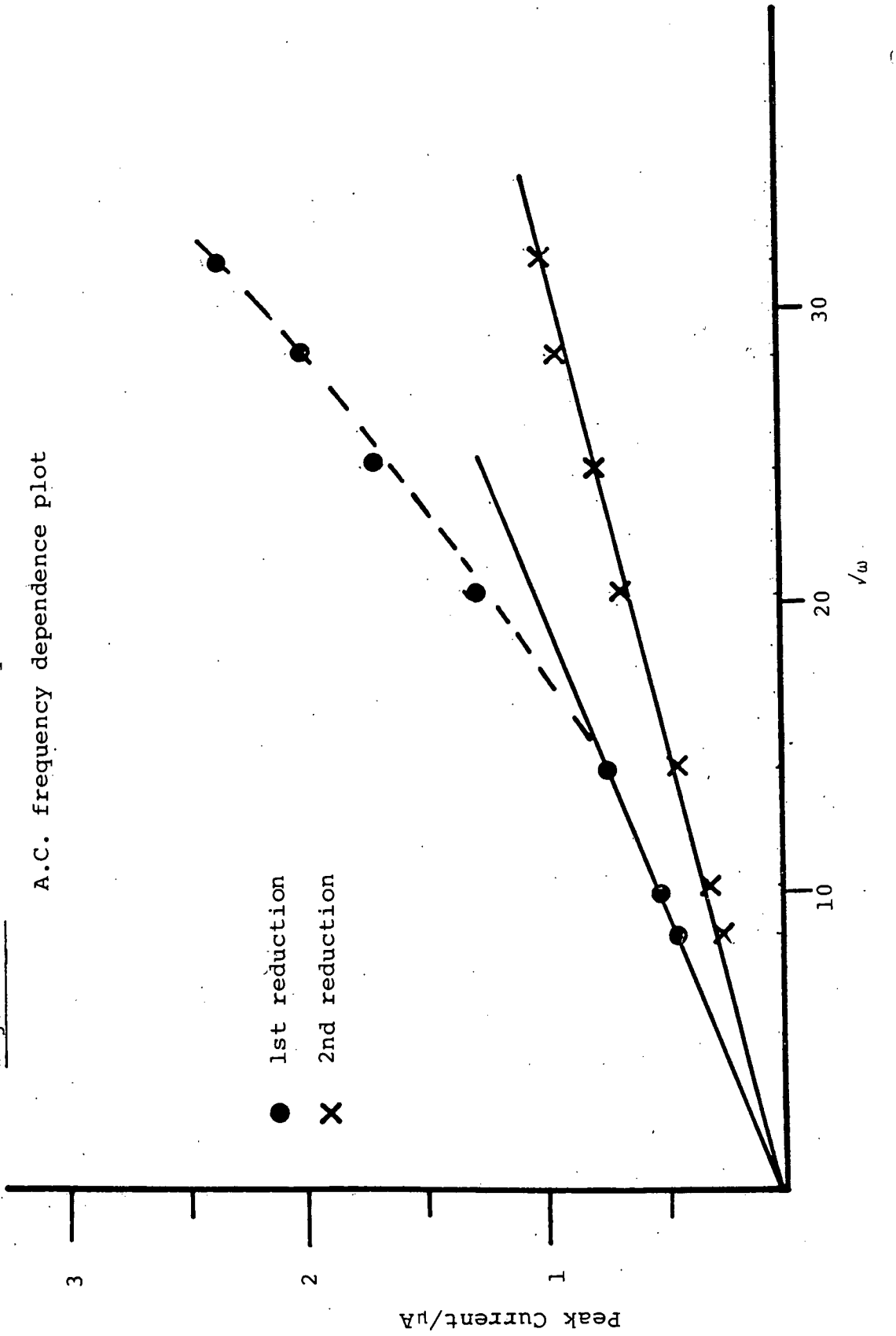

Figure 3.9 Silver Phthalocyanine

A.C. frequency dependence plot

Table 3.3 Reduction Potentials of $[MBu_4Pc]$ (a)

Central Ion	$E_{\frac{1}{2}}(1)$	$E_{\frac{1}{2}}(2)$	$\Delta E_{1,2}$ (b)
H_2	-1.17	-1.66	0.49
Fe	-1.41	-1.72	0.31
Co	-1.20	-2.13	0.93
Ni	-1.32	-1.80	0.48
Cu	-1.30	-1.74	0.44
Zn	-1.39	-1.77	0.38
Mg	-1.60	-	-
Ti(O)	-1.02	-1.44	0.42

(a) Potentials vs $Fe(cp)_2$ in 1.0M $TBABF_4$ in MeN/150°C

(b) $\Delta E = E_{\frac{1}{2}}(2) - E_{\frac{1}{2}}(1)$

In general the compounds also exhibit two well-defined reductions, as typified by the free-base [H_2Bu_4Pc] and copper compound [$CuBu_4Pc$] (Figure 3.10 and 3.11 respectively). Comparison of Figure 3.10 with the cyclic voltammogram and a.c. polarogram of [H_2Pc](Figure 3.3) indicates the larger currents achieved as a result of the greater solubility of the alkylated derivatives.

The reductions were all shown to correspond to diffusion controlled, fully reversible one-electron transfer steps in accord with a.c. frequency dependence and c.v. scan rate dependence measurements. Figure 3.12 shows the a.c. frequency dependence plot for [$ZnBu_4Pc$]. The cyclic voltammetric responce of [$Ti(O)Bu_4Pc$] is seen in Figure 3.13 and the scan rate dependence is plotted in Figure 3.14.

3.3 Discussion

(i) Nomenclature

It is appropriate at this point to outline the nomenclature used to denote the various oxidation states of metal and ligand encountered in the redox processes of metallophthalocyanines (and porphyrins). In the neutral resting state of the majority of the compounds discussed we have divalent metal ion centres in a dianionic ligand, which for convenience is written as [MPc]. In this section a more specific nomenclature is necessary; Pc^{o} specifies the normal dianionic ligand as found in the neutral complexes,

Figure 3.10 Cyclic voltammogram (A) and a.c. polarogram (B) of H_2Bu_4Pc(MeN/150°C

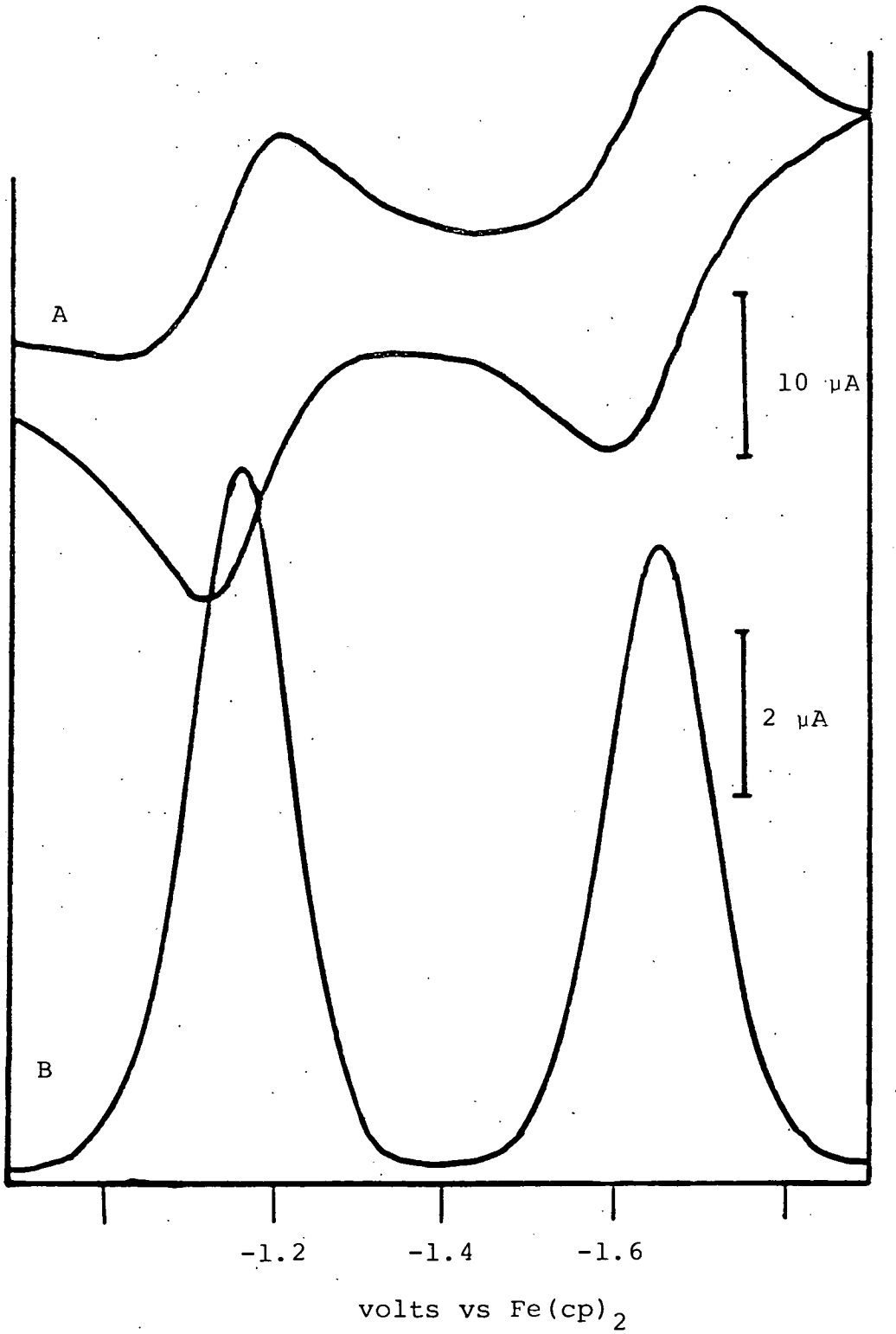

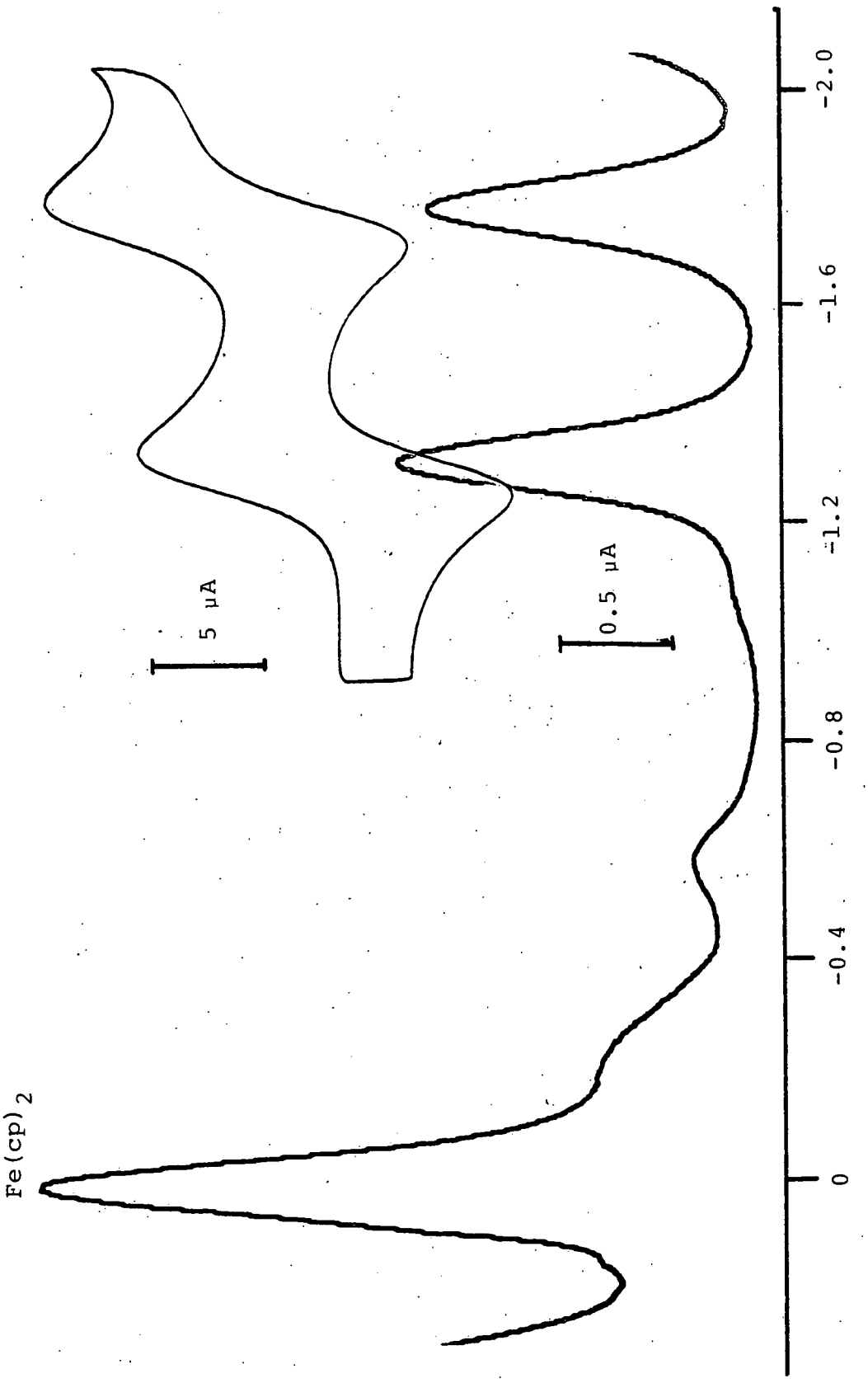

Figure 3.11 Copper tetra(^{t}butyl)Phthalocyanine/MeN/150^{o}C

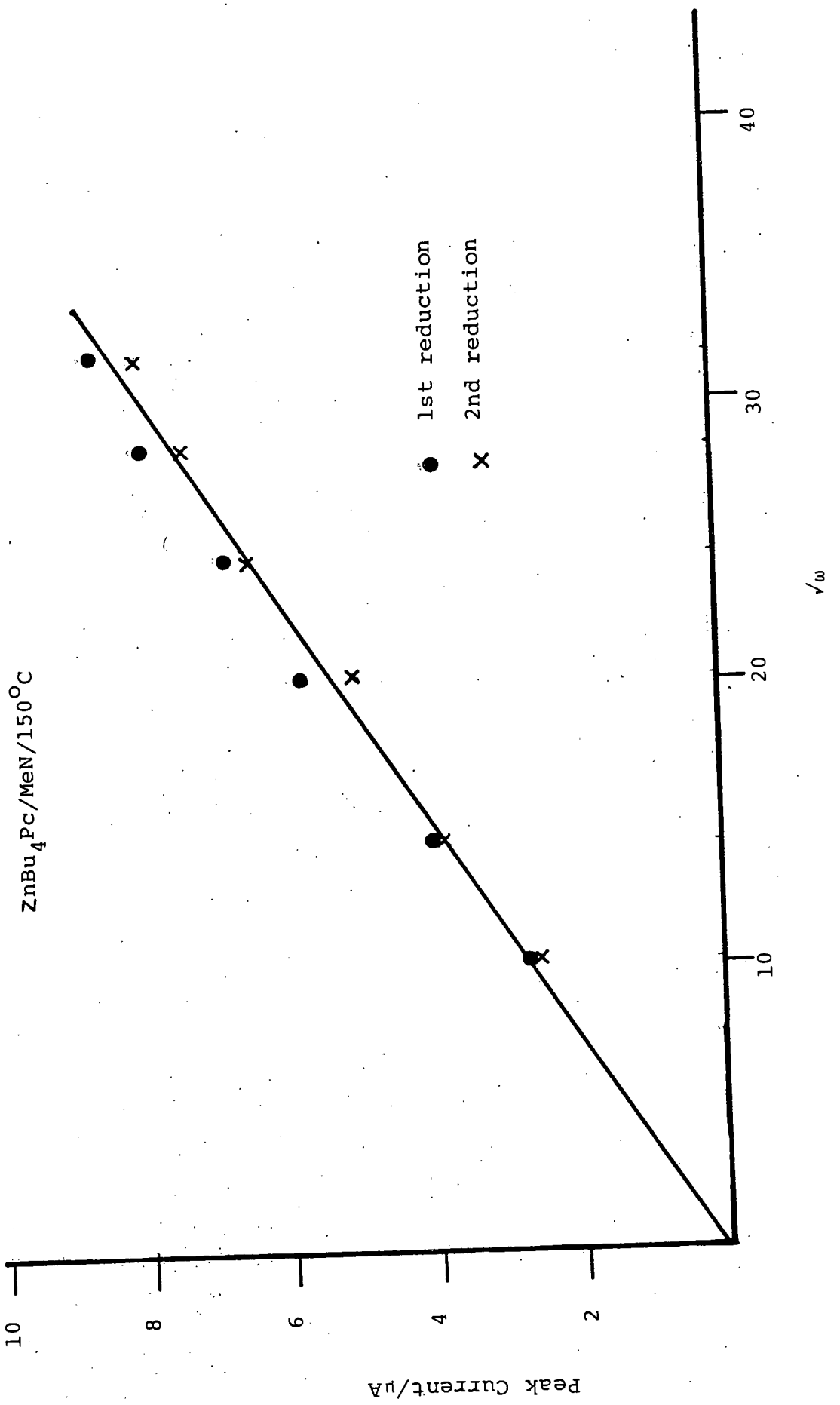

Figure 3.12 A.C. frequency dependence

$ZnBu_4Pc/MeN/150^oC$

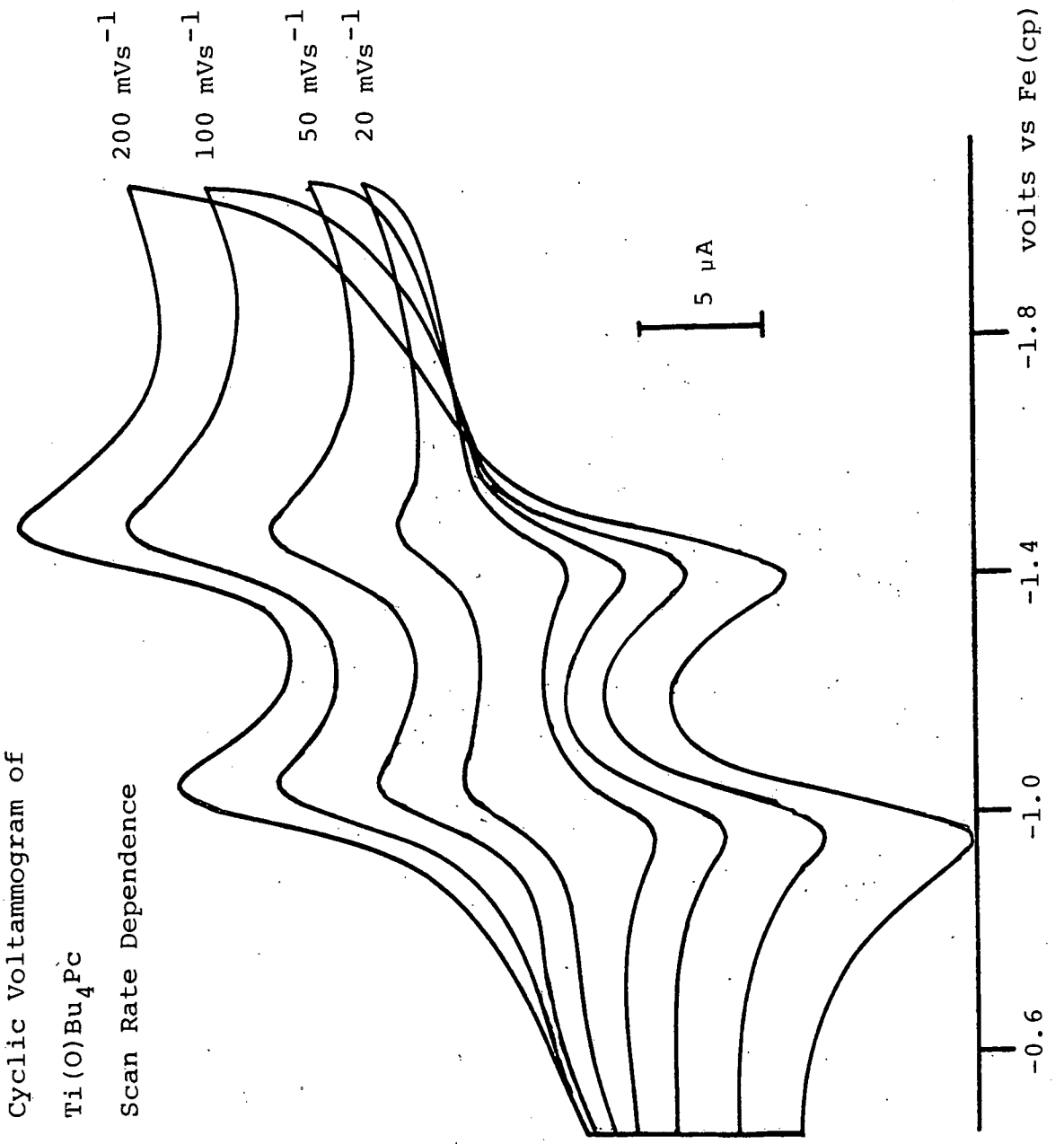

Figure 3.13 Cyclic Voltammogram of $Ti(O)Bu_4Pc$

Scan Rate Dependence

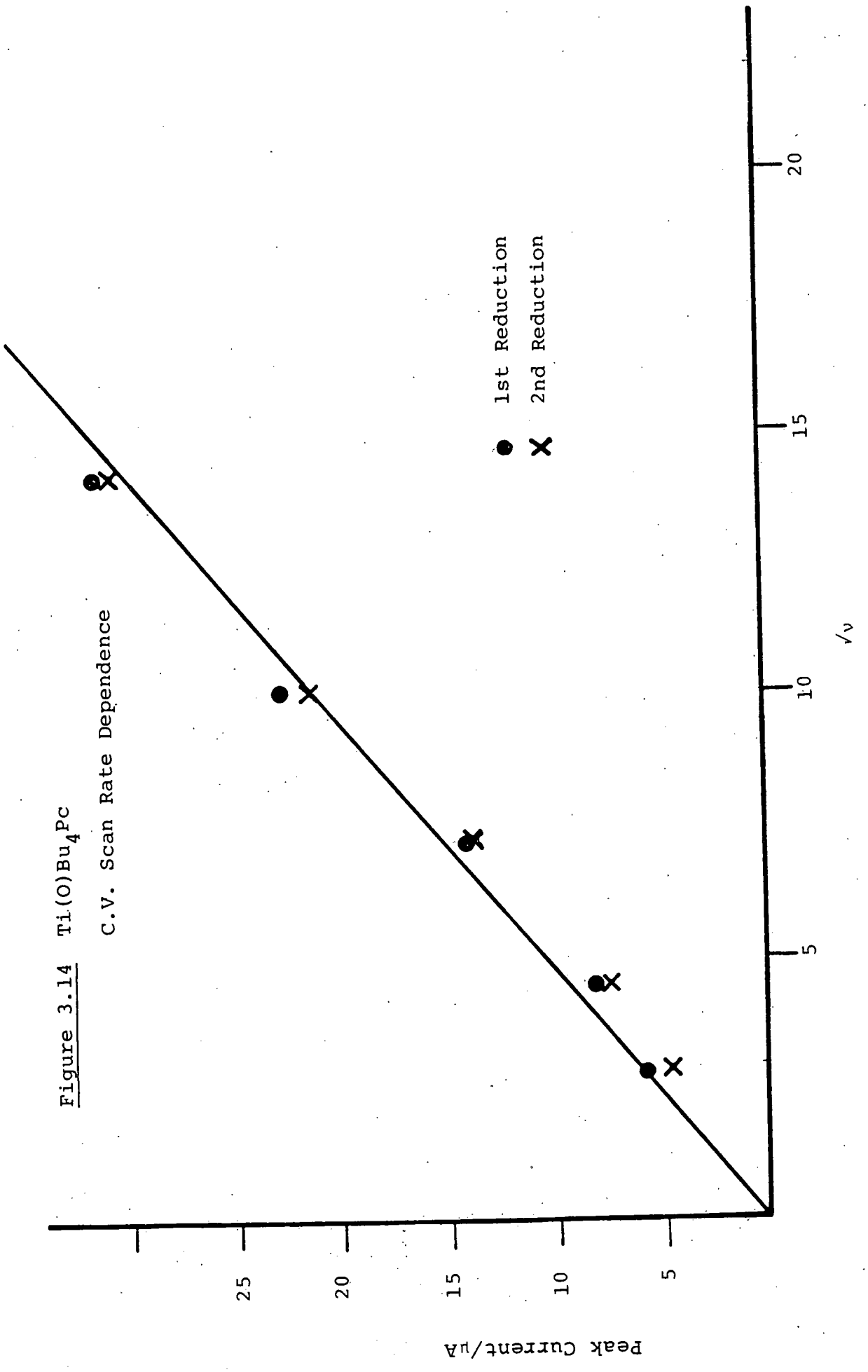

Figure 3.14 $Ti(O)Bu_4Pc$

C.V. Scan Rate Dependence

Pc^- and Pc^{2-} represent successive reduced states of the ligand, and the metal oxidation state (although redundant) is normally given. Thus, as we will show later, [CoPc], i.e. $[Co^{II}Pc^{o}]$, is reduced successively to $[Co^{I}Pc^{o}]^-$ and $[Co^{I}Pc^{-}]^{2-}$ by addition of electrons to metal and then macrocycle. Formulations such as $[CoPc]^-$ denote reduced complexes in which the site of reduction is deliberately unspecified.

(ii) Assignment of Reduction Site

In the transition metal derivatives then the possibility of metal and/or ligand-based reduction exists although clearly only macrocycle reduction can occur in $[H_2Pc]$. The separation of 0.44V between first and second reductions (ΔE) for this compound parallels that of related macrocycles e.g. $[H_2TPP]$ ΔE = 0.42 V[70,71], $[H_2OEP]$ ΔE = 0.40 V[77] and $[H_2(SO_3)_4Pc]Na_4$ ΔE = 0.44 V. This common behaviour is perhaps surprising, given the potentially significant structural distinctions between them. However this gap should be regarded as essentially a reflection of the energy terms relating to the successive addition of two electrons to a degenerate e_g orbital pair, which theoretical calculations have shown to be the L.U.M.O. of both phthalocyanine and porphyrin systems[68,69].

Separations between first and second reductions of this magnitude are therefore widely interpreted as indicative of successive ligand reductions. This behaviour is paralleled in the reductions of the phthalocyanine compounds of the redox-inert metals such as zinc(II), nickel(II) and platinum(II). Thus, the reductions of these and similar derivatives are assigned to electron addition to the macrocycle.

$$[M^{II}Pc] \overset{e^-}{\rightleftharpoons} [M^{II}Pc^{-}]^{-} \overset{e^-}{\rightleftharpoons} [M^{II}Pc^{2-}]^{2-}$$

In the case of the cobalt and iron compounds, then the possibility of metal-based reduction exists. The ΔE value of 0.70 V for [CoPc] is significantly greater than most other values of ΔE implying a different behaviour. (Though Hush's value of ΔE = 1.03 grossly distorts the contrast between [CoPc] and other [MPc] - see Figure 3.1 and later discussion). Of course the Co^{II}/Co^{I} reduction is favoured in a square planar environment, and is well known in porphyrin chemistry. The mono anion $[CoPc]^{1-}$ has been generated in bulk and the visible spectrum[132,133] of this species differs from the typical $[M^{II}Pc^{-}]^{1-}$ spectrum of the copper nickel and zinc mono-anion compounds. E.s.r.[134] and m.c.d.[135] spectra are all consistent with $[Co^{I}Pc^{o}]^{1-}$, yielding a d^8 square-planar configuration. The first reduction of [CoPc] is therefore assigned to metal-based reduction Co^{II}/Co^{I}.

The identity of the second reduction product of [CoPc] is less certain. Iwamoto[87] observed an e.s.r. spectrum for the tetra-sulphonato-substituted dianion which he found consistent with a Co(0) species implying a second metal reduction. This assignment was later questioned[136,137] and it is believed that the species he observed was in fact an oxygen adduct of $[Co^{II}(SO_3)_4Pc]$, analogous to the behaviour of cobalt porphyins[137]. Residual oxygen in the solvent is believed to be the source of this adduct and would explain the difficulty experienced by Rollman and Iwamoto in reproducing the spectrum. Later e.s.r. studies of the unsubstituted dianion were consistent with reduction of the ligand[134], and the accompanying visible spectrum of the $[CoPc]^{2-}$ closely resembled that of $[Zn^{II}Pc^{-}]^{-}$ mono-anion[132] indicating a similar ligand oxidation state in both species. Thus the reductions of [CoPc] in oxygen-free solvent are assigned as

$$[Co^{II}Pc^{o}]^{o} \overset{e^-}{\rightleftharpoons} [Co^{I}Pc^{o}]^{1-} \overset{e^-}{\rightleftharpoons} [Co^{I}Pc^{-}]^{2-}$$

The nature of the reduction steps in iron phthalocyanine is also poorly defined. In an extensive study Clack and Yandle[132] obtained visible spectra for $[MPc]^{Z-}$ ions (Z = 1 to 4, M = Mn, Fe, Co, Ni, Zn, Mg). The spectrum of $[FePc]^{2-}$ was consistent with the formulation $[Fe^{I}Pc^{-}]^{2-}$, but the authors were unable to unequivocally assign the first reduction product as either $[Fe^{II}Pc^{-}]^{1-}$ or

$[Fe^{I}Pc^{o}]^{1-}$ although favouring the former assignment. In their opinion confirmation of the sequence of reduction steps would be provided by accurately known reduction potentials, but Clack and Hush were unable to obtain reliable data for [FePc] in their polarographic study of phthalocyanines in D.M.F.[87]. This is rectified in Table 3.1.

If for the purpose of argument, the first reduction of [FePc] is hypothetically formulated as the anion $[Fe^{I}Pc^{o}]^{-}$ then legitimate comparison may be made with the well-characterised metal-based first reduction of [CoPc]. The greater effective nuclear charge (core charge) of cobalt means that one might expect the Co(II)/Co(I) d^7/d^8 reduction to occur at much more accessible potentials than the corresponding Fe(II)/Fe(I) d^6/d^7 reduction in the same square-planar environment. This conflicts with the experimental result where the first reduction potentials of [CoPc] and [FePc] are nearly equal. Furthermore, if metal reduction occurs as a first step, then the second reduction should be characteristic of phthalocyanine coordinated to a <u>univalent metal</u> ion (as in $[CoPc]^{1-/2-}$) and be considerably more negative than that actually observed for the $[FePc]^{1-/2-}$ couple. Thus we conclude that the first reduction of [FePc] cannot be metal-centred and should be assigned to reduction of the macrocycle. Given this assignment, and the spectroscopic evidence for dianion being $[Fe^{I}Pc^{-}]^{2-}$, then the second reduction should be metal-based, and we formulate the following sequence of reductions.

$$[Fe^{II}Pc] \overset{e^-}{\rightleftharpoons} [Fe^{II}Pc^-]^{1-} \overset{e^-}{\rightleftharpoons} [Fe^{I}Pc^-]^{2-}$$

The ΔE value for FePc is also consistent with two ligand reductions at an Fe(II) centre and this possibility could not be discounted at this stage. Evidence will be presented later to indicate that 'ligand then metal' reduction is the most likely reaction sequence.

While the phthalocyanines used in this work are generally well known and well characterised, the nature of the molybdenum and silver compounds has been defined for the first time in this work as outlined in Section 3.5.

(iii) Comparison with Literature Data

The clearly defined series of reduction potentials observed in our novel high-temperature medium provokes immediate comparison with the results previously obtained at room temperature in conventional solvents for Li[MPc] and $Na_4[M(SO_3)_4Pc]$.

The sequence of first reduction potentials observed in this work, easiest (least negative) to hardest, is

$$H_2 < Co < Cu < Ni < Zn$$

This sequence and the $E_{\frac{1}{2}}(2)$ vs metal ion profile closely parallel that of Rollman and Iwamoto (see Section 3.1).

Comparison of Figure 3.15 with 3.1 reveals a number of significant points. In both this and Iwamoto's study the first reductions of the cobalt are comparable with that of other phthalocyanines. As we confirmed directly at a later stage, they are therefore not far removed in absolute terms from the first reduction potential for cobalt porphyrins, which is unequivocally accepted as a Co(II)/Co(I) process. Hush had reported [CoPc] to have a much easier (approximately 0.5 V) reduction than, for example, [NiPc], paralleling the gap between the first reductions of cobalt and nickel porphyrins.

Also of significance is comparison of the various ΔE values in the three studies. Generally the values obtained by Iwamoto and ourselves are approximately equal while that observed by Clack and Hush is smaller (except for [CoPc]), e.g. $[Ni(SO_3)_4Pc]$ ΔE = 0.49 V, [NiPc] (this work) ΔE = 0.48 V, [NiPc] (Hush) ΔE = 0.38 V.

It is significant that (disregarding [ZnPc]) the second reduction potentials offer better agreement (Figure 3.16) between the results of Hush and other workers, so that the negative deviations in his <u>first</u> reduction potentials are responsible for the inconsistent $\Delta E_{1,2}$ values.

The observations outlined above and the apparent inaccuracies in the data obtained by Clack and Hush can, we feel, be attributed to the strategy used by these workers to attain sufficient concentrations of phthalocyanines in solution. Clack and Hush prepared 10^{-3}M solutions of the

Figure 3.15 Comparisons of Phthalocyanine Reduction Potential

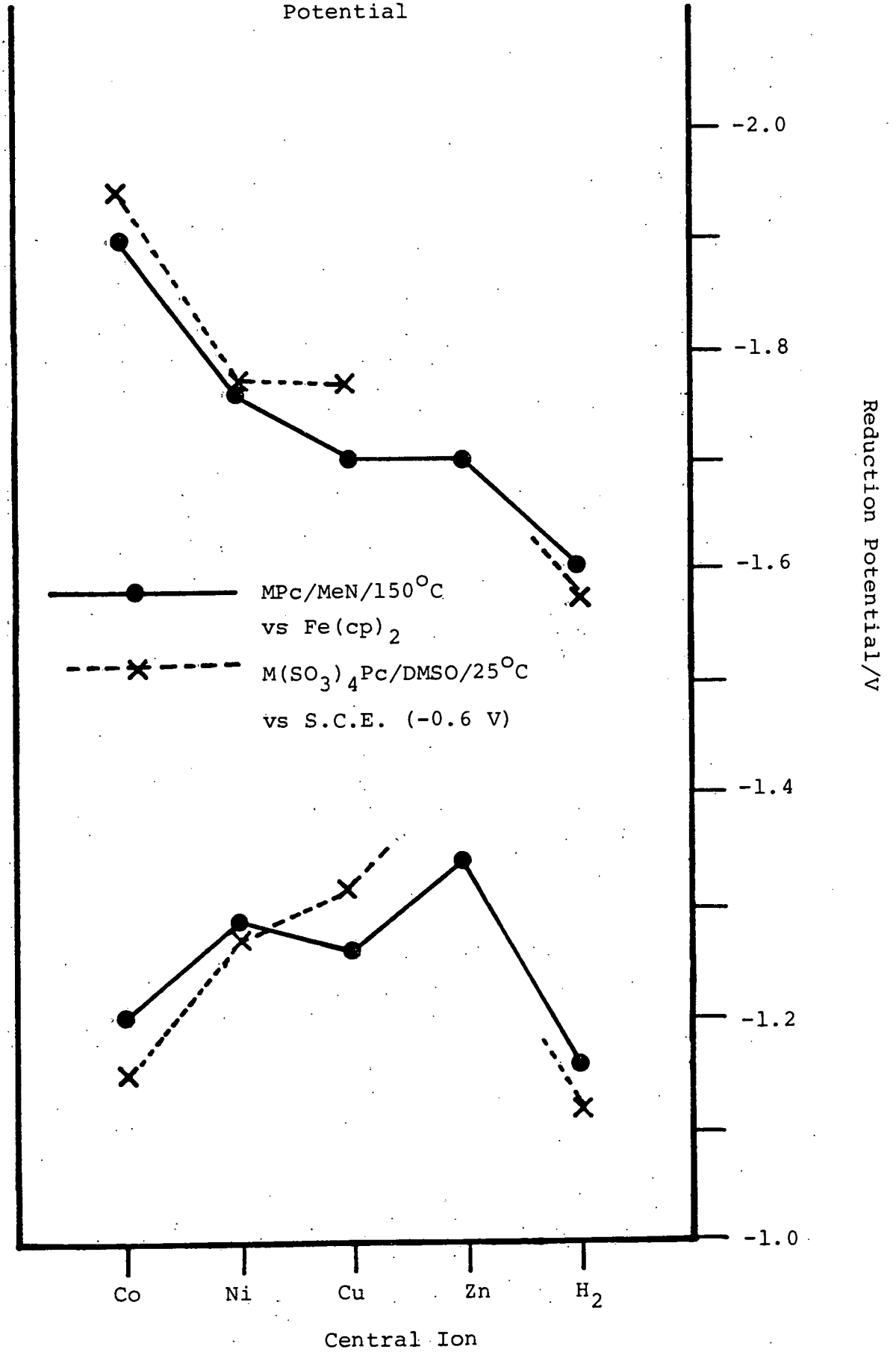

Figure 3.16 Trends in Phthalocyanine 2nd Reduction Potential

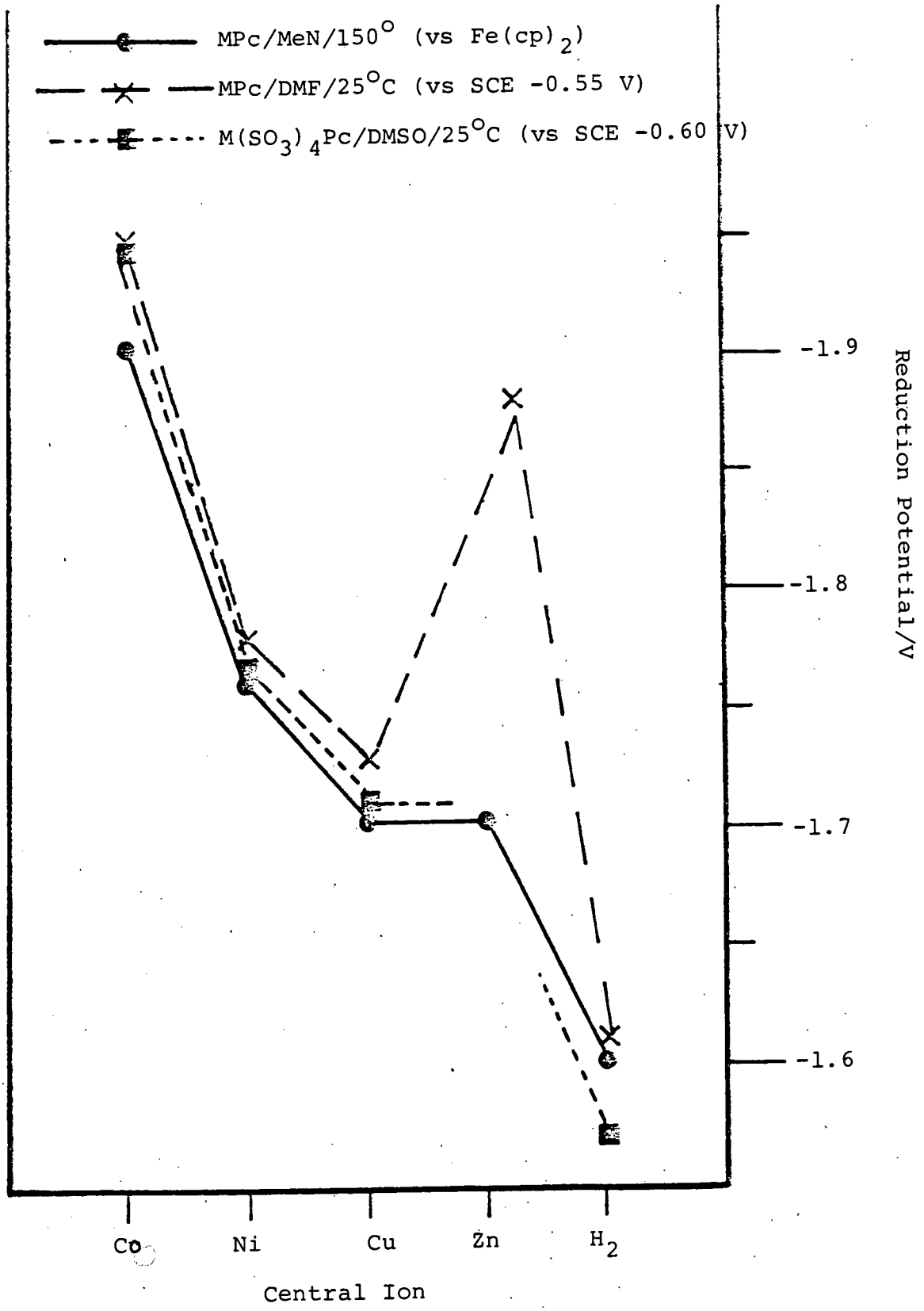

various $Li^+[MPc]^-$ salts, derived by Li reduction of the neutral species. Oxidation of the $[MPc]^-$ mono-anions was observed at potentials which Hush assumed were equivalent to first reduction of the neutral species. However the neutral compounds have a maximum solubility in DMF of approximately 10^{-6}M, about one thousand times less than the level of mono-anion and the prevailing diffusion-limited flux of $[MPc]^o$ at the electrode surface. Hence precipitation at the electrode must be expected. Thus the potentials observed by Hush are <u>not</u> those appropriate to the simple equilibrium $[MPc] + e \rightleftharpoons [MPc]^-$ but are values for this process coupled with the chemical precipitation reaction. This overall process will have a different free energy and hence a less-negative $E_{\frac{1}{2}}$ than the uncomplicated homogeneous redox process. Alternatively, consideration of the Nernst equation requires that in order that a measured potential is equivalent to the standard electrode potential then both members of the redox couple are present in equal concentration in solution. This is clearly not achieved by the method of Clack and Hush and explains the anomalous results reported by these workers. Clack and Hush observed this phenomenon (they saw shifts in first reduction potential with changing concentration of mono-anion used), without fully appreciating its significance.

Such solubility problems are absent when considering the second and subsequent reduction steps and this is reflected in the greater correlation seen in second reduction potentials in Figure 3.16.

Contrasts are also seen in the behaviour of [ZnPc]*. We have observed that in 1-methyl napthalene the second reduction of this compound is of a similar value to that of [NiPc] and [CuPc], while Clack and Hush reported a very cathodic second reduction for this species. We shall show that this is due to axial ligation of the zinc ion by the coordinating solvent, a factor which is absent in our non-polar medium.

We have therefore been able to establish for the first time a definitive series of reduction potentials for a range of unsubstituted phthalocyanines in the high temperature medium, and thus we have been able to evaluate the previously ambiguous data in the literature. The correlation of our results with those of the tetra-sulphonato-derivatives at room temperature is significant since it both validates

---

*Note No voltammetric data were presented for $[Zn(SO_3)_4Pc]$ by Rollman and Iwamoto. The compound was reported by Fukada[145] and later reported in solution, but not isolated, by Fallab[146]. Despite intensive effort we have been unable to isolate this compound by Fukada's method in this laboratory[147].

Iwamoto's pioneering study and implies that our more novel techniques have not induced any great perturbation in redox behaviour of the compounds.

In the light of this it is very significant to compare the reduction potentials obtained recently for the [MBu_4Pc] compound in Table 3.3 with the data in Table 3.1. It is evident that the reduction potentials for the [MBu_4Pc] derivatives are fairly consistently shifted to more negative values (on average by 50 mV) compared to the corresponding [MPc] as shown in Figure 3.17 The shift is generally seen in both $E_{red}(1)$ and $E_{red}(2)$, as is expected for successive ligand-based reductions where butyl substitution would raise the energy of both acceptor orbitals equally. Exceptions are however noted. The first reduction potentials of [CoPc] and [$CoBu_4Pc$] are identical. Given that this is a metal-based reduction then alkyl substitution at the ligand should exert only a slight second-order effect on the redox couple. However in the second (ligand-based) reduction of cobalt phthalocyanines, butyl substitution shifts the reduction potential from -1.90 V to -2.10 V.

In contrast to this, in iron phthalocyanines the first reduction is shifted by 120 mV while the second is shifted by only 30 mV. This strongly suggests ligand reduction followed by metal reduction, as postulated earlier. Thus the independent evidence sought by Clack and Yandle[132] is provided by the present investigation.

Figure 3.17 Phthalocyanine Reduction Potentials/MeN/150°C

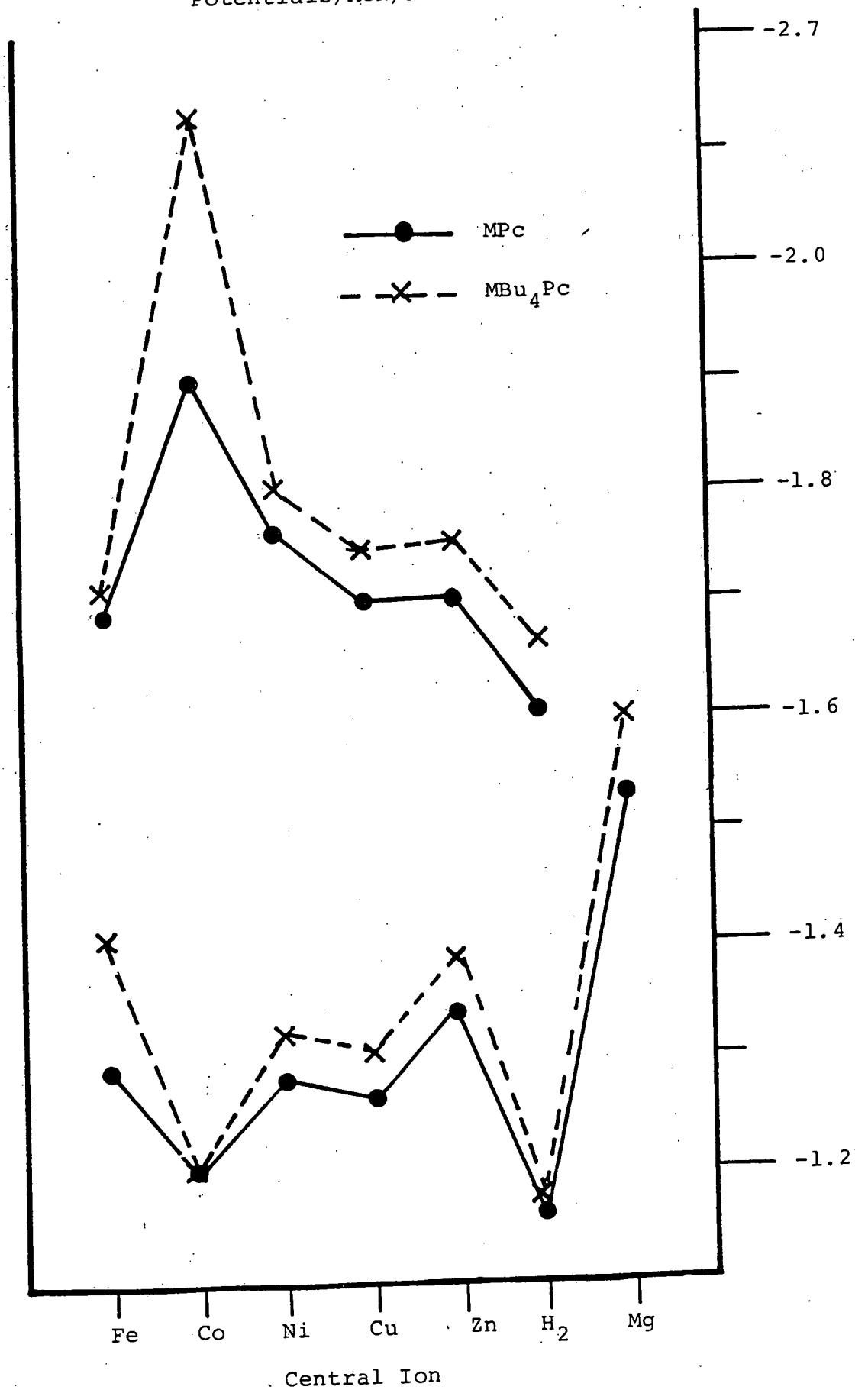

Thus the data obtained for these more soluble derivatives clearly confirm our original results for the unsubstituted compounds and vindicate our assignments of ligand or metal-based electron transfer.

The enhanced solubility of [MBu_4Pc] derivatives in a variety of media has allowed us to extend our studies to other, more conventional solvents as described below.

3.4 Electrochemistry of Phthalocyanines at Ambient Temperatures

Extension of this work on phthalocyanines to studies at ambient temperatures was desirable since it was essential to determine whether the redox behaviour seen at 150°C would be paralleled at lower temperatures. Clearly this was impossible using the unsubstituted compounds and, while Rollman and Iwamato had produced definitive data for the [$M(SO_3)_4Pc$] series in D.M.S.O. at room temperature, there are limitations on the extent and usefulness of these results.

The solvent of choice for room temperature experiments was dichloromethane (0.2 M $TBABF_4$ as supporting electrolyte). This essentially non-coordinating medium was found to offer solubility of both electrolyte and substrate for routine electrochemical work.

The familiar reductive behaviour established at elevated temperature is equally evident in this medium, the compounds exhibiting two fully reversible one electron reduction steps whose E^o values are presented in Table 3.4.

Table 3.4 Reduction Potentials of MBu_4Pc at 25^oC[a]

Central Ion	Reduction Potential[b]		
	$E_{\frac{1}{2}}(1)$	$E_{\frac{1}{2}}(2)$	ΔE
H_2	-1.17	-1.59	0.42
Fe	-1.40	-1.75	0.35
Ni	-1.34	-1.76	0.42
Cu	-1.31	-1.71	0.40
Zn	-1.385	-1.735	0.35
Ti(O)	-1.02	-1.405	0.385

(a) CH_2Cl_2/0.2M $TBABF_4$

(b) vs $Fe(cp)_2$

Comparison of this data with that obtained at 150°C (Table 3.3) shows remarkable consistency. Reduction potentials measured at 25°C in CH_2Cl_2 are almost identical with those observed at 150°C in MeN, apart from a slight consistent contraction in ΔE at the lower temperature.

The excellent correlations between the two sets of data has justified our unconventional approach to the problem of determining the electrochemical behaviour of the insoluble phthalocyanine pigments and has shown that the substituted naphthalenes provide, at elevated temperatures, an environment closely matching that of well established non-coordinating electrochemical solvents.

3.5 Characterisation of Silver and Molybdenum Phthalocyanines

(i) Silver Phthalocyanine

The compound has been variously formulated as a genuine Ag(II)[140] complex or as hydrogen silver(I)phthalocyanine[139]. Two groups have carried out e.s.r. studies on this compound. Kholmogorov and Glebovsky[139] identified the complex as diamagnetic, implying a silver(I) species. MacCragh and Koski[140] on the other hand observed lines in the e.s.r. spectrum which they regarded as characteristic of silver(II).

Our observation that the first reduction of silver phthalocyanine occurs at a more positive potential than $[H_2Pc]$ rules out the possibility that the process is a

ligand reduction of [Ag(II)Pc], since this would be expected to parallel other simple divalent metal complexes and reduce at potentials more negative than [H_2Pc].

This reduction potential is also inconsistent with Ag^{II}/Ag^{I} reduction since, as we shall demonstrate later, in the case of a genuine Ag^{II} porphyrin metal reduction occurs at potentials considerably more negative than seen here.

Further, if the first step was metal reduction then the second reduction would be that of ligand at a univalent metal centre and, as is found for [CoPc], we would expect a $\Delta E_{red}(1,2)$ value substantially greater than that actually observed for silver phthalocyanine (0.45 V).

This electrochemical evidence is therefore consistent with the formulation [Ag(H)Pc] and is reinforced by other physical studies outlined below.

Visible spectroscopy is a powerful technique in phthalocyanine chemistry. Phthalocyanine, which is of the symmetry group D_{2h}, shows an intense twin-band spectrum in the region 13,000 - 16,000 cm^{-1}, whereas typical metal phthalocyanines having the higher symmetry D_{4h} show only one band in this region. Figure 3.18 compares the visible spectra of [H_2Pc], [ZnPc] and silver phthalocyanine in 1-methylnaphthalene solution. It is readily apparent that the silver compound has a spectrum more akin to [H_2Pc] than to a simple divalent metal complex suggesting a relatively low molecular symmetry. We have observed a weak but distinct band

Figure 3.18 Phthalocyanine Visible Spectra

MeN solution, 25°C

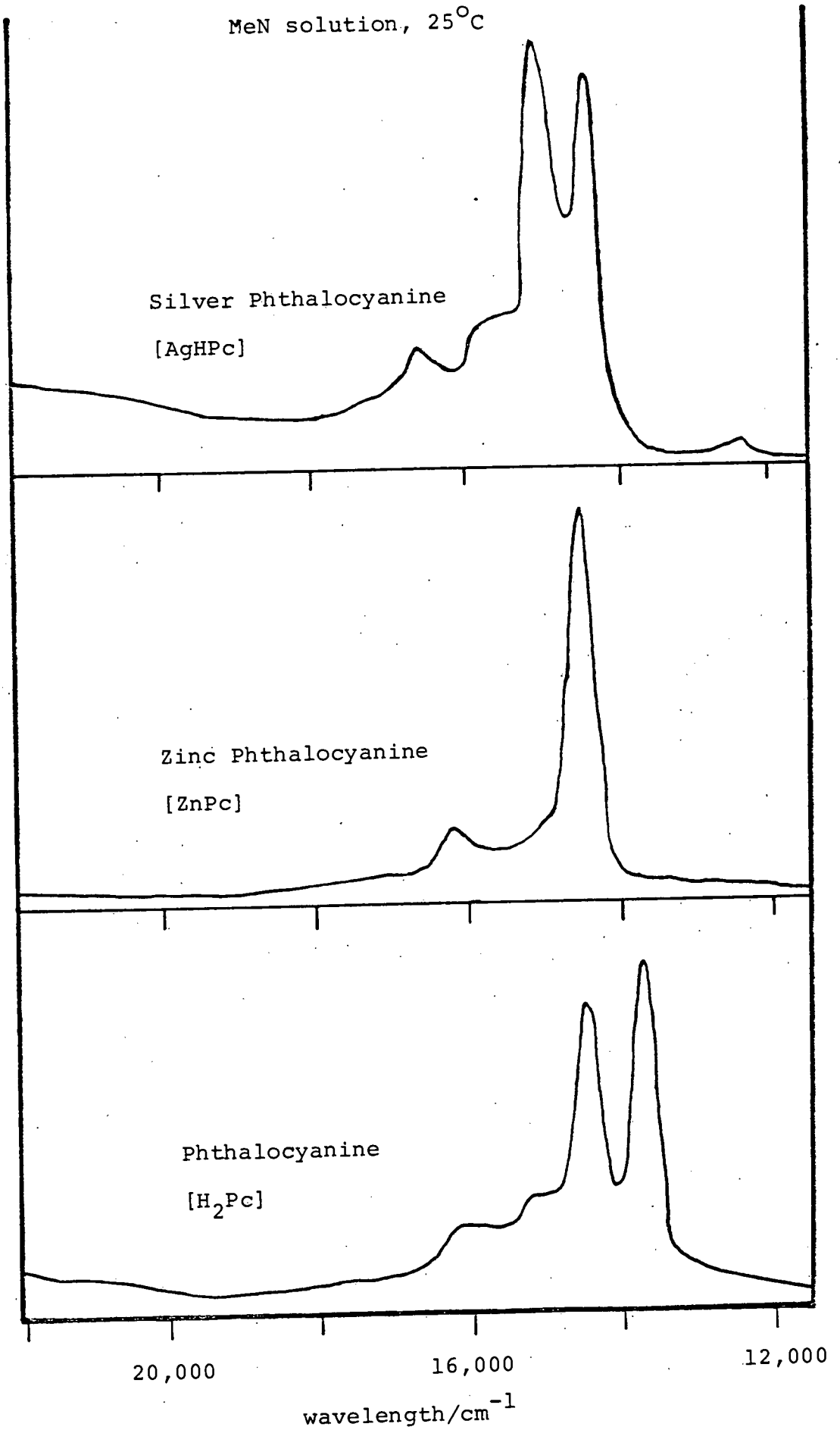

at 3280 cm^{-1} in the infra-red spectrum of the silver complex which is consistent with an N-H stretch and is in a region which is featureless in simple-divalent [MPc] complex. (We have previously established the existence of a similarly distinct ν_{N-H} band in [H_2Pc].

Thus the combined evidence (electrochemical, visible and i.r. spectral) is inconsistent with simple [AgPc] and strongly favours the formulation of this compound as [AgHPc].

(ii) Molybdenum Phthalocyanine

Such derivatives have been mentioned in the literature on a number of occasions[141] but full characterisation has never been achieved. In particular, Sharp and Moss[141] report the formation of a polymeric oxymolybdenum phthalocyanine from the reaction of phthalonitrile with molybdenum dioxide at 260°C.

A number of possible structures for molybdenum phthalocyanine can be formulated. Apart from the possibility of simple [MoPc], there are a variety of oxy-molybdenum species possible as shown below.

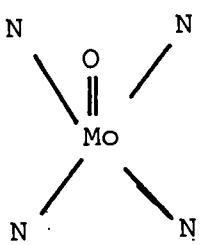

$Mo^{IV}(O)Pc$

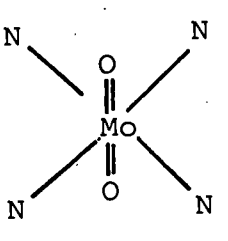

$Mo^{VI}(O)_2Pc$

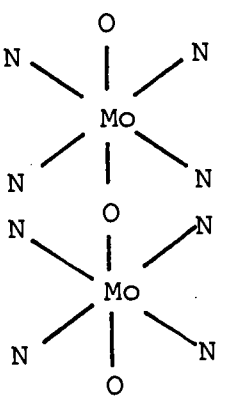

$[Mo^{IV}OPc]_n$

We note firstly that reduction potentials of molybdenum phthalocyanine are less negative than those of [H_2Pc] (or any known [MPc]) and thus militate against a simple [MoPc] structure.

Also the solubility of this compound, like V(O)Pc, is greater than that of simple divalent [MPc] species. Further, a band is present in the infra-red spectrum (KBr disc) of molybdenum phthalocyanine at 970 cm^{-1} which is not found in simple [MPc] species[141] (Figure 3.19). This is consistent with an M=O stretch[142] and is again analogous to the V=O stretch in V(O)Pc [143].

Unfortunately the distinction between Mo^{IV}=O and O=Mo=O on the basis of the i.r. spectrum is not clear cut though the former is preferred.

Differentiation between the two was made on the basis of the mass spectrum. This showed a parent ion peak at m/e = 626 consistent with [Mo^{IV}(O)Pc], with no sign of peaks corresponding to the dioxy compound at m/e = 642 or any other $Mo(O)_2$ fragments. We therefore assign "molybdenum phthalocyanine" as having the proper formulation [Mo^{IV}(O)Pc]. In accord with this, voltammetry shows a facile oxidation of the compound which is attributed to the Mo^{IV}/Mo^{V} couple (impossible for the Mo^{VI} formulation).

Figure 3.19 Infra Red Spectra of Phthalocyanines

KBr Disc/1200-650 cm^{-1}

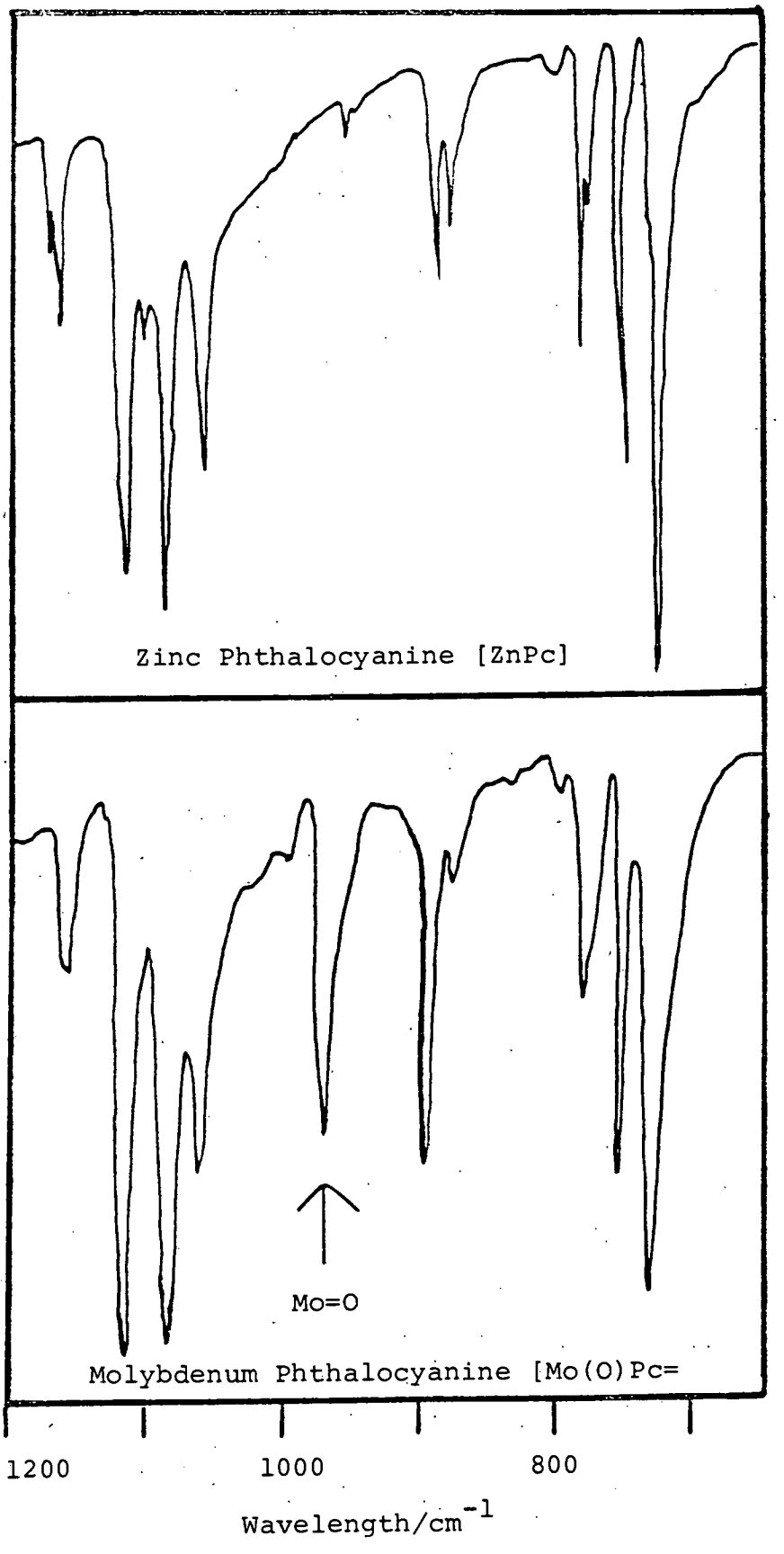

CHAPTER 4

Direct Comparison of Phthalocyanine and Porphyrin Cathodic Behaviour

4.1 Introduction

Having evaluated the order of phthalocyanine reduction potentials in a novel experimental medium we felt it significant to examine porphyrin compounds under the same conditions. This would enable direct comparison of the two macrocyclic systems in the same medium (which has not been achieved hitherto), and, in addition would provide an opportunity for comparing the extensive body of data on porphyrins obtained at room temperature in conventional solvents with the results obtained in our unusual high temperature solvent (with its particular advantages as a non-coordinating medium). A series of metallotetraphenylporphyrins (MTPP) and metallooctaethylporphyrins (MOEP) were therefore investigated by voltammetry in 1-methylnaphthalene solution at elevated temperature.

4.2 Results

(a) Metallotetraphenylporphins [MTPP]

Preliminary investigations on those compounds were carried out at Stirling University[148] in methylnaphthalene solution at 150°C using the methods outlined in Chapter 2. The compounds undergo two reductions, as typified by the copper compound (Figure 4.1). The reduction steps were shown in each case to correspond to diffusion-controlled, fully reversible one-electron transfers. As before cross-referencing experiments involving mixtures of two or more compounds were used to accurately determine the reduction potentials, and these are presented in Table 4.1.

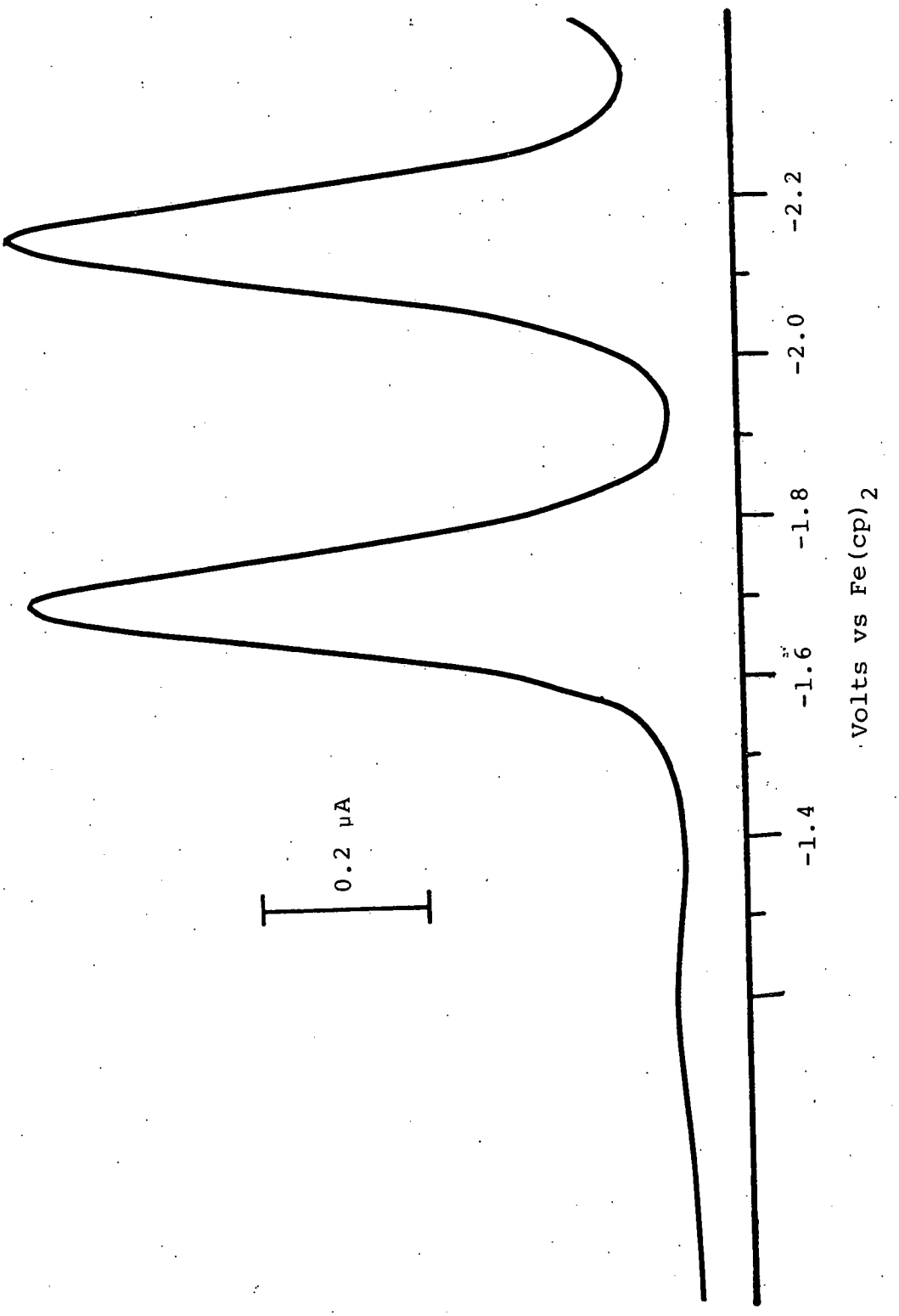

Figure 4.1 A.C. polarogram
CuTPP/MeN/150°C

Table 4.1 Reduction Potentials of meso-Tetraphenylporphins in Methyl Napthalene

Tetraphenylporphins[148]

Central Ion	Reduction Potential[a]		
	$E_{\frac{1}{2}}(1)$	$E_{\frac{1}{2}}(2)$	ΔE
H_2	-1.59	-1.99	0.40
Co	-1.29	-2.40	1.11
Ni	-1.67	-2.22	0.55
Cu	-1.70	-2.15	0.45
Zn	-1.75	-2.16	0.41
Mg	-1.89	-	-
Ag[b]	-1.45	-2.17	0.72

(a) MeN/1M TBAP/150°C vs $Fe(cp)_2$

(b) this work

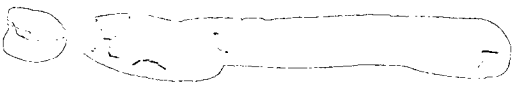

The characteristic ΔE value observed for the H_2, Ni, Cu and Zn compounds is taken as indicative of successive ligand-based reductions. This is in agreement with voltammetric results obtained by Felton and Linschitz[70,71] and confirmed by their e.s.r. and visible spectroscopic studies of the reduced species.

The distinctly easier reductions of the cobalt and silver compounds can be attributed to metal-centred processes. First reduction potentials for both these compounds are less negative than that of the free base. The Co^{II}/Co^{I} reduction is now well characterised in the literature[70,71,81]. The second reduction, being that of the ligand coordinated to a univalent metal centre, requires a very cathodic reduction potential.

$$[Co^{II}TPP^{o}] \overset{+e}{\rightleftharpoons} [Co^{I}TPP^{o}]^{-} \overset{+e}{\rightleftharpoons} [Co^{I}TPP^{-}]^{2-}$$

A similar pattern of redox-activity is seen for [AgTPP], a genuine Ag(II) compound prepared by the method of Dorough, Miller and Huennekens[149], and this is likewise attributed to initial metal-reduction followed by ligand-reduction.

(b) Metallooctaethylporphyrins [MOEP]

The reduction potentials of these compounds were obtained using our well established techniques and are tabulated in Table 4.2.

Table 4.2 Reduction Potentials of Octaethylporphyrins in Methyl Naphthalene

Central Ion	Reduction Potential[a]		
	$E_{\frac{1}{2}}(1)$	$E_{\frac{1}{2}}(2)$	ΔE
H_2	-1.78	-2.28	0.5
Fe(III)(Cl)	-0.77[b]	-1.65	0.78
Co(III)(py)(Br)	-0.64[b]	-1.44	0.80
Ni	-1.82	-	-
Cu	-1.91	-	-
Zn	-1.99	-	-

(a) MeN/1M $TBABF_4$/150°C vs $Fe(cp)_2$

(b) Irreversible, see text

The reductions of these species were observed to occur at potentials approximately 0.2 V more negative than the corresponding [MTPP], a shift which is in accord with the cumulative inductive effect of the eight ethyl groups. As a consequence of this, second-reduction potentials were rarely observed in the available potential range, indeed few have been recorded in the literature. (In contrast important oxidation steps were accessible for several compounds of the MOEP series; these will be discussed in Chapter 6).

The reductions of the H_2, Ni, Cu and Zn compounds, which are ligand-based, were all shown to be diffusion-controlled, fully reversible one-electron transfers. The compounds [Fe(Cl)OEP] and [Co(Br)(py)OEP] however, both exhibited an irreversible first reduction followed by a second reversible one, as illustrated in the cyclic voltammogram of [Fe(Cl)OEP] in Figure 4.2.

The reduction steps of iron porphyrins have been discussed by several workers. Iron protoporphyrins[78,83], tetraphenylporphins[79(a),(b)] and octaethylporphyrins[77,80(d)] have all been investigated, and the reduction assigned as Fe(III)/Fe(II). Kadish and Bottomley[80(d)] studied [Fe(Cl)OEP] in CH_2Cl_2 and observed an irreversible reduction at -0.53 V together with a reversible reduction at -1.29 V (both *vs.* S.C.E.). The separation of 0.76 V between these reductions is in excellent agreement with the value of 0.78 V observed in this work. The addition of chloride ion to solutions of [Fe(Cl)OEP] resulted in the appearance of

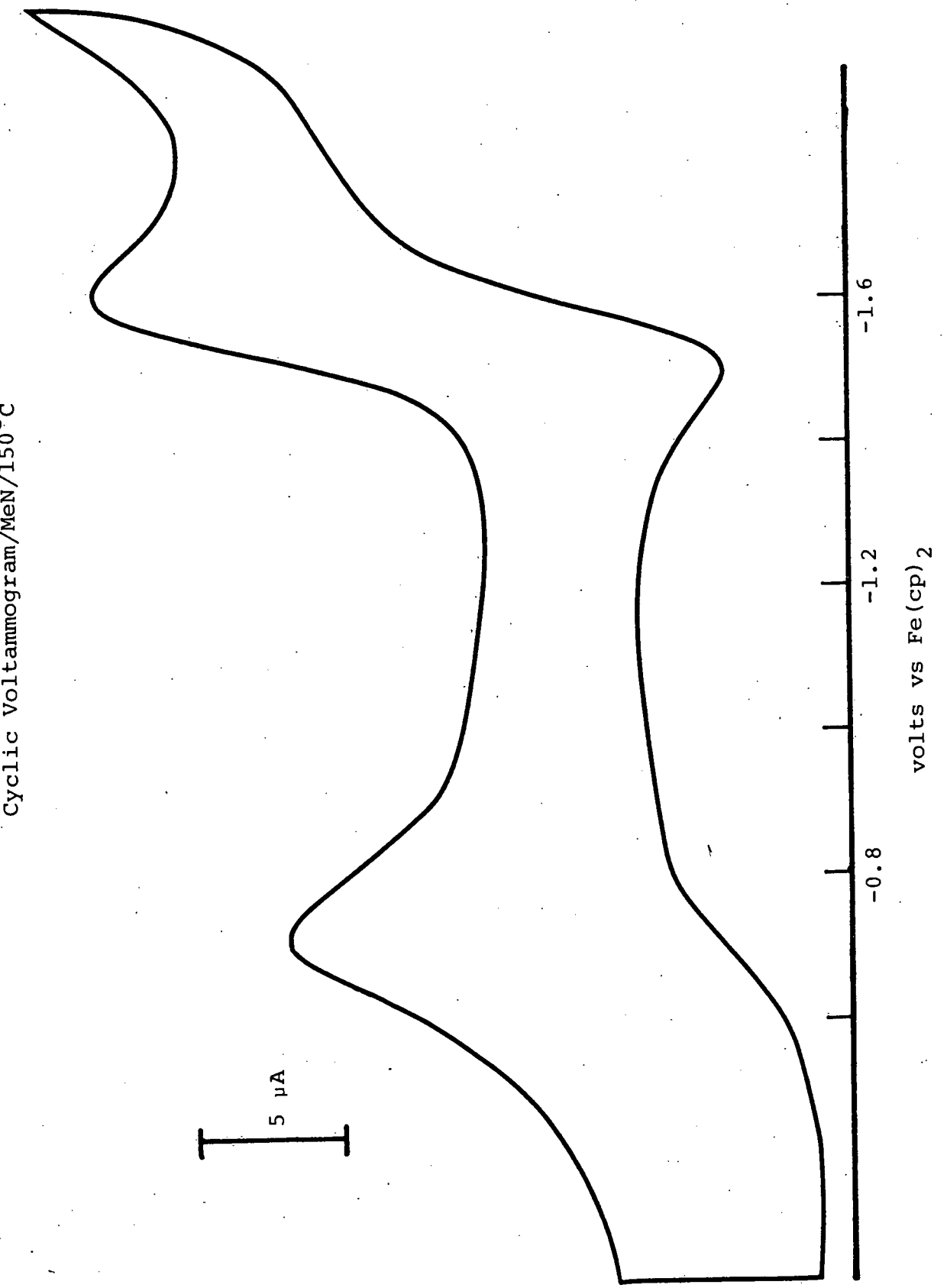

Figure 4.2 Fe(Cl)OEP

Cyclic Voltammogram/MeN/150°C

a defined re-oxidation wave associated with the first reduction. This implies that upon reduction halide is expelled from [Fe(Cl)OEP].

The second step is then the reduction of [FeOEP]. This reduction is less negative than that associated with the reduction of the ligand at a typical divalent metal centre or even of [H_2OEP] itself. This implies a further metal-base reduction has occured, i.e. Fe^{II}/Fe^{I}. This is in agreement with e.s.r.[80(a),150] and visible spectroscopic[79(a)] evidence identifying Fe^{I} in porphyrin anions. Therefore the reduction steps of the compound may be summarised as follows.

$$[Fe^{III}(Cl)OEP] \xrightarrow[-Cl^-]{+e} [Fe^{II}OEP^{o}] \overset{+e^-}{\rightleftharpoons} [Fe^{I}OEP^{o}]^-$$

This behaviour is substantially different from that of [FePc], where the ligand reduction preceeds Fe^{II}/Fe^{I} reduction. This is caused by the relatively inaccessible π^* orbitals of the porphyrin ligand lying above the unfilled metal d-orbitals while in iron phthalocyanines the π^* orbitals lie below.

$[Co^{III}(Br)(py)OEP]$ behaves analogously to $[Fe^{III}(Cl)OEP]$, and a similar Co^{III}/Co^{II} and Co^{II}/Co^{I} reduction sequence is assigned to first and second reductions of this compound.

4.3 Discussion

Our interest focussed initially on the comparison of the two sets of porphyrin data obtained at high temperature. Figure 4.3 presents the relative trends in first reduction potentials for the [MTPP] and [MOEP] series at 150°C in 1-methylnaphthalene solution. The "metal ion dependence profiles" for the two sets of data show remarkably close correlation indicating that, as expected, each metal ion has essentially the same effect on both TPP and OEP reduction potentials, irrespective of the absolute reduction potential of the ligand.

From this highly consistent data we are able to determine the effects of meso-tetraphenyl and β-pyrrole-octaalkyl substitution patterns. In absolute terms, the effect of alkyl substitution is to shift the reduction potentials by 210 mV to more negative potentials. The phenyl groups are each, of course, orthogonal to the ring, and hence no appreciable interaction between the π systems of the substituents and the porphyrin nucleus occurs. It should be noted however, that in the case of the cobalt porphyrins [CoTPP]/[CoOEP] the potential shift is significantly smaller than generally found. This is a reflection of the metal-based nature of this reduction process.

Having established the self-consistency of results obtained for the two porphyrin systems in our unfamiliar medium, it is appropriate to compare our data with the extensive data in the literature obtained at room temperature in

Figure 4.3 Trends in Porphyrin Reduction Potential MeN/150°C/vs $Fe(cp)_2$

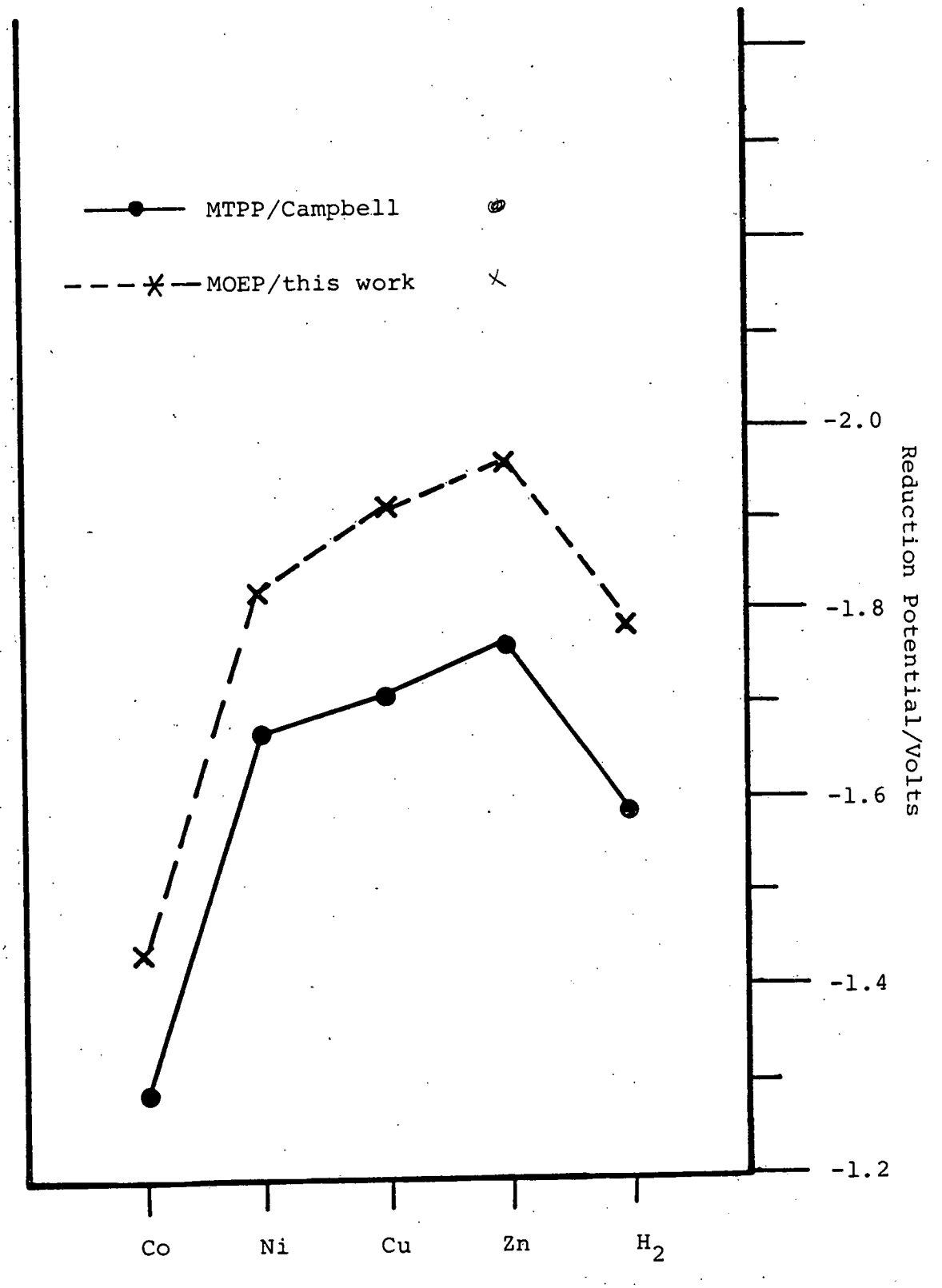

conventional solvent systems. This should provide clear-cut information on any specific temperature effects, and on solvation and coordination phenomena.

(a) Tetraphenylporphins

The single most comprehensive study of the [MTPP] compounds was that of Felton[70,71]. He observed two reductions for these complexes in dimethylformamide or dimethylsulphoxide solution. Figure 4.4 shows the trends in [MTPP] reduction potentials observed by Felton, and by Campbell[148] in MeN at 150°C. Excellent correlation is seen between the two data sets. This, again indicates that our novel experimental technique produces no gross distortion of the redox chemistry of these macrocycles and, further, that no appreciable temperature effects are present.

The greatest deviation between the two sets of data lies in the reduction potentials of [ZnTPP]. Our work indicates that both reduction potentials of this compound are relatively less negative (approximately 70 mV) than those values observed by Felton. As will be discussed later in this chapter, this cathodic shift follows as a result of specific axial coordination of the zinc ion by the dimethyl-sulphoxide solvent used in Felton's study. This underlines the value of solvent systems like methylnaphthalene where such coordination effects are minimised.

Figure 4.4 MTPP Reduction Potentials

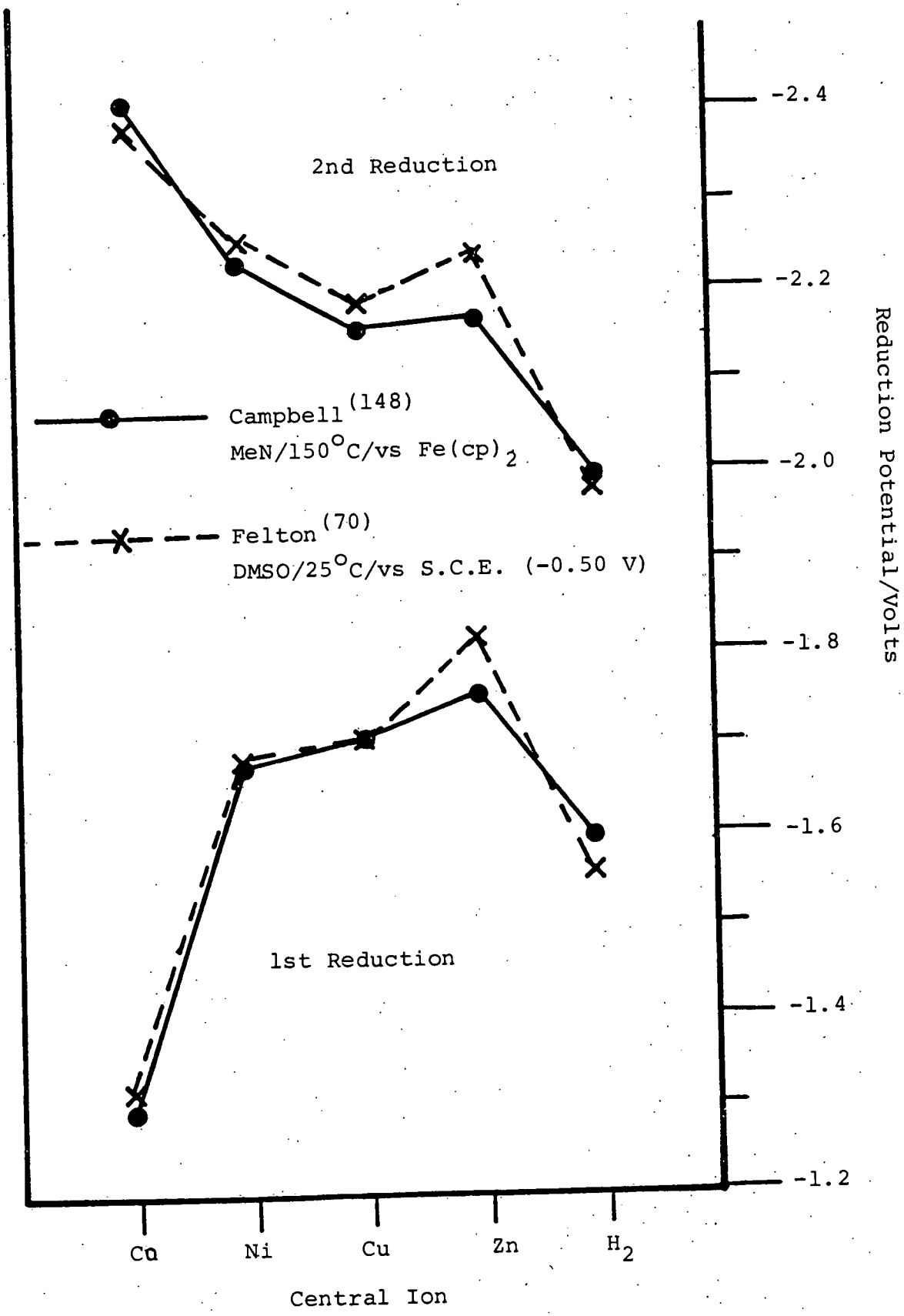

(b) Octaethylporphyrins

The work of Fuhrhop, Kadish and Davis[77] represents the most definitive study of the octaethylporphyrins to date, the solution redox chemistry of some twenty-five compounds being studied by cyclic voltammetry.

Figure 4.5 compares the relative trends in first reduction potential observed by us, and by Fuhrhop, Kadish and Davis. While the overall trend indicates good agreement between the two sets of data, there are certain deviations.

Fuhrhop et al report the first reduction of [CuOEP] to occur at potentials less negative than [NiOEP]; this contrasts not only with our MOEP data but also with our own data and Felton's data for [MTPP] complexes where the copper compounds are reduced at potentials more negative than the nickel porphyrins. Also, Fuhrhop, Kadish and Davis report equal reduction potentials for H_2OEP and CuOEP, whereas our observations on both porphyrins and phthalocyanines, as well as those of other workers including Clack and Hush[66], Kakutani, Totsuka and Senda[151] and Felton[70,71] all indicate that copper porphyrins are reduced at potentials at least 100 mV more negative than the corresponding free-base porphyrin.

Figure 4.5 Trends in MOEP Reduction Potential

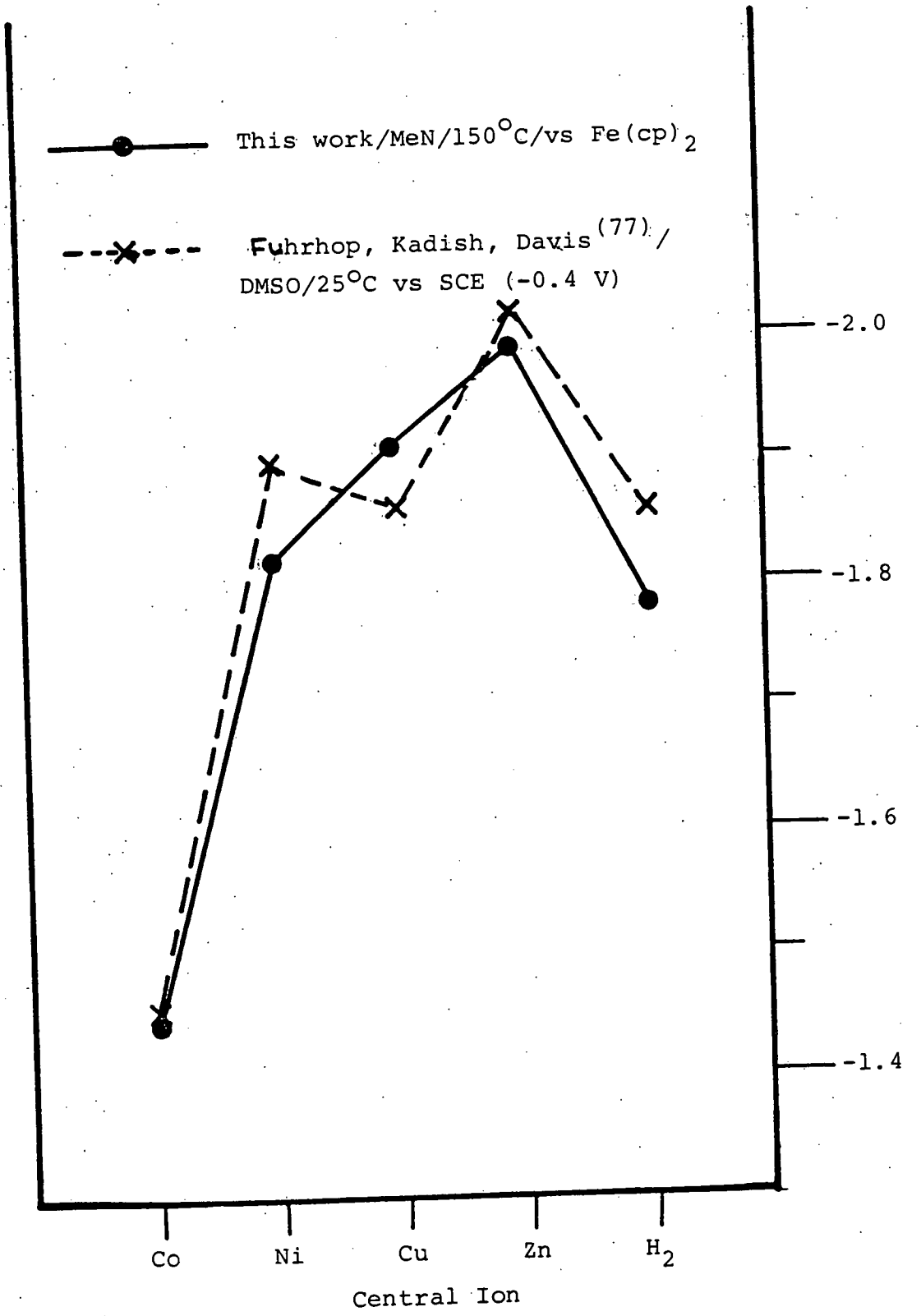

Thus there are clearly small but significant discrepancies in Fuhrhop's account of the Ni, Cu, and H_2 compounds. For unspecified reasons, NiOEP, in particular, was studied in a different solvent (benzonitrile as opposed to dimethyl sulphoxide for all other compounds), and the reduction potential is quoted to only ±0.1 V[77].

We were able to re-examine the reduction potentials of [MOEP] compounds in D.M.S.O. and, while Fuhrhop, Kadish and Davis reported the sequence (least negative to most negative),

$$Cu = H_2 < Ni ,$$

our results (they will be detailed later) reveal a sequence

$$H_2 < Ni < Cu.$$

This is in accord with our high-temperature data and with the relative order of reduction potentials recorded in different solvents by other workers, and we conclude the values presented by Fuhrhop, Kadish and Davis for these particular compounds are incorrect.

4.4 Comparative Redox Behaviour of Phthalocyanines and Porphyrins

The data accumulated in the course of this work make it possible, for the first time, to compare directly the redox behaviour of the porphyrin and phthalocyanine macrocycles under identical experiment conditions. Figure 4.6 shows the absolute values of first reduction potentials of the [MPc], [MTPP] and [MOEP] series obtained in 1-methyl-

Figure 4.6 Relative Trend in Reduction Potential/ MeN/150°C vs $Fe(cp)_2$

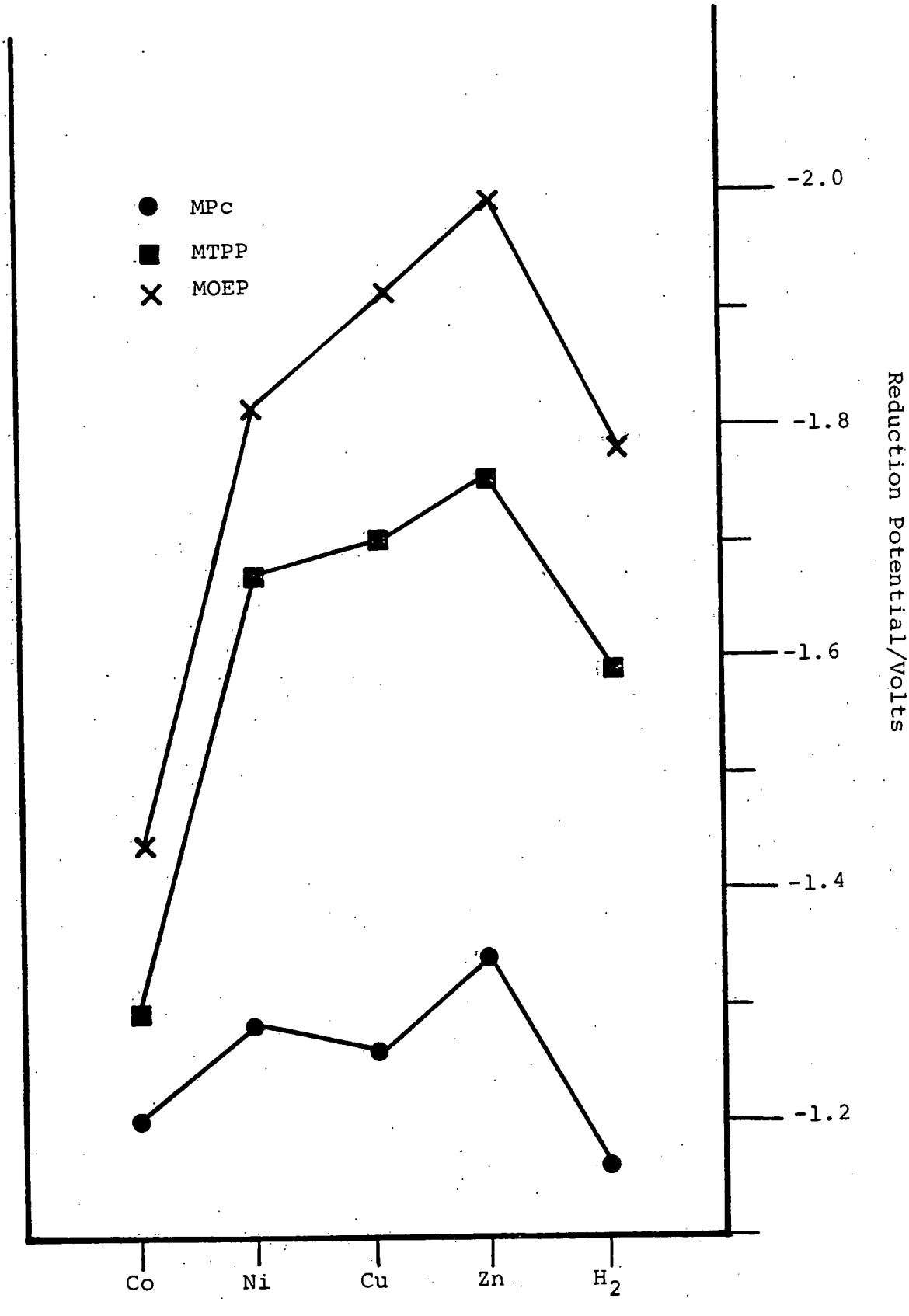

napthalene solution at 150°C. Consideration of the nickel, copper, zinc and free-base compounds (which have confirmed ligand reductions) shows that each phthalocyanine reduces at a potential on average 0.42 V less negative than the corresponding tetraphenylporphyrin. This enhanced electron-affinity of the phthalocyanine moiety must reflect the two main structural differences between the two tetrapyrollic macrocyclic systems. The increased conjugation pathway of phthalocyanines resulting from the fusion of the four benzenoid rings, might lead to lower orbital energies, and the replacement of the C-H bridge of porphyrin by the more electronegative nitrogen atom in phthalocyanine could likewise lead, straightforwardly, to easier reductions. However both suppositions may be complicated by the consideration that, in these reductions, we are dealing with π^* (rather than π) acceptor orbitals. The separation of these effects requires the synthesis of compounds intermediate in structure between porphyrin and phthalocyanine and is discussed later in this work.

The trends in first and second reduction potential for the [MPc] and [MTPP] series are compared in Figure 4.7 where, to emphasise the close parallels between the two series the [MPc] data are shifted by 0.40 V (causing near-superposition). While excellent correlation exists between the two sets of data, both this and Figure 4.6 show the apparently distinct behaviour of first reduction potentials of the cobalt macrocycles. This reflects the inherent metal-based rather

Figure 4.7 Trends in Reduction Potential/MeN/150°C/vs $Fe(cp)_2$

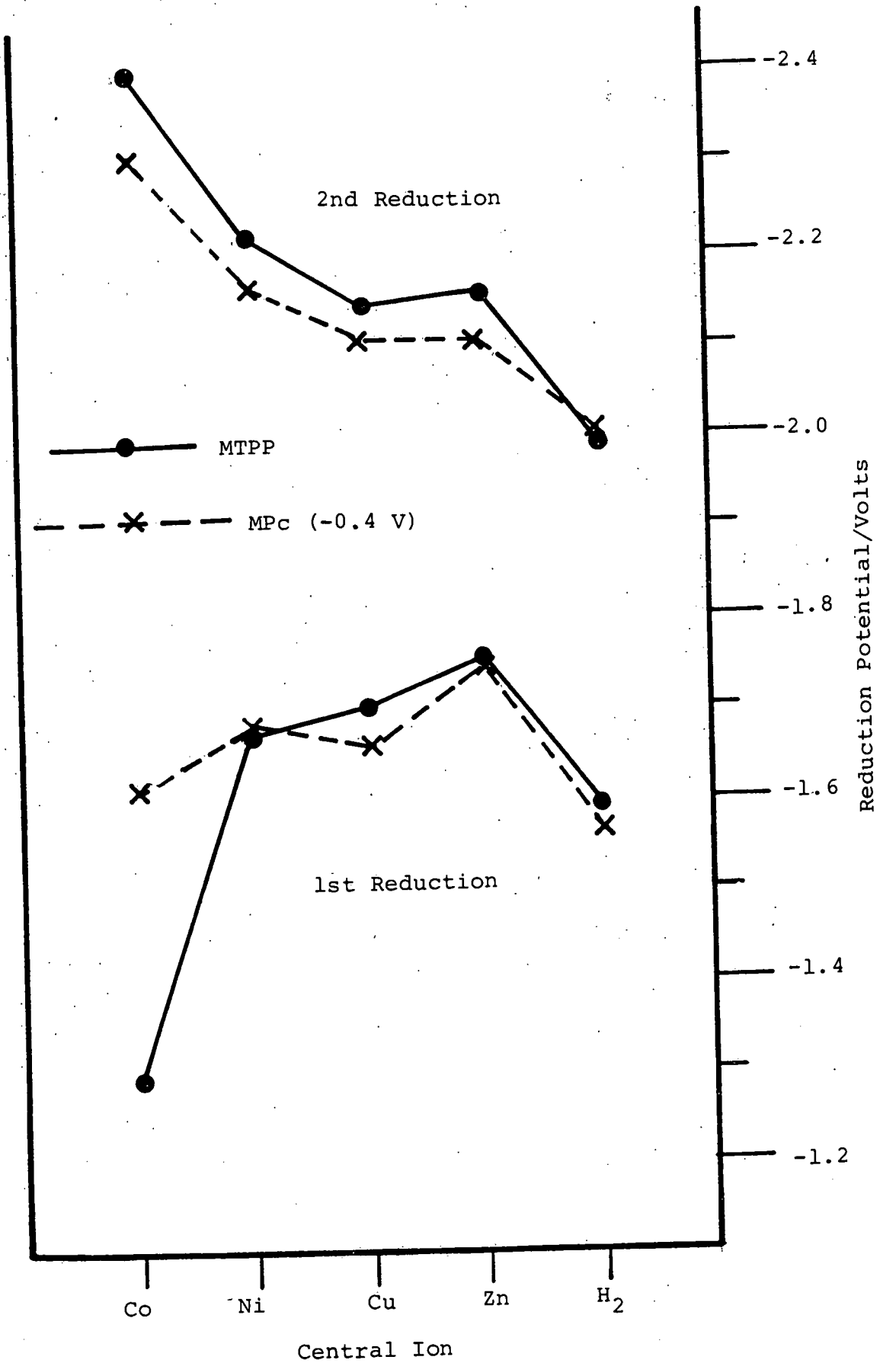

than ligand-based first reduction of these compounds. The Co(II)/Co(I) reduction in [CoTPP] is only 90 mV more negative than the corresponding [CoPc] reduction, in contrast to the general shift of ca. 420 mV between [MTPP] and [MPc] systems. Thus, this reduction potential is characteristic of Co(II)/Co(I) in a square planar environment, the identity of the coordinating ligand producing only a secondary effect on the redox couple. In most other complexes, conversely, the ligand is the redox-active centre and the coordinated metal exerts only a secondary effect.

Also of interest is the consistent inversion in the order of reduction potentials seen for the nickel and copper compounds, established above (Figure 4.7). Our data indicate nickel porphyrins are reduced at potentials less negative than copper porphyrins while for nickel and copper phthalocyanines the inverse is true.

The ligand reduction in all these divalent metal compounds is shifted to negative potentials compared with the parent macrocycle (H_2TPP, etc.). It has been argued that the detailed trend in E^o values reflects the residual charge on the ligand (which influences the frontier orbital energies), and is thus determined by the various central ion electronegativities[68,69]. Thus, for example, the derivatives of electropositive Mg^{2+} are exceptionally hard to reduce (see Tables 3.1, 3.3, 4.1).

If we consider the relative ability of $2H^+$ and M^{2+} to remove charge from the ligand upon formation of, for example, [H_2TPP] and [MTPP] respectively, then clearly the metal ion may not be as effective at σ-electron withdrawal, since the M-N bond is less covalent in nature. Moreover the Lewis acid ability of a metal ion may be also reduced by mis-matching of its steric requirements with that of the macrocycle.

Of course, transition metal ions can also transfer negative charge towards the ligand, directly into the π system, via dπ - pπ 'back-bonding'. This effect would be expected to diminish over the later transition metals (especially Zn^{2+}) as the d_π-orbitals descend into the core. Thus if the distinctions between such metal ions were principally determined by π-bonding interactions, then the zinc complexes should be the easiest to reduce, whereas they are found to be the hardest, even in our strictly non-coordinating media. This suggests that the straightforward polarising effect of each metal ion is the dominant factor.

In particular the Zn^{2+} ion, being relatively large and not prone to planar geometry, is poorly matched with the macrocyclic cavity. These factors probably explain the relatively negative electrode potentials of the zinc complexes in coordinating media where axial solvation occurs with some displacement of the d^{10} ion from the macrocyclic plane.

Inspection of Figure 4.6 (cf. Tables 3.1, 4.1 and 4.2) makes it clear that the apparent "inversion" of the order of reduction of nickel and copper macrocycles is essentially due to the anomalously easy reduction of nickel porphyrins. Thus, reduction of [NiPc] is 0.12 V more difficult than [H_2Pc] whereas [NiOEP] is only 0.04 V more difficult than the reduction of [H_2OEP]. For comparison, the corresponding shifts associated with the copper derivatives are 0.10 V and 0.13 V respectively. Therefore, while Cu^{2+} exerts a similar influence on both porphyrin and phthalocyanine reduction, Ni^{2+} has a far smaller influence on porphyrin than on phthalocyanine reduction.

Accordingly, it proves significant to consider aspects of the comparative structural data for the relevant macrocyclic complexes. In general the central cavity of the porphyrin ring is bigger than that of phthalocyanines[152]. Nickel(II) is the smallest of the ions under consideration (nickel, copper, zinc) and while in [NiPc] the Ni-N bond length of 1.83 Å [14] is typical of nickel-nitrogen bonds, in contrast in [NiOEP][18] the Ni-N bond length of 1.958 Å is according to Hoard[152], "fully 0.1 Å longer than the bonds that are rather commonly formed by the diamagnetic d^8 nickel(II) atom with the nitrogen atoms of four monodentate ligands". The adoption of a (S_4) tetragonal geometry[17] in which the macrocycle is "ruffled" leads to a shorter Ni-N bond length of 1.929 Å. Even in this complex the Ni-N bonds is still over-long,

although this latter form is understood to be the lower energy state of the molecule and is liable to be adopted in solution.

It is noted that even in [NiPc] the central section of the molecule is distorted, shrinking the cavity, compared with $[H_2Pc]$[12] or [CuPc][153].

In contrast to the nickel complexes, the Cu-N bond lengths in [CuTPP][154] and [CuPc][153] of 1.981 and 1.935 Å respectively compare favourably with typical Cu-N bond lengths of 1.95 Å, as exemplified by the copper dimethyl glyoxime compounds[155].

This bond lengthening in nickel porphyrins will reduce back-bonding which should result in easier reduction but will equally diminish σ-donation, which we have argued above is more important. Thus we feel the non-planarity of the nickel porphyrins (caused by cavity shrinkage induced by the small Ni(II) ion) has affected the π* molecular orbitals. Such a distortion of the macrocycle should result in lower π* molecular orbital energies and result in easier reduction as we have observed.

In summary, we feel confident that the small but significant deviations in first reduction potential for nickel porphyrins established in our detailed studies (and concealed hitherto by inaccurate literature data) are related to the mismatch of cavity and metal ion sizes, and the consequent structural distortions peculiar to Ni^{2+} (as defined by Hoard's investigations). The interpretation of this is less certain but we prefer to emphasise the effect of macrocyclic "ruffling" on molecular orbital energy.

Detailed theoretical M.O. calculation exist for the porphyrins[68,69] which evaluate the participation of metal d-orbitals. However, as far as we can discover, the effect of small systematic distortions of the planar macrocycle on the energies of the macrocycle "frontier orbitals" have yet to be explored.

4.5 Solvent Coordination and its Effect on Redox Behaviour

Throughout this work we have laid great emphasis on the value of having access to non-coordinating solvents in the study of macrocyclic complexes. The studies of phthalocyanines and their alkylated derivatives in our unique naphthalene solvents at elevated temperatures have, as outlined in Chapter 3, been extended to investigations in dichloromethane/$TBABF_4$ at ambient temperatures. The consistency of the two sets of data indicates the essentially non-coordinating nature of the latter electrolyte medium.

It seemed worthwhile therefore to investigate porphyrin derivatives as well in CH_2Cl_2, in order to confirm that the parallel with methylnaphthalene is not restricted to phthalocyanines. This having been established, it was then possible in further investigations to assess the effect by added coordinating agents on the electrochemistry of the metallated macrocycles at room temperatures.

Accordingly, the redox characteristics of octaethylporphyrin [H_2OEP] and its copper, nickel and zinc complexes were investigated in dichloromethane solution at 25°C as tabulated in Table 4.3 (column 1). These results and those obtained previously at elevated temperatures in methylnaphthalene are compared in Figure 4.8. The data sets are closely parallel indicating the absence of specific metal-coordinating effects in both these media. Particularly significant is the consistency of the data for the zinc complexes for reasons made clear below.

From the observations so far accumulated it is clearly evident that the most marked differences between data in non-coordinating media and the literature values in typical (coordinating) electrochemical solvents relate to the zinc macrocycles. In general, zinc porphyrins and phthalocyanines are reported to reduce at potentials relatively more negative than we have observed (Figures 3.16, 4.4).

Initially therefore, we examined the effects of adding coordinating ligands to CH_2Cl_2 solutions of zinc macrocycles to test the proposition that the divergence noted is indeed attributable to coordination effects.

Figure 4.9 shows the a.c. polarogram of a mixture of [CuOEP] and [ZnOEP] in (A) CH_2Cl_2/TBABF$_4$ above, and (B) in the presence of pyridine (0.2M). The reduction of [CuOEP] is unaltered while the [ZnOEP] reduction is shifted by 100 mV to more negative potentials. While in this

Table 4.3 Reduction Potentials of Octaethylporphyrins in Selected Solvents

MOEP M =	Reduction Potential[a] Solvent		
	CH_2Cl_2	C_3H_7CN[b]	$(CH_3)_2SO$[b]
Ni	-1.285	-1.305	-1.300
Cu	-1.385	-1.370	-1.380
Zn	-1.490	-1.480	-1.550
H_2	-1.250	-1.250	-1.250

(a) 0.2M $TBABF_4$/25°C/*vs* (Ag/AgCl/CH_2Cl_2)

(b) uniformly corrected by 40 mV (junction potential, general solvation terms).

Figure 4.8 Trends in MOEP Reduction Potential at Different Temperatures

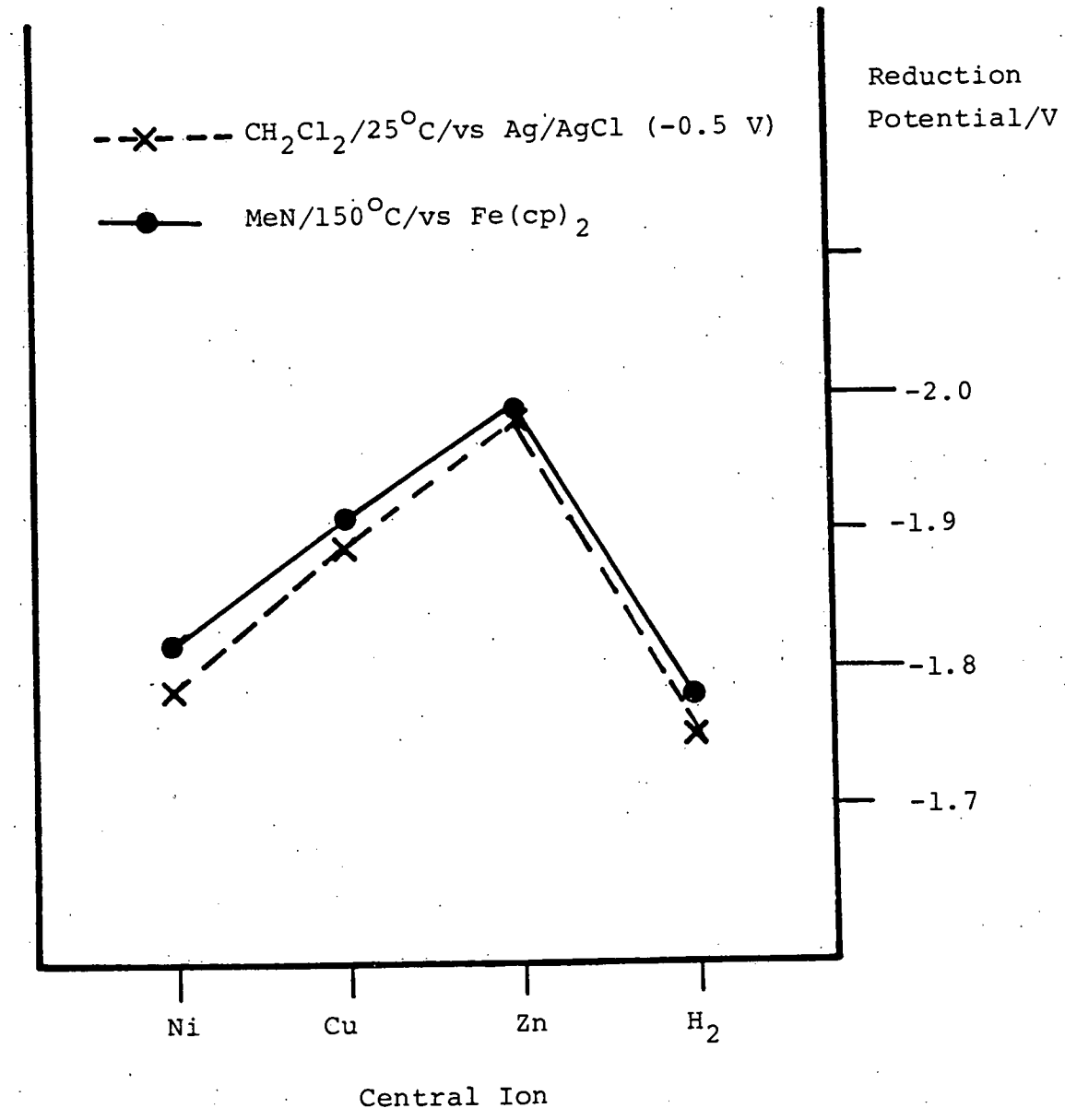

Figure 4.9 A.C. Polarogram of mixture of [CuOEP] and [ZnOEP] in

(A) CH_2Cl_2 solution

(B) CH_2Cl_2/0.2M pyridine solution

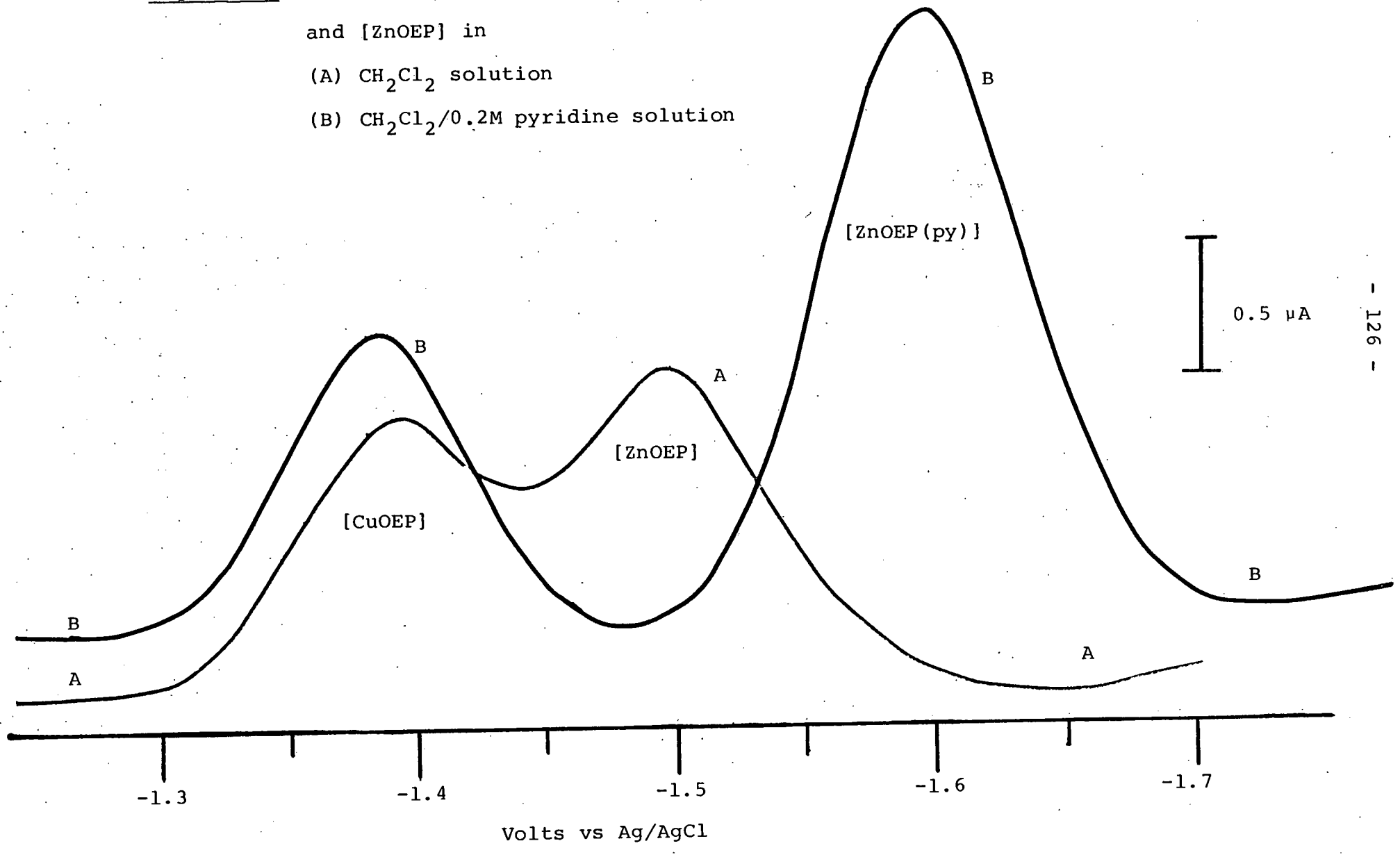

particular experiment gross concentrations of pyridine relative to [ZnOEP] (10^{-5}M) were used, it was later found that even equimolar quantities of pyridine would produce virtually the same shift in reduction potential. (In the particular experiment reproduced in Figure 4.9 a saturated solution of [ZnOEP] was used and the solubility was seen to increase on addition of pyridine; hence the larger current).

By comparison [CuOEP] reductions were unshifted over the range of pyridine concentrations used here (10^{-4} to 10^{-1} M) while a maximum shift of 30 mV was exhibited by [NiOEP] only at excessive pyridine concentrations (4 M pyridine, 10^{-4}M [NiOEP]) and no shift observed in the range 10^{-4} to 1 M pyridine.

Similarly [$ZnBu_4Pc$] reductions were observed to shift in the presence of a coordinating ligand. Equimolar pyridine (10^{-4}M) shifted the reduction potentials of this compound to -1.44 V and -1.89 V (vs $Fe(cp)_2$) compared with -1.37 V and -1.72 V in pure CH_2Cl_2/$TBABF_4$ solution, and as with [ZnOEP], further increase in pyridine concentration over three orders of magnitude gave no further movement.

If the initial reduction of [$ZnBu_4Pc(py)$] caused pyridine to be expelled from the complex anion (as might occur due to accumulation of negative charge) then the shift of $E_{\frac{1}{2}}$ with added pyridine should be progressive, moving 60 mV for every ten-fold increase in pyridine.

Equally the observation that second reduction is even more influenced than the first by pyridine (throughout the concentration range) suggests that the axial ligand is retained by the mono-anion. This system deserves further attention particularly since Kadish has concluded that for zinc (case the) axial ligand is expelled after the first reduction[161].

Spectroscopic studies of the equilibrium coordination of nitrogenous bases to metalloporphyrins[158,161] have yielded formation constants β_1 of typically 10^4 for zinc, 10^2 for nickel, and 10^{-1} in the case of copper compounds. This evidently accords with our preliminary electrochemical investigations, where zinc complexes exhibit the greatest dependence on axial ligand and copper porphyrins the least. However it must be remembered that in the electrochemical experiment E_1(red) responds to the relative stabilization of oxidised and reduced forms of the couple by axial ligation, i.e. to the ratio of β values for [MP] and $[MP]^{1-}$. This area requires further investigation, particularly by use of linked spectroscopic (visible and n.m.r.) and electrochemical studies, since voltammetric techniques provide classical and powerful methods for evaluating stability constants for metal ion complexation.

Our studies on axial interactions were then expanded to investigate the redox behaviour of a range of [MOEP] complexes in bulk solvents of varying donor ability.

Butyronitrile, having a Gutman donor number[119] of 16.6, presents a solvent of medium coordinating power, while dimethyl sulphoxide is highly coordinating with a donor number of 29.8. Combined with the pyridine studies outlined above (donor number for pyridine 33.1), these media span the range characteristic of the solvents normally used in published studies of the porphyrins.

The reduction potentials for a range of [MOEP] (M = H_2, Cu, Ni and Zn) in butyronitrile and dimethyl-sulphoxide are included in Table 4.3, and the variation of E^o values with solvent is shown in Figure 4.10.

A common ($Ag/AgCl/CH_2Cl_2$) non-aqueous reference electrode was used throughout, isolated by a fritted salt bridge containing the appropriate electrolyte (0.2 M $TBABF_4$ in CH_2Cl_2, C_3H_7CN or DMSO). The quoted reduction potentials are corrected by 40 mV in C_3H_7CN and DMSO, to allow for estimated junction potentials and general solvation terms. This has the effect of making the first reduction of [H_2OEP] in all three solvents coincident, which is ideal for detection of specific metal-coordination effects.

Inspection of the figure immediately shows the distinctly different behaviour exhibited by [ZnOEP] in dimethyl sulphoxide. Thus, in sufficiently coordinating media the reduction of this compound and of similar zinc macrocycles, e.g. [ZnTPP], [$ZnBu_4Pc$], is shifted to more negative potentials (60 mV for [ZnOEP]).

Figure 4.10 Variation of Reduction Potential with Solvent [MOEP]/25°C/vs (Ag/AgCl)

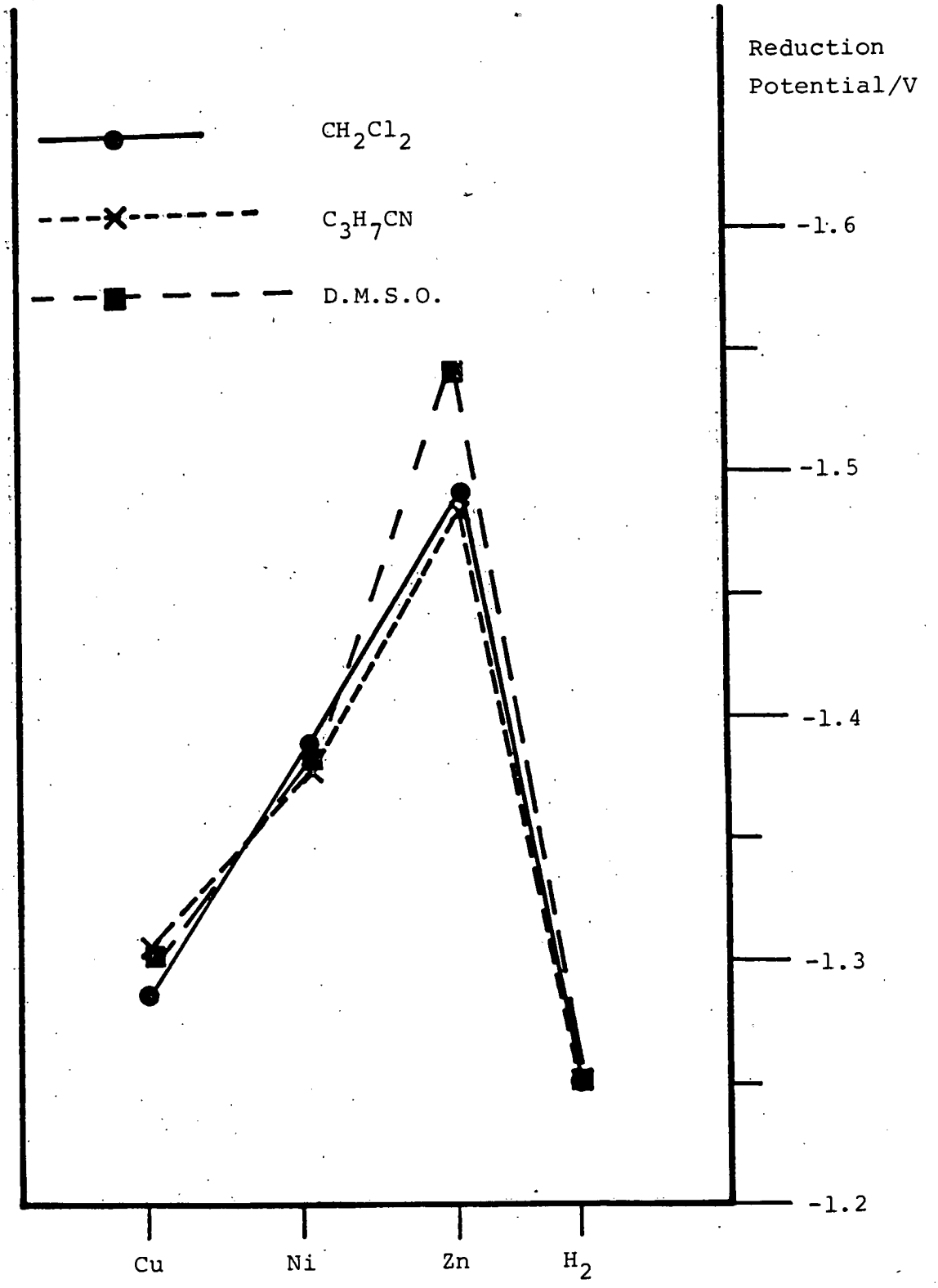

This individual behaviour can be understood as follows. The d^{10} zinc(II) ion is spherically symmetric and hence an octahedral, tetrahedral, or similar three-dimensional environment is preferred to the square-planar geometry found in porphyrin or phthalocyanine. Crystal structure data show that zinc porphyrins crystallised from coordinating media[19,152] retain an axial ligand (e.g. pyridine[19]) and that the zinc ion is displaced from the plane of the macrocycle towards the axial ligand, adopting a distorted square pyrimidal structure. Absorption spectra have shown that [ZnTPP] is monoligated in the presence of sufficient concentrations of nitrogenous bases[156-158].

Thus, in the presence of a coordinating agent zinc will bind axial ligands, distorting from square planar geometry, and as a consequence the interaction between metal and macrocycle ligand is altered, resulting in the shift in reduction potential. This decrease in the metal ion's polarising power is due to the combined effect of displacement from the macrocycle plane and the negative-charge donation of the axial ligand.

Naturally, nothing is known at this stage of the structural features of a reduced adduct such as the hypothetical $[ZnOEP(py)]^{1-}$.

4.6 The Relationship between Macrocycle Structure and Electron Affinity

Our previous studies have enabled us to determine the absolute differences in electron affinity between the phthalocyanine and porphyrin macrocycles. The substantially easier reduction of phthalocyanines must reflect the sum of the two structural differences between the macrocycles, namely the fusion of a benzene ring to each pyrrole and the replacement of the methine bridges by nitrogen in phthalocyanine. It was of interest to determine separately the influence of each of these structural features on the redox activity of such macrocycles. We have therefore, investigated the synthesis and redox activity of compounds intermediate in structure between phthalocyanine and porphyrin.

The two relevant macrocyclic derivatives are the tetrabenzoporphyrin (TBP) (Figure 4.11) and the tetraaza-porphyrin or porphyrazine (Pz) (Figure 4.12).

Figure 4.11

Tetrabenzoporphyrin

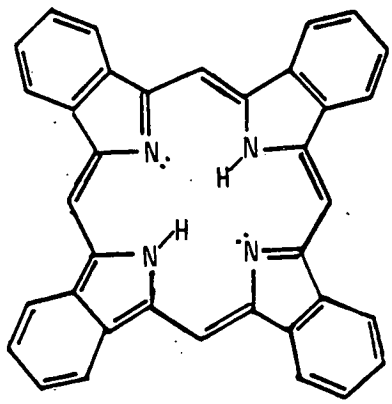

Figure 4.12

Tetraazaporphyrin

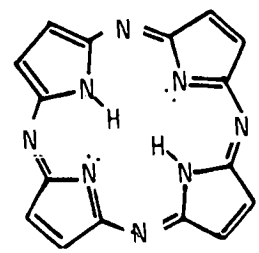

Successful synthesis of zinc tetrabenzoporphyrin was achieved (methods are discussed in detail in Chapter 8) and the redox activity of this compound was investigated in 1-methylnaphthalene solution at 150°C. The compound was observed to undergo a fully reversible one-electron reduction at -1.90 V vs ferrocene (a reversible oxidation was also noted). This value should now be compared with the first reduction potentials of the other zinc macrocycles [all vs $Fe(cp)_2$/MeN/150°C];

$[ZnTPP]^{0/1-}$	-1.75 V
$[ZnPc]^{0/1-}$	-1.34 V
$[ZnTBP]^{0/1-}$	-1.90 V

Ideally, comparisons should be made with zinc porphin itself, [ZnPor], rather than [ZnTPP]. However, the meso-tetraphenyl substituents are perpendicular to the major ring and are generally understood to exert little influence on the redox activity of the porphin. This is confirmed by the very similar redox potentials recorded for corresponding pairs of [MTPP] and [MPor] (M = H_2, Ni, Cu, Zn)[159] i.e. under the same conditions. The changes in reduction potential as a function of structure are represented schematically below.

Figure 4.13

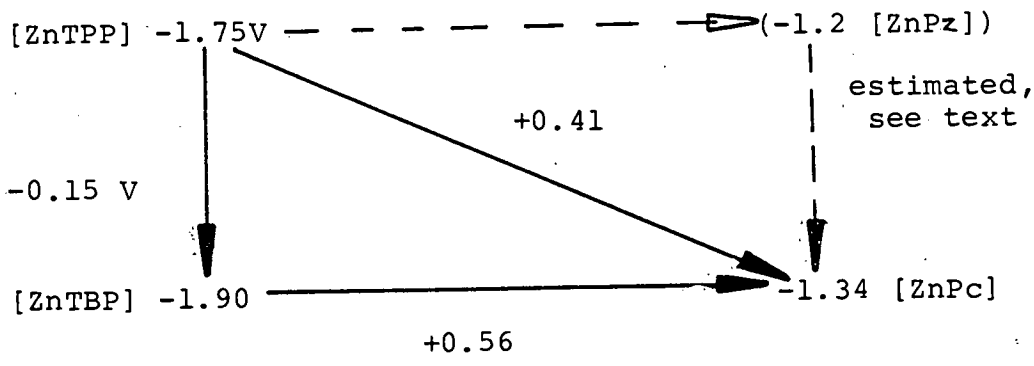

It is important to note that we have obtained this data in a non-coordinating medium. Previous scattered data in coordinating solvents preclude strict comparisons of the type presented here.

The point of immediate significance in the data is that the fusion of the benzene ring to the porphin has shifted the reduction by 0.15 V to more negative potentials, that is the acceptor orbital (L.U.M.O.) has been raised in energy relative to simple porphyrins. One might expect that increased delocalisation as in [ZnTBP] would lead to a general lowering of orbital energies, however, in reductions we are dealing with antibonding levels, certain of which may be destabilized by the fusion of benzene rings[160].

In any event, the limitations of such instinctive expectations are indicated by the fact that the oxidation of [ZnTBP] is easier by 0.4 V than that of [ZnTPP], demonstrating that, in such molecules with extended π-systems, perturbations

on the energy of individual orbitals can only be considered in relation to the whole manifold of levels.

Our results are consistent with appropriate theoretical analysis. Thus Schaffer, Gouterman and Davidson[69] derived molecular orbital schemes using extended Hückel calculations. These methods are semi-empirical in the sense that they are calibrated to fit the observed optical (π/π^*) spectra for each macrocycle. They predicted shifts of macrocyclic L.U.M.O. by ca. +0.5 eV on aza-substitution and by -0.2 eV on fusion. Schaffer et al succeeded in modelling the narrower frontier orbital gap in ZnTBP (1.84 V c.f. our value 1.90 V) and in predicting the correct order of reduction potentials:

(most negative) [ZnTBP], [ZnPor], [ZnPc], [ZnPz] (least negative)

The differences in calculated orbital energy arising from these semi-empirical methods are shown in Figure 4.14, and should be compared with our experimental results in Figure 4.13.

Figure 4.14 Calculated Differences in LUMO (e_g) Energies (eV)

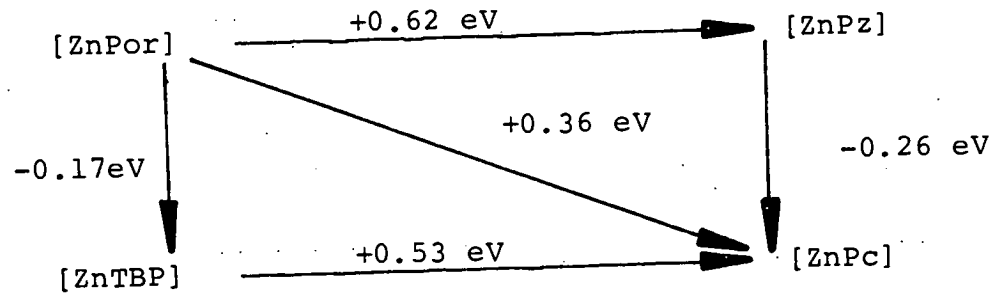

The detailed consistency between theoretical and experimental results is excellent. Thus it is clear that the enhanced electron affinity of the phthalocyanines is due entirely to the replacement of C-H bridge by the more electronegative nitrogen atom, which indeed overcomes the destablising effect of the fused benzene rings. A zinc porphyrazine, having the nitrogen bridges but no benzene ring would therefore be expected to possess the least negative reduction of all four macrocycles, at about -1.1 to -1.2 V on our scale (Figure 4.13). Investigations to test this prediction by synthesis of metallo-porphyrazines are in hand at the time of writing.

CHAPTER 5

Reduction Potential/Electronegativity Correlations for Metallophthalocyanines and Metalloporphyrins

Throughout the preceding discussions, great emphasis has been laid on the "metal ion dependence profiles", the variations in ligand reduction potential as a function of central metal ion. These profiles are, in general, independent of the nature of the macrocycle or its substituents, indicating that the change in reduction potential induced by insertion of any metal is specific to that metal. For example, insertion of magnesium shifts the reduction potentials of most macrocycles by 400 mV relative to the free base while for copper the corresponding shift is 100 mV.

This implies that the metal ion is exerting a systematic second-order effect on the ligand and suggests that the variation of ligand reduction potential might be linked to specific identifiable metal properties. Throughout the last twenty years various workers have advocated the existence of a systematic relationship between metal ion electronegativity and porphyrin reduction potential, and identified linear electronegativity/E^{o} relationships. Given the similar "metal ion profiles" observed in this work, we intially anticipated that this straightforward relation extended to the phthalocyanine series as well, and so were led to examine its nature.

The concept was apparently first advanced by Felton in his study of [MTPP] complexes[10]. From his results on a small series of compounds (M = Mg, Zn, Cd, Cu, Ni, Pb) he proposed

a correlation of first reduction potential with metal-electronegativity. The more electronegative metals were observed to give less negative reduction potentials, the rationale being that the more electronegative elements would withdraw more electron density from the macrocycle leading to easier reduction. In the same laboratories, Gouterman's[68] theoretical calculations for metalloporphins (M = Mn, Fe, Co, Ni, Cu, Zn) were linked to a similar prediction.

Later Stanienda and Biebl[72] investigated the variation of ligand oxidation potential with ionic radius and metal ionisation energy. The latter function produced a more systematic relationship with oxidation potential although the dependence was non-linear.

Metal electronegativity correlations were most vigorously advocated by Fuhrhop, Kadish and Davis[77] in their study of octaethylporphyrin derivatives. The large range of compounds studied by these workers provided a broader test of the concept of a direct relationship between reduction potential and metal electronegativity. They reported a linear dependence of reduction potential on electronegativity in the case of divalent metal ions (M^{II} = Co, Mg, Mn, Cd, Zn, Ni, Pd) and felt sufficiently confident in this data to use this correlation to define an effective "induction parameter" (determined from the reduction potentials) for M^{III} and M^{IV} ions in species such as [Al(OH)OEP] and [$Sn(OH)_2$OEP], where electronegativity values were inappropriate. By virtue of their definition these data naturally fall on excellent straight-line plot versus E^{o}.

If we examine more carefully the analysis of Fuhrhop et al then a number of points emerge. The electronegativity values were obtained from the paper of Gordy and Thomas[162]. This was essentially a tabulation of three earlier electronegativity scales, based on bond energy (Pauling), ionisation energy (Mulliken) or force constant calculations, from which Gordy and Thomas selected one numerical value as characteristic of each element. Thus the electronegativity values used by Fuhrhop, Kadish and Davis represent a conceptually random selection of parameters in the range 1.0 to 2.0, determined in most cases to only one decimal place.

After consideration of the relationship between the metal ion electronegativity values and reduction potentials to hand, Fuhrhop, Kadish and Davis stated that "Linearity is obtained for the case of divalent metal ions".

In the paper, seven [MOEP] complexes are used to define this straight line and it is worthwhile to examine the data relating to these complexes.

Zinc and cadmium have the same assigned Gordy electronegativity (1.5) yet the reduction potentials of [ZnOEP] and [CdOEP] differ by 90 mV, a substantial divergence when the whole span of first reduction potentials is only 220 mV. Equally, since cadmium and palladium have Gordy electronegativities of 1.5 and 2.0, it might be expected that [CdOEP] and [PdOEP] are reduced at quite different potentials, whereas potentials of -1.53 V and -1.52 V respectively were recorded.

Thus, the assertion of a faithful linear relationship for these complexes must be qualified by admitting that substantial discrepancies exist in the data presented. While we have noted inconsistencies in the reported reduction potential values we initially supposed that the main source of uncertainty lay in the quality of electronegativity data selected by these workers. We sought therefore to reassess the relationship identified by Fuhrhop, Kadish and Davis, using more accurate (and modern) electronegativity values derived from a single scale. This seemed particularly important for the general argument, given the lack of internal conceptual consistency in the origin of electronegativity parameters used hitherto.

The concept of electronegativity was first proposed by Pauling, and defined by him as

"The power of an atom in a molecule to attract electrons to itself".

Various methods have been used to estimate numerical values of electronegativity, the three main scales being those of Pauling, Allred-Rochow and Mulliken. Pauling and Allred-Rochow scales of electronegativity (which are available for all relevant elements[163]) have been used throughout this work. The reduction potentials reported by Fuhrhop, Kadish and Davis are plotted against the Allred-Rochow and Pauling values in Figures 5.1 and 5.2 respectively. In Figure 5.1 there is apparently a random scatter of data while in Fig. 5.2 a better correlation of electronegativity with

Figure 5.1 Variation of MOEP reduction potential (Fuhrhop) with Allred-Rochow Electronegativity

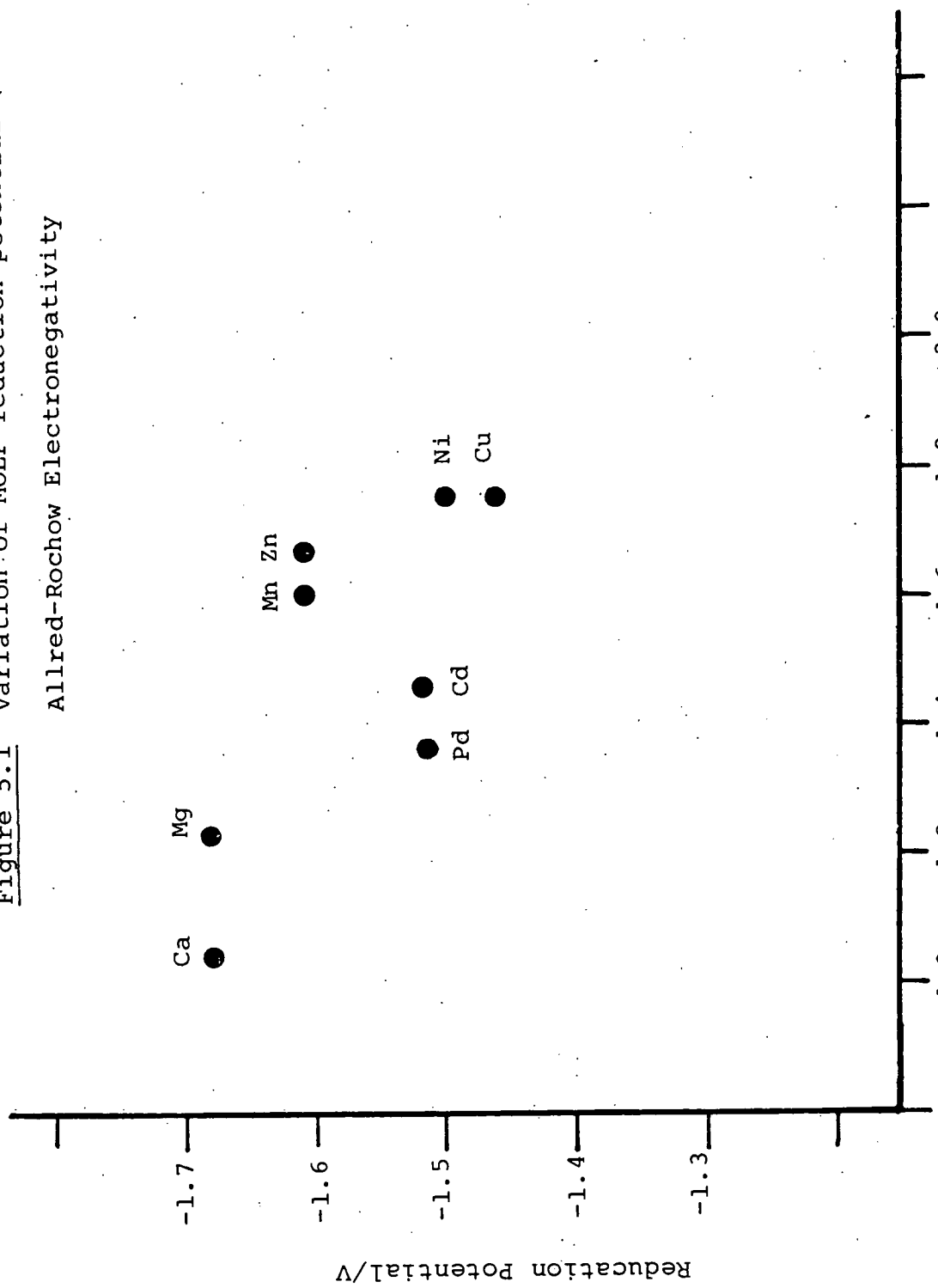

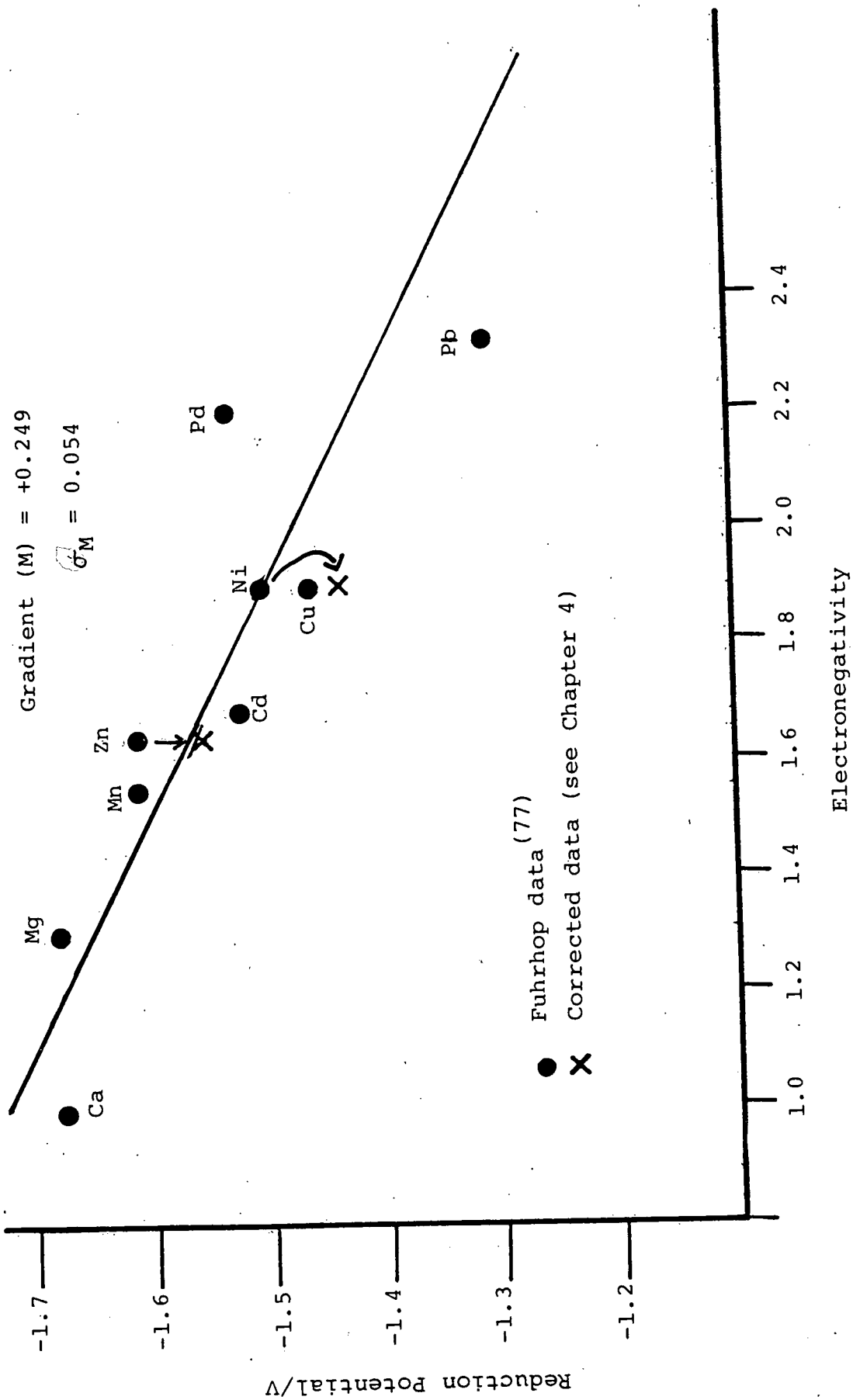

Figure 5.2 Variation of [MOEP] Reduction Potential (Fuhrhop) with Pauling Electronegativity

Gradient (M) = +0.249

σ_M = 0.054

reduction potential is observed. A similar pattern of behaviour is exhibited by our own data for the phthalocyanine series. The variation of phthalocyanine reduction potential with Allred-Rochow electronegativity (Figure 5.3) is unsystematic while Pauling electronegativities produce a more ordered response (Figure 5.4).

Pauling's concept of electronegativity is founded on the observation that the energy of any (X-Y) bond was usually not the average of (X-X) and (Y-Y) bond energies; the difference between the actual (X-Y) bond energy and this "averaged" value is taken as a measure of the difference in electronegativities of the two elements X and Y. Therefore from a series of thermochemical measurements, he was able to determine relative electronegativities and assuming certain standards (electronegativity of hydrogen, 2.1) then absolute values were assigned.

Allred and Rochow[164] used a different approach. The force of attraction between an electron and a nucleus is given by:

$$\text{Force} = \frac{e^2 Z}{r^2}$$

where e = electronic charge, Z = effective nuclear charge and r = distance between the electron and nucleus. The size of this force is a measure of the power of an atom or ion to attract electrons to itself, i.e. the electronegativity of the element. Allred and Rochow used the ratio Ze/r^2 as a

Figure 5.3 Variation of MPc first reduction potential (this work) with Allred-Rochow Electronegativity

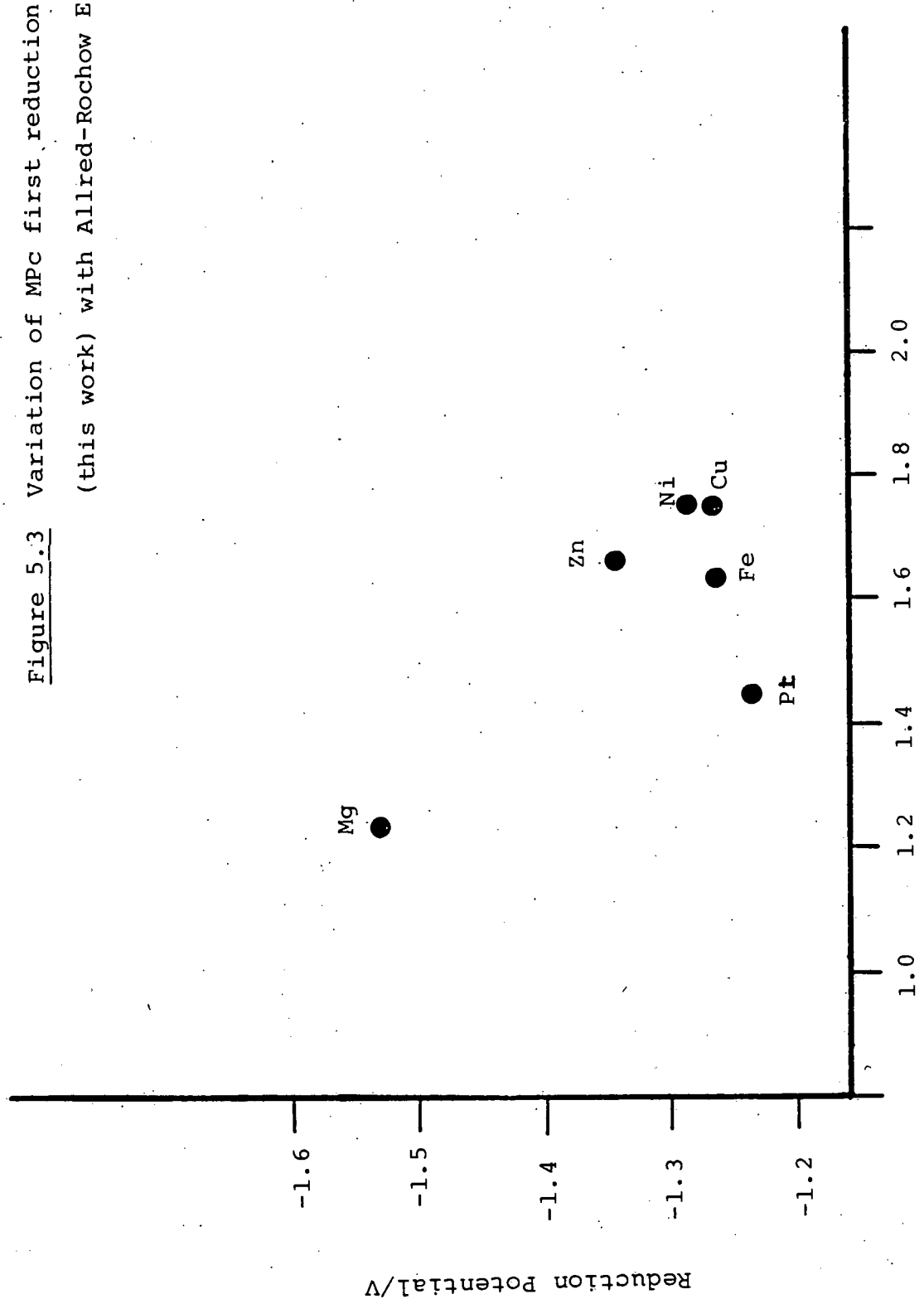

Figure 5.4 Variation of [MPc] Reduction Potential with Pauling Electronegativity

Gradient (M) = 0.25

σ_M = 0.13

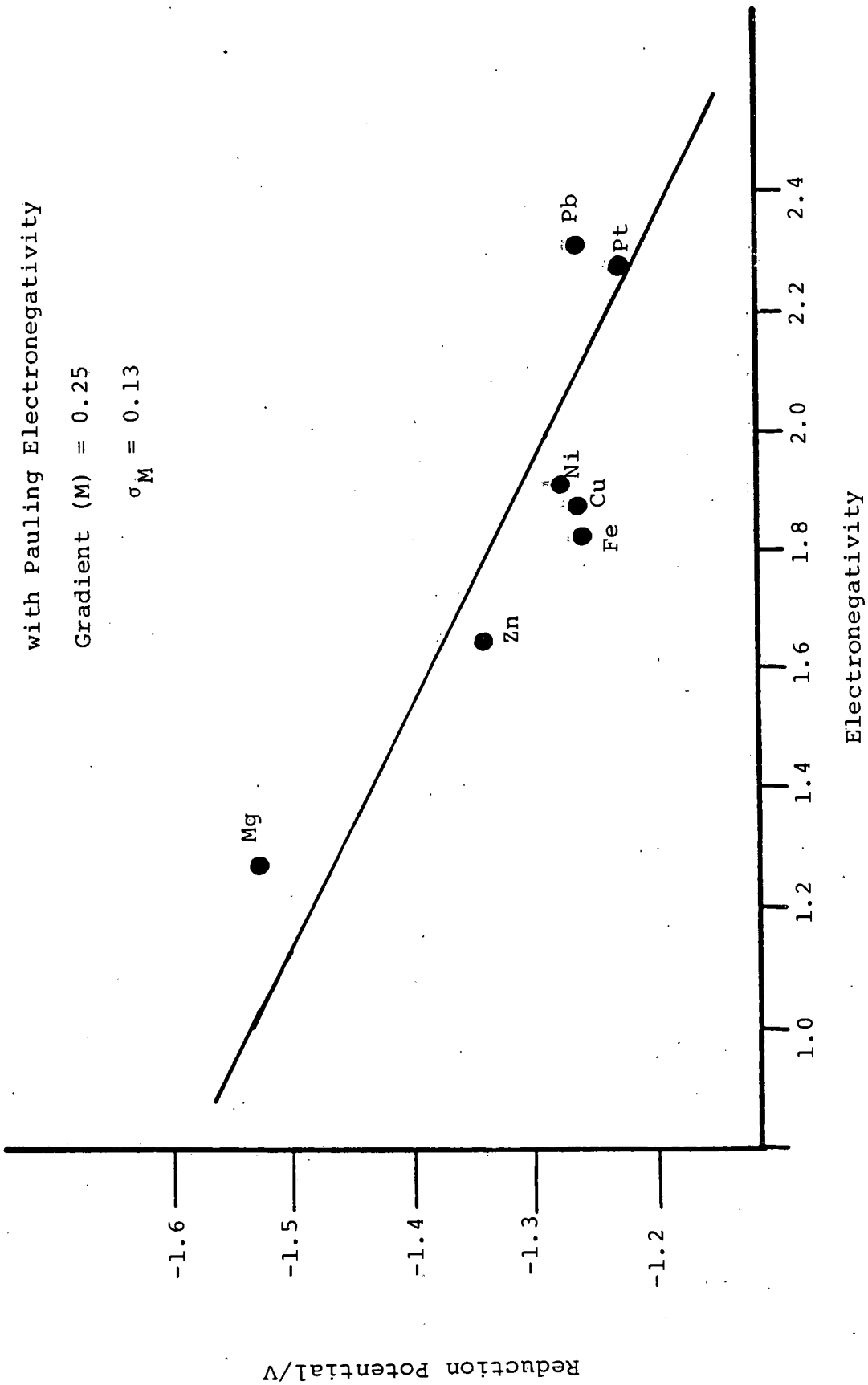

measure of the electronegativity of a range of elements. The two scales can be made to coincide (with the least possible deviation) by using the expression

$$\text{Electronegativity (Allred-Rochow)} = \frac{0.359Z}{r^2} + 0.744$$

Inspection of Figures 5.1 - 5.4 shows that, for both porphyrin and phthalocyanine series, the apparent order (or disorder) of the data hinges on the electronegativity values of a few key metals. For the lighter metals (e.g. first row transition metals) the two scales of electronegativity are very similar. However the scales diverge seriously for the heavier (second or third row) elements i.e. "soft" metals such as Pd, Pb, Pt or Cd.

The Allred-Rochow scale is based wholly on electrostatics (ionic charge and size) while the Pauling method takes into account all contributions to bonding, both ionic and covalent (covalent type bonding is more significant in the heavier elements). Given Gouterman's theoretical viewpoint[68] that the metal ion is simply <u>polarizing</u> the macrocycle, we might have expected Allred-Rochow electronegativity to produce the more straightforward correlation.

This confusion led us to consider whether or not electronegativity is a suitable parameter at all in this context. Electronegativity as a property of each element should depend on oxidation state and stereochemistry and

presumably refers generally to situations where each metal ion is in a three-dimensional environment, rather than the rigid planar geometry under discussion.

Alternative metal properties were then examined, such as electron affinity, ionisation energy and work function, to determine whether or not a simple correlation with reduction potential could be identified. Our preference was for a parameter which could be purely empirically defined and accurately measured for the elements in hand. Despite these precautions no particular improvement in correlation has been achieved. For example, Figure 5.5 shows the variation of phthalocyanine first reduction potential with metal work function. The work function of a metal is strictly defined as,

> "the minimum energy required to remove an electron from an atom in a metal surface"(165)

It is appropriate at this point however, to discuss general points regarding the concept of relating macrocyclic reduction potentials to specific metal properties. As noted, most of the metal properties under discussion are related to the element in a totally symmetric environment rather than the planar geometry encountered in these macrocyclic complexes, although specific metals will adopt a symmetric environment by binding axial ligands with, as we have noted, significant changes in reduction potential, at least in the case of Zn^{2+}. Thus, in coordinating solvents, reduction potentials are being influenced by factors other than central metal electronegativity contrary to the simple expectation.

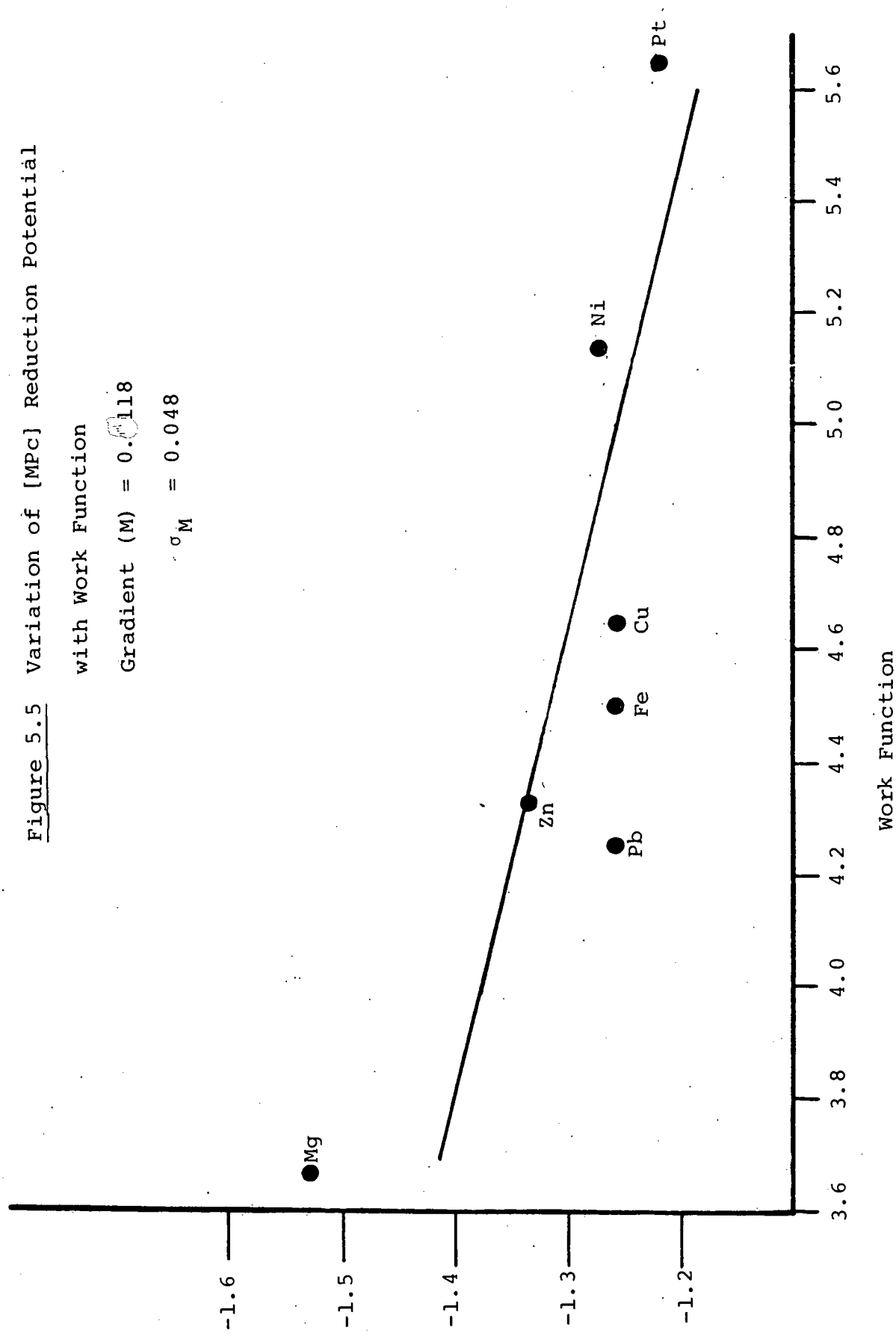

Figure 5.5 Variation of [MPc] Reduction Potential with Work Function

Gradient (M) = 0.118

σ_M = 0.048

We have discussed in section 4.3 the reality of the inversion of the order of copper/nickel phthalocyanines and porphyrins. This inversion evidently negates the possibility of a strict correlation between macrocyclic reduction potential and any wholly metal-based parameter, since clearly such a correlation demands a constant order of relative reduction potentials. The question still remains as to whether this in an anomaly in an otherwise consistent overall trend.

Actually the rate of change of reduction potential with metal ion parameter is small. Thus, for example the gradient of the line in Figure 5.5, by least squares analysis is -0.12 (σ 0.048). Thus, though having a high degree of scatter (high standard deviation), the line is almost horizontal (i.e. nearly independent of metal identity).

We feel therefore that while extreme differences in metal electronegativity or similar function are qualitatively helpful in remembering the sense of shifts in reduction potential (for example, [MgPc] vs [PtPc]), no strict quantitative correlation and no direct causative influence should be sought, especially among the important transition metal derivatives.

While this thesis was in preparation, Lever[166] proposed that phthalocyanine reduction potentials could be linked to metallic ion charge and radius. He considered [MPc] reduction potentials as a function of the charge-to-radius ratio (Ze/r) of various metal ions.

He notes:

"A plot of these quantities E° vs (Ze/r) is curved. A linear plot is conveniently obtained by plotting E° against (r/Ze)"

Thus a mathematical manipulation has been used to obtain a straight line. The "inverse charge/radius ratio" (r/Ze) has no hitherto recognised physical significance, in contrast to (Ze^2/r^2), and unfortunately large ions such as Pb^{2+} which deviate grossly must be excluded from Lever's consideration.

The qualitative influences of ionic radius and charge are no doubt as indicated, but this particular correlation is no more satisfactory numerically and even less conceptually appealing than that which has gone before. It should simply be appreciated that the influence of a metal ion on the macrocycle reduction is related to its Lewis Acid strength and therefore to its size and charge. Electronegativity and E° values both follow from the primary characteristics of the metal ion (which explains their loose parallel) but the specifically planar nature of the macrocyclic ligand and detailed considerations of ion-cavity matching lead to a subtle control of E° order which it is futile to ascribe to electronegativity or any other parameter peculiar to the metal alone.

CHAPTER 6

The Anodic Behaviour of Porphyrins and Phthalocyanines

6.1 Introduction

Our previous discussions have centred on the reductions of phthalocyanine and porphyrins. The latter compounds also have a rich oxidative chemistry which has been extensively documented in the literature. The phthalocyanines however, have received little attention in this context.

One of the earliest reports of cationic phthalocyanine species was that of Cahill and Taube[61] who observed a one-electron oxidation product of copper phthalocyanine on treatment with Ce^{IV}. Later, chemical oxidation studies by Lever[89] yielded nuclear addition products such as $[Mn^{III}(Br)Pc]$.

Voltammetric studies of phthalocyanine oxidations have been limited. Rollman and Iwamoto reported degradative oxidations for the $[M(SO_3)_4Pc]$ complexes[74]. Lever's study of phthalocyanines in pyridine[88] is complicated by the effects of coordination to the central metal and spin-state effects. More recently (while this work was in progress) Gavrilov, Lukyanets and Shelepin reported studies on alkylated phthalocyanines. They reported an anomalous voltammetric behaviour for certain complexes (this will be detailed later in this chapter) which contrasted with the apparantly well-behaved potentiometric response noted earlier by these workers. The numerical values for first oxidation potentials determined by the two methods deviated grossly.

Oxidation studies clearly allow us to probe the filled π orbitals of the macrocycles, whereas hitherto only the π^* acceptor orbitals (LUMO) have been investigated through our studies on the reduction of the complexes. The combination of the two is significant since it provides information on the H.O.M.O./L.U.M.O. separation for comparison with theoretical[67] and spectroscopic data. Given the close parallels between phthalocyanine and porphyrin reductions and the voltammetrically well-defined oxidative processes of the porphyrins, similar anodic behaviour was expected for the phthalocyanines.

In this chapter therefore, following a discussion of the oxidative processes of porphyrins at elevated temperatures, the results of our studies of the anodic response of a range of phthalocyanines are presented and discussed in detail.

6.2 Porphyrin Oxidations at Elevated Temperatures

These studies were designed to complement our reduction studies in naphthalene solvents at elevated temperatures. The broad parallel between our reduction studies and literature data indicated that our novel approach has apparently produced no systematic perturbation of the macrocycles under investigation, or at least of their π^* levels. Equally it is important to determine whether or not naphthalene solvents have any effect on filled π orbitals (H.O.M.O.s). The well-defined oxidative

chemistry of porphyrins provided a standard against which results in naphthalene solvent could be assessed prior to any investigations of the phthalocyanines.

Oxidations were recorded for six porphyrins, as exemplified by [ZnTPP] whose a.c. polarogram and cyclic voltamogram are shown in Figure 6.1. The oxidations are all characterised as fully reversible one-electron transfer processes according to the standard criteria (Chapter 3) and values of oxidation potential are presented in Table 6.1.

For the redox-inert metals such as copper, zinc and magnesium, oxidation occurs unambiguously at the ligand. In the case of cobalt porphyrins, Co^{II}/Co^{III} oxidation is possible. This has been formulated as the first oxidation process of [CoTPP] by a number of workers, in accord with e.s.r. and visible spectroscopic measurements[72,73,76,81] in coordinating solvents. The oxidation of nickel porphyrins is the subject of debate. Fuhrhop and Mauzerall prepared the mono-cation of [NiOEP], by reaction with ferric perchlorate and assigned the compound as $[Ni^{II}OEP^{+}]^{+}$ on the basis of visible and e.s.r. spectroscopic measurements. Later, in their paper on electrochemical studies of [MTPP] complexes in benzonitrile, Wolberg and Manassen suggested nickel-based oxidation. They reported that the mono-cation, formulated $[Ni^{III}TPP^{o}]^{+}$, undergoes a slow ($t_{\frac{1}{2}}$ = 45 minutes) irreversible intra-molecular electron transfer to yield $[Ni^{II}TPP^{+}]^{+}$ [167]. In contrast, in dichloromethane solution, Dolphin and co-workers reported successive ligand oxidations of [NiTPP][168].

$$[Ni^{II}TPP^{o}]^{o} \underset{}{\overset{-e^-}{\rightleftharpoons}} [Ni^{II}TPP^{+}]^{+} \overset{-e^-}{\rightleftharpoons} [Ni^{II}TPP^{2+}]^{2+}$$

Figure 6.1 Voltammetry of [ZnTPP]/MeN/150°C

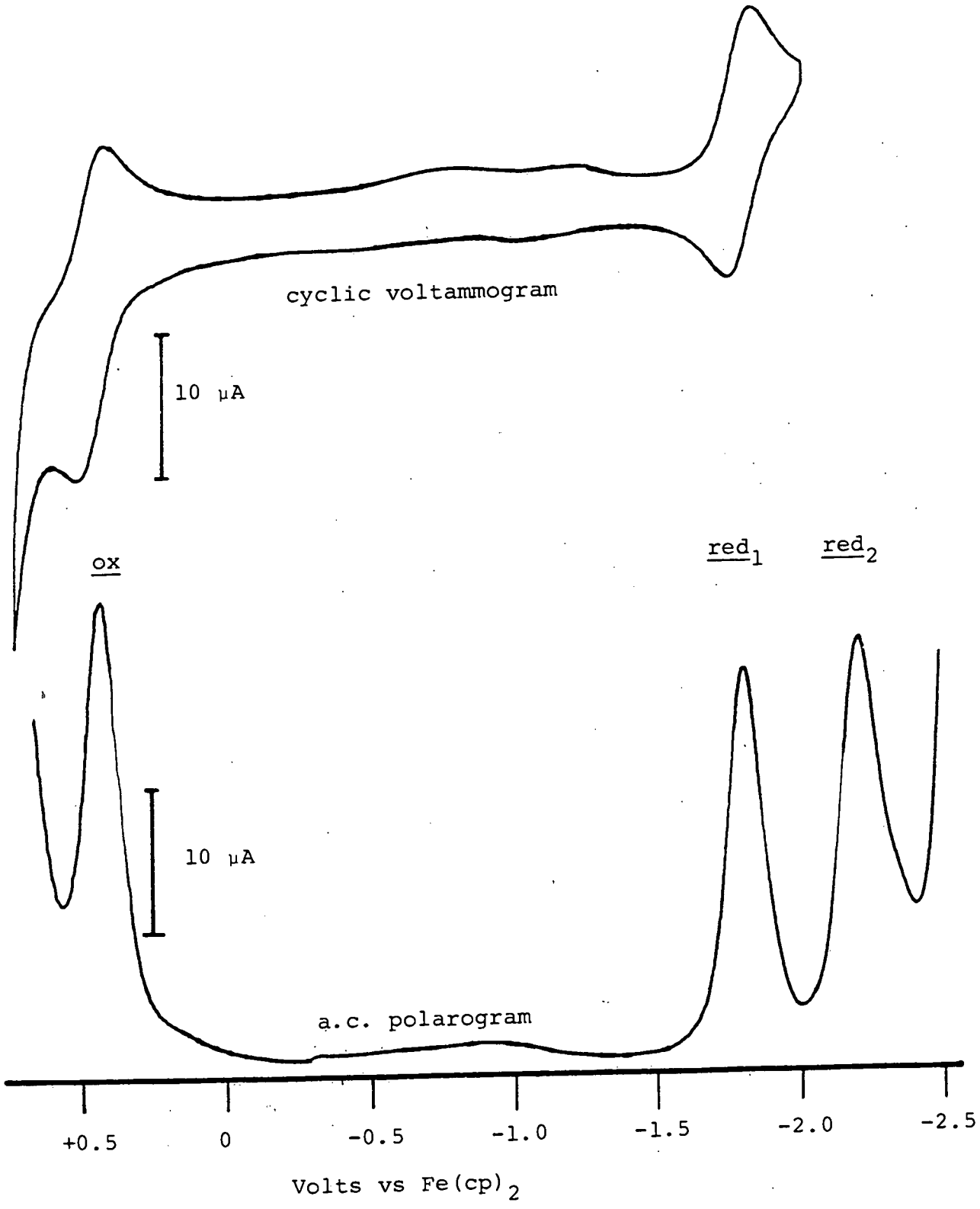

Table 6.1 Redox Potentials of Metalloporphyrins at Elevated Temperatures[a]

[MP]	E_{ox}	E_{red}	$\Delta E_{(ox-red)}$
CoTPP	+0.50	-1.29	1.79
ZnTPP	+0.40	-1.75	2.15
MgTPP	+0.15	-1.89	2.04
NiOEP	+0.36	-1.82	2.18
CuOEP	+0.31	-1.91	2.22
ZnOEP	+0.28	-1.99	2.27

(a) MeN solution/150°C/$TBABF_4$/vs. $Fe(cp)_2$

Table 6.2 [MOEP] Redox Potential Separations[a]

MOEP M =	E_{ox}	E_{red}	$\Delta E_{(ox-red)}$
Ni	+0.900	-1.285	2.185
Cu	+0.850	-1.385	2.235
Zn	+0.755	-1.49	2.245

(a) CH_2Cl_2/25°C/$TBABF_4$/vs. [Ag/AgCl]

E.s.r. spectra were consistent with porphyrin mono- and di-cations respectively. Curiously in solutions of the mono-cation cooled to 77 K the e.s.r. spectrum changed to one consistent with $[Ni^{III}TPP^{O}]^{+}$ but unlike Wolberg and Manassen, Dolphin found this reaction was reversed on raising the temperature. On balance, it seems that for the nickel macrocycles the available evidence suggests that removal of an electron from the ligand is favoured, at least in non-coordinating solvents and particularly for the more readily oxidisable octa-ethyl derivatives.

If we consider our data for the triad of [MOEP] complexes with (M = Cu, Ni, Zn) we note that the order of oxidation is the reverse of the order of reduction. For example, [ZnOEP] which has the hardest (most cathodic) reduction has the easiest (least anodic) oxidation. Thus the electrostatic effect of the metal which raises π^* orbitals to higher energy is also transmitted to the filled π orbitals of the macrocycles.

Of great significance is the separation of first oxidation and first reduction potentials which are also recorded in Table 6.1 (ΔE(ox-red)). This can be regarded as a measure of the separation in eV between highest occupied and lowest unoccupied molecular orbitals. The theoretical calculations of Gouterman[68] (matched to π/π^* spectra) describe a gap of 2.18 V between H.O.M.O. and L.U.M.O. and this accords with our results (the deviation observed for [CoTPP] in Table 6.1 is, of course, due to the metal-based nature of the redox steps for this compound).

For comparison the oxidation potentials of [NiOEP], [CuOEP] and [ZnOEP] were also recorded in dichloromethane (0.2M $TBABF_4$) solution at 25°C in our laboratory, and are presented in Table 6.2. Correlation between the two sets of data is good. Both sets are in close agreement with literature ΔE values of 2.19 V (this is corrected for the inaccuracies we feel are present in Fuhrhop's data), 2.25 and 2.24 V for the nickel, copper and zinc octaethyl-porphyrins respectively[77]. Care should be taken in interpreting these results since coordinating solvents are expected to affect redox behaviour. Donor solvents can, we have noted, shift reductions to more negative potentials. Likewise oxidations may be facilitated by coordination of axial ligand. Clearly now, when considering the overall oxidation/reduction gap these effects are concealed and oxidation and reduction are best dealt with in isolation, i.e. in terms of absolute potential. Such a partition is not possible in optical measurements. Investigations into the effects of axial ligand on oxidations are in progress at the time of writing. We have noted that for example [ZnOEP] is oxidised at less anodic potentials (+0.69 V vs Ag/AgCl) in donor solvents (D.M.S.O.) than in CH_2Cl_2 (+0.755 V), although the ΔE value is maintained (2.240 and 2.245 respectively).

6.3 Oxidations of Phthalocyanines

In the case of porphyrins there is good agreement between the measurements of the H.O.M.O./L.U.M.O. gap by spectroscopic and electrochemical methods, and it was hoped that this principle could be extended to the phthalocyanines. On this basis, the energy of the principle band in the electronic spectrum of metallophthalocyanines at 14,500 - 15,000 cm^{-1} corresponds to a H.O.M.O./L.U.M.O. separation of ca. 1.8 V, i.e. slightly smaller than in porphyrins. Therefore it was expected that, where only ligand redox processes were involved, oxidation of metallo-phthalocyanines would be observed at potentials about 1.8 V positive of first reduction. Clearly the compounds relevant for study of ligand oxidation are the free base [H_2Bu_4Pc] and its complexes with the "redox inert" metals, zinc, nickel and copper, and our studies have centred on these compounds. However, as we shall show, with the exception of zinc macrocycles, the voltammetric oxidation of phthalocyanines is complex, in contrast to their well-defined reductions.

In methyl-naphthalene solution* only [ZnPc] and [$ZnBu_4Pc$] were observed to undergo reversible one-electron oxidations as shown in Figures 3.4 and 6.3 respectively, at the potentials recorded in Table 6.3. As we expected, the

---

*Note A reversible oxidation was also noted for [Mo(O)Pc] at +0.16 V vs. $Fe(cp)_2$. No unequivocal assignment can be made on the site of oxidation in the absence of supporting spectroscopic data, but the Mo^{IV}/Mo^{V} couple has been observed in [Mo(O)TPP] (169) and thus metal oxidation is suggested. (Figure 6.2).

Figure 6.2 A.C. Polarogram

[Mo(O)Pc]/MeN/150°C

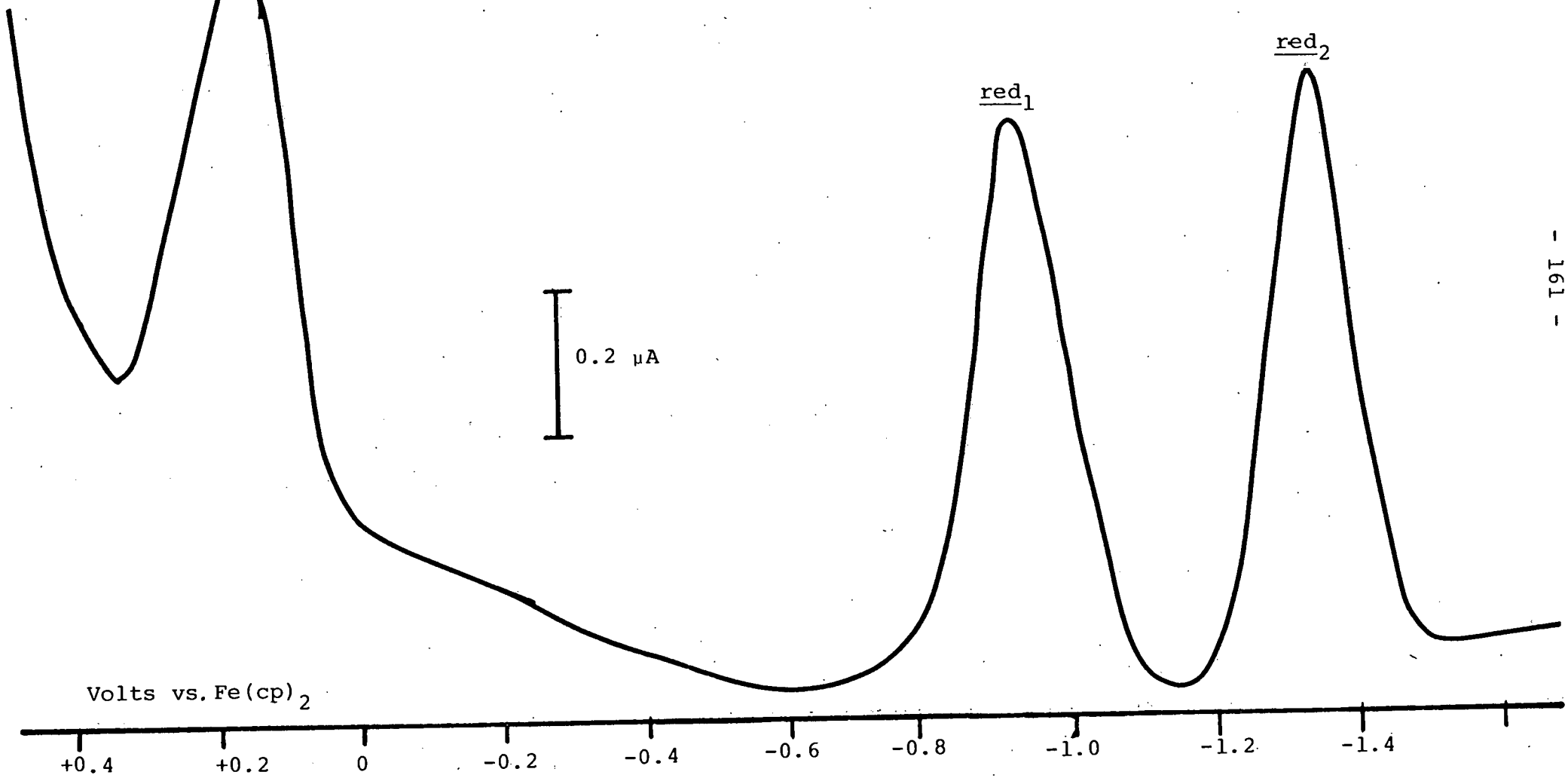

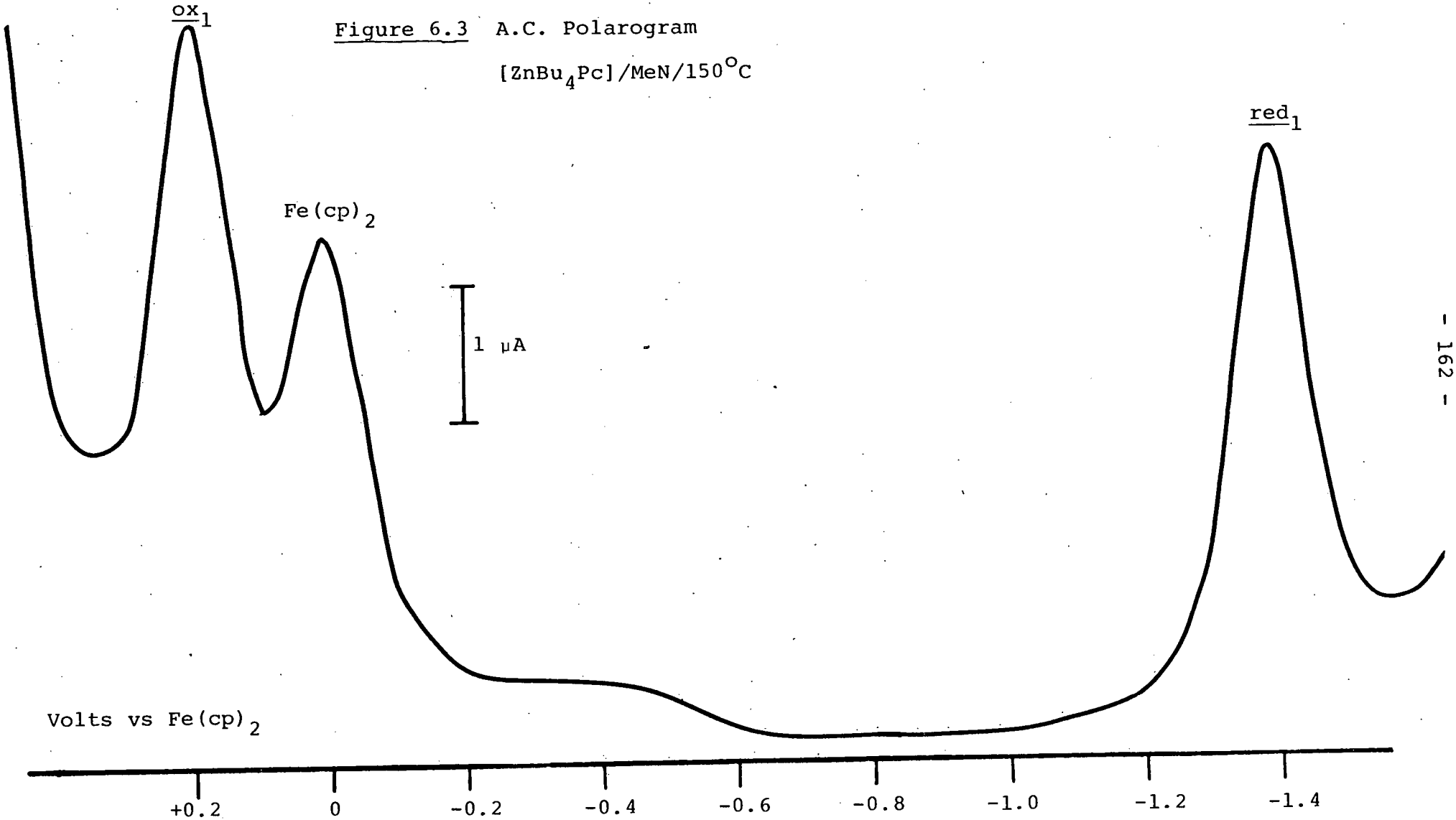

Figure 6.3 A.C. Polarogram

[$ZnBu_4Pc$]/MeN/150°C

Table 6.3 Oxidation Potentials of Metallophthalocyanines

MPc/MBu_4Pc	Solvent[a]	Temperature	Oxidation Potential/V[b]
[ZnPc]	MeN	150°C	+0.22
[$ZnBu_4Pc$]	MeN	150°C	+0.19
[Mo(O)Pc]	MeN	150°C	+0.16
[$ZnBu_4Pc$]	1,2-D.C.B.	100°C	+0.19, +0.83[c]
[$CoBu_4Pc$]	1,2-D.C.B.	100°C	+0.20

(a) Supporting electrolyte $TBABF_4$

(b) vs. $[Fe(cp)_2]$

(c) Irreversible

effect of butyl substitution is to shift oxidation potentials marginally to less anodic values. However it should be noted that the ΔE(ox-red) values of 1.56 V and 1.58 V for [ZnPc] and [$ZnBu_4Pc$] are less than the separation (1.8 V) calculated from spectroscopic data.

In view of the low solubility of the unsubstituted phthalocyanines (at ambient temperatures) and the limited anodic range of 1-methylnaphthalene, two courses of action were open. A different high-temperature solvent with a wider anodic range than methylnaphthalene might be used to study the oxidative behaviour of [MPc] and [MBu_4Pc].

Alternatively, the enhanced solubility of [MBu_4Pc] derivatives at ambient temperatures should allow anodic studies in dichloromethane solution, and, given our knowledge of the effect of butyl substitution on the reductions of phthalocyanines, interpretation of reduction potentials should be straightforward.

Interestingly, at this time some voltammetric studies of [$ZnBu_4Pc$] and [$CoBu_4Pc$] oxidations in 1,2-dichlorobenzene (1,2 D.C.B.) solution at room temperature were reported in the Soviet Union[90].

The high boiling point (180°C) of this solvent and its ability to dissolve [MBu_4Pc] suggested that it might be an alternative solvent for the study of oxidations at high temperature as well. Experiments were therefore carried out in this solvent at 100°C using 0.2M $TBABF_4$ as supporting electrolyte.

Initial investigations in this medium on the porphyrin series were encouraging. Figure 6.4 shows the two oxidations of [CoTPP] (+0.4 V and +0.66 V vs. $Fe(cp)_2$). The limited cathodic range meant that only early reductions could be observed in this solvent.

In 1,2-dichlorobenzene solution at 100°C the reversible oxidation of [$ZnBu_4Pc$] was again observed and a further irreversible oxidation was also noted at the potential recorded in Table 6.3. This was in agreement with the observations of Gavrilov, Tomilova, Shelepin and Lukyanets[90] who observed oxidations at +0.88 V (reversible) and +1.47 V (irreversible) (vs. SCE). The reported ΔE_{ox} 1,2 value of 0.59 V compares with 0.64 V observed in our work.

The oxidation of [$CoBu_4Pc$] was also observed by Shelepin et al[90] at +0.87 V (vs. NHE), and found to be very close to that of [$ZnBu_4Pc$] (+0.88 V). Likewise, we have independently observed approximately equal oxidation potentials for [$ZnBu_4Pc$] and [$CoBu_4Pc$] (+0.19 and 0.20 V vs. $Fe(cp)_2$ respectively).

In the case of [H_2Bu_4Pc] and its nickel and copper derivatives however, an anomalous oxidative behaviour or electrode response was noted, which contrasted with the well defined reduction. For example Figure 6.5 shows the voltammetry of [$CuBu_4Pc$] in 1,2-D.C.B. The low solubility of [MPc] compounds in 1,2-D.C.B. precluded voltammetric studies in this solvent of the pigments themselves.

Figure 6.4 Cyclic Voltammogram

[CoTPP]/1,2 D.C.B./100°C

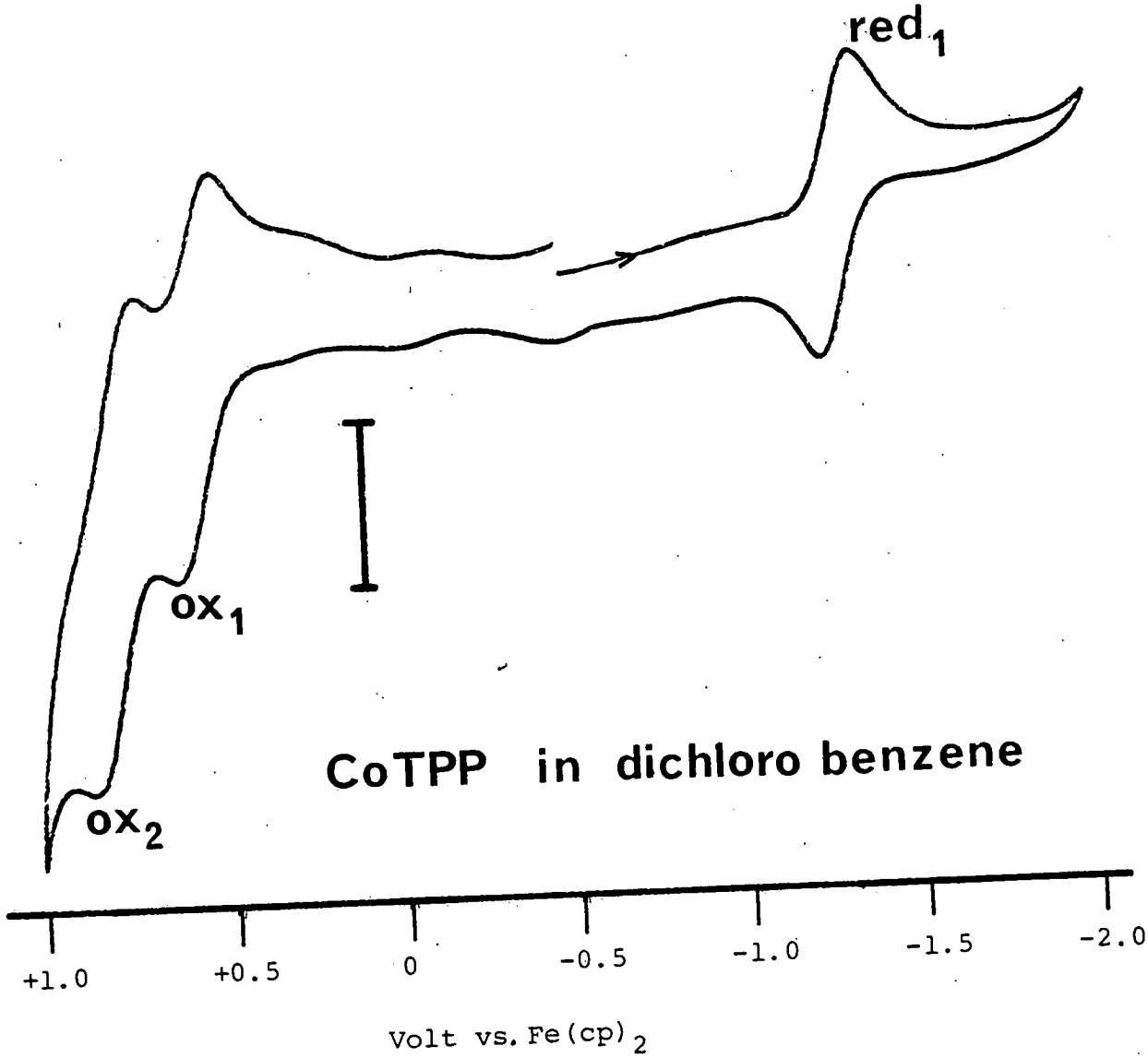

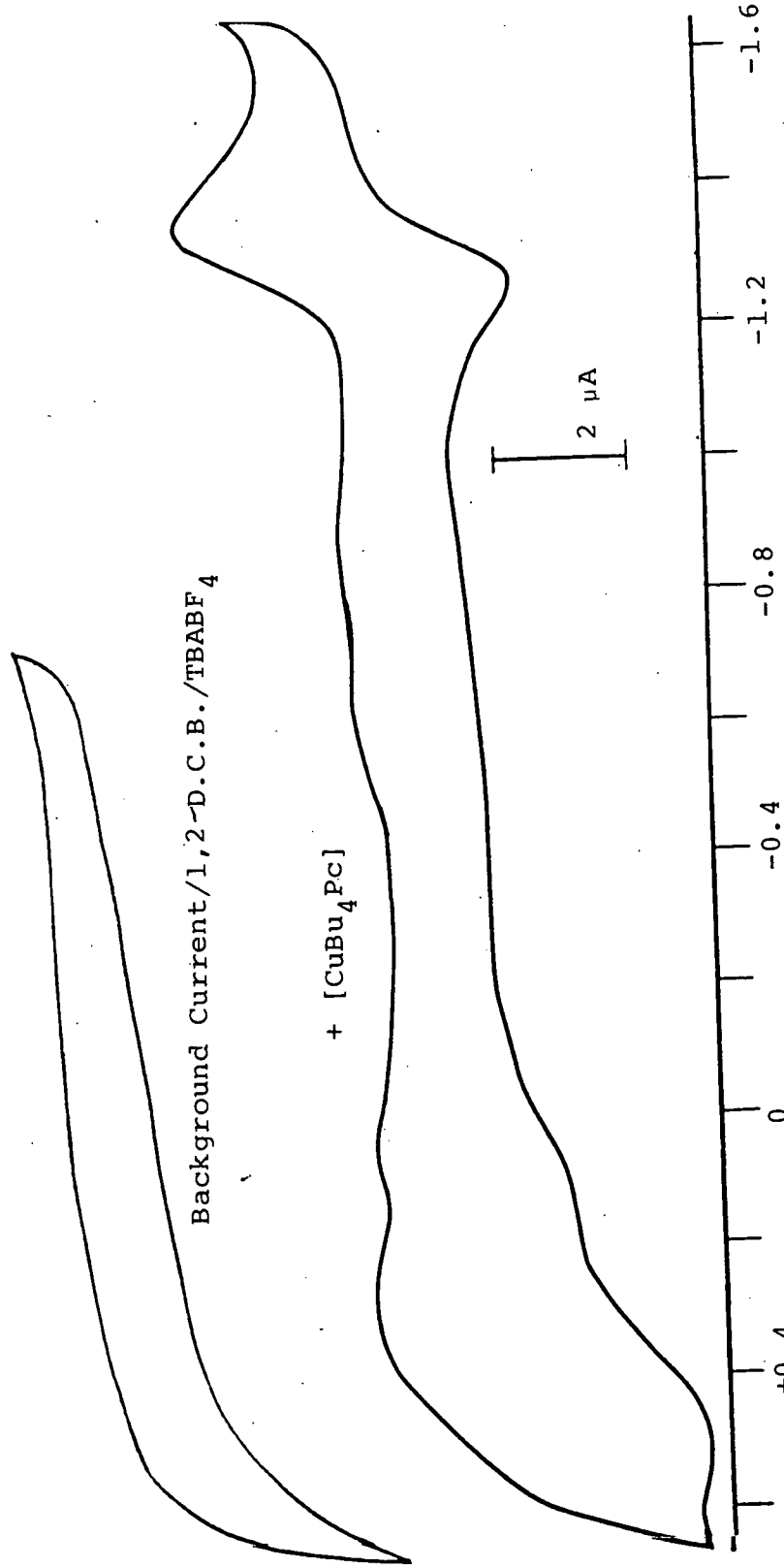

Figure 6.5 Voltammetry of $[CuBu_4Pc]/100^{o}C/1,2$ D.C.B.

In the light of this, it was decided to continue these studies on the [MBu_4Pc] compounds in dichloromethane solution, where a larger potential range and better solvent purity could be achieved.

Again, in dichloromethane solution, only [$ZnBu_4Pc$] was seen to undergo a well-defined reversible ligand oxidation. The irreversible second oxidation was also noted as before, both oxidations occuring at potentials virtually identical to those recorded in 1,2-D.C.B. (Table 6.3).

In the case of [H_2Bu_4Pc] and its nickel and copper complexes, the complex oxidative behaviour observed at higher temperature was also observed in $CH_2Cl_2/TBABF_4$ solution. Figures 6.6, 6.7 and 6.8 show the voltammetric responses of [H_2Bu_4Pc], [$CuBu_4Pc$] and [$NiBu_4Pc$] respectively.

In all three cases a similar oxidative response containing two diffuse waves is seen. Linear voltammograms recorded on a platinum rotating disc electrode have shown that these oxidations, like that of [$TiOBu_4Pc$] (Figure 6.9), correspond to the loss of one electron per molecule.

Figure 6.6 Cyclic Voltammogram

$[H_2Bu_4Pc]/25^{o}C/CH_2Cl_2$

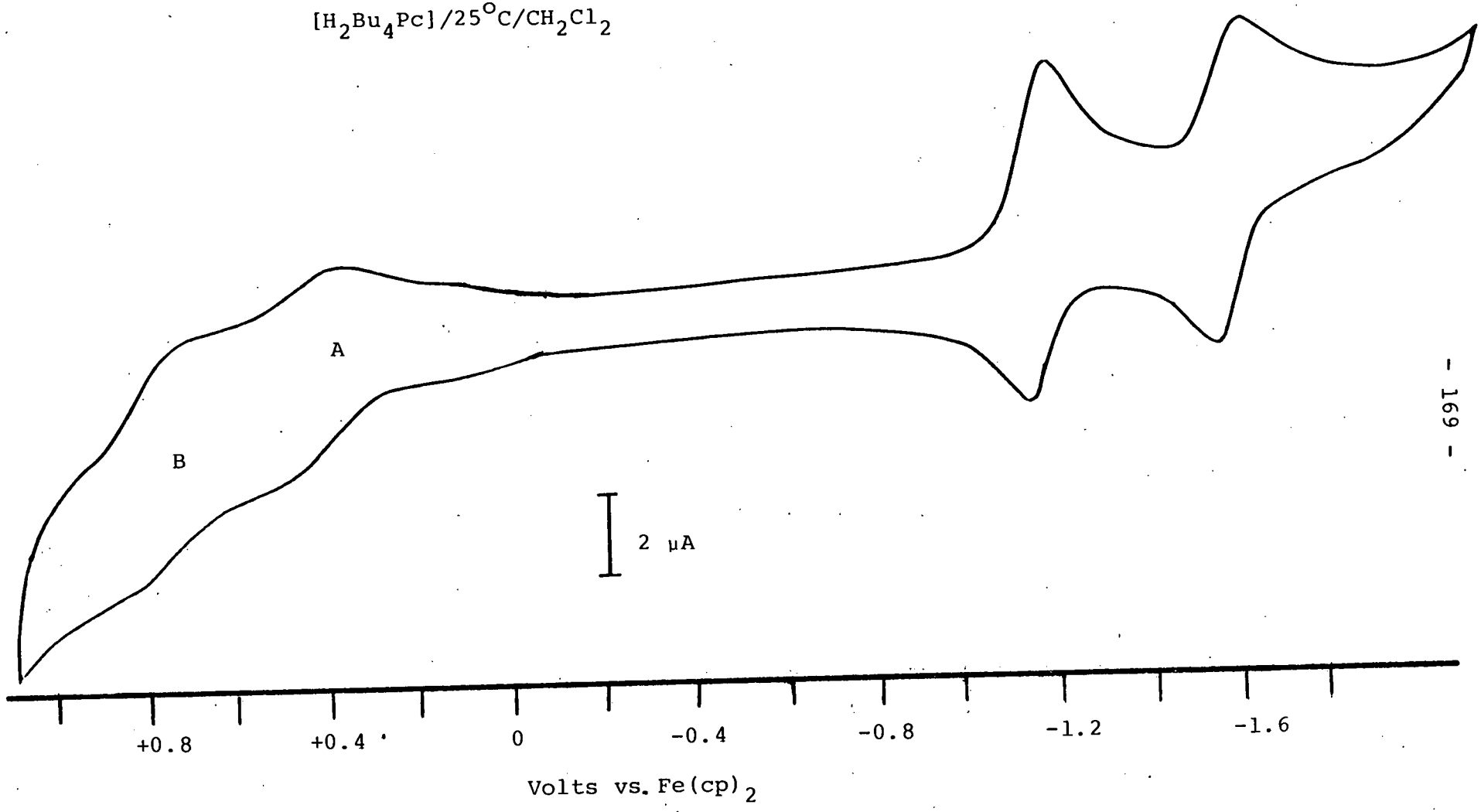

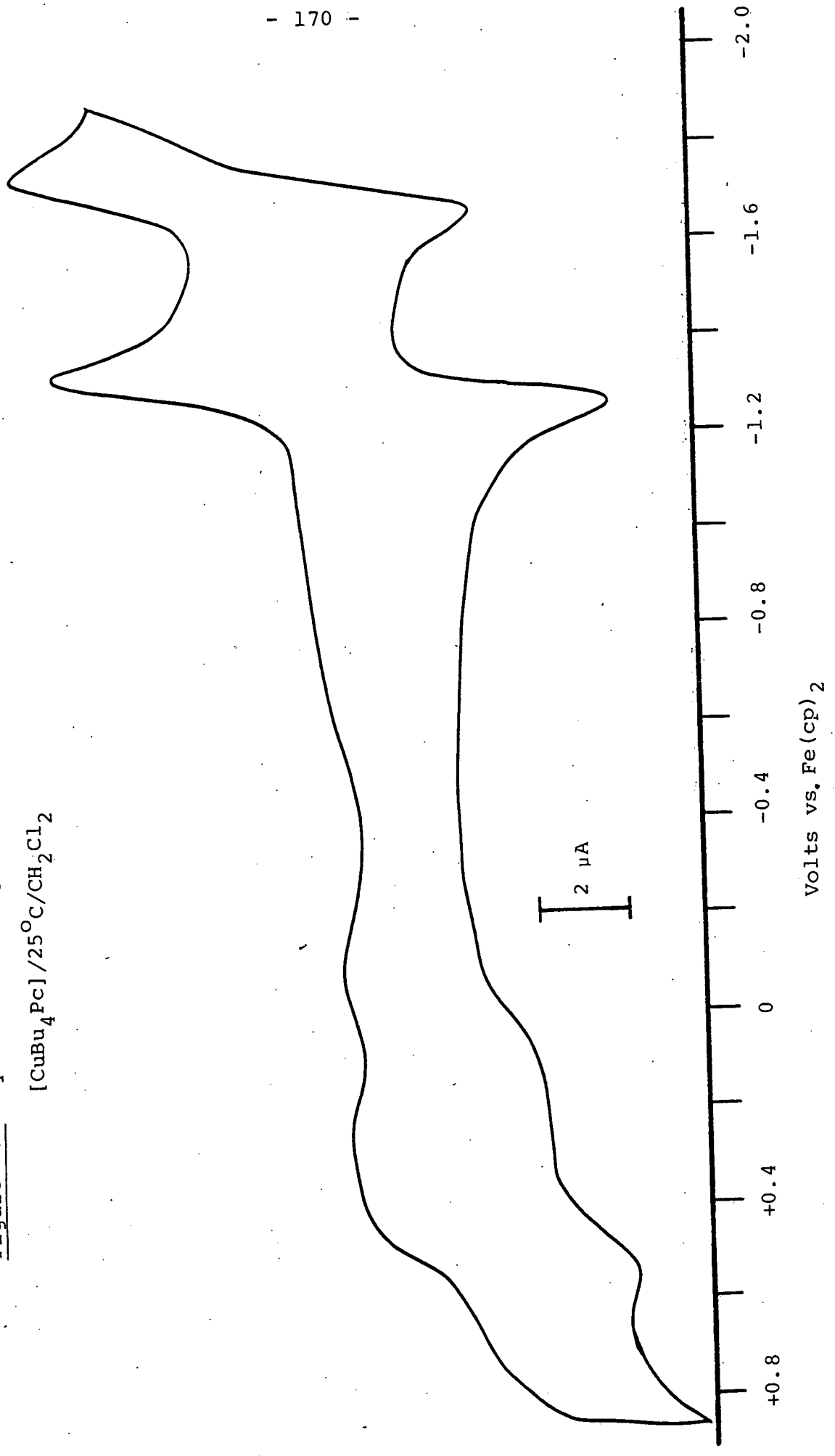

Figure 6.7 Cyclic Voltammogram

[$CuBu_4Pc$]/25°C/CH_2Cl_2

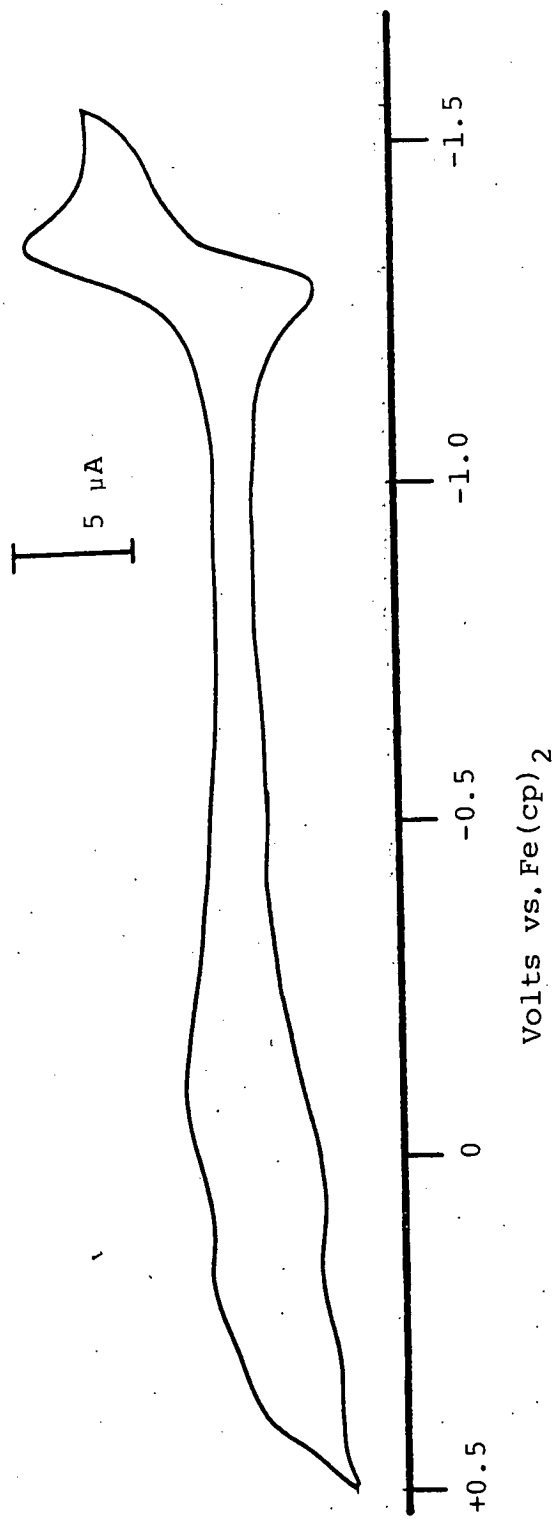

Figure 6.8 Cyclic Voltammogram

$[NiBu_4Pc]/25^oC/CH_2Cl_2$

Figure 6.9 Voltammetry of [Ti(O)Bu_4Pc]

CH_2Cl_2/25°C

A Linear Voltammogram

B Cyclic Voltammogram

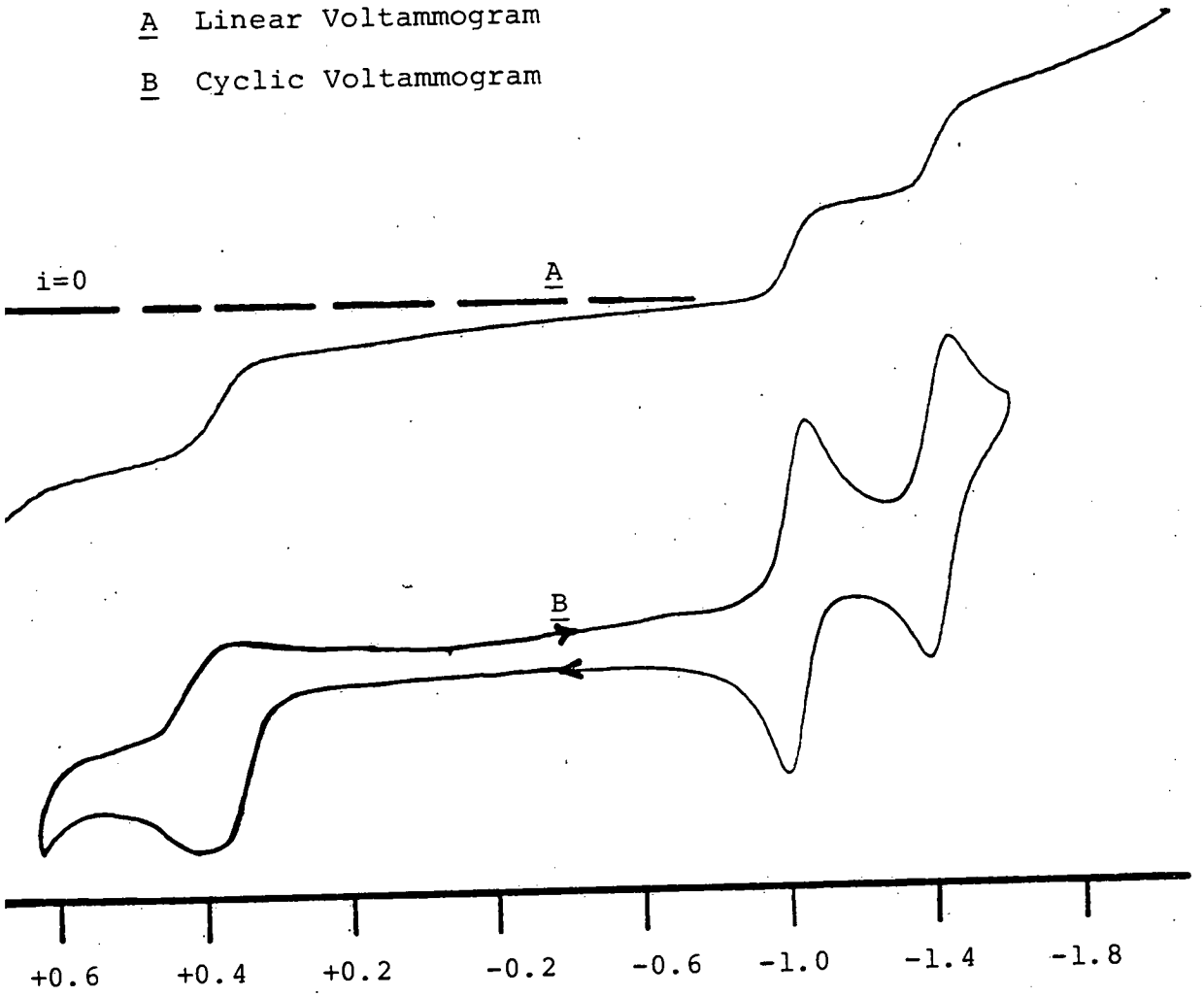

Volts vs $Fe(cp)_2$

This oxidative response of these compounds is unchanged by scan rate (5 mVs^{-1} to 5 Vs^{-1}), concentration (10^{-4}M to 10^{-6}M) or temperature (20°C to -45°C).

These observations have been borne out by recent studies in the Soviet Union[91]. Gavrilov, Lukyanets and Shelepin report similar twin oxidation waves for $[H_2Bu_4Pc]$ and $[CuBu_4Pc]$, although their lack of reduction data restricted their analysis. This voltammetric data obtained by these workers contrasted with the apparently well-defined potentiometric results reported earlier by Lukyanets et al[170]. However Gavrilov, Lukyanets and Shelepin were able to electrogenerate the mono-cations of $[H_2Bu_4Pc]$ and $[CuBu_4Pc]$ and reported electronic spectra closely matched to that of $[ZnBu_4Pc]^+$ indicating that the overall oxidative process corresponded to one-electron oxidation of the ligand.

It should be noted that for $[H_2Bu_4Pc]$, $[NiBu_4Pc]$ and $[CuBu_4Pc]$ the separation between reduction and the mid-point of the oxidative wave is approximately 1.5 V, of similar magnitude to $[ZnBu_4Pc]$. Recently Lever investigated the electrochemistry of a range of closed-shell main-group phthalocyanine complexes in coordinating solvents[166]. He reported a consistent separation of 1.575 V between first oxidation and first reduction which compares with 1.56 V and 1.58 V for [ZnPc] and $[ZnBu_4Pc]$ in non-coordinating solvents. This confirms our observation that coordinating solvents affect the complete manifold of energy levels, shifting oxidation and reduction potentials equally.

In porphyrins there is excellent agreement between voltammetric and spectroscopic measures of the π/π^* orbital separation. However, in phthalocyanines the separation of 1.575 eV measured electrochemically is appreciably less than the 1.8 eV calculated from electronic spectra. This may reflect the possibility that the different techniques are "mapping" different orbitals within the macrocycle in the present case. The main absorption band of phthalocyanine, the Q band, is known to be the transition from $a_{1u} \rightarrow e_g$. The e_g orbital is the L.U.M.O. and is thus the "acceptor" orbital in both optical transition and electrochemical reduction. However the a_{1u} orbital while being the symmetry-allowed donor orbital for the intense electronic transition is <u>not</u> the H.O.M.O. of the phthalocyanine macrocycle according to Gouterman's calculations[69]. It is from these other higher-energy $N_{P\sigma}$ orbitals that oxidation should occur; hence it appears that the disparity between electrochemical measurements and optical data in the case of phthalocyanines reflects a meaningful and important distinction between these systems and the porphyrins.

Detailed consideration of spectroscopic evidence will be necessary to elucidate the electronic structures of $[MPc]^+$ systems, derivable by electrogeneration, and hence resolve these questions.

CHAPTER 7

Bonellin Dimethyl Ester

7.1 Introduction

It has always been hoped that the systematic studies on symmetrically substituted model porphyrins in our laboratory would serve as a basis for future work on biologically relevant systems where both the macrocycle itself can be modified (as in chlorins or corrins) and the pattern of peripheral substitution is more elaborated. These investigations are just beginning, but are represented in this work by a brief intensive study of a remarkable pigment called Bonellin (Figure 7.1).

Although this compound has been known for over a century the structure has only recently been established by Pelter and co-workers[171,172]. A supply of this very rare material (approximately 10^{-3} g are obtained from 10^3 g of tissue) was generously donated by Professor Pelter, 5 mg of the pure pigment proving sufficient for a complete study of its voltammetric behaviour.

Figure 7.1 Bonellin

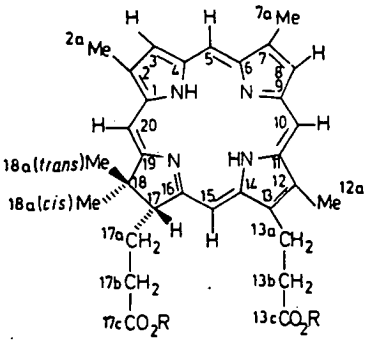

Bonellin (Figure 7.1 R = H) is the green pigment responsible for masculinisation in the marine worm Bonellia viridis. It is structurally unique among naturally occuring chlorins in possessing a gem-dimethyl grouping (C-18), and no substituents on C-3, C-8 or on the bridging methine C-15. Most remarkable of all, it is as yet the only tetrapyrrolic macrocycle found to have no coordinated metal ion in the natural state. Nonetheless, in common with other porphyrins and chlorin derivatives, its biochemical action is known to involve a photo-redox mechanism[173].

A detailed analysis of the redox behaviour of Bonellin, coupled with spectroscopic studies of the oxidised and reduced forms, may help to elucidate the functions of this remarkable pigment.

7.2 Results

The compound, examined as the dimethyl ester ([H_2BDME]*, Figure 7.1, R = CH_3), undergoes two successive reductions and an oxidation step as shown in Figure 7.2. These were all shown to correspond to fully reversible one-electron transfer processes by a.c. frequency and c.v. scan-rate dependence measurements.

---

*Note We follow the conventional porphyrin electrochemical nomenclature by indicating the two displacable hydrogen atoms of the free base.

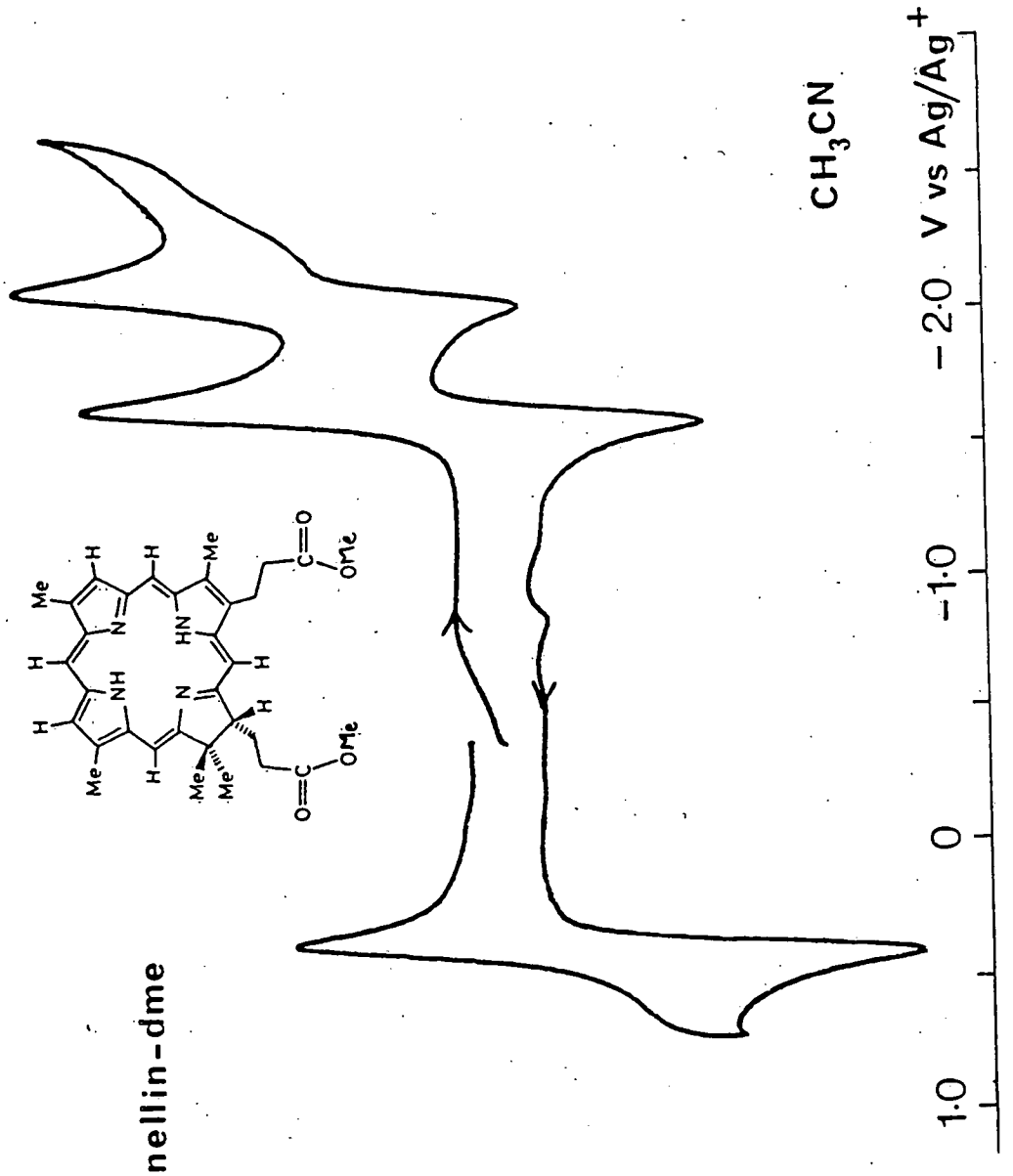

Figure 7.2 Cyclic Voltammogram

A further well-defined oxidation is observed by a.c. voltammetry at +0.86 V (Figure 7.3) which, although not fully characterised, coincides with the second one-electron reversible oxidation observed in a parallel study of octaethylchlorin, $[H_2OEC]$.

These electrode processes are summarised below,

$$^{*}[H_2BDME]^{2+} \overset{e^-}{\rightleftharpoons} [H_2BDME]^{+} \overset{e^-}{\rightleftharpoons} [H_2BDME]^{\circ} \overset{e^-}{\rightleftharpoons} [H_2BDME]^{-} \overset{e^-}{\rightleftharpoons} [H_2BDME]^{2-}$$

*inferred product, see text.

The relevant electrode potential values are presented in Table 7.1 and are clearly independent of electrode material and voltammetric techniques.

A complementary study of $[H_2BDME]$ over a more limited range in strictly non-coordinating liquid naphthalene media at 150°C shows that the first reduction and oxidation are unaltered ($E_{ox} - E_{red}$) = 1.99 V), and are clearly simple electron-transfers uncomplicated by subsequent rearrangements or solvent interactions.

Related studies in this laboratory[178] have shown that the effect of the characteristic Bonellin substitution pattern is to shift the reduction potentials by +0.15 to 0.2 V relative to octaethylchorin $[H_2OEC]$, while leaving the internal separations unchanged. (Absolute values of first reduction potential for $[H_2OEC]$ and $[H_2OEP]$ are virtually

Table 7.1 Redox Potentials of $[H_2BDME]$

(i) Reductions

Electrode[c]	Solvent[d]	Electrode Potential/V[a] $E_{red}(1)$	$E_{red}(2)$	$\Delta E(1/2)$
Pt (a.c.)	CH_3CN	-1.62	-2.06	0.44
Pt (c.v.)	CH_3CN	-1.63	-2.08	0.45
Hg (a.c.)	CH_3CN	-1.63	-2.08	0.45
Hg (a.c.)	MeN	-1.74[b]	-	-

(ii) Oxidation

Electrode	Solvent[d]	Electrode Potential/V[a] $E_{ox}(1)$	$E_{ox}(2)$	ΔE(ox-red)
Pt (a.c.)	CH_3CN	+0.37	+0.86	1.99
Pt (c.v.)	CH_3CN	+0.37	-	2.00
Hg (a.c.)	CH_3CN	+0.36	-	1.99
Hg (a.c.)	MeN	+0.25[b]	-	1.99

(a) vs. Ag/Ag^+ reference unless otherwise stated.

(b) vs. $Fe(cp)_2/MeN$ (note: $Fe(cp)_2$ is oxidised at ca. +0.1 V[a] in CH_3CN)

(c) a.c. - alternating current voltammetry;
c.v. - cyclic voltammetry

(d) $CH_3CN/TBABF_4/25^oC$ or $MeN/TBABF_4/150^oC$

Figure 7.3 A.C. voltammogram

$[H_2BDME]$ oxidations

$CH_3CN/25^{\circ}C$

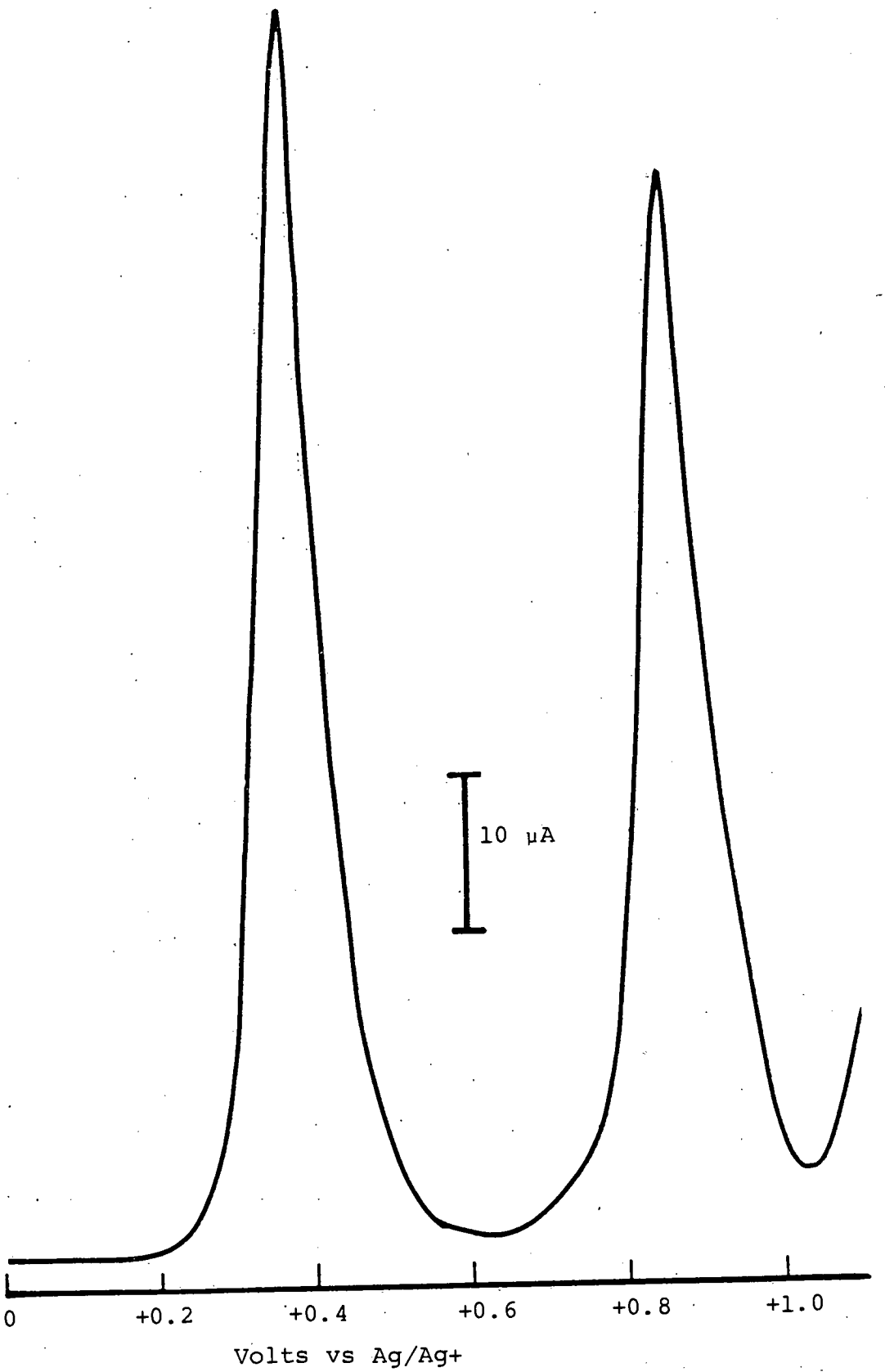

equal). Compared to porphyrins the first oxidation of both $[H_2OEC]$ and $[H_2BDME]$ is characteristically facile, with $E_{ox}(1)-E_{red}(1) = 2.00$ V, c.f. 2.25 V for $[H_2OEP]$.

Studies of the absorption spectrum of Bonellin have revealed a π/π^* transition energy of 1.94 V[176] which closely matches our electrochemically determined separation between donor and acceptor levels. This indicates that the two experiments map the same molecular orbital levels.

The fully reversible voltammetric behaviour noted above for Bonellin suggests that the simple electrode products can exist as independent stable moieties and should be capable of electrosynthesis at controlled potentials. Thus there existed the prospect of characterising the absorption spectra of $[H_2BDME]^+$ and $[H_2BDME]^-$ which are the feasible intermediates in the quenching of photoactivated $[H_2BDME]$.

The *in situ* spectroscopic monitoring of the electrogeneration of $[H_2BDME]^-$ in CH_3CN was undertaken in a chilled optically transparent thin layer cell, developed in this laboratory for use at low temperatures[177].

The changes in absorption spectra upon production of $[H_2BDME]^-$ are detailed elsewhere[178] but a remarkable spectral sequence is noted. Two distinctly different stages are observed in the electrolysis. Initially the characteristic band of Bonellin at 639 nm collapses with the growth of a band of similar appearance at 725 nm. This latter band is then lost so that the final spectrum is dominated by a broad band centred at 680 nm. The two

stages of this process are also distinguished by two independent sets of isosbestic points relating $[H_2BDME]$ with intermediate and intermediate with the final product. It should be noted that these changes occur at the voltammetrically determined first reduction potential of $[H_2BDME]$, and that $[H_2BDME]$ is completely regenerated (original $[H_2BDME]$ spectrum is recovered) if the applied potential is removed.

These observations are consistent with an intermediate complexation of $[H_2BDME]^-$ by $[H_2BDME]^o$ to form a dimer anion radical.

$$2[H_2BDME] \underset{}{\overset{e^-}{\rightleftharpoons}} [H_2BDME]^- + [H_2BDME] \overset{e^-}{\rightleftharpoons} 2[H_2BDME]^-$$

639nm $\qquad\qquad$ 680nm

$$\Updownarrow$$

$$[H_2BDME...H_2BDME]^-$$

725 nm

Our present data cannot determine the final state of $[H_2BDME]^-$ as monomer or dimer.

At the time of writing, studies are in hand in this laboratory on this compound and on other simple chlorins e.g. $[H_2OEC]$.

7.3 Experimental

Electrochemical methods were as outlined in Chapter 2. Acetonitrile, purified by the method of Walter and Ramaley[174] was used as solvent. The reference electrode for this work was Ag/Ag^+ (0.01 M $AgBF_4$/0.09 M $TBABF_4$). For ease of handling the sample was treated as follows. The compound (4.8 mg) was dissolved in pure CH_3CN (10 ml) and $TBABF_4$ (0.2 g) added. This solution was stirred for 10 minutes and the solvent removed under vacuum. The resulting mass was intimately ground and divided into four equal quantities. These were compressed under pressure (10 tons/sq. in for 5 minutes). The resulting pellets, each containing approximately 1.2 mg of compound, could then be conveniently used in routine electrochemical work. Solution concentrations of 4×10^{-4} M were used (1 pellet in 5 ml of 0.1 M $TBABF_4/CH_3CN$ solution). These manipulations and all electrochemical experiments were carried out in the absence of light.

CHAPTER 8

Synthetic Procedures

8.1 Introduction

The synthesis of the tetra-pyrrolic macrocycles has been reviewed in depth in the literature[44,57,179]. A brief outline of the general synthetic methods available will be given before a detailed account of the synthetic routes used in this work.

The strategies of porphyrin and phthalocyanine synthesis are quite different. The synthesis of the porphyrin macrocycle requires substituted pyrrole precursors, which are themselves elaborate and sometimes difficult to prepare. Four of these sub-units must then react to give the free base macrocycle. The conditions necessary for the cyclisation may give rise to a high proportion of open-chain and other polymeric pyrrole derivatives, so that cumulative yields in porphyrin synthesis are low. For example, even the simplest known porphyrin preparation, the single-step synthesis of [H_2TPP] from pyrrole and benzaldehyde has a yield of only 26%[180].

In contrast, in the preparation of phthalocyanines it is generally unnecessary to pre-form the "pyrrole" unit; this reaction occurs *in situ* from simpler, more readily obtainable sub-units (e.g. phthalic anhydride and urea). In addition, the phthalocyanine macrocycle can be synthesised around the template metal ion, facilitating the condensation of the four sub-units with simultaneous metal ion incorporation.

This template approach cannot be effectively applied in most metallo-porphyrin syntheses, indeed all known metalloporphyrin biosyntheses involve the insertion of metal ion into the free-base porphyrin with the displacement of the central hydrogen atoms.

$$M^{2+} + [H_2P] \longrightarrow [MP] + 2H^+$$

The synthesis of the substituted pyrroles has been documented in great depth and is not discussed here.

The methods of phthalocyanine synthesis were developed by Linstead and co-workers[4-8,181-184] and have been extended to a wide range of metals over the last forty years with the result that phthalocyanine complexes of the majority of main group, transition, and lanthanide metals are now known.

The starting materials in phthalocyanine synthesis are any of a number of phthalic acid derivatives, phthalic anhydride (with urea), phthalimide, phthalamide, phthalonitrile and o-cyanobenzamide. Phthalimide was the inadvertant source in the first recognised synthesis of ferrous phthalocyanine (see Chapter 1), while current industrial production of copper phthalocyanine is from a mixture of copper chloride, phthalic anhydride and urea.

Although the anhydride is the common starting material, the ideal precursor is phthalonitrile ($C_8H_4N_2$); this is essentially the "monomer" of phthalocyanine ($C_{38}H_{16}N_8$). The cyclisation of four molecules of phthalonitrile to yield the phthalocyanine macrocycle is formally represented in Figure 8.1.

Figure 8.1 Cyclisation of Phthalocyanines

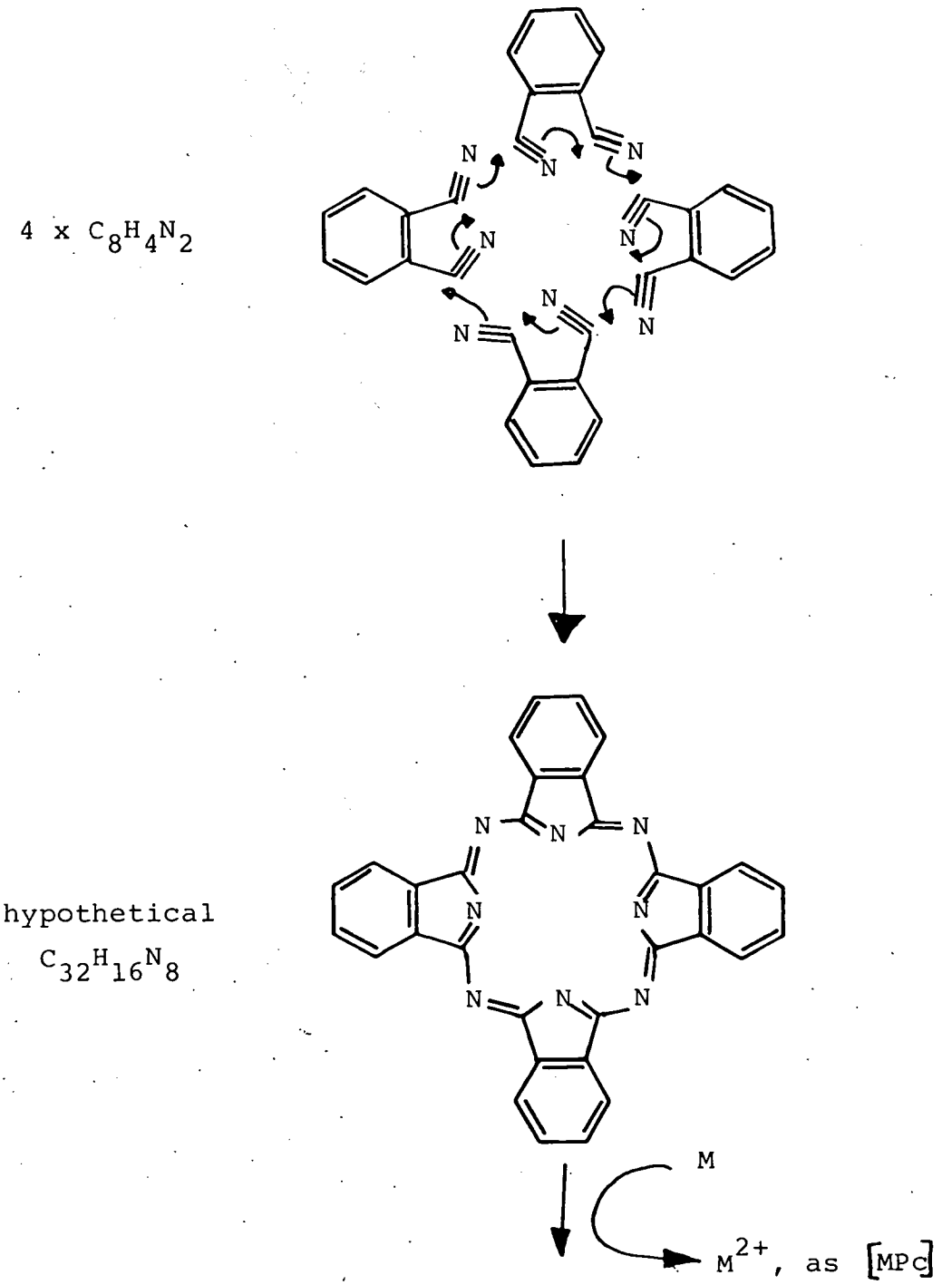

Interestingly, the electrosynthesis of [MPc] complexes by generation of the dianion of phthalonitrile in the presence of the appropriate metal ion (M = Co, Ni, Cu, Mg, Pb) has been recently reported[185].

8.2 Synthesis of Porphyrins

Tetraphenylporphin [H_2TPP], octaethylporphyrin [H_2OEP], [Fe(Cl)OEP] and [Co(Br)(py)OEP] were the generous gift of Professor A.W. Johns and were used without further purification. Standard literature methods[179] were used for the preparation of [MTPP] compounds (M = Co, Ni, Cu, Zn, Ag) and [MOEP] compounds (M = Ni, Cu, Zn), using the metal acetates in the preparation of cobalt, nickel, copper, zinc and silver complexes and magnesium perchlorate in the preparation of [MgTPP]. Purity of these compounds was assessed by visible/ultra-violet spectroscopic measurements and ultimately by their electrochemical examination.

8.3 Synthesis of Phthalocyanines

Phthalocyanine [H_2Pc] and its iron, cobalt, nickel, copper, zinc and magnesium complexes were prepared by literature methods[44]. Platinum, lead, silver, molybdenum and vanadyl phthalocyanines were obtained from Pfaltz and Bauer Inc. U.S.A. and were used without further purification.

The synthesis of substituted phthalocyanines requires the preparation of the appropriate substituted phthalic acid. In this work 4-t-butyl phthalic acid and its derivatives have been prepared; the steps involved are based on the methods of Lukyanets et al[186] with modifications and are summarised in Figure 8.2.

It is noticable that, from the o-xylene starting point, we are presented with a three-stage synthesis culminating in the direct condensation of the nickel and copper complexes (overall yield <5%), or a six-stage route to [H_2Bu_4Pc] (20% overall yield) leading to seventh stage metal-insertion reactions (overall yield 5-10%).

1-t-butyl-3,4-dimethyl-benzene (4(t-butyl)o-xylene) ($C_{12}H_{18}$)

o-xylene (203 g) and anhydrous ferric chloride (17.6 g) were chilled to ice temperature, and t-butyl chloride (203 g) added dropwise over a four-hour period with temperature maintained below 5°C. After stirring overnight the mixture was drowned in dilute HCl/ice and the organic layer washed with water (2 x 200 ml), saturated sodium carbonate solution (2 x 150 ml), and saturated salt solution (200 ml), and dried over anhydrous sodium sulphate. The resulting brown liquid was distilled under vacuum to yield 1-t-butyl-3,4-dimethyl-benzene, 266g; 66% yield.

Boiling Point 92°C/13 mm Hg; 65°C/8 mmHg

Analysis	Calculated	88.9% C;	11.1% H
	Observed	89.0% C;	11.0% H

Figure 8.2 Synthetic Routes to [MBu_4Pc]

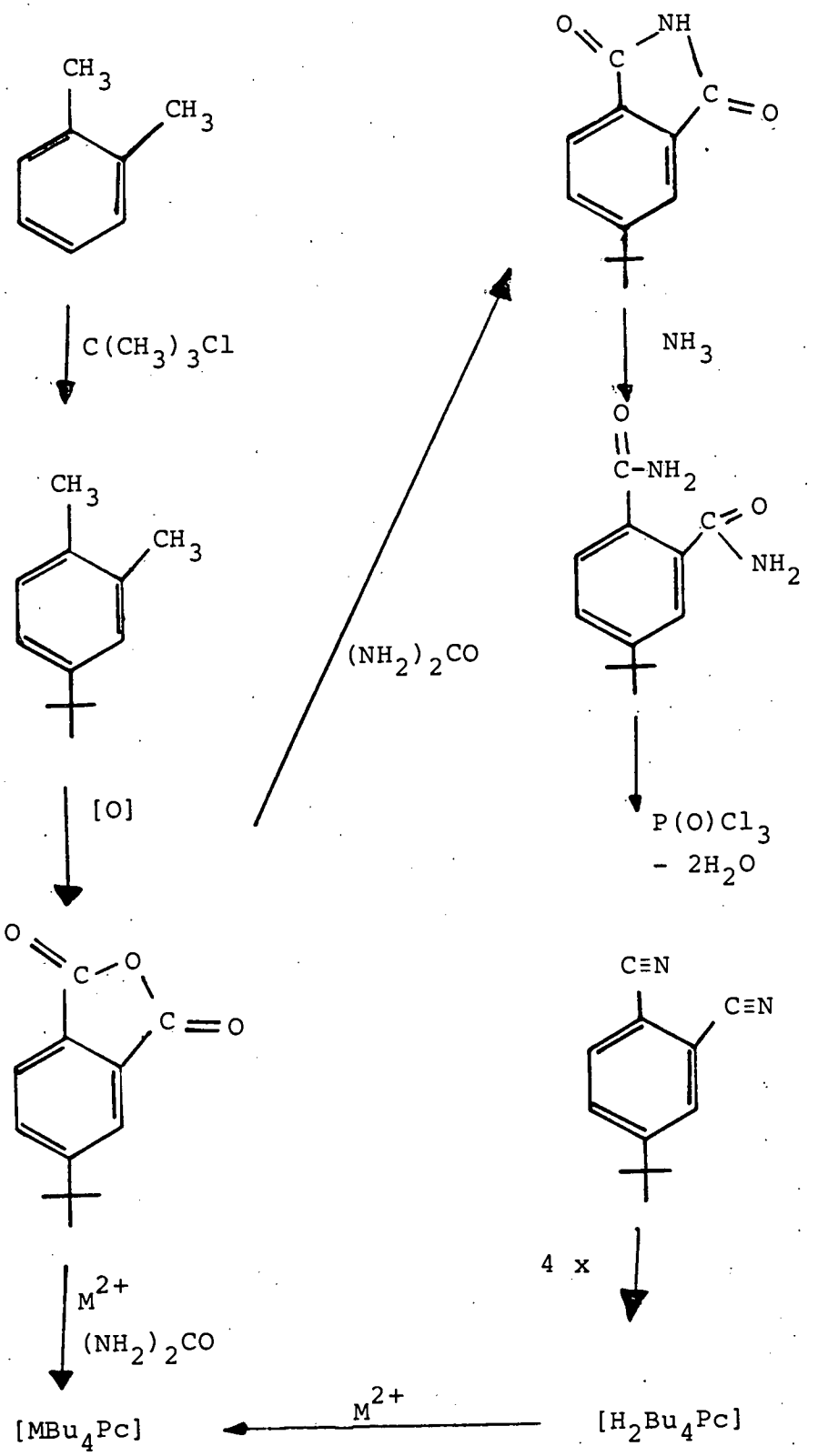

[^{1}H] n.m.r. spectrum ($CDCl_3$/TMS)

. 1.3 δ, 9H, singlet

2.15 δ, 3H, singlet

2.25 δ, 3H, singlet

7.05-7.15 δ, 3H, aromatic, complex

Infra Red Spectrum (neat liquid)

2970 cm^{-1}(s), 1505 cm^{-1}(s), 1450 cm^{-1}(s), 1140 cm^{-1}(m), 1025 cm^{-1}(m), 995 cm^{-1}(m), 925 cm^{-1}(m), 815 cm^{-1}(s).

Spectrum A (The infra red spectrum of this, and other compounds are presented at the end of this chapter).

4-t-butyl-phthalic anhydride ($C_{12}H_{12}O_3$)

Lukyanets et al used the method of Contractor and Peters[187], however the method used here[188] although involving longer reaction times gave the required compound in higher yield (typically 55%, compared wtih 35%).

A solution of t-butyl o-xylene (100 g), cobalt^{II} bromide (15 g) and manganese^{II}acetate (5 g) in propionic acid (500 ml) was refluxed for ca. 60 hours while compressed air was passed through the solution. (The use of compressed oxygen decreased reaction time to ca. 36 hours). After cooling the solvent was removed in vacuo and the residue extracted into chloroform (400 ml). This was washed with water (3 x 150 ml), saturated sodium carbonate solution (150 ml) and saturated salt solution. The chloroform solution was dried over anhydrous sodium sulphate, after removal of the solvent, the brown solid was recrystallised from 40-60 petroleum ether to yield white 4-(t-butyl)phthalic anhydride (69 g; 55%).

Melting Point 76°C (lit[187] 75.5-76.5°C)

Analysis Calculated 70.6% C; 5.9% H

Observed 70.5% C; 5.8% H

[^{1}H] n.m.r. spectrum ($CDCl_3$/TMS)

1.43 δ, 9H, singlet

7.95-8.10 δ, 3H, aromatic complex

Infra Red Spectrum (KBr Disc)

2960 cm^{-1}(m), 1845 cm^{-1}(s), 1770 cm^{-1}(s), 1470 cm^{-1}(m), 1240 cm^{-1}(s), 910 cm^{-1}(s), 880 cm^{-1}(s), 855 cm^{-1}(m), 740 cm^{-1}(s), 705 cm^{-1}(m), 685 cm^{-1}(s).

Spectrum B

This anhydride is produced by the *in situ* dehydration of the corresponding dicarboxylic acid.

In some experiments this conversion was not complete. In such cases, when the chloroform solution was washed with sodium carbonate, the sodium salt of the acid separated out. This could be filtered off, and warming the sodium salt with concentrated hydrochloric acid regenerated 4-t-butyl-phthalic acid ($C_{12}H_{14}O_4$).

Melting Point 154°C (lit[188] 154°C)

Analysis Calculated 64.9% C, 6.3% H

Observed 64.9% C, 5.9% H

[^{1}H] n.m.r. spectrum ($CDCl_3$/TMS)

1.34 δ, 9H, singlet

7.6-7.9 δ, 3H, aromatic complex

12.2 δ, 2H, singlet, labile

Infra Red spectrum (KBr Disc)

3500-2700 cm^{-1} (broad, s, OH), 2950 cm^{-1}(w), 1690 cm^{-1}(vs), 1430 cm^{-1}(m), 1320 cm^{-1}(s), 920 cm^{-1}(m), 845 cm^{-1}(m), 800 cm^{-1}(m), 705 cm^{-1}(m).

Spectrum C

4-t-butyl-phthalimide[186] ($C_{12}H_{13}NO_2$)

4-t-butyl-phthalic anhydride (21.1 g) was heated to 170°C for 2 hours with an equimolar quantity of urea (6.2 g). The melt was then allowed to cool and water (100 ml) added. The resulting precipitate was filtered off and dried. Recrystallisation from toluene gave 4-t-butyl-phthalimide (19.8 g, 93% yield).

Melting Point 131°C (lit[186] 131-132°C)

Analysis Calculated 70.0% C; 6.40% H; 6.89% N

Observed 69.8% C; 6.28% H; 6.87% N

[^{1}H] n.m.r. spectrum ($CDCl_3$/TMS)

1.3 δ, 9H, singlet

7.7-7.8 δ, 3H, aromatic complex

8.2 δ, 1H, singlet labile

Infra Red spectrum (KBr disc)

3200 cm^{-1}(s), 3060 cm^{-1}(w), 2960 cm^{-1}(m), 1775 cm^{-1}(m), 1720 cm^{-1}(vs), 1360 cm^{-1}(s), 1305 cm^{-1}(s), 1115 cm^{-1}(m), 1085 cm^{-1}(s), 1045 cm^{-1}(m), 870 cm^{-1}(s), 750 cm^{-1}(s)

Spectrum D

4-t-butyl phthalamide[186] ($C_{12}H_{16}N_2O_2$)

4-t-butyl phthalimide (18.0 g) was stirred with concentrated ammonia solution (100 ml) for 24 hours at room temperature. The resulting precipitate was then filtered off and dried under vacuum for 24 hours to yield 4-t-butyl-phthalamide (15.1 g, 77% yield).

Melting Point 180°C (decomposed) (lit[186] 181°C)

Analysis Calculated 65.3% C; 7.3% H; 12.7% N

Observed 64.83% C; 7.35% H; 12.32% N

[^{1}H] n.m.r. spectrum ($CDCl_3/d_6$ DMSO/TMS)

1.30 δ, 9H, singlet

7.4-7.6 δ, 3H, aromatic complex

7.2 δ, 4H, single labile

Infra Red Spectrum (KBr Disc)

3290 cm^{-1}(s), 3160 cm^{-1}(s), 2960 cm^{-1}(m), 1665 cm^{-1}(vs), 1590 cm^{-1}(m), 1405 cm^{-1}(s), 1125 cm^{-1}(m), 845 cm^{-1}(w,sharp), 690 cm^{-1}(m), 845 cm^{-1}(w,sharp), 690 cm^{-1}(s,broad).

Spectrum E

4-t-butyl phthalonitrile[186] ($C_{12}H_{12}N_2$)

4-t-butyl phthalamide (14 g) was dissolved in dry pyridine (100 ml) and phosphoryl chloride (25.0 g) added dropwise over a period of 45 minutes while the temperature was kept in the region 0 to 5°C. After addition was complete the mixture was stirred at room temperature for 3 hours and then drowned into ice. The brown precipitate was filtered off, washed with ice-cold water and dried.

This material was of sufficient quality for synthetic work; sublimation under vacuum (10^{-3} mmHg) at 60°C using an acetone/dry ice cold finger yielded white, crystalline 4-t-butyl phthalonitrile (10.2 g, 87% yield).

Melting Point 55°C (lit 55-57°C(186))

Analysis Calculated 78.26% C; 6.52% H; 15.21% N

Observed 78.51% C; 6.45%H; 14.98% N

[^{1}H] n.m.r. spectrum ($CDCl_3$/TMS)

1.35 δ, 9H, singlet

7.6-7.8 δ, 3H, aromatic complex

Infra Red spectrum (KBr disc)

3060 cm^{-1}(w), 2960 cm^{-1}(s), 2240 cm^{-1}(s, sharp, C≡N), 1580 cm^{-1}(s), 1480 cm^{-1}(s), 1395 cm^{-1}(s), 1195 cm^{-1}(m), 930 cm^{-1}(m), 845 cm^{-1}(s), 525 cm^{-1}(s).

Spectrum F

Tetra-(4-t-butyl)phthalocyanine $[H_2Bu_4Pc]$ $(C_{48}H_{50}N_8)$

Sodium (0.15 g) was dissolved in iso-amyl alcohol (60 ml) and the solution brought to reflux. t-butyl phthalonitrile (1.8 g) and sodium molybdate (catalytic amount; 1 mg) were then added and the mixture refluxed for 5 hours during which time the initially colourless solution became yellow, then green and finally intensely blue. The solution was then concentrated to approximately 5 ml on the rotary evaporator and 75 mls of methanol added. This was stirred overnight at room temperature, the deep blue

precipitate was then filtered, washed with ice cold methanol and dried. Chromatography on a silica column with carbon tetrachloride:acetone (95:5) as eluent followed by recrystallisation from chloroform-methanol, yielded tetra(4-t-butyl)phthalocyanine (0.65 g, 36%)

Analysis	Calculated	78.02% C;	6.82% H;	15.17% N
	Observed	77.38% C;	6.81% H;	14.16% N

The physical and spectroscopic (infra-red, n.m.r. and visible) properties of this and other [MBu_4Pc] compounds are discussed collectively later in this chapter.

Copper tetra(4-t-butyl)phthalocyanine [$CuBu_4Pc$] ($C_{48}H_{48}N_8Cu$)

A mixture of 4-t-butyl phthalic anhydride (15 g), urea (35 g), copper^{II} chloride (4.0 g) and sodium molybdate (0.1 g) in 1,2,4-trichlorobenzene (150 ml) was stirred under reflux for 16 hours. After cooling, the mixture was washed with dilute hydrochloric acid, dilute sodium hydroxide and water. The solvent was then removed and the residue extracted with carbon tetrachloride. This was then chromatographed on a silica gel column using carbon tetrachloride:acetone (95:5) as eluent. The blue solid obtained after removal of the solvent was recrystallised from chloroform/methanol to yield copper tetra(4-t-butyl)-phthalocyanine (1.1 g, 7.5% yield).

Analysis	Calculated	72.0% C;	6.0% H;	14.0% N
	Observed	71.9% C;	5.9% H;	13.7% N

Nickel tetra(4-t-butyl)phthalocyanine [$NiBu_4Pc$]

This compound was obtained in a manner analogous to [$CuBu_4Pc$] using nickel^{II} chloride hexahydrate in place of copper chloride to give nickel tetra(4-t-butyl)phthalocyanine in similar yield (9%).

Analysis	Calculated	72.5% C;	6.08% H;	14.1% N
	Observed	72.6% C;	6.3% H;	14.0% N

Zinc tetra(4-t-butyl)phthalocyanine [$ZnBu_4Pc$]

2 ml of saturated solution of zinc acetate in acetic acid were added to a refluxing solution of [H_2Bu_4Pc] (0.1 g) in toluene (25 ml). Heating was continued for 2 to 3 hours, the progress of the reaction being monitored by visible spectroscopy. After cooling, the solution was washed with water (100 ml), sodium carbonate solution (2 x 100 ml) and then dried over sodium sulphate. The solvent was removed and the solid extracted with carbon tetrachloride. This was chromatographed on silica using carbon tetrachloride: acetone (75:25) as eluent. Recrystallisation from chloroform:methanol give zinc tetra(4-t-butyl)phthalocyanine (0.045 g, 41%).

Analysis	Calculated	71.88% C;	6.03% H;	14.0% N
	Observed	71.5% C;	6.2% H;	12.5% N

Cobalt tetra(4-t-butyl)phthalocyanine

This was prepared in 28% yield in a similar manner to [$ZnBu_4Pc$], using cobalt^{II} acetate in place of zinc acetate. Electrochemistry and visible spectroscopy showed that this compound contained a small quantity (ca. 5%) of unreacted [H_2Bu_4Pc] which could not be separated from the required compound.

Magnesium tetra(4-t-butyl)phthalocyanine

Magnesium perchlorate (1.0 g) was added to a refluxing solution of [H_2Bu_4Pc] (0.1 g) in dry pyridine (50 ml). After 3 hours the cooled solution was added to CCl_4 (100 ml) and washed with water (2 x 100 ml) and the organic layer dried over anhydrous sodium sulphate for 24 hours. Chromatography on alumina using carbon-tetrachloride:acetone (80:20) as eluent gave magnesium tetra(4-t-butyl)phthalocyanine which was pumped under vacuum at 10^{-4} mmHg at 60°C for 24 hours.

Iron tetra(4-t-butyl)phthalocyanine [$FeBu_4Pc$]

Iron pentacarconyl ($Fe(CO)_5$|m|, 1.5 g) was added to a solution of [H_2Bu_4Pc] (0.1 g) in refluxing toluene under nitrogen (25 ml). After 3 hours the solution was evaporated to dryness. The residue was extracted with carbontetrachloride, washed with water (2 x 100 ml) and dried over sodium sulphate. The resulting blue solution was then chromatographed on alumina using carbon tetrachloride:acetone

(95:5) as eluent. The blue solution separated from a brown impurity which remained on the column. The blue solid obtained from this solution was recrystallised from chloroform/methanol to yield iron tetra(4-t-butyl) phthalocyanine.

Oxo-titanium tetra(4-t-butyl)phthalocyanine ($Ti(O)Bu_4Pc$)

This reaction was originally undertaken on the presumption that it would yield [H_2Bu_4Pc] according to the known synthesis of [H_2Pc] via $TiCl_4$-catalysed condensation of phthalic anhydride and urea[188]. Presumably in the case of the alkylated derivative, hydrolysis led to the formation of the oxotitanium complex (in low yield).

The electrochemistry of this compound was anomalous reductions occuring at less negative potentials than expected. The compound was tentatively identified in our laboratory as a [$(M=O)Bu_4Pc$] derivative on the basis of its single band visible spectrum (rather than the twin band spectrum expected for [H_2Bu_4Pc]), the absence of a N-H stretch in the infra red spectrum and the presence of a new band at 965 cm^{-1} ($\nu_{Ti=O}$). This was confirmed by X-ray fluorescence studies at I.C.I. Organics Division, Manchester, which revealed the presence of one atom of titanium per molecule.

A solution of 4-t-butyl phthalic anhydride (15 g), urea (36 g) and titanium tetrachloride (1.9 g) in trichlorobenzene (150 ml) was heated to 170°C with stirring when 2-aminoethanol was added. The mixture was then

heated to reflux (190°C) for 16 hours. The mixture, after cooling, was evaporated to dryness and the residue extracted with carbon tetrachloride. This was washed with dilute hydrochloric acid, dilute sodium hydroxide, and water. After drying over sodium sulphate, the blue solution was chromatographed on a silica column using carbontetrachloride: acetone as eluent. Recrystallisation from chloroform:methanol gave oxo-titanium tetra(4-t-butyl)phthalocyanine.

Physical Properties of tetra(4-t-butyl)phthalocyanines

(i) Melting Points

No definitive melting points could be recorded for the [MBu_4Pc] compounds. They are all high (>350°C) and many compounds tended to sublime rather than melt. The problem of sublimation also made it difficult to obtain accurate and reproducible combusion analyses, hence data are not recorded for certain compounds. These latter compounds were however spectroscopically and electrochemically "pure".

(ii) Infra Red Spectra

The infra-red spectra of [MPc] compounds are complex with approximately 30 bands of differing intensity being observed in the region 1700 to 250 cm^{-1} (44). For example spectrum G shows the infra red spectrum of copper phthalocyanine. Fortunately the spectra of all [MPc] compounds are very similar and thus the infra red spectrum may be used as a "finger print" for the phthalocyanine

compound, in certain cases this spectrum being used as proof of formation of a new phthalocyanine derivative[44]. The free base [H_2Pc] exhibits a spectrum similar to that of [MPc] but, helpfully, contains an additional band at 3290 cm^{-1} (N-H stretch) and an intense band at 1007 cm^{-1} also associated with the central hydrogen atoms (Spectrum H).

The infra red spectra of the [MBu_4Pc] systems are naturally even more elaborate. However the free base [H_2Bu_4Pc] exhibits a band characteristic of a N-H stretch at 3280 cm^{-1} and, as in [H_2Pc], an intense band is seen at 1005 cm^{-1} (Spectrum J).

The [MBu_4Pc] compounds (M = Fe, Co, Ni, Cu, Zn, Mg) all reveal remarkably similar infra red spectra, as exemplified by the copper and zinc derivatives (Spectra K and L respectively). The oxo-titanium derivative [Ti(O)Bu_4Pc] has, in addition to the characteristic "finger print" spectrum, an additional band at 965 cm^{-1} assigned to the Ti=O stretch (Spectrum M).

The infra red absorption frequencies of [H_2Bu_4Pc] and its metallated derivatives have not been described elsewhere and are recorded in Table 8.1.

Table 8.1 Infra red spectra of [MBu_4Pc] (Frequency/cm^{-1})

	[MBu_4Pc] M =						
H_2	Fe	Co	Ni	Cu	Zn	Mg	Ti(O)
3280[a]	-	-	-	-	-	-	-
2950	2960	2950		2950	2940	2950	2940
1615	1610	1610		1610	1620	1610	1605
1500	b	b		1505	b	b	b
1480	1480	1485		1485	1490	1470	1480
1390	1390	1390		1385	1390	1380	1380
1365	1355	1360		1355	1360	1365	1360
1315	1310	1320		1315	1330	1325	1320
1280	1275	1280		1275	1280	1280	1275
1255	1255	1260		1250	1255	1250	1250
1085	1090	1090		1085	1090	1085	1070
1005[a]	-	-	-	-	-	-	965[c]
910	935	940		925	920	915	915
830	800	800		820	825	795	820
750	760	750		755	760	750	755
-	740	-		740	740	750	745
680	690	690		685	685	680	680
665	670	665		660	665	650	660
520	-	-		530	530	-	520

[a] (N-H) mode

[b] concealed by neighbouring absorption

[c] (Ti=O) mode

(iii) Visible Spectra and Aggregation Phenomena for Phthalocyanines

The visible spectra of phthalocyanines are characterised by intense absorptions in the region 650 to 700 nm, which are responsible for their vivid colour.

The high symmetry (D_{4h}) metal complexes possess a single intense almost invariant absorption band in this region. For example, in chloronaphthalene solution the copper, nickel and zinc derivatives have maximum absorbances at 678, 671 and 680 nm respectively, with molar extinction coefficients of ca. 10^5 $M^{-1}dm^3cm^{-1}$. Phthalocyanine [H_2Pc] which is of lower symmetry (D_{2h}) exhibits a two-band spectrum (698 nm and 665 nm) in the same region.

The tetra-t-butyl-phthalocyanines possess similar spectroscopic characteristics. For example, the free base [H_2Bu_4Pc] has two strong absorption bands in dichloromethane solution, almost unshifted with respect to [H_2Pc], while the metal complexes show a single band at approximately 670 nm. The relevant absorption maxima and extinction coefficients for [H_2Bu_4Pc] and its metal complexes are presented in Table 8.2.

Aggregation phenomena are well-known for porphyrins, and for derivatised phthalocyanines in polar media, at all but the most dilute concentrations. Aggregation, if present, would clearly bear on interpretation of the electrochemical data. The voltammetric concentration range is generally $<5 \times 10^{-4}$ M, and $<10^{-5}$ M (of necessity) for the phthalocyanine pigments themselves, in methyl naphthalene at 150°C.

Table 8.2 Absorption Maxima of MBu_4Pc

(i) $[H_2Bu_4Pc]$

λ_{max}/nm	698	662	638	600	339	228
ε^a (x 10^{-3})	202	176	64.2	36.7	104	53.2

(ii) $[CoBu_4Pc]$

λ_{max}/nm	669	641	605	325	285
ε^a (x 10^{-3})	178	58.5	42.6	89.4	97.7

(iii) $[NiBu_4Pc]$

λ_{max}/nm	670	640	603	362	331	293
ε^a	144	42.7	32.1	28.8	46.9	55.1

(iv) $[CuBu_4Pc]$

λ_{max}/nm	677	635	600	338	286
ε^a (x 10^{-3})	269	69.3	61.0	122.1	54.5

(v) $[ZnBu_4Pc]$

λ_{max}/nm	678	646	611	340	286
ε^a (x 10^{-3})	204	48.7	38.2	86.9	34.7

(vi) $[MgBu_4Pc]$

λ_{max}/nm	679	648	612	350	289
ε^a (x 10^{-3})	182	26.1	23.9	70.6	29.4

(vii) $[Ti(O)Bu_4Pc]$

λ_{max}/nm	697	665	626	347	295
ε^a (x 10^{-3})	151	41.8	36.4	148	68.7

[a] ($M^{-1}dm^3cm^{-1}$) in CH_2Cl_2 solution

We investigated the possiblity of aggregation by looking for characteristic changes in the visible spectrum. For this investigation it was necessary to develop a very short path-length (0.05 mm) high-temperature cell (<200^{o}C), controlled by a circulating thermostat bath, as in our electrochemical experiments. The short path-length is dictated by the extreme visible extinction coefficients and the need to examine concentrations as 'high' as 10^{-3} M.

At room temperature, the free base [H_2Bu_4Pc] was found to obey the Beer-Lambert Law in methylnaphthalene in the concentration range 10^{-7} to 10^{-4} M. For the corresponding metallo-complexes, in contrast, deviations from ideal Beer-Lambert Law behaviour were noted above 10^{-5} M. These deviations were characterised by a broadening of the primary absorption band and a change in relative intensity of bands at ca. 600 and 640 nm. However on systematically raising the temperature of such concentrated solutions, the spectrum was observed to change progressively, and above 100^{o}C to coincide with that seen in ideal dilute solution. Presumably we are observing some form of aggregation of the metal complexes in the non-polar medium which is overcome at elevated temperature. The ideal behaviour of the free base at all accessible concentrations contrasts with that of the metal derivatives and suggests the aggregation observed in the latter derivatives involves metal-nitrogen interactions similar to those found in the crystalline state (see Chapter 1).

For the present purpose, the important point is that, notwithstanding the achievement of unprecedented solubility levels of the phthalocyanines and their tetra-alkyl analogues in liquid naphthalene media, the high operating temperature of the electrochemical experiments precludes any aggregation phenomena.

8.4 Synthesis of Zinc Tetrabenzoporphin [ZnTBP]

This compound was first synthesised by Linstead and co-workers[189-192] and later by Edwards, Gouterman and Rose[193]. Both methods were based on cyclisations using iso-indolinone-3-acetic acid. More recently, Vogler and Kunkley[194] reported the synthesis of [ZnTBP] in a single-step template reaction using a readily available starting material, 2-acetyl benzoic acid, condensed with NH_3 in the presence of zinc acetate. This latter method was followed closely in this work, the purified compound being isolated in 5% yield as purple crystals which dissolve in pyridine, toluene, dichloromethane etc. to give an intense green solution. The visible spectrum is consistent with that described by Edwards, Gouterman and Rose[193]. Limited infra-red spectroscopic data were reported by these workers but the spectrum itself was not presented. Therefore we include here the infra red spectrum of [ZnTBP] over the region 4000-250 cm^{-1} (Spectrum N), as well as listing the principal bands below.

Infra Red Spectrum (KBr Disc)

3060 cm^{-1}(w), 2930 cm^{-1}(w), 2860 cm^{-1}(w), 1580 cm^{-1}(m), 1420 cm^{-1}(m), 1285 cm^{-1}(m), 1115 cm^{-1}(s), 1055 cm^{-1}(m), 755 cm^{-1}(s), 735 cm^{-1}(s), 700 cm^{-1}(s).

Analysis	Calculated	75.4% C;	3.5% H;	9.8% N
	Observed	74.4% C;	3.79% H;	9.35% N

8.5 Experimental Procedure

All melting points were obtained on a hot stage microscope and are uncorrected. Infra red spectra in the region 4000-250 cm^{-1} were obtained on a Perkin-Elmer Model 557 Infra Red Spectrometer as KBr Discs or as Nujol Mulls. ^{1}H N.m.r. Spectra were run on a Perkin Elmer R32 Spectrometer. Ultraviolet-visible spectra were recorded on a Pye Unicam SP8-400 Spectrophotometer over the range 900-250 nm. Elemental analyses (carbon, hydrogen and nitrogen) were obtained by the microanalytical services of the Chemistry Department, University of Edinburgh and Organics Division, I.C.I. Grangemouth.

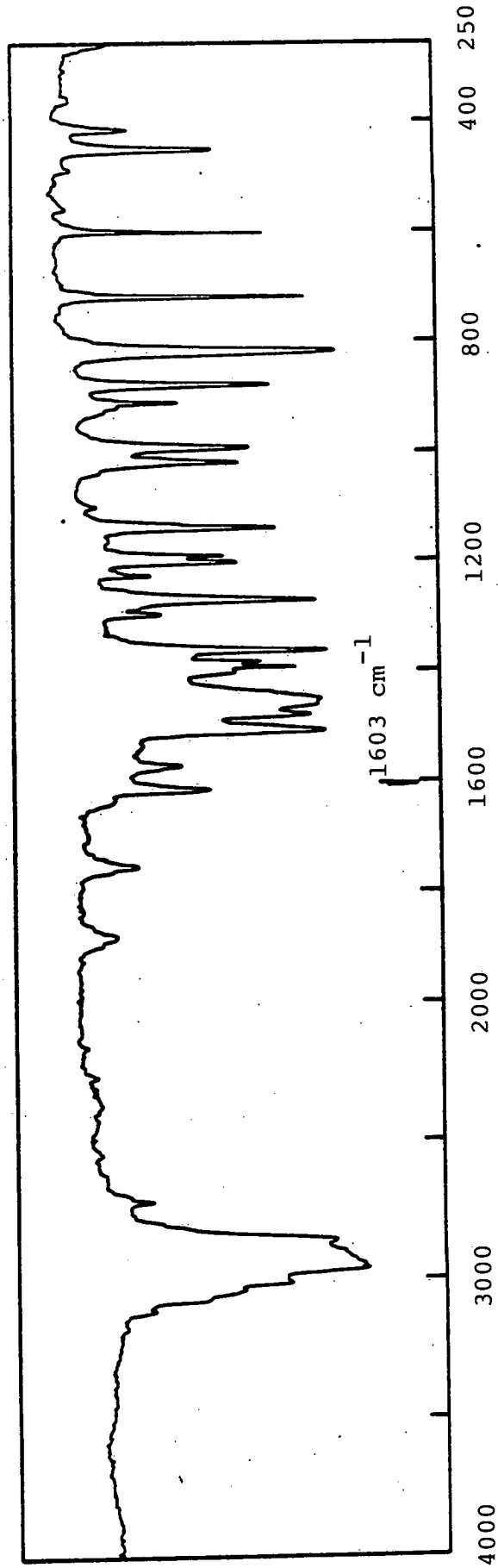

Spectrum A 1-t-butyl-3,4-dimethyl-benzene (neat liquid)

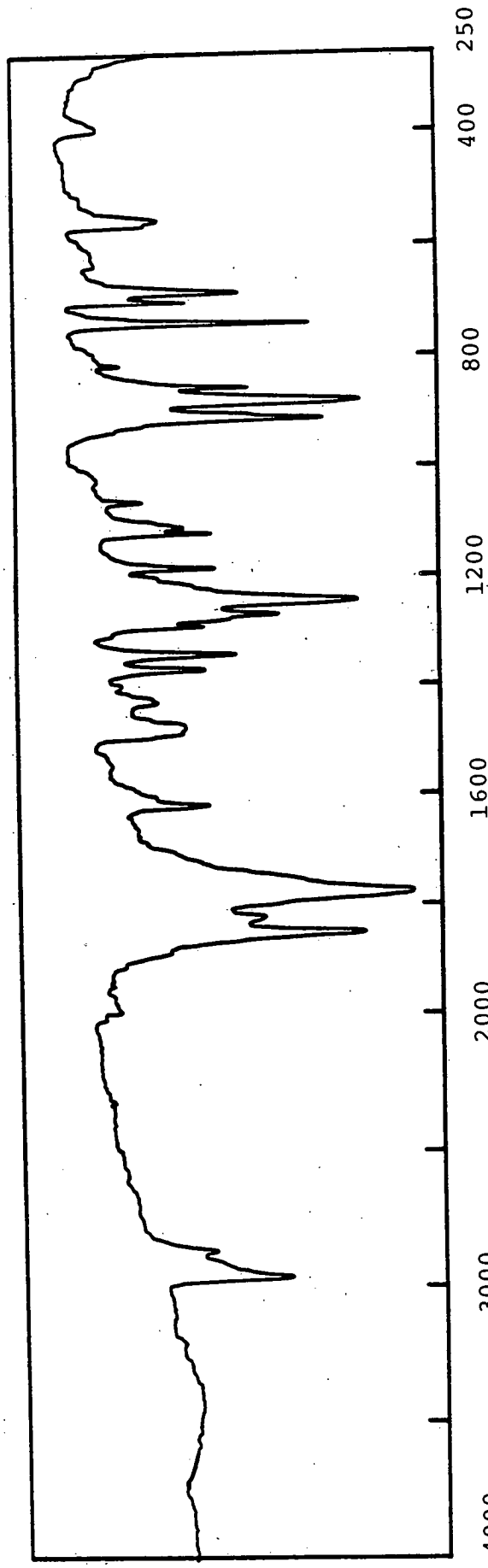

Spectrum B 4-t-butyl phthalic anhydride (KBr Disc)

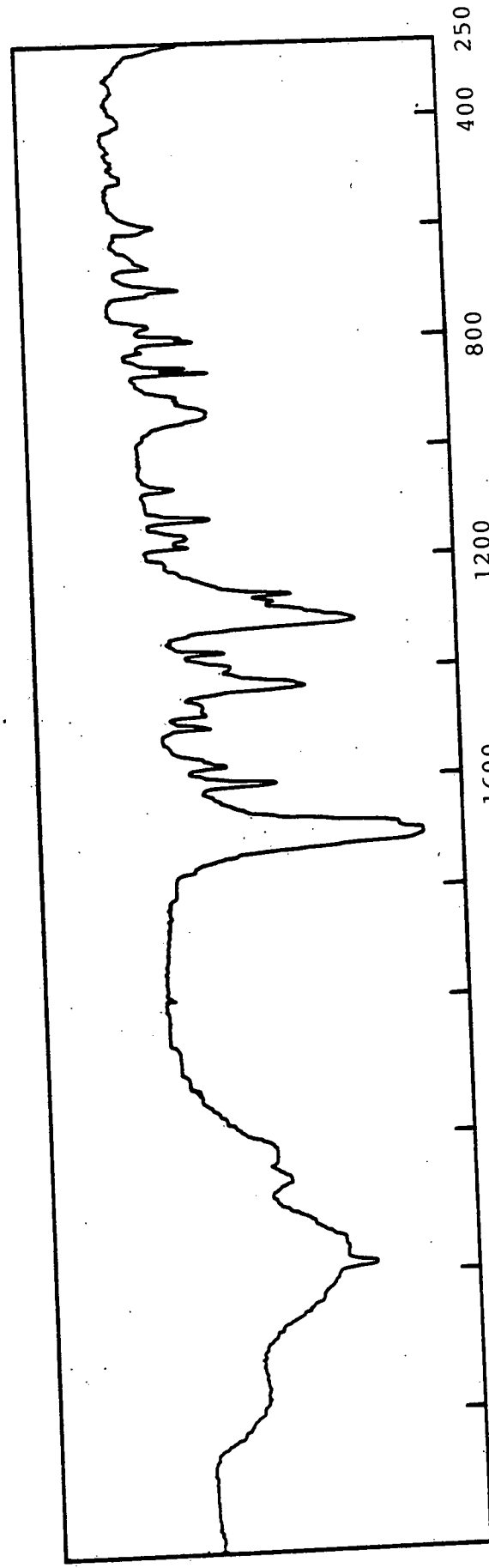

Spectrum C 4-t-butyl phthalic acid (KBr Disc)

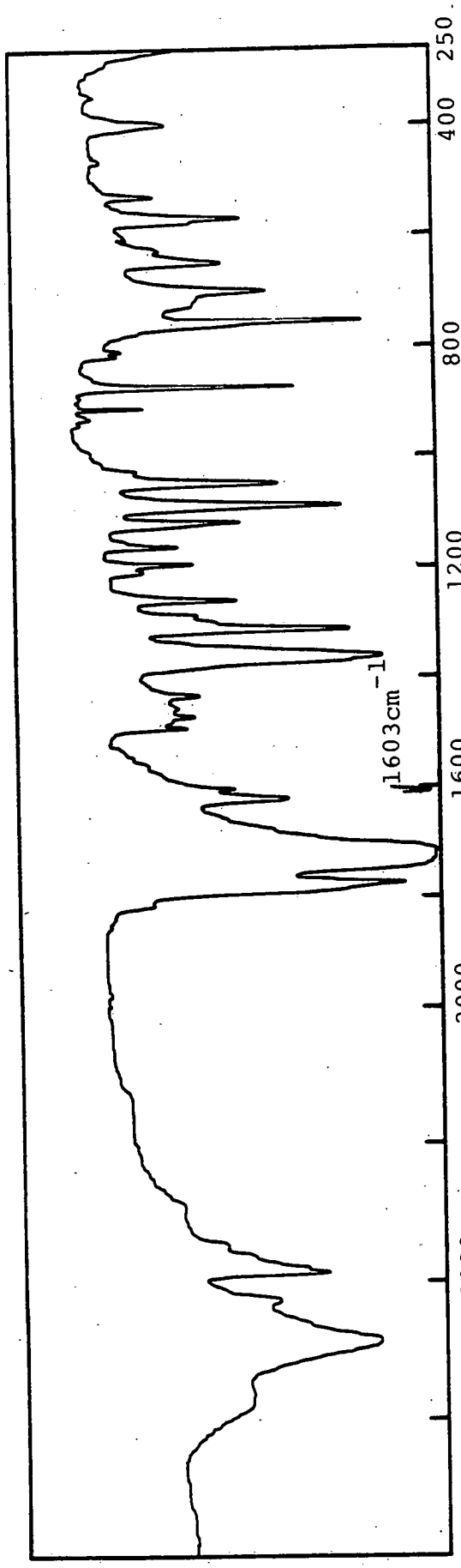

Spectrum D 4-t-butyl phthalimide (KBr Disc)

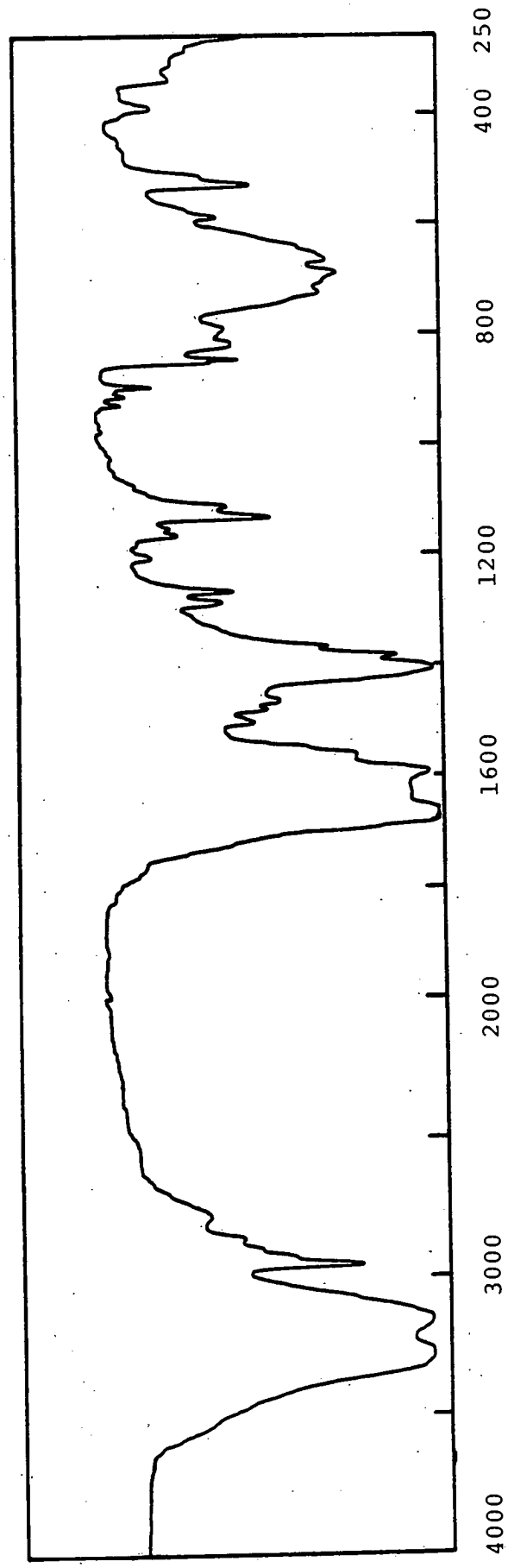

Spectrum E 4-t-butylphthalamide (KBr Disc)

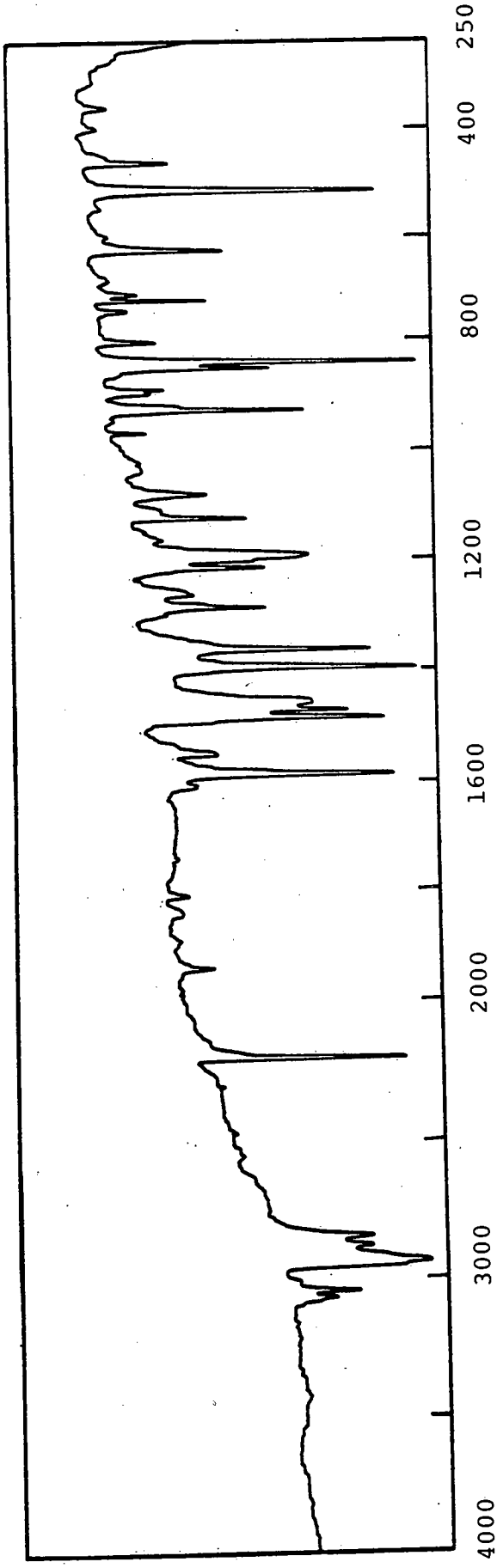

Spectrum F 4-t-butyl phthalonitrile (KBr Disc)

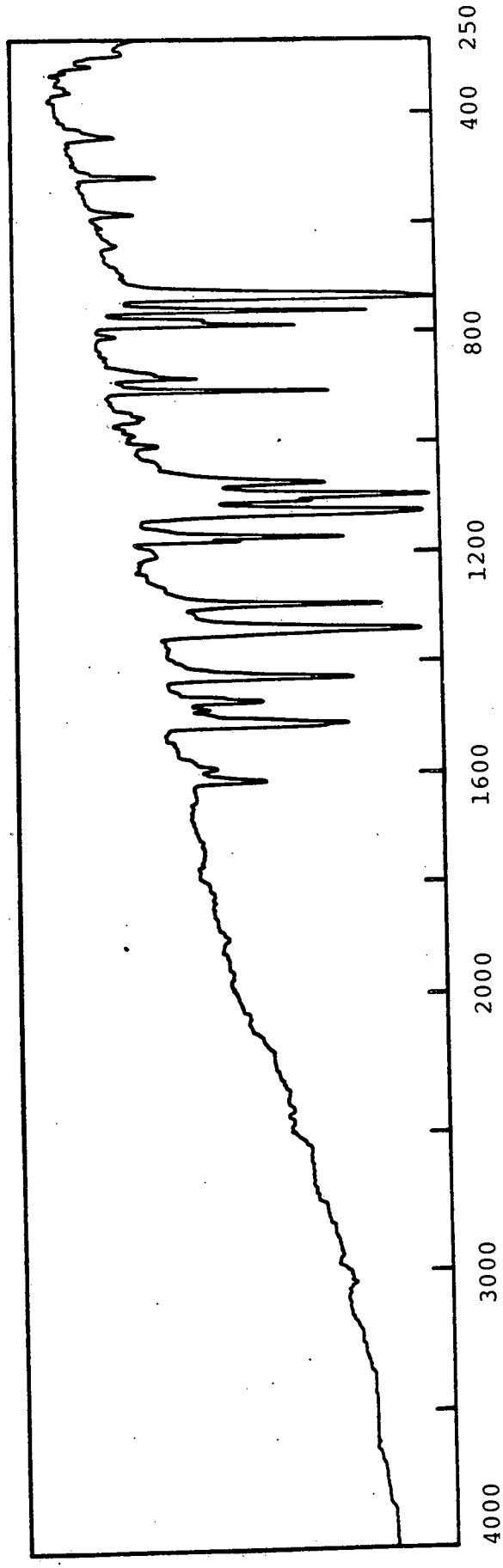

Spectrum G Copper Phthalocyanine [CuPc] (KBr Disc)

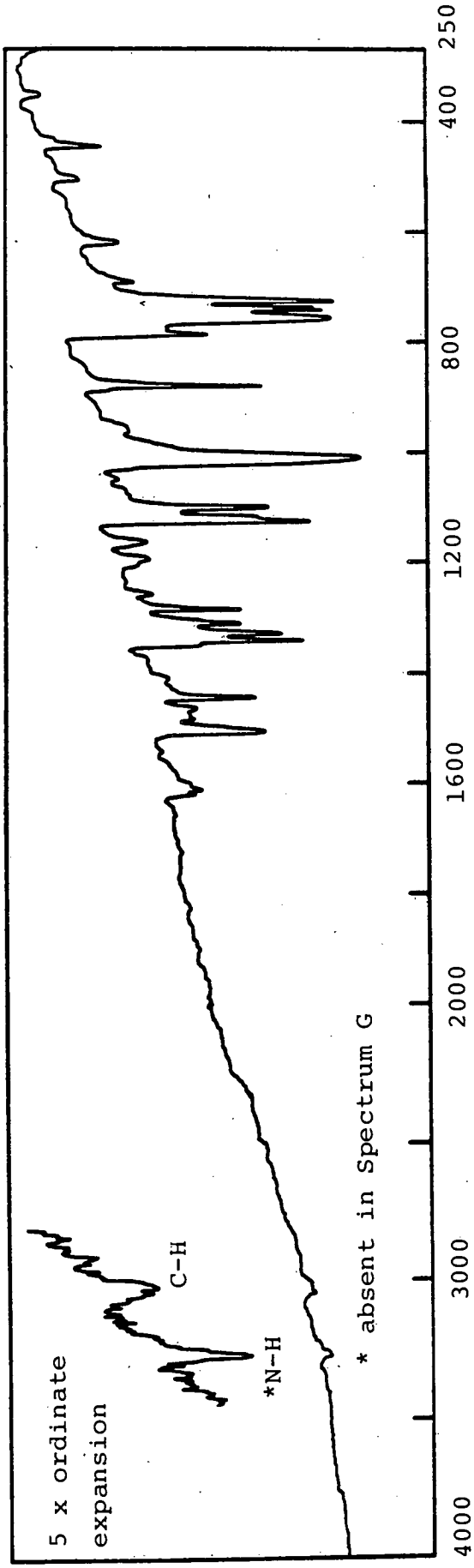

Spectrum H Phthalocyanine [H_2Pc] (KBr Disc)

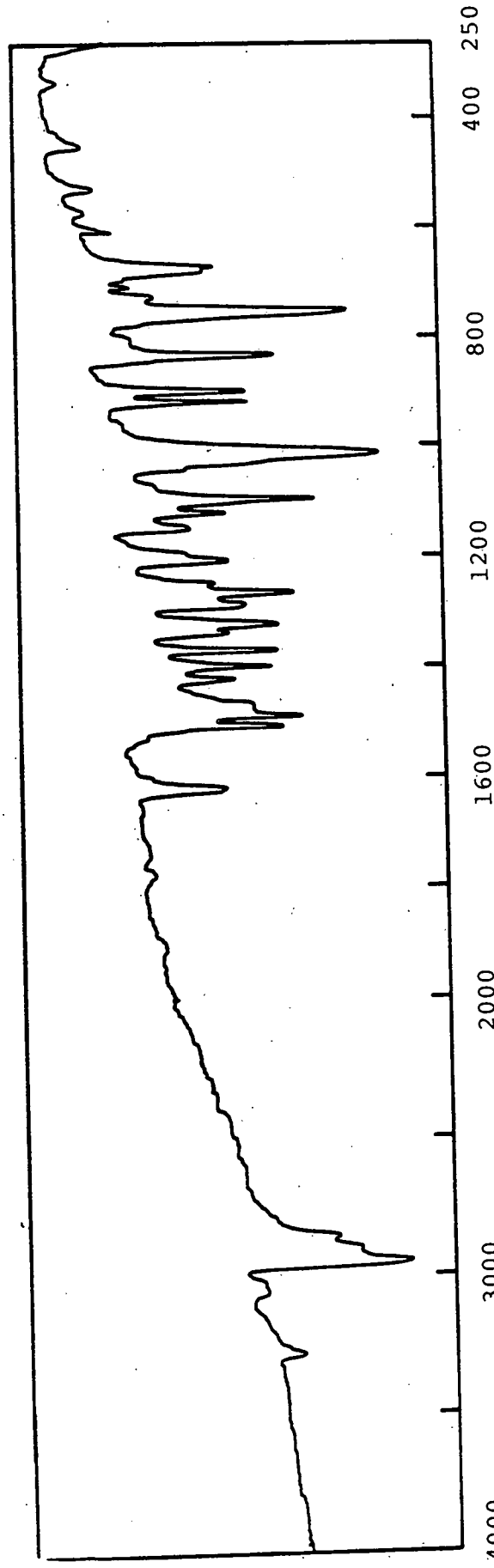

Spectrum J Tetra(4-t-butyl)phthalocyanine [H_2Bu_4Pc] (KBr Disc)

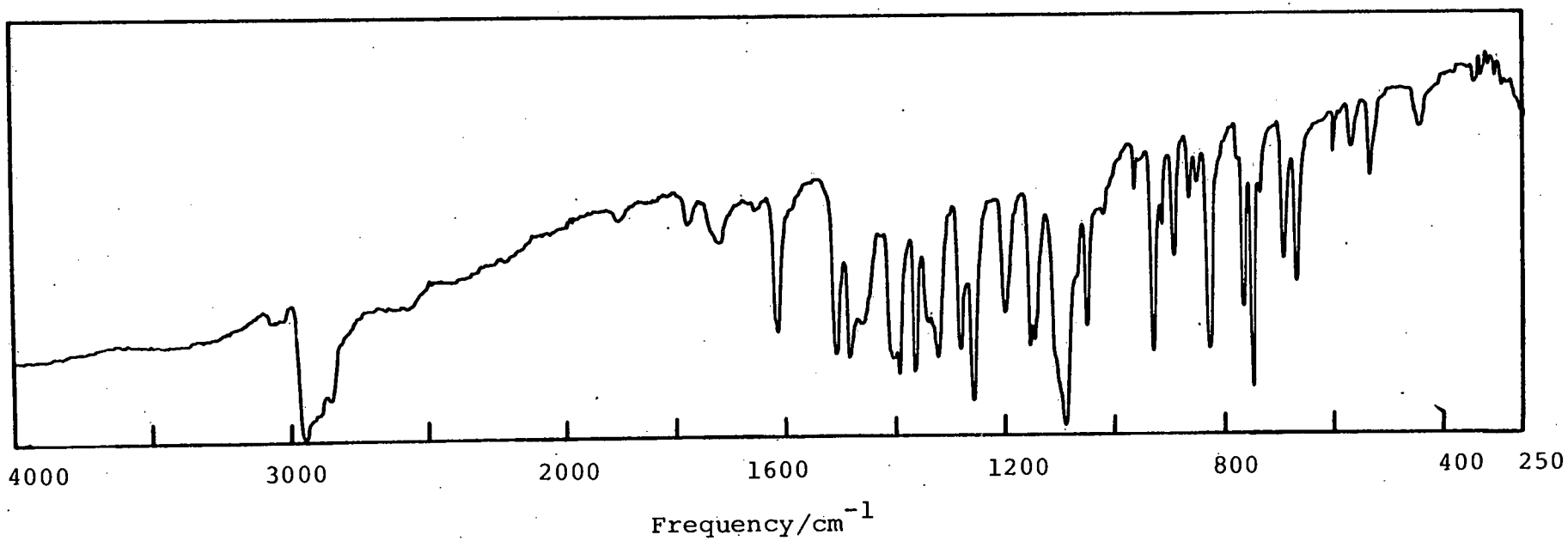

Spectrum K Copper tetra(4-t-butyl)phthalocyanine [$CuBu_4Pc$] (KBr Disc)

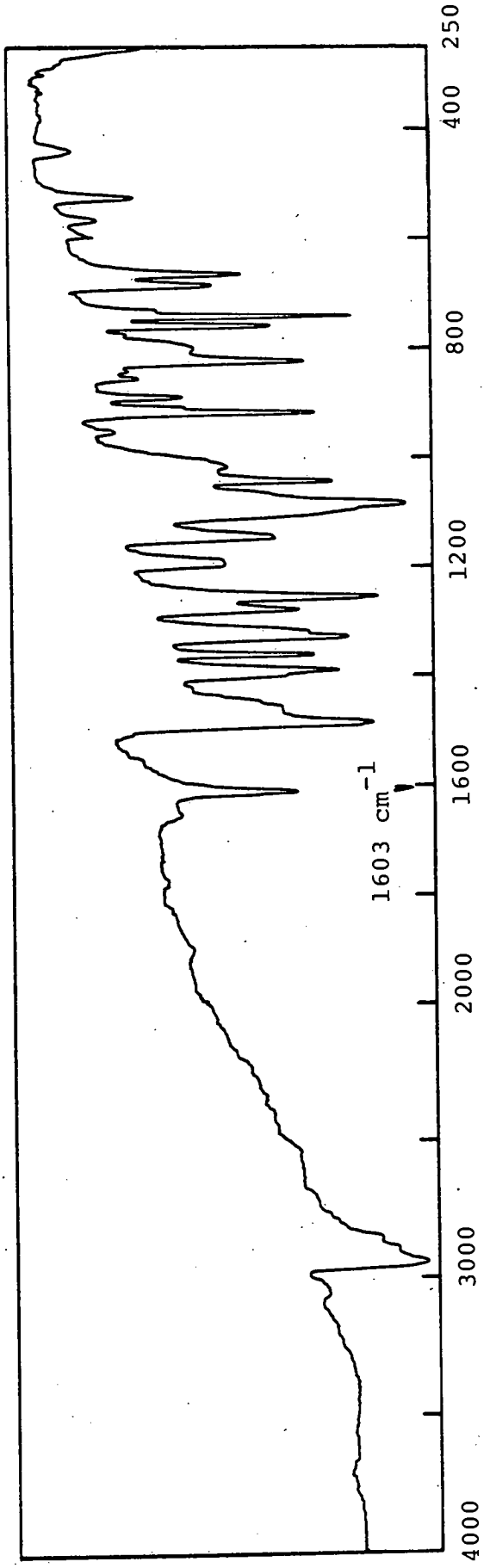

Spectrum L Zinc tetra(4-t-butyl)phthalocyanine [$ZnBu_4Pc$] (KBr Disc)

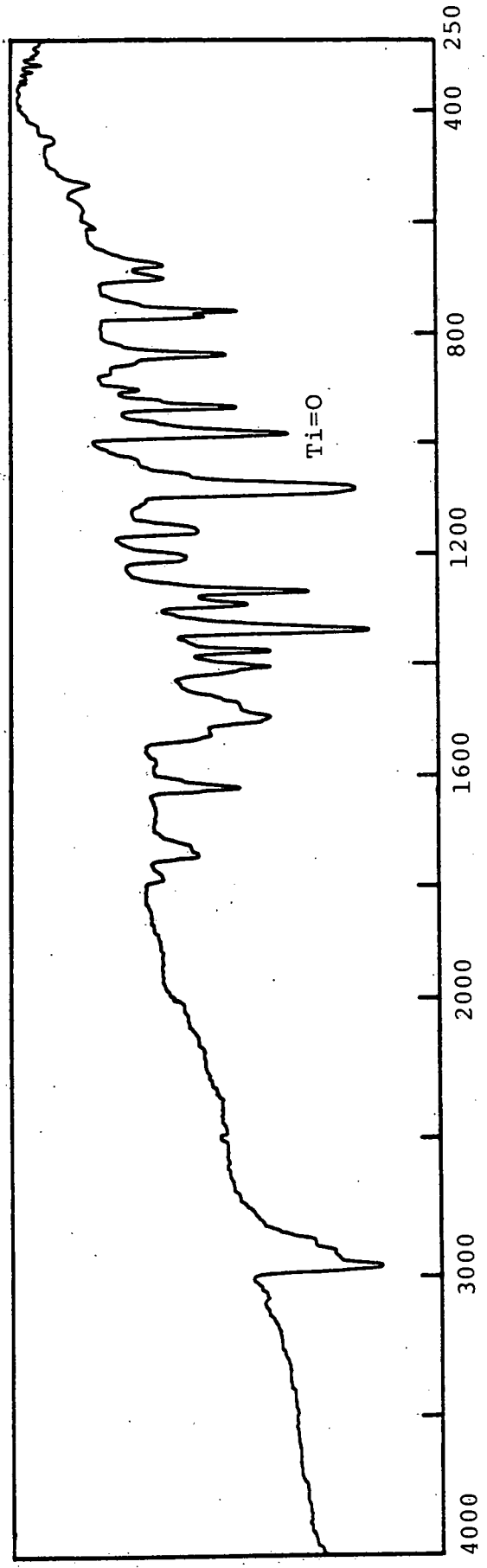

Spectrum M Titanyl tetra(4-t-butyl)phthalocyanine [Ti(O)Bu_4Pc] (KBr Disc)

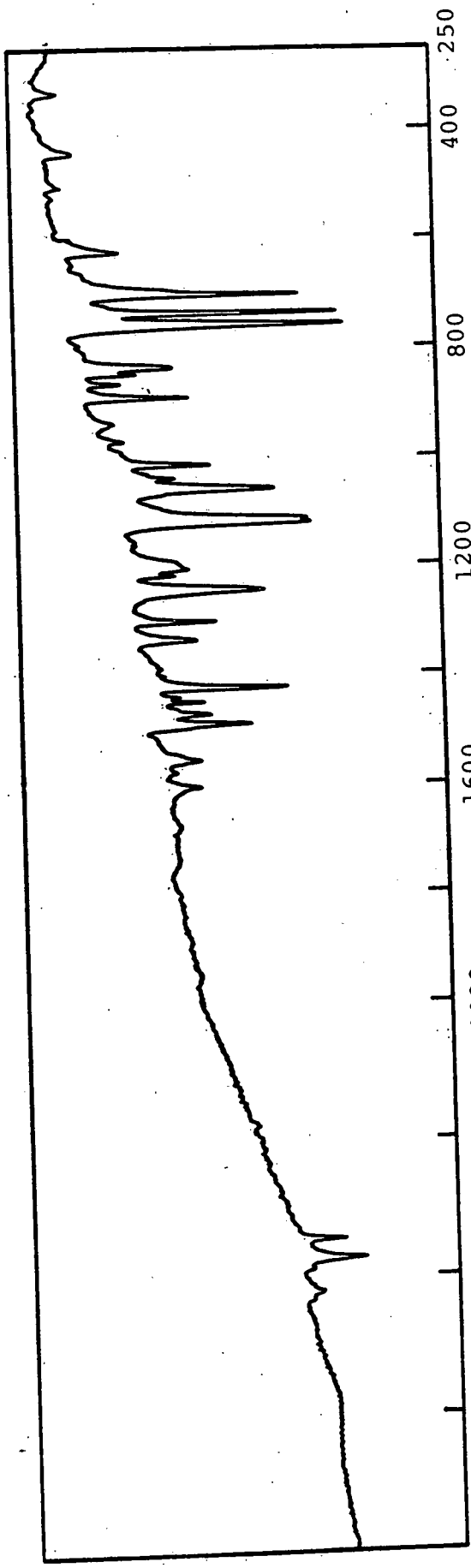

Spectrum N Zinc tetrabenzoporphin [ZnTBP] (KBr Disc)

References

1. W. Kuster, Hoppe-Seyler Z. Physiol.Chem., 82 (1912), 463.
2. H. Fischer, K. Zeile, Ann.Chem., 468 (1928), 98.
3. H. de Diesbach, E. van der Weid, Helv.Chim.Acta., 10 (1927), 886.
4. R.P. Linstead, J.Chem.Soc., (1934), 1016.
5. G.T. Byrne, R.P. Linstead, A.R. Lowe, J.Chem.Soc., (1934), 1017.
6. R.P. Linstead, J.Chem.Soc., (1934), 1022.
7. R.P. Linstead, J.Chem.Soc., (1934), 1031.
8. C.E. Dent, R.P. Linstead, A.R. Lowe, J.Chem.Soc., (1934), 1033.
9. J.L. Soret, Comp.Rend., 97, (1883), 1267.
10. E.A. Lawton, J.Phys.Chem., 62, (1958), p.384.
11. R.P. Linstead, J.M. Robertson, J.Chem.Soc., (1935), 615.
12. R.P. Linstead, J.M. Robertson, J.Chem.Soc., (1936), 1195.
13. R.P. Linstead, J.M. Robertson, J.Chem.Soc., (1936), 1736.
14. J.M. Robertson, I. Woodward, J.Chem.Soc., (1937), 219.
15. B.M.L. Chen, A. Tulinsky, J.Am.Chem.Soc., 94, (1972), 4144.
16. J.W. Lauher, J.A. Ibers, J.Am.Chem.Soc., 95, (1973), 5148.
17. E.F. Meyer, Acta.Cryst., B28, (1972), 2162.
18. D.L. Cullen, E.F. Meyer, J.Am.Chem.Soc., 96, (1974), 2095.
19. D.M. Collins, J.L. Hoard, J.Am.Chem.Soc., 92, (1970), p.3761.
20. R.E. Dickerson, I.Geis, "The Structure and Action of Proteins Harper and Row, 1969.
21. E. Ochiai, "Bioinorganic Chemistry", Allyn & Beacon, Boston, U.S.A., Chapter 7, 1977.
22. V. Ullrich, Angew Chem.Int. Ed., 11 (1972), p.701.

23. A. Harriman, G. Porter, J.Chem.Soc., Faraday Trans. 2, (1979), p.1532.

24. A. Harriman, G. Porter, J.Chem.Soc., Faraday Trans. 2, (1979), p.1543.

25. N. Carnieri, A. Harriman, G. Porter, J.Chem.Soc., Dalton Trans., (1982), p.931.

26. F. Basolo, B.M. Hoffman, C.J. Weschler, J.Am.Chem.Soc., 97, (1975), p.5278.

27. F. Basolo, D.A. Summerville, R.D. Jones, J.Am.Chem.Soc., 100, (1978), p. 4416.

28. J.A. Elvidge, A.B.P. Lever, Proc.Chem.Soc., (1959), p. 195.

29. K. Uchida, S. Naito, M. Soma, T. Onishi, K. Tamaru, J.Chem.Soc., Chem.Comm., (1978), p. 217.

30. A.B.P. Lever, J.P. Wilshire, S.K. Quan, Inorg.Chem., 20 (1981), p.761.

31. A.B.P. Lever, J.P. Wilshire, S.K. Quan, J.Am.Chem.Soc., 101 (1979), p. 3668.

32. E.W. Abel, J.M. Pratt, R. Whelan, J.Chem.Soc., Chem.Comm., (1971), p. 449.

33. F. Cariati, D. Galizzioli, F. Morazzoni, C. Busetto, J.Chem.Soc., Dalton Trans, (1975), p. 556.

34. H. Przywarska-Boniecka, E. Panejko, L. Trynda, J. Biernat, Material Science, 4 (1978), p. 139.

35. J.P. Collman, J.I. Brauman, K.S. Suslick, J.Am.Chem.Soc., 97 (1975), p. 7185.

36. R. Jasinski, Nature, 201 (1964), p. 1212.

37. A.J. Appleby, J. Fleisch, M. Savy, J.Catal., 44, (1976), p. 281.

38. A.J. Appleby, M. Savy, Electrochim.Acta., 21 (1976), p. 567.

39. S.M. Maroie, M. Savy, J.J. Verbist, Inorg.Chem., 18, (1979), p. 2560.

40. N. Kobayashi, M. Fujihira, K. Sunakawa, T. Osa, J.Electroanal.Chem., 101, (1976), p. 269.

41. H. Jahnke, Photosyn. Oxygen Evol. Symp., (1979), p. 439.

42. J. Zagal, P. Bindra, E. Yeager, J.Electrochem.Soc., 127 (1980), p. 1506.

43. E. Putseiko, Dokl.Akad.Nauk, SSSR, 59 (1948), p. 471.

44. A.B.P. Lever, Adv. Inorg.Chem. Radiochem., 7 (1965), 27 and references therein.

45. S.C. Dahlberg, M.E. Husser, J.Chem.Phys., 70, (1979), p.5021.

46. R.O. Loutfy, J.H. Sharp, J.Chem.Phys., 71 (1979), p. 1211.

47. F.R. Fan, L.R. Faulkner, J.Chem.Phys., 69, (1978), p. 3334.

48. F.R. Fan, L.R. Faulkner, J.Chem.Phys., 69 (1978), p. 3341.

49. R.A. Nelson, J.Chem.Phys., 27 (1957), p. 864.

50. A.M. Fiabane, D.R. Williams, The Principles of Bio-Inorganic Chemistry, Chem.Soc. Monograph, No. 31, London 1977.

51. H. Eckert, I. Ugi, Angew.Chem.Int.Ed., 15 (1976), p. 681.

52. H. Eckert, I. Listl, I. Ugi, Angew Chem.Int. Ed., 17, (1978), 361.

53. H. Eckert, I. Ugi, Angew Chem.Int.Ed., 14 (1975), p. 825.

54. H. Eckert, I. Ugi, J.Organomet.Chem., 118 (1976), C59.

55. H. Eckert, A. Lagerlund, I. Ugi, Tetrahedron, 33 (1977), p. 2243.

56. A.H. Cook, J.Chem.Soc., (1938), p. 1761.

57. L.J. Boucher "Coordination Chemistry of Macrocyclic Compounds", Ed G.A. Nelson, Plenum; New York, 1979, p. 461-516.

58. V.M. Kotheri, J.J. Tazuma, J.Catal., 41, (1976), p. 180.

59. H. Kropf, Angew.Chem.Int.Ed., 11 (1972), p. 239.

60. E. Rabinowitch, J. Weiss, Proc.R.Soc. London, A162, (1937), 251.

61. A.E. Cahill, H. Taube, J.Am.Chem.Soc., 73, (1951), p.2847.

62. P. George, D.J.E. Ingram, J.E. Bennett, J.Am.Chem.Soc., 79 (1957), p. 1870.

63. J.F. Gibson, D.J.E. Ingram, Nature, 178 (1956), p. 871.

64. G.L. Closs, L.E. Closs, J.Am.Chem.Soc., 85 (1963), 818.

65. J.W. Dodd, N.S. Hush, J.Chem.Soc., (1964), p. 4607.

66. D.W. Clack, N.S. Hush, J.Am.Chem.Soc., 87 (1965), p. 4238.

67. (a) R. Taube, Z.Chemie, 6, (1966), p. 8.
(b) R. Taube, Angew.Chem.Int.Ed., 6 (1967), p. 358.

68. M. Zerner, M. Gouterman, Theor.Chim.Acta., 4 (1966), p. 44.

69. A.M. Schaffer, M. Gouterman, E.R. Davidson, Theor.Chim.Acta., 30 (1973), p. 9.

70. R.H. Felton, Harvard University, U.S.A., Ph.D. Thesis, 1964.

71. R.H. Felton, H. Linschitz, J.Am.Chem.Soc., 88 (1966), p.1113.

72. A. Staniendo, G. Bield, Z.Physi.Chem.Neue.Folge, 52, (1967), p. 254.

73. A. Wolberg, J. Manassen, J.Am.Chem.Soc., 92 (1970), p.2982.

74. L.D. Rollman, R.T. Iwamato, J.Am.Chem.Soc., 90 (1968), p.145

75. J.H. Fuhrhop, D. Mauzerall, J.Am.Chem.Soc., 91 (1969), p.417

76. D. Dolphin, A. Forman, D.G. Borg, J. Fajer, R.H. Felton, Proc.Nat.Acad.Sci., 68 (1971), p. 614.

77. J.H. Fuhrhop, K.M. Kadish, D.G. Davis, J.Am.Chem.Soc., 95 (1973), p. 5140.

78. D.G. Davis, D.J. Olreron, Anal.Chem., 38 (1966), p. 179.

79. (a) D. Lexa, M. Momenteua, J. Mispelter, Biochem.Biophys. Acta, 338, (1974), p. 151.

(b) D. Lexa, M. Momenteau, J. Mispelter, Bioelectrochem. Bioenergy, 1 (1974), p. 108.

80. (a) K.M. Kadish, G. Larson, D. Lexa, M. Momenteau, J.Am.Chem.Soc., 97 (1975), p. 282.

(b) K.M. Kadish, L.A. Bottomley, J.Am.Chem.Soc., 99, (1977), p. 2380.

(c) K.M. Kadish, L.A. Bottomley, D. Bericz, Inorg.Chem., 17 (1978), p. 1124.

(d) K.M. Kadish, L.A. Bottomley, Inorg.Chem., 19 (1980), p. 832.

(e) K.M. Kadish, D. Schaeper, J.Chem.Soc.Chem.Comm., (1980), p. 1273.

81. L.A. Truxillo, D.G. Davis, Anal.Chem., 47 (1975), p. 2260.

82. F.A. Walker, D. Berioz, K.M. Kadish, J.Am.Chem.Soc., 98 (1976), p. 3484.

83. L.A. Constant, D.G. Davis, Anal.Chem., 47 (1975), p. 2253.

84. L.J. Boucher, H.K. Garber, Inorg.Chem., 9 (1970), p. 2646.

85. K.M. Kadish, M. Sweethand, J. Cheung, Inorg.Chem., 17 (1978), p. 2795.

86. R.H. Felton, "The Porphyrins", Ed. D. Dolphin, Academic Press, New York (1980), Vol. 5, p. 53.

87. D.W. Clack, N.S. Hush, I.S. Woolsey, Inorg.Chim.Acta., 19 (1976), p. 129.

88. A.B.P. Lever, J.P. Wilshire, Can.J.Chem., 54 (1976), p.2514.

89. A.B.P. Lever, J.P. Wilshire, Inorg.Chem., 17 (1978), p. 1145.

90. V.I. Gavrilov, L.G. Tomilova, I.V. Shelepin, E.A. Lukyanets, Elektrokhimiya, 15 (1979), p. 1058.

91. V.I. Gavrilov, E.A. Lukyanets, I.V. Shelepin, Electrokhimiya, 17 (1981), p. 1183.

92. J.F. Myers, G.W. Rayner Cauham, A.B. Plever, Inorg.Chem., 14 (1975), p. 461.

93. R.D. Lowfy, E.R. Menzel, J.Am.Chem.Soc., 102 (1980), p. 4963.

94. R.F. Fan, L.R. Faulkner, J.Chem.Phys., 69 (1978), p. 3334 and references therein.

95. R.O. Loutfy, J.H. Sharp, J.Chem.Phys., 71 (1979), p. 1211.

96. S.F. Vulfson, O.L. Kaliya, O.L. Lebedev, E.A. Lukyanets, Z.Org.Khim., 12 (1976), p. 123.

97. J. Heyrovsky, Chem.Listy., 16 (1922), p. 256.

98. J. Heyrovsky, P. Zuman, "Practical Polarography", Academic Press, London (1968).

99. O.H. Muller in "Physical Methods of Chemistry", Ed. Weissberger and Rossiter, Wiley Intersicnece, New York, (1971), Part IIa, Chapter 4.

100. A.J. Bond, L.R. Faulkner, "Electrochemical Methods Fundamental and Applications", Wiley, New York (1980).

101. D.T. Sawyer, J.L. Roberts, "Experimental Electrochemistry for Chemists", Wiley, New York, (1974).

102. E.R. Brown, R.F. Large in "Physical Methods of Chemistry", Ed. Weissberger and Rossiter, Wiley Interscience, New York (1971), Part IIa, Chapter 6.

103. B. Breyer, F. Gutmann, Trans.Faraday Soc., 43 (1947), p.785.

104. P. Arthur, P.A. Lewis, N.A. Lloyd, R.K. Vanderkan, Anal.Chem., 33 (1961), p. 488.

105. W.B. Schaap, P.S. McKinney, Anal.Chem., 36 (1964), p. 29.

106. E.R. Brown, T.G. McCord, D.E. Smith, D.D. Deford, Anal.Chem., 38 (1966), p. 1119 and references therein.

107. G.L. Booman, W.B. Holbrook, Anal.Chem., 35 (1963), p. 1793.

108. W.L. Underkofler, I. Shain, Anal.Chem., 35 (1963), p. 1778.

109. G.L. Booman, W.B. Holbrook, Anal.Chem., 37 (1965), p. 795.

110. Handbook of Chemistry and Physics, ed. R. Weist, C.R.C. Press, U.S.A., 62nd Edition (1980).

111. W.M. Heston, E.J. Hennelly, C.P. Symth, J.Am.Chem.Soc., 72 (1950), p. 2071.

112. J.W. Hayes, C.N. Reilley, Anal.Chem., 37 (1965), p. 1322.

113. P. Arthur, R.H. Vanderkam, Anal.Chem., 33 (1961), p. 765.

114. E.R. Brown, D.E. Smith, Anal.Chem., 46, (1968), p. 1411.

115. E.R. Brown, H.L. Huny, T.G. McCord, D.E. Smith, Anal.Chem., 40 (1968), p. 1425.

116. W.B. Schaap, P.S. McKinney, Anal.Chem., 36 (1964), p. 1251.

117. P.E. Whitson, H.W. Vandenborn, D.H. Evans, Anal.Chem., 45 (1973), p. 1298.

118. D. Garreau, J.M. Saveant, J. Electroanal.Chem., 35 (1972), p. 35.

119. V. Gutmann, E. Wychera, Inorg.Nucl.Chem.Lett., 2 (1966), p. 257.

120. A.M. Bond, J.Electroanal.Chem., 35 (1972), p. 343.

121. D.E. Smith, "Electroanalytical Chemistry", Ed. A.J. Bard, Dekker, New York (1961), Vol. 1.

122. M.R. Pesce, S.L. Knesbach, R.K. Ladisch, Anal.Chem., 25, (1953), p. 979.

123. G. Jones, R.C. Josephs, J.Am.Chem.Soc., 50 (1928), p. 1049.

124. T. Shedlovsky, J.Am.Chem.Soc., 52 (1930), p. 1793.

125. P.H. Daum, D.F. Nelson, Anal.Chem., 45 (1973), p. 463 and references therein.

126. G.A. Heath, R.H. Campbell, G.T. Hefter, in preparation.

127. J. Timmermaus, "Physiochemical Constants of Pure Organic Compounds", Elesevier, New York, Vol. 1, 1950, p. 180; Vol. 2, 1965, p. 132 and references therein.

128. J.A. Riddick, W.B. Burger, "Techniques of Chemistry", Wiley, New York, Vol. III, Organic Solvents, 3rd Ed., 1970, p. 347 and references therein.

129. G.B. Arrowsmith, G.H. Jeffery, A.I. Vogel, J.Chem.Soc., (1965), p. 2072.

130. "Table of Dielectric Constants of Pure Liquids", N.B.S. Circular 514, U.S. Govt. Printing Office, Washington, 1951.

131. F. Danials, R.A. Albuty, "Physical Chemistry", Wiley, New York, (1961), 2nd Edition, p. 506.

132. D.W. Clack, J.R. Yandle, Inorg.Chem., 11 (1972), p. 1738.

133. P. Day, H.A.O. Hill, M.G. Price, J.Chem.Soc., A, (1968), p.90

134. D.W. Clack, N.S. Hugh, J.R. Yandle, Chem.Phys.Lett., 1, (1967), p. 157.

135. M.J. Stillman, A.J. Thomson, J.Chem.Soc., Faraday II, (1974), p. 790.

136. C.M. Guzy, J.B. Raynor, L.P. Stadulskii, M.C.R. Symons, J.Chem.Soc., A, (1969), p. 997.

137. F.A. Walker, J.Am.Chem.Soc., 92 (1970), p. 4235.

138. R. Taube, Pure and Appl.Chem., 38 (1974), p. 427.

139. V.E. Kholmogorov, D.N. Glabovsky, Opt. i Spektroskopiya, 12 (1962), p. 728.

140. A. MacCragh, W.S. Koski, J.Am.Chem.Soc., 85 (1963), p. 2375.

141. A.B.P. Lever, Adv. Inorg.Radiochem., 7 (1965), p. 51, and references therein.

142. N.N. Greenwood, E.J.F. Ross, B.P. Stranghan, "Index of Vibrational Spectra of Inorganic and Organometallic Compounds" Butterworth Press, 1972, Vol. 1, and references therein.

143. J. Selbin, L.H. Holmes, S.P. McGlynn, J.Inorg.Nucl.Chem., 25 (1963), p. 1359.

144. E.A. Cuellar, T.J. Marks, Inorg.Chem., 20 (1981), p. 3766.

145. N. Fukada, Nippou Kagaka Zasshi, 75 (1954), p. 1141.

146. K. Bernauer, S. Fallab, Helv.Chim.Acta., 44 (1961), p. 1287.

147. F.M. McLaren, M.Sc. Thesis, University of Stirling, 1980.

148. R. Campbell, Honours Project Report, Stirling University 1978.

149. G.D. Dorough, J.R. Miller, F.M. Huennekens, J.Am.Chem.Soc., 73 (1951), p. 4315.

150. I.A. Cohen, D. Ostfield, B. Lichenstein, J.Am.Chem.Soc., 94 (1972), p. 4522.

151. T. Kakutani, S. Totsuka, M. Senda, Bull.Chem.Soc. Japan, 46 (1973), p. 3652.

152. L.J. Hoard in "Porphyrins and Metalloporphyrins", Ed. K.H. Smith, Elsevier, Amsterdam, (1975), Chapter 8, p. 323.

153. C.J. Brown, J. Chem. Soc. A. (1968), p 2488.

154. (a) E.B. Heischer, J.Am.Chem.Soc., 85 (1963), p. 1353.
(b) E.B. Heischer, C.K. Miller, L.E. Webb, J.Am.Chem.Soc., 86 (1964), p. 2342.

155. E. Frasson, R. Berdi, S. Bezzi, Acta Cryst., 12 (1959), p.201.

156. K.M. Kadish, P.K. Rhodes, Inorg.Chem., 20 (1981), p. 2961.

157. M. Nappa, J.S. Valentine, J.Am.Chem.Soc., 100 (1978), p. 5075.

158. P. Hambright in "Porphyrins and Metalloporphyrin", Ed. K.M. Smith, Elsevier, Amsterdam (1975), Chapter 6, p. 259, and references therein.

159. D.G. Davis in "The Porphins" ed D. Dolphin, Academic Press (1980), Volume 5, Chapter 3.

160. I. Flemming in "Frontier Orbitals and Organic Chemical Reactions", Wiley Intersience, 1976, Chapter 2.

161. K.M. Kadish, K.L. Thomson, D. Berioz, L.A. Bottomly, in "Electrochemical Studies of Biological Systems", A.C.S. Symposium Series 38, Washington (1977), 51.

162. W. Gordy, W.J.O. Thomas, J.Chem.Phys., 24 (1956) p. 436.

163. F.A. Cotton, G. Wilkinson,"Advanced Inorganic Chemistry", Wiley, U.S.A. 1972, 3rd Edition, p. 115 and references therein.

164. A.L. Allred, E.G. Rochow, J.Inorg.Nucl.Chem., 5 (1958), p.264

165. H.B. Michaelson, J.Appl.Phys., 48 (1977), p. 4729.

166. A.B.P. Lever, P.C. Minor, Inorg.Chem., 20 (1981), p. 4015.

167. A. Wolberg, J. Manassen, Inorg.Chem., 9 (1970), p.2365.

168. D. Dolphin, T. Niem, R.H. Felton, I. Fujita, J.Am.Chem.Soc., 97 (1975), p. 5288.

169. K.M. Kadish, T. Malinski, H. Ledon, Inorg.Chem., 21 (1982), p. 2982.

170. S.F. Vul'fson, O.L. Kaliya, O.L. Lebedeo, E.A. Lukyanets, Zh.Organ.Khim., 12 (1976), p. 123.

171. A. Pelter, J.A. Ballantine, V. Ferrito, V. Jaccarini, A.F. Psaila, P.J. Schembri, J.Chem.Soc.,Chem.Comm., (1976), p. 999.

172. A. Pelter, J.A. Ballantine, A.F. Psaila, P. Murray-Rust, V. Ferrito, P. Schembri, V. Jaccarini, J.Chem.Soc., Perkin Trans 1, (1980), p. 1080.

173. L. Agius, Comp.Biochem.Physiol.B., 63 (1979), p. 109.

174. M. Walter, L. Ramaley, Anal.Chem., 45, (1973), p. 165.

175. M. Low, Honours Project Report, Edinburgh University, 1982.

176. J.I. Matthews, S. Braslavsky, P. Camilleri, Photochem. Photobiol., 32 (1980), p. 733.

177. (a) G.A. Heath, L.J. Yellowless, P.S. Braterman, J.Chem.Soc., Chem.Comm., (1981), p. 287.

(b) G.A. Heath, A.J. Lindsay, T.A. Stephenson, D.K. Vattis, J.Organomet.Chem., 233 (1982), p. 353.

178. G.A. Heath, M.H. Low, R.C.S. McQueen, A. Pelter, J.Chem.Soc., Perkin II, in preparation.

179. J.H. Fuhrhop, K.M. Smith, "Porphyrins and Metalloporphyrins" Ed. K.M. Smith, Elsevier, Amsterdam (1975), Chapter 19, p. 757.

180. A.D. Alder, F.R. Long, J.D. Finarelli, J.Org.Chem., 32, (1967), p. 476.

181. R.P. Linstead, C.E. Dent, J.Chem.Soc., (1934), p. 1022.

182. R.P. Linstead, C.E. Dent, J.Chem.Soc., (1934), p. 1027.

183. P.A. Barrett, C.E. Dent, R.P. Linstead, J.Chem.Soc., (1936), p. 1719.

184. R.P. Linstead, J.Chem.Soc., (1953), p. 2873.

185. C.H. Yang, S.F. Liu, H.L. Chan, G.T. Chang, Inorg.Chem., 19 (1980), p. 3541.

186. S.A. Mikhalenko, S.V. Barkanoon, O.L. Lebedev, E.A. Lukyanets, Zh.Obschi.Chim., 41 (1971), p. 2735.

187. R.B. Contractos, A.T. Peters, J.Chem.Soc., (1949), p. 1314.

188. I.C.I. Personal Communication.

189. R.P. Linstead, G.A. Rowe, J.Chem.Soc., (1940), p. 1070.

190. R.P. Linstead, G.A. Rowe, J.Chem.Soc., (1940), p. 1076.

191. P.A. Barrett, R.P. Linstead, F.G. Rundell, G.A.P. Tuey, J.Chem.Soc., (1940), p. 1079.

192. R.P. Linstead, F.T. Weiss, J.Chem.Soc., (1950), p. 2975.

193. L. Edwards, M. Gouterman, C.B. Rose, J.Am.Chem.Soc., 98 (1976), p. 7638.

194. A. Vogler, H. Kunkley, Angew.Chem.Int.Ed., 17 (1978), p. 760.

The following postgraduate courses were attended:

Homogeneous Catalysis	Dr. T.A. Stephenson University of Edinburgh
Fourier Transform Infra-Red Spectroscopy	Dr. S. Cradock University of Edinburgh
Inorganic Cluster Chemistry	Dr. A.J. Welch University of Edinburgh
Synchroton Radiation	Dr. C.D. Garner University of Manchester
Aspects of Industrial and Inorganic Chemistry	Dr. H.L. Roberts I.C.I.
Mass Spectroscopy	Professor J.H. Beynon University College of Swansea
Using the Results of Crystallography	Dr. A.J. Welch, Dr. R.O. Gould, Dr. M. Walkinshaw University of Edinburgh

U.S.I.C. Conferences, Galashiels, 1981 and 1982

All Inorganic Research Seminars and Colloquia